Lawrence Berkeley National Laboratory
Lawrence Berkeley National Laboratory

Title
I. THE SYNTHESIS AND CHARACTERIZATION OF ANNULATED URANOCENES II. THE VARIABLE TEMPERATURE 1H NMR OF URANOCENES

Permalink
https://escholarship.org/uc/item/4gn1n2rh

Author
Luke, Wayne Douglas

Publication Date
1980

Peer reviewed

eScholarship.org Powered by the California Digital Library
University of California

DISCLAIMER

This book was prepared as an account of work sponsored by an agency of the United States Government. Neither the United States Government nor any agency thereof, nor any of their employees, makes any warranty, express or implied, or assumes any legal liability or responsibility for the accuracy, completeness, or usefulness of any information, apparatus, product, or process disclosed, or represents that its use would not infringe privately owned rights. Reference herein to any specific commercial product, process, or service by trade name, trademark, manufacturer, or otherwise, does not necessarily constitute or imply its endorsement, recommendation, or favoring by the United States Government or any agency thereof. The views and opinions of authors expressed herein do not necessarily state or reflect those of the United States Government or any agency thereof.

I. The Synthesis and Characterization of Annulated Uranocenes

II. The Variable Temperature ^1H NMR of Uranocenes

Abstract

A general synthetic route to alkyl annulated cyclooctatetraene dianions and the corresponding annulated uranocenes has been developed. Dideprotonation of bicyclooctadienes resulting from reaction of cyclooctatetraene dianion with 1,n-dialkylbromides or methanesulfonates, affords alkyl annulated cyclooctatetraene dianions in moderate yields. Three diannulated uranocenes, dicyclopenteno-, bisdimethylcyclopenteno- and dicyclohexenouranocene were prepared from the corresponding cyclooctatetraene dianions and UCl_4. The structures of dicyclobuteno- and dicyclopentenouranocene were elucidated by single crystal X-ray diffraction and the effects of annulation on the uranocene skeleton are discussed. Attempted synthesis of benzocyclooctatetraene and a benz-annulated uranocene are reported.

The variable temperature ^1H NMR spectrum of uranocene has been reinvestigated from -100 to 100°C. The isotropic shift was found to be linear in T^{-1} with an extrapolated intercept of 0 at $T^{-1} = 0$. Variable temperature ^1H NMR spectra, from -80 to 70°C, of 17 substituted uranocenes are reported. The energy barrier to ring rotation in 1,1',4,4'-tetra-t-butyluranocene was determined to be 8.24 ± 0.5 kcal/mole while the barrier in the corresponding 1,1',3,3'-tetra-t-butylferrocene was determined to be 13.1 kcal/mole.

Conformational analysis of 1,1'-dialkyluranocenes by

DISTRIBUTION OF THIS DOCUMENT IS UNLIMITED

variable temperature ^1H NMR shows that primary substituents prefer a conformation where the substituent is farthest from the uranium and the dihedral angle between the $C_\alpha - C_\beta$ bond and the ring plane is 90° while secondary substituents prefer a conformation where the ring plane and the methine C-H bond dihedral angle is close to zero.

Alkyl substitution is shown to have little effect on the electronic and magnetic properties of the uranocene skeleton, and thus alkyl substituted uranocenes are treated as having effective axial symmetry in analysis of the observed isotropic shifts. Using diannulated uranocenes as model systems an analysis of the contact and pseudocontact components of the observed isotropic shifts in uranocene and alkyl substituted uranocenes is presented.

Synthesis of 1,1'-dimethyluranocene-4d is reported and an assignment of the individual ring proton resonances in 1,1'-dimethyluranocene is given.

to my parents

ACKNOWLEDGEMENT

The author wishes to express his gratitude to Professor Thomas C. Flood, who as his undergraduate advisor at USC, taught him how to think like an organic chemist and encouraged him to go to graduate school. Likewise I owe a debt of gratitude to Professor Andrew Streitwieser Jr., without whose patience and guidance this project would not have been possible and the kind collaboration of Dr. Alan Zalkin, of Lawrence Berkeley Laboratories, in determination of the two X-ray crystal structures reported.

A major portion of this thesis represents the fruitation of an NMR study begun by a previous Streitwieser graduate student, Stuart Berryhill. I am grateful for Stuart's initial encouragement on this project and the lengthy discussion of ideas with fellow colleagues in the Streitwieser group.

WAYNE D. LUKE

This work was conducted under the support of the U. S. Department of Energy under Contract W-7405-ENG-48.

TABLE OF CONTENTS

Chapter 1. A Brief Survey of Uranocene Chemistry

I. Historical Background 1

II. The Chemical Properties of Uranocene 3

III. The Physical Properties of Uranocene 9

References 12

Chapter 2. Annulated Uranocenes

I. Introduction 14

II. Synthesis of Diannulated Uranocenes 18

A) Synthesis of Dicyclopentenouranocene . . . 20

B) Reaction of Cyclooctatetraene Dianion with Alkyl Halides 25

C) Synthesis of Bis(dimethylcyclopenteno)-uranocene 30

III. Structural Characterization of Annulated Uranocenes 30

IV. Discussion 44

Experimental 49

References 57

Chapter 3. The NMR of Alkyl Substituted Uranocenes

I. Introduction and Historical Background 59

A) Theory 59

1) Contact Shift 63

2) Pseudocontact Shift 67

3) Factoring of Isotropic Shifts 74

a) Ratio Methods 75

b) Computational Methods 76

B) NMR of Uranium(IV) Organometallic Compounds . . 77

1) Tricyclopentadienyl Uranium(IV) Compounds . 77

2) Uranocenes 85

II. The Variable Temperature ^1H NMR of Uranocene and Substituted Uranocenes 99

A) Diamagnetic Reference Compounds 101

B) The Temperature Dependent ^1H NMR of Uranocene . 102

C) The Effect of Substitution on the ^1H NMR of Uranocene 106

1) The Energy Barrier to Ring Rotation in 1,1',4,4'-Tetra-t-Butyluranocene . . . 110

2) The Energy Barrier to Ring Rotation in 1,1',3,3'-Tetra-t-Butylferrocene . . . 120

3) The Energy Barrier to Ring Rotation in Monosubstituted Uranocenes 124

4) The Ring Rotation Energy Barrier in 1,1'-Dialkyluranocenes 131

D) The Effect of Substitution on the Magnetic Susceptibility of Uranocene 132

E) The Temperature Dependence of Ring Proton Resonances in Substituted Uranocenes . . . 135

F) The Temperature Dependence of Substituent Proton Resonances in Substituted Uranocenes . 182

1) Methyl and t-Butyl Substituted Uranocenes . 207

2) 1,1'-Diethyluranocene 215

3) 1,1'-Di-n-Butyluranocene 219a

4) 1,1'-Dineopentyluranocene 219a

5) 1,1'-Diisopropyluranocene 220

6) 1,1'-Bis(triphenylmethyl)uranocene 224

7) 1,1'-Diaryluranocenes 225

8) 1,1'-Di(cyclooctatetraenyl)uranocene . . . 226

9) Diannulated Uranocenes 230

III. Factoring the ^{1}H Isotropic Shifts in Alkyl Substituted Uranocenes 232

IV. Discussion and Summary 247

V. The ^{13}C NMR Spectra of Uranocenes 250

Experimental 260

References 266

Chapter 4. Deuterium Labeling of Ring Positions in 1,1'-Dialkyluranocenes

I. Introduction 272

II. Preparation of Ring Deuterated Uranocenes 273

A) Deuteration of n-Butylcyclooctatetraene . . . 273

B) 4-Deutero-Methylcyclooctatetraene 282

III. Assignment of the Ring Proton Resonances in 1,1'-Dialkyluranocenes 286

Experimental 293

References 300

Chapter 5. Annulated Uranocenes Part II. Approaches to Dibenzouranocene

I. Introduction 301

II. Approaches to Dibenzouranocene 302

A) Attempted Benzannulation of Uranocene 304

B) Attempted Synthesis of Benzocyclooctatetraene . 307

1) Attempted Diels-Alder Trapping of 1,2-Dehydrocyclooctatetraene 307

2) Reaction of Cyclooctatetraene Dianion with Alkyl Halides 311

III. Preparation of Stable Annulated Uranocenes with Fused 6-Membered Rings 316

A) Attempted Preparation of Bis[10,11-Dimethyl-9,12-Dihydrobenzo]uranocene 316

B) Preparation of Dicyclohexenouranocene 317

Experimental 323

References 331

CHAPTER I A BRIEF SURVEY OF URANOCENE CHEMISTRY

I. HISTORICAL BACKGROUND

Organometallic chemistry of the early actinide elements, thorium, protactinium, uranium and neptunium, is still in its infancy. The first actinide organometallic complex, Cp_3U-Cl, was synthesized by Wilkinson and co-workers,[1] in 1956. Since this initial report, a wide variety of organoactinide complexes containing both σ and π bonded organic ligands have been synthesized. Most of the early work in organoactinide chemistry was devoted to synthesis and structural characterization of thermally and kinetically stable complexes. More recently, mechanistic studies which attempt to extend and consolidate the reaction chemistry of organoactinide complexes with the vast body of knowledge on transition metal organometallic complexes have appeared. Thus, α elimination to form metal carbenes,[2,4,5] β-hydride elimination,[2,3,4,5] CO-insertion into actinide-carbon σ bonds,[5] and temperature dependent changes from monohapto to trihapto bonding[2,4,5] of an allyl ligand have all been observed in organoactinide complexes.

The chemistry of biscyclooctatetraene actinide sandwich complexes has played a central role in the development of organoactinide chemistry. Fischer[6] was the first to suggest the possibility of cyclooctatetraene actinide complexes. However, Streitwieser[7,8] was the first to realize the

similarity between the symmetry of cyclooctatetraene dianion molecular orbitals (MO's) and valence f-orbitals, and the symmetry of cyclopentadienyl anion MO's and the valence d-orbitals on the metal in ferrocene and ferrocene-type sandwich organometallic complexes. In ferrocene, and ferrocene-type organometallic type complexes, the covalency of the ligand-metal bond results principally from a symmetry allowed orbital overlap between the highest occupied ligand MO's and vacant d-orbitals on the metal. In analogy, Streitwieser proposed that a similar symmetry allowed orbital overlap between filled ligand orbitals of cyclooctatetraene dianion and vacant f-orbitals on an actinide metal would confer covalent character to the ligand-metal bonds in a similar series of sandwich organometallic complexes of the early actinide elements.

Indeed, the initial reaction of cyclooctatetraene dianion with UCl_4 afforded an emerald green, air sensitive complex, which could be purified by sublimation.[7] A subsequent crystal structure[9] confirmed the proposed sandwich structure, and established that this compound was the structural homolog of ferrocene. Hence, the complex was given the trivial name "uranocene." Since this initial preparation of uranocene by Müller-Westerhoff and Streitwieser[7] slightly over 10 years ago, subsequent work has established that all of the early actinides form similar biscyclooctatetraene, or actinocene, complexes.[10-12] However, both from a safety standpoint and due to its ease of synthesis, most of the work in this area has been done with the uranium complex.

II. THE CHEMICAL PROPERTIES OF URANOCENE

In the decade since the initial synthesis of uranocene, a great deal of effort has been devoted to elucidation of the character of the ligand-metal bond, and the possible role that f-orbitals play in contributing to covalency in the ligand-metal bond. Since uranocene was proposed as the f-orbital analog of ferrocene, initially both were assumed to display similar chemistry. Unfortunately, the reaction chemistry of uranocene is not as rich or as varied as that of ferrocene. Three well known properties of ferrocene, its oxidative stability, its hydrolytic stability, and its stability toward hydrogenation, all reflect the covalent character of the ligand-metal bond.

Unlike ferrocene, which is air stable, but can be easily and reversibly oxidized to the ferrocinium cation, most uranocenes are highly air sensitive and on exposure to air decompose to UO_2 and the corresponding cyclooctatetraene within minutes. An early report[19] suggests that uranocenes are explosively pyrophoric, however, this appears to have been due to dianion impurities rather than the organometallic species. Only 1,1',3,3',5,5',7,7'-octaphenyluranocene, where the metal center is effectively shielded from oxygen attack, is air stable, suggesting that steric congestion around the metal center will impart air stability to uranocenes.[13] However, other substituted uranocenes bearing moderately bulky substituents such as 1,1',4,4'-tetra-t-butyluranocene show no enhanced air stability.

Attempted oxidation of uranocene in solution both electrochemically and with a variety of chemical oxidants, results in destruction of the uranocene.[14] In the presence of mild oxidizing agents such as nitro compounds uranocenes react to form UO_2, the free cyclooctatetraene ligand and either a reduced azo or amino species.[15] The reaction is extremely fast except for 1,3,5-tri-t-butyl-nitrobenzene, suggesting that the rate determining step involves attack at the metal in uranocenes. However, kinetic studies do not substantiate this and indicate that the reaction is extremely complex. Importantly, in oxidation of uranocene, the oxidation state of the metal does not change as a result of the reaction.

Ferrocene displays remarkable hydrolytic stability even upon exposure to strong mineral acids. On the other hand, uranocene shows only limited hydrolytic stability to weak Brönsted acids.[16] However, comparison with the instantaneous hydrolysis of ionic cyclooctatetraene dianion complexes, indicates the covalent character of the ligand - metal bonds in uranocenes. While the uranium containing decomposition products have not been characterized in hydrolysis reactions, the sole formation of cyclooctatrienes suggests that the uranium has not changed oxidation state during hydrolysis.

Ferrocene shows remarkable stability to hydrogenation such that olefins appended to the ferrocene moiety can be hydrogenated without destruction of the ferrocene moiety. Similarly, uranocene is reported to remain unchanged upon exposure to 1 atm. of hydrogen in the presence of palladium on carbon, and vinyl uranocene is quantitatively converted to

ethyl uranocene under similar conditions.[17] However, attempted hydrogenolysis of uranocene esters resulted in hydrogenation of the uranocene moiety without cleavage of the ester.[18] Thus, verification of the stability of uranocene and substituted uranocenes toward hydrogenation conditions is certainly an area for further study.

Typically the reaction chemistry of ferrocene is dominated by the stability of the basic sandwich structure and the aromatic character of the ligands. Like other electron rich aromatic systems, ferrocene forms a charge transfer complex with TCNE both in solution and upon mixing the dry solids. While an initial report suggests that uranocene behaves similarly, we have found that grinding solid uranocene samples with TCNE results in no apparent reaction while mixing the two compounds in solution results in decomposition of the uranocene and formation of the TCNE radical anion.[19]

Ferrocene readily undergoes electrophilic aromatic substitution under Friedel-Crafts or Vilsmeier conditions affording a wide variety of substituted ferrocenes. Unfortunately, substituted uranocenes cannot be prepared in a similar manner. Uranocenes do not undergo electrophilic aromatic substitution and are decomposed in the presence of strong electrophiles.[16]

Reports on the behavior of uranocenes with strong bases are conflicting. Uranocene appears to be stable to alkyllithium reagents but does not undergo metallation.[16] However, attempted metallation of alkyl substituted uranocenes which are significantly more soluble than uranocene has not been thoroughly investigated. Preliminary studies show that brief

treatment (ca. 15 min) of 1,1'-diethyluranocene with n-butyllithium in THF at -70°C results in no significant amount of metallation. Although treatment of uranocenes with alkyllithium reagents does not result in rapid metallation, some interaction between the two species does occur as evidenced by a change in the visible spectrum. Solutions of alkyluranocenes either darken in color or change color to red, similar to the behavior of alkoxyuranocenes on exposure to alkyllithium reagents. This color change may reflect formation of a charge transfer complex since the green color of uranocene is regenerated upon quenching with water.

Treatment of quaternary amino and alkoxy uranocenes with alkyllithium reagents results in substitution of the amino or alkoxy group with the alkyl group of the lithium reagents.[20] Indeed, outside of hydrogenation or carbene addition to the double bond in 1,1'-divinyluranocene, this is the only reaction which preserves the uranocene moiety throughout the course of the reaction. The reaction is proposed to proceed via a metal complexed 1,2-dehydrocyclooctatetraene. An attempt at Diels-Alder trapping of this species will be discussed in Chapter 5. However, the reaction of alkyllithium reagents with substituted uranocenes is certainly an area for further study.

Uranocene has been reported to decompose in the presence of alkoxide and amine bases.[16] We have found that treatment of 1,1'-dimethyluranocene with sublimed potassium t-butoxide in THF results in no apparent reaction or decomposition. Similarly, several aminoalkyl substituted uranocenes have

been synthesized and solutions of these compounds show no sign of decomposition after several years. Furthermore, in a subsequent section we shall discuss the preparation and stability of uranocene in liquid ammonia. Thus, the decomposition reported in earlier work undoubtedly resulted from impurities, and uranocenes are stable in the presence of weak as well as strong bases.

The assumed decomposition of uranocene by alkoxide bases resulted from the observation that uranocene hydrolysis is faster in aqueous THF with added potassium hydroxide or in ethanolic sodium ethoxide, than in aqueous THF.[16] However, the observed decomposition clearly results from the presence of the proton source, i.e., the water or the alcohol, and the base only serves to accelerate this process. Indeed, the fact that the oxidation state of the uranium ion remains apparently unchanged during hydrolysis suggests that base attack at the metal center occurs concurrently with protonation of the cyclooctatetraene rings, rather than initial protonation occuring at the metal center. This could be verified by kinetic studies on the decomposition of uranocene and particularly the more soluble alkyl substituted uranocenes with weak acids such as alcohols, water, and acetic acid both with and without added base.

All attempts to reduce uranocenes to the corresponding uranium (III) species have failed. No reaction occurs upon treatment of uranocene with potassium naphthalide or potassium metal.[21] However, reducing species with extremely high

reduction potentials, such as 1,3,5,7-tetra-t-butylcyclooctatetraene dianion will reduce uranocene to the corresponding ligand dianion and uranium metal.[22]

Although the reaction chemistry of uranocene is certainly limited this has not hindered the synthesis of a wide variety of functionalized uranocenes. Uranocenes have been synthesized by four types of approaches: 1)reaction of cyclooctatetraene dianions with UCl_4; 2)reaction of cyclooctatetraene dianion with uranium organometallic species; 3)reaction of cyclooctatetraene with finely divided uranium metal; 4)functional group transformations of substituted uranocenes. To date these synthetic routes have afforded uranocenes with alkyl, alkoxy, amino, phosphino, silyl, stanyl and ester functionality. Unlike ionic cyclooctatetraene dianion complexes, the ligands in uranocenes do not exchange with cyclooctatetraenes. However, in the presence of added dianion, ligand exchange is observed but this reaction has not been used in the synthesis of uranocenes.[23]

In total, the reaction chemistry of uranocene is dominated by three important characteristics: 1)a failure to behave as a purely ionic compound indicative of some covalent character in the ligand-metal bond; 2)a pronounced instability toward proton or electrophilic reagents; 3)a pronounced propensity to undergo oxidative decomposition in the presence of extremely mild oxidizing agents. Further, in reactions which result in decomposition of the uranocene moiety, no evidence exists to suggest the metal changes oxidation state.

III. PHYSICAL PROPERTIES OF URANOCENE

Insight into the character of the ligand-metal bond in uranocenes through measurement and interpretation of the physical properties of uranocene has proven a very fruitful area of research. Typically the visible spectrum of uranocenes display one major and two or three less intense absorption bands in the visible spectrum with extinction coefficients of ca. 1.5×10^3 l $mole^{-1}cm^{-1}$ and ca. 0.5×10^3 l $mole^{-1}cm^{-1}$, respectively. The λ_{max} of the principal band varies from 600 to 660 nm while the resolution of the lesser bands varies depending upon the substituent with λ_{max} ranging from 640 to 740 nm. The λ_{max} are substituent dependent. In uranocene the λ_{max} are 616, 643, 661 and 671 nm. Electron-withdrawing groups on the rings shift the λ_{max} toward shorter wavelength while electron-donating groups shift the absorbance to longer wavelength.[24] The magnitude of the shift increases with increasing substitution. Both the magnitude of the extinction coefficients and the substituent induced shift in λ_{max} are indicative of a charge transfer transition rather than an f-to-f transition. Streitwieser, et al. have proposed that the visible spectrum results from a ligand-to-metal charge transfer transition.[16] Subsequently, Spiro and co-workers[25] have confirmed this from resonance Raman spectroscopic studies which showed that the visible absorption bands at 616 and 661 nm are resonance coupled to the symmetrical ring-metal stretch and the ring-breathing deformations, respectively.

The spectral bands in both the IR and the Raman spectrum of uranocene have been assigned: the symmetrical ring-metal stretch at 211 cm^{-1} and the asymmetrical stretch at 240 cm^{-1}. Comparison of calculated primary force constants for both ferrocene (3.17 mdy A^{-1}) and uranocene (2.31 mdy A^{-1}) shows the weaker ligand-metal bonds in uranocene consistent with the smaller overlap of f-orbitals than d-orbitals.[25] Unfortunately, substituent induced shifts in the ring-metal stretching frequencies have not been studied.

Uranocenes are paramagnetic, with two unpaired f-electrons. The bulk magnetic susceptibility of uranocene displays Curie-Weiss behavior above 20°K with μ_{eff} = 2.4 ± 0.2 B.M.[27] Several workers have found that agreement between the experimental bulk susceptibility and calculated values from crystal field models only results when the crystal field calculations are corrected for reduction in orbital size resulting from covalent contributions to ligand-metal bonding.[25,28-30] However, this interpretation is not universally accepted,[31] and the controversy will not be resolved until better magnetic susceptibility data is available.

Recent interpretation of the photoelectron spectrum (PES) of uranocene[32] has confirmed the Streitwieser, et al.,[8,16] proposal of orbital overlap between metal f-orbitals and ligand MO's. In addition, the PES spectrum also showed a significant interaction between metal d-orbitals and ligand MO's of appropriate symmetry. To date, the PES spectrum of uranocene provides the most convincing evidence for f-orbital

contributions to the covalent character of the ligand-metal bonds in uranocene.

Since uranocenes are paramagnetic, NMR spectroscopy can be used to evaluate electron delocalization and the covalent character of the ligand-metal bond.[33,34] Such an analysis will form a major portion of this thesis and will be discussed in Chapters 3 and 4. The remaining chapters will be concerned with the synthesis of annulated uranocenes, both for their use as model systems in the NMR analysis and to assess the effects of annulation on the uranocene skeleton.

REFERENCES

1) L. T. Reynolds and G. Wilkinson, Inorg. Nucl. Chem. Let., 2, 246 (1956).

2) T. J. Marks, A. M. Seyam and J. R. Kolb, J. Am. Chem. Soc., 95, 5529 (1973).

3) T. J. Marks and A. M. Seyam, J. Organometal. Chem., 67, 61 (1964).

4) T. J. Marks, Accts. Chem. Res., 9, 223 (1976).

5) P. J. Fagan, J. M. Manuquez and T. J. Marks in "Organometallics of the f-Elements", T. J. Marks and R. D. Fischer, Eds., D. Reidel Pub. Co., Boston, Mass., (1979), p. 113.

6) R. D. Fischer, Theoret. Chim. Acta., 1, 418 (1963).

7) A. Streitwieser, Jr. and U. Muller-Westerhoff, J. Am. Chem. Soc., 90, 7364 (1968).

8) A. Streitwieser, Jr. in "Topics in Nonbenzenoid Aromatic Chemistry", T. Nozoe, R. Breslow, K. Hafner, S. Ito and I. Murata, Eds., Hirokawa Publ Co., Inc., Tokyo (1973), p. 221.

9) A. Avdeef, K. N. Raymond, K. O. Hodgson and A. Zalkin, Inorg. Chem., 11, 1083 (1972).

10) D. G. Karraker and J. A. Stone, J. Am. Chem. Soc., 96, 6885 (1974).

11) A. Streitwieser, Jr. and N. Yoshida, J. Am. Chem. Soc., 91, 7528 (1969).

12) D. F. Starks, T. C. Parsons, A. Streitwieser, Jr. and N. Edelstein, Inorg. Chem., 13, 1307 (1974).

13) A. Streitwieser, Jr. and R. Walker, J. Organomet. Chem., 97, C41 (1975).

14) J. A. Butcher, Jr., J. Q. Chambers and R. M. Pagni, J. Am. Chem. Soc., 100, 1012 (1978).

15) C. B. Grant and A. Streitwieser, Jr., J. Am. Chem. Soc., 100, 2433 (1978).

16) A. Streitwieser, Jr., U. Muller-Westerhoff, G. Sonnichsen, F. Mares, D. G. Morrell, K. O. Hodgson and C. A. Harmon, J. Am. Chem. Soc., 95, 5529 (1973).

17) A. Streitwieser, Jr. and C. A. Harmon, Inorg. Chem., 12, 1102 (1973).

18) H. Burghard, unpublished results.

19) C. A. Harmon, Ph.D. Thesis, U.C. Berkeley (1975).

20) C. A. Harmon and A. Streitwieser, Jr., J. Am. Chem. Soc., 94, 8926 (1972).

21) M. Halpern, unpublished results.

22) M. Miller, Ph.D. Thesis, U.C. Berkeley (1978).

23) C. LeVanda, unpublished results.

24) S. Berryhill, Ph.D. Thesis, U.C. Berkeley (1977).

25) R. F. Dallinger, P. Stein and T. G. Spiro, J. Am. Chem. Soc., 100, 7865 (1978).

26) L. Hecks, J. Goffart, G. Duyckaerts and P. Teyssie, Spectrochimica. Acta., 30A, 907 (1974).

27) H. D. Amberger, R. D. Fischer and B. Kanellakopolus, Theoret. Chim. Acta., 37, 105 (1975).

28) R. G. Hayes and N. Edelstein, J. Am. Chem. Soc., 94, 8688 (1972).

29) D. G. Karraker, Inorg. Chem., 12, 1105 (1975).

30) K. D. Warren, Structure and Bonding, 33, 97 (1977).

31) R. D. Fischer in ref. 5, p. 337.

32) J. P. Clark and J. C. Green, J. Organomet. Chem., 112, C14 (1976).

33) N. Edelstein, G. N. La Mar, F. Mares and A. Streitwieser, Jr., Chem. Phys. Let., 8, 399 (1971).

34) A. Streitwieser, Jr., D. Dempf, G. N. La Mar, D. G. Karraker and N. Edelstein, J. Am. Chem. Soc., 93, 7343 (1971).

CHAPTER 2 ANNULATED URANOCENES

I. INTRODUCTION

The dianion 2 of bicyclo[6.2.0]deca-1,3,5,7-tetraene, 1, is formally the 10π electron homolog of benzocyclobutene 3.

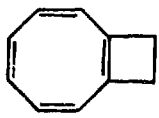

1

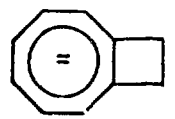

2

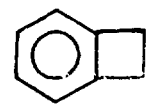

3

In general, cyclooctatetraene dianions are prepared by the reduction of the hydrocarbon. Sondheimer and co-workers[1,2] first prepared 1 in 0.4% overall yield from benzene and dimethylacetylenedicarboxylate, according to Scheme 2-1. While 1 is reduced to 2 upon treatment with potassium metal,[3] the poor synthetic yield of 1 from readily available starting materials, coupled with its rapid decomposition in the neat state at ambident temperatures, precludes this as a reasonable synthetic route to the dianion 2.

Staley and co-workers[3] found that 2 could be readily

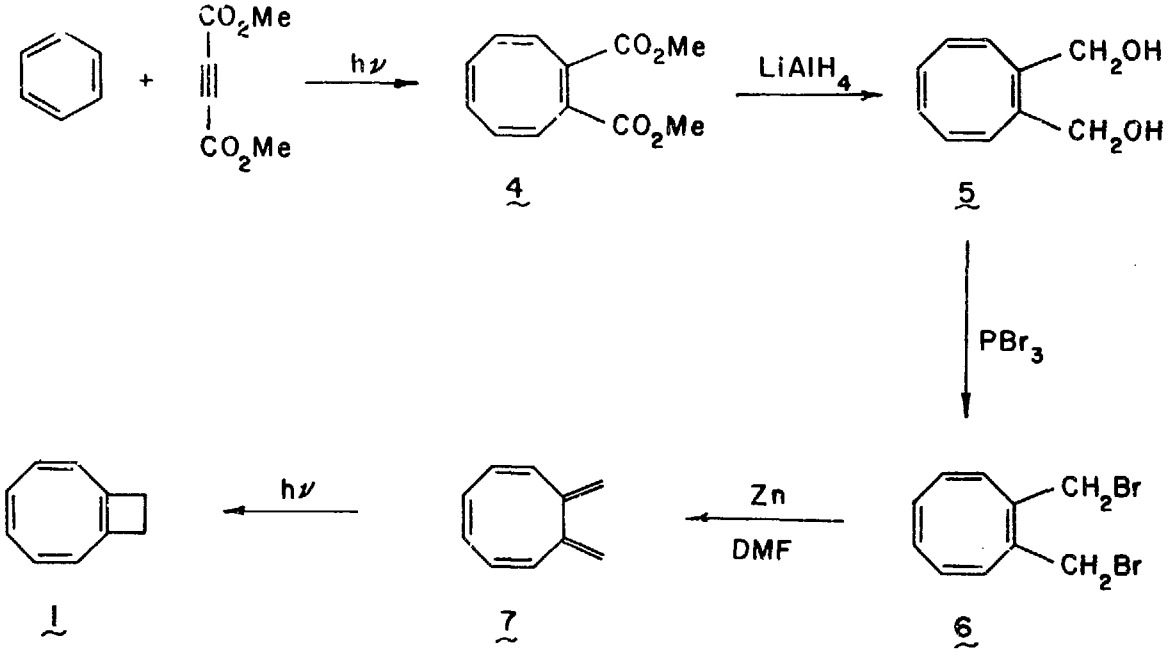
CO2Me
CO2Me
hν
CO2Me
CO2Me
LiAlH4
CH2OH
CH2OH
4
5
PBr3
hν
Zn
DMF
CH2Br
CH2Br
1
7
6

Scheme 2-1

prepared in high yield by the dideprotonation of 8 with potassium amide in liquid ammonia. The requisite bicyclooctatriene 8 was readily synthesized by the addition of 1,2-dibromoethane to cyclooctatetraene dianion (Scheme 2-2).[4]

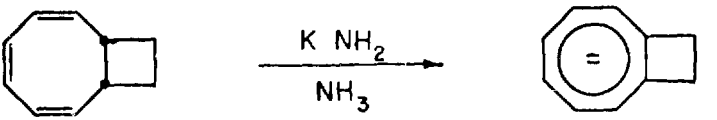

8 2

This facile two-step synthesis of 2 from cyclooctatetraene led Berryhill[5] to investigate 2 as a possible uranocene ligand. Ideally, in a uranocene formed from 2, the interplay of both the electron donating alkyl substituents coupled with the strain induced by the fused ring could confer unique physical and chemical properties to the uranocene moiety. Reaction of 2 with UCl_4 in THF resulted in the green air sensitive dicyclobutenouranocene 9, in 83% yield.

The visible spectrum of 9 (Table 2-1) showed the expected bathochromic shift for an alkyl-substituted uranocene with the λ_{max} at 623 nm similar to that of 1,1'-dialkyluranocenes, λ_{max} 619-625 nm, but less than that of 1,1',3,3',5,5',7,7'-

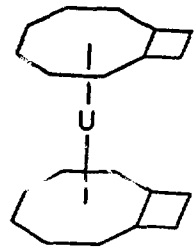

9

octamethyluranocene, with λ_{max} at 650 nm.[6] The visible spectrum was unusual in that the band at 732 nm is at a longer wavelength than any absorption observed in other alkyl-substituted uranocene. Berryhill suggested that the position of this band may be related to the strain introduced by the fused ring. Bulk magnetic susceptibility measurements (Table 3-11) showed that annulation had little if any effect on the bulk magnetic properties of uranocene.

The ^{1}H NMR spectrum of 9 was extremely interesting. The exo and endo protons of the methylene groups are non-equivalent with a remarkable shift difference of 46.41 ppm, at 30°C (Table 2-2). Each of the resonances is a doublet with a coupling constant of 9.64 Hz. While the resonances of the three unique ring protons fall within the range of ring proton resonances

for substituted uranocenes (Table 3-7), their spread in frequency is larger. Berryhill suggested this resulted from distortion of the 8-membered ring resulting from fusion with the 4-membered ring.

As part of a study on the factorization of isotropic ^{1}H NMR shifts in 1,1'-dialkyluranocenes into pseudocontact and contact components, described in Chapter 3, a need arose for alkylated uranocenes whose substituent was constrained to a known conformation(s). The apparent rigidity of the substituent in 9 suggested that constraining the alkyl substituent in a fused ring would limit the number of possible conformations of the alkyl substituent on the uranocene moiety. This approach is not unique. During the course of this project, Rettig, et al.,[7] reported a similar approach, wherein the substituent is constrained in a fused ring in analysis of the ^{1}H isotropic shifts in nickelocenes. In preliminary work using an assumed structure for 9, Berryhill showed that factorization of the ^{1}H isotropic shifts in 9 leads to qualitatively similar results as those found by Edelstein, et al.,[8] in analysis of 1,1',3,3', 5,5',7,7'-octamethyluranocene.

II. SYNTHESIS OF DIANNULATED URANOCENES

Our goal was the synthesis and structural characterization of a series of diannulated uranocenes in order to assess the effect of annulation on the uranocene skeleton, and to use these compounds as model systems in NMR studies. Initially we were interested in synthesizing uranocenes 10 and 11 which

have protons in the β and γ positions, respectively.

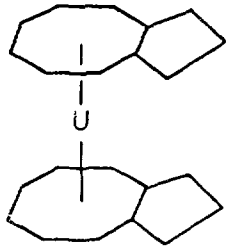

10

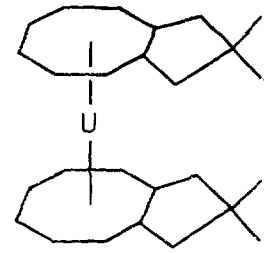

11

The annulated cyclooctatetraene dianion precursors, 12 and 13, to these uranocenes are unknown. Paquette and co-workers,[9-14]

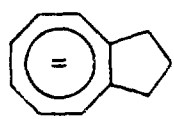

12

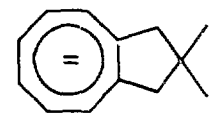

13

in several papers, have reported the synthesis of annulated cyclooctatetraenes with fused five, six and seven membered rings by either pyrolysis of the propellanes 14, or photolysis of the bridged tricyclic ketones 15 or the sulfones 16. While the yields of annulated cyclooctatetraenes from these precursors

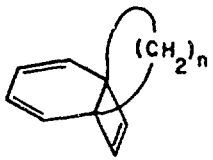

14

	n
a	3
b	4
c	5

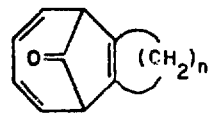

15

	n
a	4

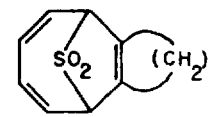

16

	n
a	3
b	4
c	5

are high, the multi-step synthesis of 14, 15 and 16 greatly lowers the yield from readily available starting materials and renders these approaches useless for the large scale synthesis of annulated cyclooctatetraenes.

A) SYNTHESIS OF DICYCLOPENTENOURANOCENE

The bicyclic cyclooctatriene homologs of 8 are readily available from reaction of cyclooctatetraene dianion with dibromoalkanes[15] (Scheme 2-2).

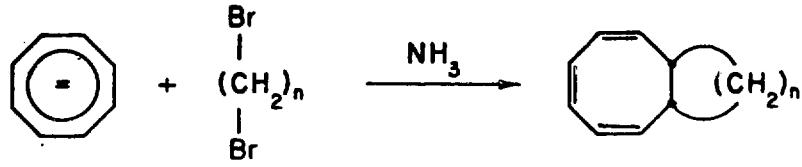

17

	n
a	2
b	3
c	4

Scheme 2-2

In principle, dideprotonation of these trienes would provide a general two-step synthetic route to annulated cyclooctatetraene dianions from cyclooctatetraene. Using $\overset{\oplus}{Na}\overset{\ominus}{NH_2}/NH_3$ under conditions identical to those used in dideprotonation of 8, Berryhill[5] was unsuccessful in an attempt to dideprotonate 17b. The failure appeared to result from the insolubility of the triene in liquid ammonia. In a large number of dissolving metal reductions in liquid ammonia, up to 25% of ethereal cosolvents are added to facilitate solvation of the reactants.[16] Similarly, treatment of 17a with $\overset{\oplus}{Na}\overset{\ominus}{NH_2}$ in 20% THF/80% NH_3 afforded a deep red-brown solution of the desired dianion which could be isolated as an impure tan solid upon solvent removal. Redissolution in THF was highly exothermic leading to red-brown

solutions of the dianion which were characterized by NMR: ^{1}H NMR (THF-d_8); 5.5 ppm, ring; 2.0 ppm, α-CH_2; 1.3 ppm, β-CH_2; ^{13}C NMR; 99.9 ppm, quaternary; 96.9, 89.8, 87.0 ppm, ring; 46.4 ppm, α-methylene; 27.2 ppm, β-methylene.

Addition of a THF solution of UCl_4 (1 eq.) to a THF solution of the dianion (2 eq.) resulted in an immediate color change from red-brown to emerald green indicative of uranocene formation. Removal of solvent gave a greyish green air sensitive solid which was purified by Soxhlet extraction with hexane affording 10 in 15.9% yield. A mass spectrum of this material showed major m/e peaks of 526 (100%), 382 (57%), 144 (18%), corresponding respectively, to the molecular ion, loss of one ligand, and the cyclooctatetraene ligand. The visible spectrum (Table 2-1) showed λ_{max} of 632, 656, 663 and 680 nm. The principal band of 632 nm is at a slightly longer wavelength than the corresponding band in dicyclobutenouranocene but within the bathochromic shift range expected for a tetraalkyl-substituted uranocene. The six well resolved resonances observed in the ^{1}H NMR spectrum could be assigned by a combination of integration and comparison with the ^{1}H NMR spectra of other uranocenes, with the shifts and assignment summarized in Table 2-2. In the ^{13}C NMR spectrum six resonances are observed with the four at 308.0, 296.9, 279.0, and 268.5 ppm corresponding to the ring carbon resonances, and the two at 13.4 and -32.5 ppm corresponding to the β and α carbon resonances, respectively. A comparison of the IR of 10, with that of uranocene and other annulated uranocenes is shown in Table 2-3.

Magnetic susceptibility measurements on the bulk solid

Fig. 2-1 Plot of 1/X vs T for dicyclopentenouranocene

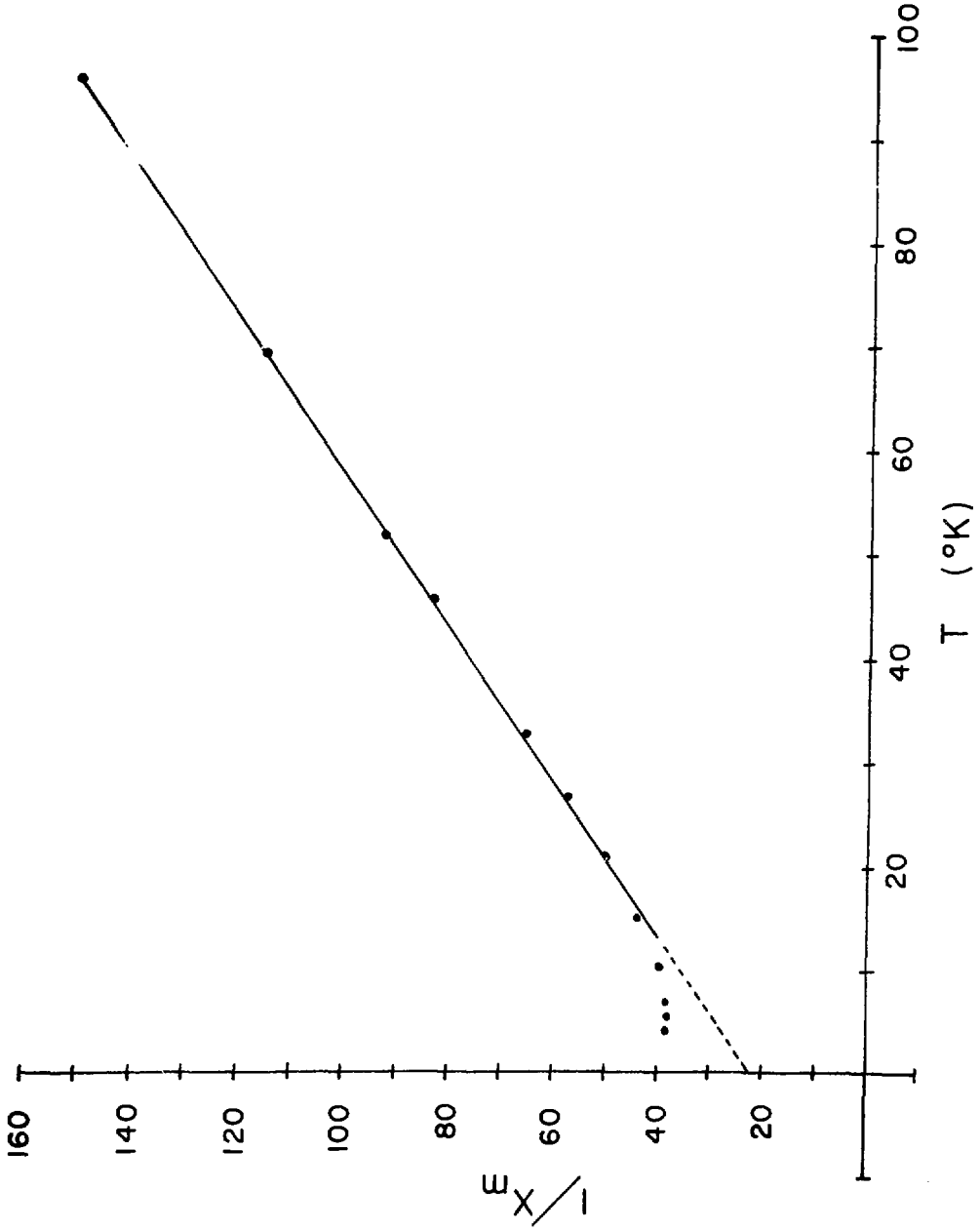
160
140
120
100
80
60
40
20
$1/\chi_m$
20
40
60
80
100
T (°K)

from 4.2 to 95.6°K are shown in Fig. 2-1. Above 20°K the magnetic susceptibility follows the Curie-Weiss Law with $C = 0.743 \pm 0.005$ emu °K mole^{-1}, $\mu = 2.4 \pm 0.1$ B.M. and $\theta = 16.6° \pm 0.05°K$. Below 10°K the magnetic moment was independent of temperature with $X_m = 2.56 \pm 0.03 \times 10^{-2}$ csu/mole. Using a diamagnetic correction of -187×10^{-6} emu mol^{-1} the corrected values are $C = 0.714 \pm 0.005$ emu °K mole^{-1}, $\mu = 2.4 \pm 0.1$ B.M. and $\theta = 16.1° \pm 0.5°K$.[18]

B) REACTION OF CYCLOOCTATETRAENE DIANION WITH ALKYL HALIDES

During the synthesis of 18 the bicyclooctatriene precursor

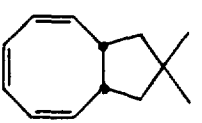

18

to 13, we became interested in the mechanism of the reaction of cyclooctatetraene dianion with alkyl halides. The reaction of cyclooctatetraene dianion with two alkyl halides involves two discrete sequential steps, each of which can occur by either

a direct Sn_2 displacement or by an electron transfer radical coupling type mechanism (Scheme 2-3). If one of the steps proceeds via an Sn_2 displacement, then a methanesulfonate should react faster than the corresponding alkyl bromide. Conversely, in a step which involves electron transfer, an alkyl bromide will react faster than the corresponding methanesulfonate.

In analogy with the preparation of 8 and 17, the preparation of 18 would involve the reaction of cyclooctatetraene dianion with 1,3-dibromo-2,2-dimethylpropane, which in turn is prepared from the readily available 2,2-dimethyl-1,3-propanediol.[17] Since in general, the synthesis of methanesulfonates is easier than the synthesis of bromides, the reaction of the di-methanesulfonate of 2,2-dimethyl-1,3-propanediol with cyclooctatetraene dianion was investigated.

Addition of a THF solution of the dimethanesulfonate to cyclooctatetraene dianion in liquid ammonia followed by oxidative workup, similar to the preparation of 17a, resulted in cyclooctatetraene and the unreacted dimethanesulfonate. However, preparation of 1,3-dibromo-2,2-dimethylpropane from the diol and PBr_3, followed by reaction with cyclooctatetraene dianion under identical conditions afforded the desired triene 18 as a yellow oil in 17.9% yield.

This result suggests that the first step in the reaction of cyclooctatetraene dianion with an alkyl halide involves electron transfer rather than Sn_2 displacement. Further evidence for an initial electron transfer step comes from the work of Monthony and Okamura[19] who found that the reaction of 1,2,3-trichloropropane with cyclooctatetraene dianion results in

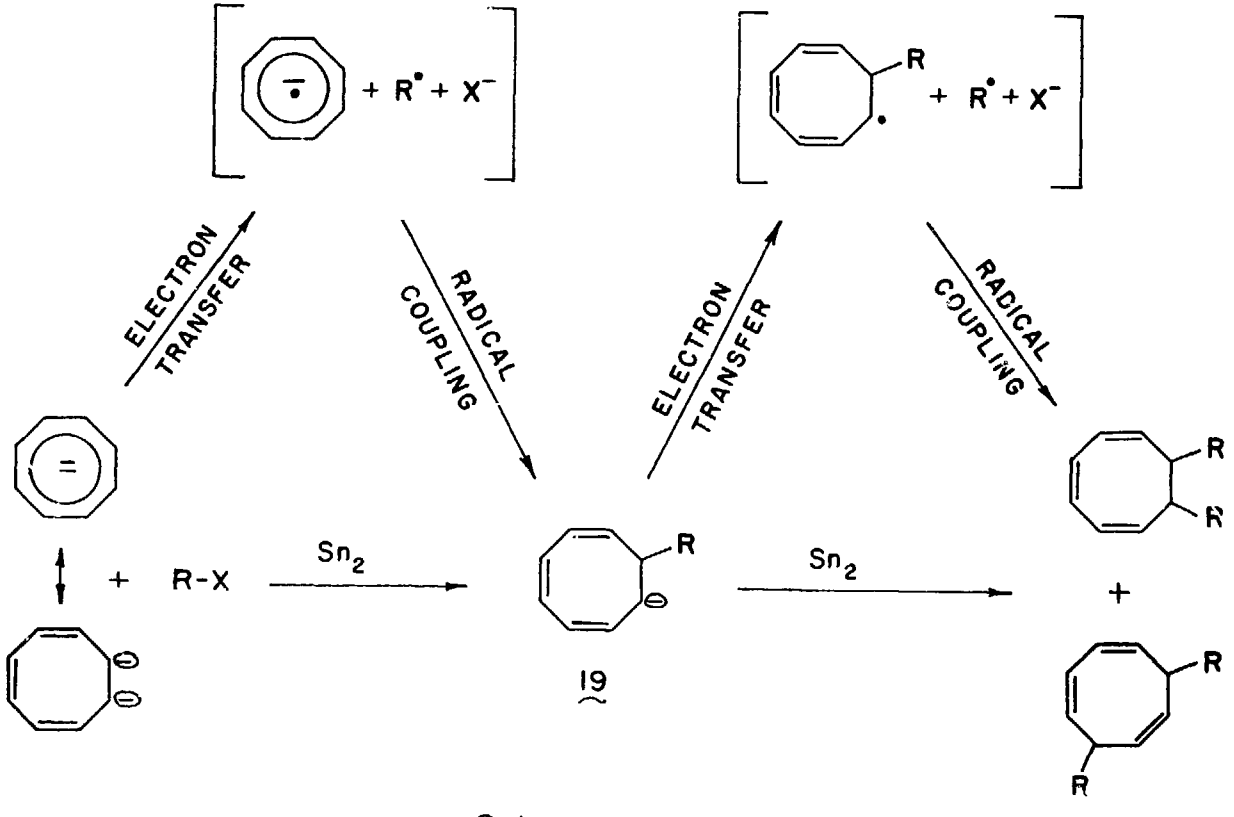
+ R• + X⁻
ELECTRON TRANSFER
RADICAL COUPLING
ELECTRON TRANSFER
RADICAL COUPLING
R
+ R• + X⁻
+ R-X
Sn2
Sn2
19
R
R
R
R

Scheme 2-3

exclusive formation of 20 in 7.25% yield. This product suggests that the secondary rather than the primary halide

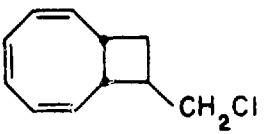

20

reacted in the initial step, consistent with an electron transfer rather than a direct displacement mechanism. Since 19 can be viewed as a heptatrienyl anion, it should preferentially react as a nucleophile rather than as an electron transfer reagent. Thus, the second step in the reaction of cyclooctatetraene dianion with alkyl halides should involve an Sn_2 nucleophilic displacement. This suggests that the dimethanesulfonate of 1,3-propanediol will not react with cyclooctatetraene dianion while the reaction of the methanesulfonate of 1-bromo-3-propanol will provide a probe for the mechanism of the second step in the reaction of cyclooctatetraene dianion with alkyl halides.

However, reaction of the dimethanesulfonate of 1,3-propanediol with cyclooctatetraene dianion in liquid ammonia led to 17a in 58.4% yield. Without kinetic data, it is

impossible to tell whether the dimethanesulfonate or the dibromide reacted faster. It does, however, suggest that the initial step in the reactions of cyclooctatetraene dianion with alkyl halides can proceed via either an electron transfer or an Sn_2 displacement type mechanism. The failure of the dimethanesulfonate of 2,3-dimethyl-1,3-propanediol to react undoubtedly reflects the fact that the Sn_2 displacement reaction involves displacement at a neopentyl center.

We have also found that the reaction of alkyl halides and methanesulfonates with cyclooctatetraene dianion can be run in THF. For example, the addition of 1,3-dibromopropane to cyclooctatetraene dianion in THF afford 9b in 63.2% yield. However, use of THF suffers from the disadvantage that the reduction of cyclooctatetraene to its dianion with potassium metal is slow in THF and often incomplete, thus leaving the desired triene contaminated with small amounts of cyclooctatetraene upon workup. Use of liquid ammonia as a solvent has the advantage that dissolving metal reduction of cyclooctatetraene at -30°C is instantaneous and the reaction is easily monitored by the immediate color change from blue to yellow upon complete consumption of the metal. However, caution should be employed in dissolving metal reductions run in liquid ammonia. Similar to the temperature dependent formation of potassium amide, dissolving metal solutions at ca. -70 to -40°C will not reduce cyclooctatetraene to the dianion, and thus, large amounts of cyclooctatetraene can be added with no apparent reaction. Formation of the dianion is exothermic, and thus warming such solutions leads to an extremely violent reaction above ca. -40°C.

C) SYNTHESIS OF BIS(DIMETHYLCYCLOPENTENO)URANOCENE

Dideprotonation of 18 with potassium amide in liquid ammonia/THF afforded a deep red solution of the dianion which was isolated as a tan solid upon solvent removal. Redissolution in THF resulted in a muddy brown solution which on slow addition to a THF solution of UCl_4 gave a dark black solution. Solvent removal yielded a silver grey highly pyrophoric powder which was washed with hot hexane affording a green solution. Centrifugation followed by solvent removal gave the desired uranocene 11 in 7% yield.

The visible spectrum of this material showed the typical uranocene cascade with λ_{max} of 627, 655 and 670 nm; while the mass spectrum showed major m/e peaks of 582 (78%, molecular ion), 410 (43%, loss of one ligand), 172 (72%, free ligand). The ^1H NMR shifts, at 30°C, and their assignments are recorded in Table 2-2.

III. STRUCTURAL CHARACTERIZATION OF ANNULATED URANOCENES

We have found that most substituted uranocenes can be readily recrystallized from hot hexane in an Ar atmosphere glove box. The technique involves preparing a saturated solution of the desired uranocene in boiling hexane, followed by centrifugation, and reheating to boil off a small amount of solvent. Allowing such saturated solutions to slowly cool to ambident temperature affords analytically pure crystalline uranocenes in 2 to 5 hrs. In this manner, single crystals of

Table 2-1

Visible Spectra of Annulated Uranocenes[a]

	λ_{max} nm			
Uranocene[b]	616	643	661	671
1,1'-Dimethyl-	623	650	670	681(s)
Dicyclobuteno-	623	652		732
Dicyclopenteno-	632	656	663	680
Bis(Dimethylcyclopenteno)-	627	655	670(s)	

s = shoulder

[a]spectra run in hexane

[b]spectra run in THF

Table 2-2

The ^1H NMR of Annulated Uranocenes in Toluene-d_8 at 30°C

δ From TMS

	Substituent	Ring
Dicyclobuteno-	-26.76(α_{endo}), 19.65(α_{exo}) J=9.64 Hz	-27.70, -35.90, -43.80
Dicyclopenteno-	-32.58(β_{endo}, m), -8.28(β_{exo}, m) -18.78(α_{endo}, m), 24.43(α_{exo}, m)	-32.12, -34.20, -41.15
Bis(dimethylcyclo-penteno)-	-12.91($CH_{3\,endo}$), 5.39($CH_{3\,exo}$) -22.90(α_{endo}), 8.28(α_{exo}) J=14.5 Hz	-32.43, -33.26, -39.83

Table 2-3

The IR of Annulated Uranocenes

cm^{-1} in NUJOL

Uranocene[a]	Dicyclobuteno-	Dicyclopenteno-	Bis(dimethyl-cyclopenteno)-
		1870(w)	
1730(w)		1765(w)	
		1320(m)	
1262(s)[b]	1262(m)	1260(m)	1265(s)
	1195(w)		
	1165(w)		1050(vs)[b]
1018(s)[b]	1120(s)	1020(m)	
	979(s)		
	918(s)	900(s)	
799(s)	820(m)	790(m)	790(vs)[b]
	818(s)		
	795(w)		
	791(s)		
	780(m)		
		745(s)	
720(s)	719(NS)	720(NS)	720(vs)

w = weak; m = medium; s = strong; NS = very strong

[a]See ref. 29 for assignments of spectral bands in uranocene

[b]broad

Fig. 2-2 Ortep ball and spoke view of dicyclobutenouranocene

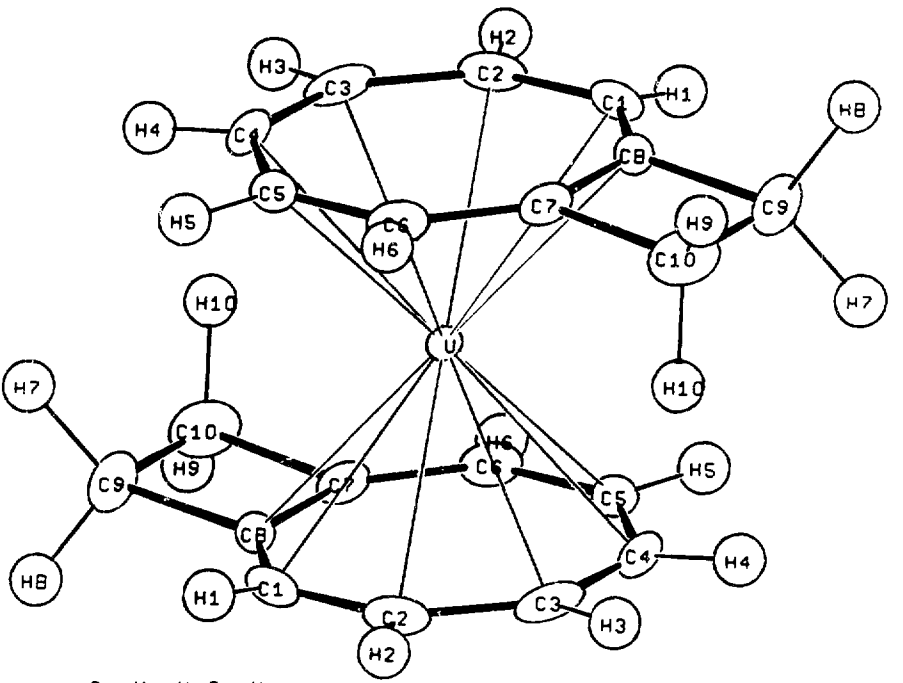

$C_{10}H_{10}U\ C_{10}H_{10}$

XBL 7711-10665

Table 2-4

Interatomic Distances (A) in Dicyclobutenouranocene

U	-2C(1)	2.675(7)	C(1)-H(1)	0.87(5)
	-2C(2)	2.654(7)	C(2)-H(2)	0.96(8)
	-2C(3)	2.618(7)	C(3)-H(3)	0.94(9)
	-2C(4)	2.631(8)	C(4)-H(4)	0.93(6)
	-2C(5)	2.637(8)	C(5)-H(5)	0.87(9)
	-2C(6)	2.674(7)	C(6)-H(6)	0.79(8)
	-2C(7)	2.637(6)	C(9)-H(7)	1.16(9)
	-2C(8)	2.626(6)	-H(8)	1.06(14)
			C(10)-H(9)	0.92(11)
C(1)-C(2)		1.38(2)	-H(10)	1.15(8)
C(2)-C(3)		1.41(2)		
C(3)-C(4)		1.39(2)		
C(4)-C(5)		1.41(2)		
C(5)-C(6)		1.40(2)		
C(6)-C(7)		1.38(2)		
C(7)-C(8)		1.40(2)		
C(8)-C(1)		1.38(2)		
C(8)-C(9)		1.54(2)		
C(9)-C(10)		1.47(2)		
C(10)-C(7)		1.55(2)		

Table 2-5

Selected Bond Angles (deg) in Dicyclobutenouranocene

C(8)-C(1)-C(2)	131.7(8)
C(1)-C(2)-C(3)	134.0(8)
C(2)-C(3)-C(4)	136.7(8)
C(3)-C(4)-C(5)	135.0(9)
C(4)-C(5)-C(6)	135.7(8)
C(5)-C(6)-C(7)	130.6(7)
C(6)-C(7)-C(8)	137.2(7)
C(7)-C(8)-C(1)	139.0(7)
C(6)-C(7)-C(10)	131.0(9)
C(1)-C(8)-C(9)	129.2(11)
C(8)-C(7)-C(10)	91.3(9)
C(7)-C(8)-C(9)	91.4(10)
C(8)-C(9)-C(10)	89.0(9)
C(7)-C(10)-C(9)	88.4(8)
C(8)-C(9)-H(7)	132(4)
C(8)-C(9)-H(8)	112(6)
H(7)-C(9)-H(8)	106(6)
C(7)-C(10)-H(9)	121(5)
C(7)-C(10)-H(10)	113(4)
H(9)-C(10)-H(10)	102(6)

Fig. 2-3 Ortep ball and spoke view of dicyclopenteno-uranocene. The hydrogens are omitted for clarity.

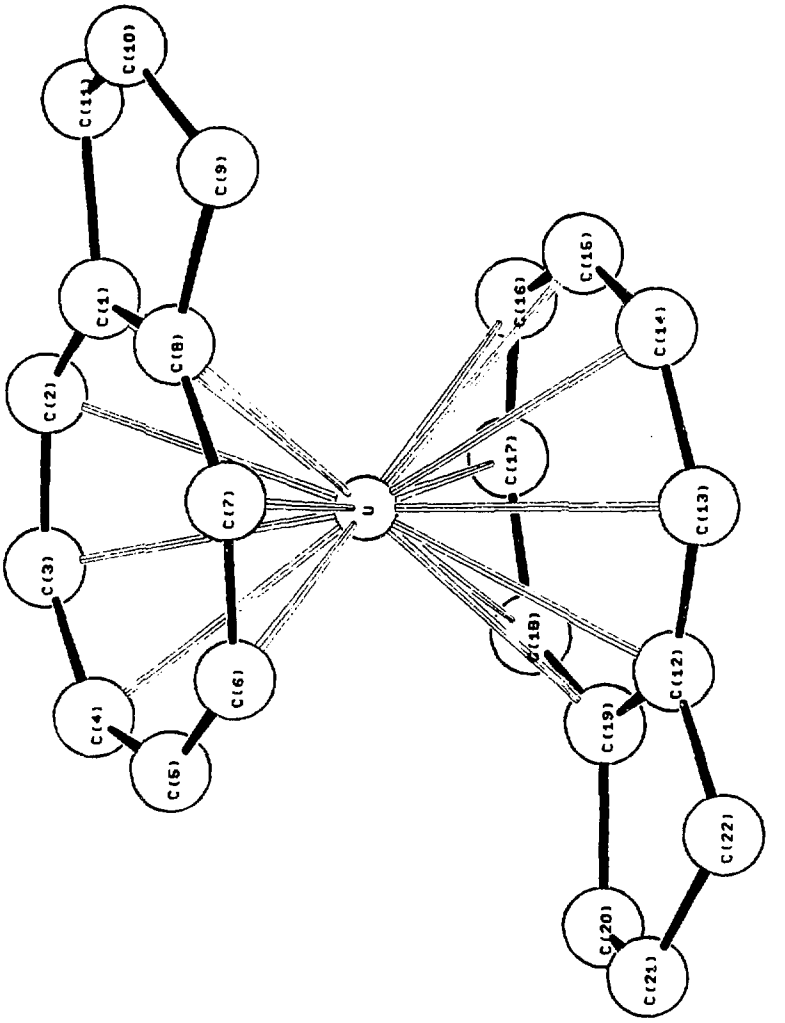

XBL 7811-12981

Fig. 2-4 Ortep ball and spoke view of the molecule perpendicular to the cyclooctatetraene rings. Hydrogen atoms are omitted for clarity.

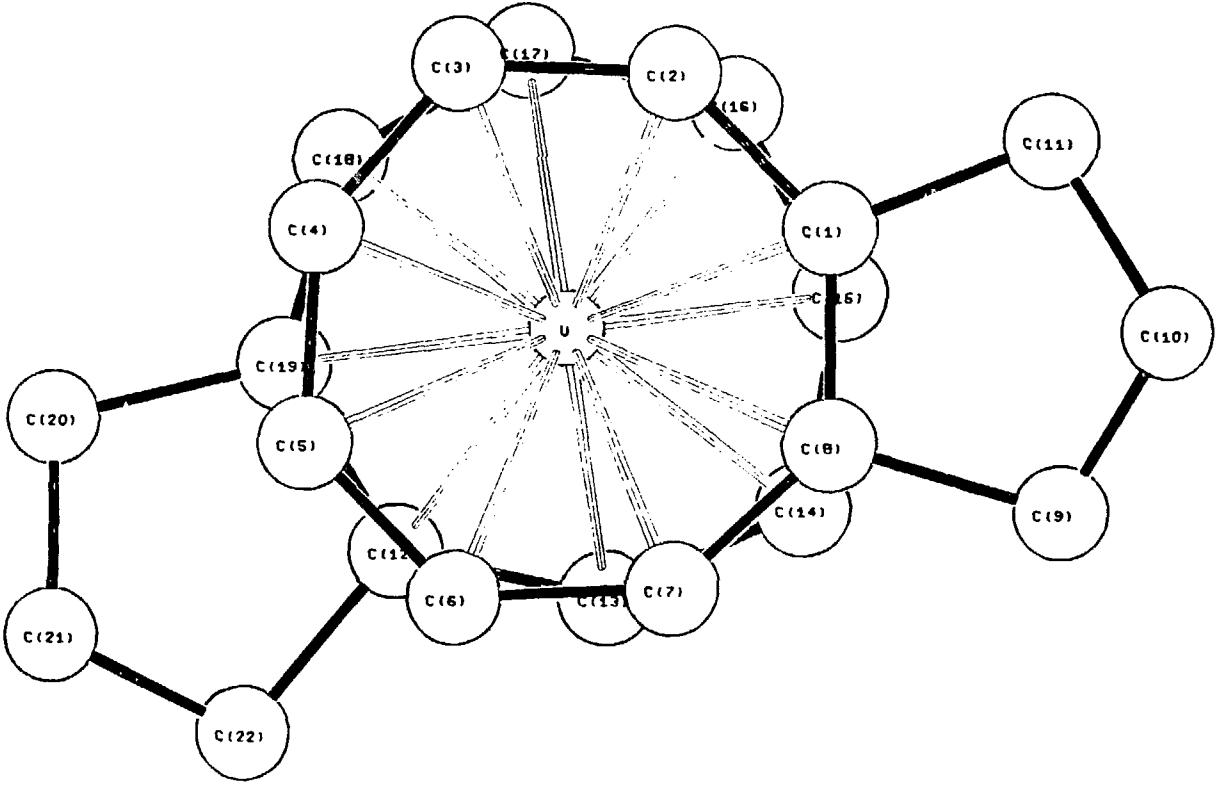

XBL 7811-12980

Table 2-6

Selected Interatomic Distances (A) in Dicyclopentenouranocene

U	-	C(1)	2.66(3)
		C(2)	2.63(3)
		C(3)	2.65(4)
		C(4)	2.60(3)
		C(5)	2.66(3)
		C(6)	2.64(3)
		C(7)	2.62(2)
		C(8)	2.68(2)
		C(12)	2.66(2)
		C(13)	2.66(3)
		C(14)	2.68(4)
		C(15)	2.58(3)
		C(16)	2.61(3)
		C(17)	2.67(2)
		C(18)	2.61(2)
		C(19)	2.66(2)
C(1)		C(2)	1.41(2)
C(2)		C(3)	1.40(2)
C(3)		C(4)	1.40(2)
C(4)		C(5)	1.39(2)
C(5)		C(6)	1.38(2)
C(6)		C(7)	1.40(2)
C(7)		C(8)	1.39(2)
C(8)		C(1)	1.40(2)
C(12)		C(13)	1.39(2)
C(13)		C(14)	1.40(2)
C(14)		C(15)	1.40(2)
C(15)		C(16)	1.39(2)
C(16)		C(17)	1.39(2)
C(17)		C(18)	1.40(2)
C(18)		C(19)	1.39(2)
C(19)		C(20)	1.40(2)
C(8)		C(9)	1.55(2)
C(9)		C(10)	1.38(5)
C(10)		C(11)	1.46(6)
C(11)		C(1)	1.53(2)
C(19)		C(20)	1.54(2)
C(20)		C(21)	1.43(5)
C(21)		C(22)	1.43(5)
C(22)		C(12)	1.53(2)

Table 2-7

Selected Angles (deg) in Dicyclopentenouranocene

C(1)	- U -	C(2)	31.0(5)
C(2)	- U -	C(3)	30.7(5)
C(3)	- U -	C(4)	31.0(5)
C(4)	- U -	C(5)	30.6(5)
C(5)	- U -	C(6)	30.2(5)
C(6)	- U -	C(7)	31.0(5)
C(7)	- U -	C(8)	30.1(4)
C(8)	- U -	C(1)	30.3(4)
C(12)	- U -	C(13)	30.4(5)
C(13)	- U -	C(14)	30.4(5)
C(14)	- U -	C(15)	30.8(5)
C(15)	- U -	C(16)	31.1(5)
C(16)	- U -	C(17)	30.5(4)
C(17)	- U -	C(18)	30.7(4)
C(18)	- U -	C(19)	30.5(4)
C(19)	- U -	C(12)	30.6(5)

C(8)	- C(1) -	C(2)	134(3)
C(1)	- C(2) -	C(3)	138(4)
C(2)	- C(3) -	C(4)	128(4)
C(3)	- C(4) -	C(5)	143(3)
C(4)	- C(5) -	C(6)	133(3)
C(5)	- C(6) -	C(7)	131(3)
C(6)	- C(7) -	C(8)	140(3)
C(7)	- C(8) -	C(1)	133(3)
C(19)	- C(12) -	C(13)	133(2)
C(12)	- C(13) -	C(14)	143(3)
C(13)	- C(14) -	C(15)	124(4)
C(14)	- C(15) -	C(16)	142(3)
C(15)	- C(16) -	C(17)	132(3)
C(16)	- C(17) -	C(18)	135(2)
C(17)	- C(18) -	C(19)	135(2)
C(18)	- C(19) -	C(12)	134(2)
C(2)	- C(1) -	C(11)	113(3)
C(8)	- C(1) -	C(11)	113(3)
C(1)	- C(11) -	C(10)	98(3)
C(11)	- C(10) -	C(9)	115(4)
C(10)	- C(19) -	C(8)	104(3)
C(1)	- C(8) -	C(9)	105(2)
C(7)	- C(8) -	C(9)	122(3)
C(18)	- C(12) -	C(22)	118(3)
C(19)	- C(12) -	C(22)	110(2)
C(12)	- C(22) -	C(21)	104(3)
C(22)	- C(21) -	C(20)	112(3)
C(21)	- C(20) -	C(19)	105(3)
C(20)	- C(19) -	C(12)	107(2)
C(20)	- C(19) -	C(18)	119(3)

dicyclobutenouranocene 9, and dicyclopentenouranocene 10, suitable for single crystal X-ray analysis were prepared and the crystal and molecular structures were determined by the kind collaboration of Alan Zalkin and David Templeton of Lawrence Berkeley Laboratories. The details of the structural determinations have been published elsewhere.[20-21] The pertinent bond lengths and angles are summarized in Fig. 2-2 through 2-4 and Tables 2-4 through 2-7.

IV. DISCUSSION

Dideprotonation of bicyclooctatrienes with potassium amide in THF/NH_3 offers a facile and simple synthesis of annulated cyclooctatetraene dianions from readily available starting materials. The relatively low yields of annulated uranocenes derived from such dianions undoubtedly results from incomplete deprotonation of the triene precursors. In particular, the lower yields of the fused 5-membered ring uranocenes in comparison to the yield of dicyclobutenouranocene may result from the difference in the known tautomeric equilibrium 21a $\rightleftharpoons$ 21b of the precursor cyclooctatrienes.[15]

Both Berryhill[5] and Cotton, et al.,[15] have shown that 17a exists preferentially in the bicyclic form while Cotton, et al, has shown that 7b exists in the tricyclic form. We have found that ^{13}C NMR provides an unambiguous method of distinguishing the two tautomers 21a and 21b. Spectroscopic analysis of freshly distilled 17b shows a significant amount of the

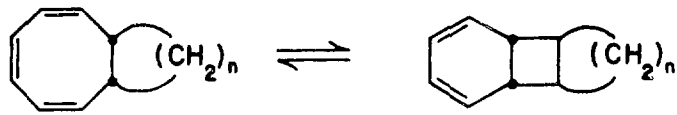

21a 21b

bicyclic tautomer (^{13}C; 135.3, 127.7, 126.3 ppm, olefinic; 43.5 ppm, bridgehead; 32.3 ppm, α-methylene; 19.5 ppm, β-methylene), which slowly rearranges to the tricyclic tautomer (^{13}C; 126.6, 120.3 ppm, olefinic; 51.0, 35.6 ppm, bridgehead; 32.9 ppm, α-methylene; 24.7 ppm, β-methylene). Similar spectra of 18 show only the presence of the tricyclic tautomer (^{13}C; 127.0, 120.7 ppm, olefinic; 51.1, 49.1 ppm, bridgehead; 48.9 ppm, quaternary; 37.6 ppm, α-methylene; 28.6, 28.3 ppm, methyl). If only the bicyclic isomer deprotonates to form the dianion, then the slow interconversion of the two tautomers could account for the lower yields of the dianion and the corresponding uranocenes.

The crystal structures of the two annulated uranocenes clearly show that annulation has little if any effect on the uranocene skeleton. Importantly, in both dicyclobuteno- and

dicyclopentenouranocene, the uranium atom is centrosymmetrically located between the two 8-membered rings and the uranium ring distance of 1.92 A is in excellent agreement with that of other uranocenes. In dicyclobutenouranocene, the fused ring induces a small but statistically significant distortion of the 8-membered ring from that of a regular octagon, which is not observed in dicyclopentenouranocene. While this distortion is small, it may account for the fact that the lowest field ring proton resonance in dicyclobutenouranocene is approximately 5 ppm lower in field than the corresponding resonances in either of the two annulated uranocenes with fused 5-membered rings. Outisde of this possible effect on the ^{1}H NMR spectrum, comparison of the physical properties of the annulated uranocenes with those of other alkyl substituted uranocenes shows that annulation does not effect the physical properties of uranocene.

In the solid state, the crystal structures show that the rings in dicyclobutenouranocene are eclipsed with the uranium at a center of inversion, while in dicyclopentenouranocene, the two rings are twisted away from an eclipsing position by about 10°. In other uranocenes, the rings have been found to be both staggered[22,23] and eclipsed[23,24] seeming to indicate that, as in ferrocenes, the relative orientation of the rings in uranocene crystals results from crystal packing and not from significant steric interactions between the rings which are 3.84 A apart.

Further, the crystal structures of both of the annulated uranocenes show that the α-carbons of the substituent are not

co-planar with the 8-membered ring but bent slightly inwards toward the uranium atom. The average tip angle for dicyclobutenouranocene is 6.9°, and somewhat less for dicyclopentenouranocene. The crystal structure of only one other alkyl substituted uranocene, 1,1',3,3',5,5',7,7'-octamethyluranocene has been reported, and it also shows that the α-carbons are bent inward ca. 3.5° toward the uranium.[22] Thus, this bending appears to be a general feature in alkyl substituted uranocenes where steric interactions between the rings is small.

Comparable bending has been observed in a variety of organometallic compounds with planar 5 and 6-membered rings.[25,26] Two possible explanations have been offered to account for this bending;[22] 1)bending the substituent toward the metal makes each carbon slightly more pyramidal with the π orbital of the carbocyclic ring bent inward toward the metal and providing greater directionality for overlap between π orbitals and metal orbitals; 2)contraction in volume of the electron density on the side of the ring adjacent to the highly charged metal ion. Non-bonding interaction between the substituted bond and the more diffuse electron density on the uncomplexed side of the ring would result in an inward bend of the substituent. This latter explanation suggests the inward bending should be independent of ring size. However, it appears that for 3- and 4-membered rings the substituents bend outward away from the metal.[26] Theoretical calculations on d-transition metal compounds attribute this bending to the former explanation and predict an outward bend for 3- and 4-membered rings and an inward bend in the substituent for rings larger than 5.[26]

Theoretical Xα calculations on uranocene have also suggested that this bend may result from an increase in directionality of the ligand π orbital and metal orbitals on uranium.[27] We believe that this bending of the substituent in toward the metal is a general feature in all substituted uranocenes where steric interactions between the rings is small and may reflect the proposed covalency in ligand-metal bonding in these systems.

EXPERIMENTAL

All reactions requiring air free anhydrous conditions were conducted under an Ar or N_2 atmosphere or under Ar in a Vacuum Atmospheres recirculating glove box. Solvents were distilled from CaH_2, $LiAlH_4$ or Na/benzophenone and degassed prior to use. Visible spectra were obtained on a Cary 118 spectrometer, infra-red spectra on a Perkin Elmer 297 spectrometer, ^1H NMR spectra on a Varian T-60 (60 MHz) spectrometer or the Berkeley FT-NMR system (180 MHz) and ^{13}C NMR spectra on a Brucker TT-23 spectrometer. Mass spectra and elemental analyses were performed by the Analytical Services Laboratory, University of California, Berkeley. Magnetic susceptibility measurements were measured on a vibrating-sample magnetometer previously described in the literature.[28] All melting points and boiling points are uncorrected.

cis-Bicyclo[6.3.0]undeca-2,4,6-triene, 17b. -- Under an Ar atmosphere 1.4 g (0.2 mol) of lithium wire (1% sodium) was added to 300 mL of anhydrous liquid ammonia in a 500 mL round bottom flask. To this deep blue solution was added 10.4 g (0.1 mol) of freshly distilled cyclooctatetraene (33°C/ 14 Torr) (BASF), at -40°C, via syringe. The resulting yellow suspension of dianion was stirred for 1.5 h at -40°C followed by dropwise addition (1 drop every 2 seconds) of 20.2 g (0.1 mol) of 1,3-dibromopropane (Aldrich) in 20 mL of ether. The reaction mixture was stirred for 4.5 h at ca. -40°C followed by overnight evaporation of the ammonia affording a red brown

solid which was suspended in 200 mL of saturated ammonium chloride and extracted with ether (4x100 mL). The ether extracts were washed with water (3x100 mL) and dried over $MgSO_4$. Removal of solvent followed by vacuum distillation (25°C/0.1 Torr) yielded 6.83 g (46.8%) of a clear yellow liquid; mass spectrum parent m/e = 156. The ^1H and ^{13}C NMR ($CDCl_3$) of this material indicated that it was a mixture of both the bicyclic and tricyclic valence isomers; bicyclic ^1H NMR ($CDCl_3$): δ 5.80 (s, 6H, vinyl), 2.77 (br m, 1.4H, bridgehead), 1.65 (complex multiplet, 5.3H, cyclopentyl); tricyclic ^1H NMR ($CDCl_3$): δ 5.57 (s, 4H, vinyl), 2.77 and 2.43 (br m, 2H, bridgehead), 1.67 (complex multiplet, 5.3H, cyclopentyl); ^{13}C NMR: see text. After standing for 4 days at room temperature the material had rearranged completely to the tricyclic isomer.

Preparation of 17b from 1,3-bis(methanesulfonyloxy)-propane. -- Following the same procedure but using 23.2 g (0.1 mol) of 1,3-bis(methanesulfonyloxy)propane in 100 mL of THF instead of 1,3-dibromopropane in 10 mL of ether afforded the same product in 54.8% yield.

Preparation of 17b in THF. -- A solution of cyclooctatetraene dianion in THF was prepared by the addition of 0.7 g (0.1 mol) of lithium metal (1% sodium) to an Ar degassed solution of 5.2 g (0.05 mol) of cyclooctatetraene (BASF as supplied) in 400 mL of THF. After stirring for 24 h at room temperature the green solution of dianion was cannulated into

a 1 L round bottom flask and 10.1 g (0.05 mol) of 1,3-dibromopropane (Aldrich) in 20 mL of THF was slowly added dropwise. The reaction was exothermic and to prevent solvent reflux the reaction vessel was immersed in an ice bath. Upon completion of the addition of the dihalide, the reaction mixture changed color from dark green to pale yellow. After stirring for 1 h, the reaction mixture was washed with brine (1x 200 mL) and dried over $MgSO_4$. Removal of solvent followed by reduced pressure distillation gave 4.02 g (63.2%) yield of 17b.

Bicyclo[6.3.0]-1,3,5,7-tetraene potassium, 12. -- Under Ar, a suspension of potassium amide in liquid ammonia was prepared by distilling 300 mL of ammonia from a lithium metal-ammonia solution into a 500 mL round bottom flask containing several mg of anhydrous $FeCl_3$. Subsequent addition of 2.14 g (0.055 mol) of potassium metal at -40°C afforded a blue solution which was stirred (ca. 5 min) until the blue color disappeared indicating formation of the amide. A 4.0 g (0.027 mol) aliquot of 17b was added via syringe and the resulting red brown solution was stirred for 1.5 h at -35°C. The solution was slowly warmed to room temperature and the ammonia was swept out with a steady Ar purge overnight, to afford 4.66 g of the crude dianion as a highly air sensitive grey brown solid; ^1H NMR (THF-d_8): δ 5.67, 1.3, 0.93, broad singlets; ^{13}C (THF-d_8): δ 99.9 (quaternary), 96.9, 89.8, 87.0 (ring), 46.4 (α-CH_2), 27.2 (β-CH_2). No attempt was made to purify this material.

Dicyclopentenouranocene, 10. -- In an Ar atmosphere glove box 2.56 g (0.0068 mol) of UCl_4 in 25 mL of THF was added to a solution of 3.0 g (0.0135 mol) of 12 in 100 mL of THF in a 500 mL round bottom flask, and the resulting green solution was stirred for 18 h. Removal of the solvent by vacuum transfer afforded a green solid which was purified by Soxhlet extraction with hexane; yield 0.57 g (15.9%); mass spectrum, parent peak m/e 526; visible spectrum in hexane, nm ($\varepsilon \times 10^3$) 632 (2.1), 656 (0.9), 663 (0.9), 680 (0.7). See text for NMR and IR data.

1,3-Bis(methylsulfonyloxy)propane. -- To a stirred 0°C solution of 15.22 g (0.2 mol) of 1,3-propanediol (Aldrich), 70 mL (0.5 mol) of triethylamine and 1 L of CH_2Cl_2 in a 2 L round bottom flask was added dropwise 32.5 mL (0.42 mol) of methanesulfonyl chloride (Eastman) over 5 min. The resulting reaction mixture was stirred for 0.5 h during which time a white precipitate formed. After sequential extractions with 200 mL ice water, 200 mL cold 10% HCl, 200 mL saturated sodium bicarbonate and 200 mL brine, the organic layer was dried over $MgSO_4$ and stripped of solvent to afford a white solid which was recrystallized from hot methanol; yield 38.4 g (82.7%); mp 40.5-41.5°C; ^1H NMR ($CDCl_3$): δ 4.37 (t, 4H, $-OCH_2-$), 3.07 (s, 6H, $-CH_3$), 2.19 (p, 2H, $-CH_2-$).

Anal. Calcd for $C_5H_{12}O_6S_2$: C, 25.85; H, 5.21; S, 27.61

Found: C, 26.04; H, 5.26; S, 27.42

1,3-di-Methanesulfonyloxy-2,2-dimethylpropane. -- Over a 5 min period 46.17 g (0.40 mol) methanesulfonyl chloride was added to a stirred solution of 2,2-dimethyl-1,3-propanediol (Aldrich) (20 g, 0.19 mol) and triethylamine (48.57 g, 0.48 mol), in 1 L of CH_2Cl_2 at 0°C. After stirring for 0.5 h at 0°C, during which time a white precipitate formed, the material was extracted with ice water (200 mL) followed by cold 10% HCl (200 mL), saturated sodium bicarbonate (200 mL), and saturated NaCl (200 mL). The organic layer was dried over $MgSO_4$. Removal of solvent afforded white crystals which were recrystallized from hot methanol: yield 42.37 g (84.8%); mp 73-75°C; ^1H NMR ($CDCl_3$): δ 4.00 (s, 4H, CH_2), 3.03 (s, 6H, S-CH_3), 1.07 (s, 6H, C-CH_3).

Anal. Calcd for $C_7H_{16}S_2O_6$: C, 32.29; H, 6.19

Found: C, 32.75; H, 6.38

1,3-di-Methanesulfonyloxy-2,2-dimethylpropane and cyclooctatetraenyl lithium. -- Under an N_2 atmosphere 1.4 g (0.2 mol) of lithium wire (1% sodium) was added to a 500 mL 3-necked round bottom flask containing ca. 300 mL of anhydrous ammonia. The resulting deep blue solution was stirred at 40°C while 10.4 g (0.1 mol) of cyclooctatetraene (BASF as supplied) was added via syringe. After stirring the yellow suspension of dianion for 1 h at -40°C, 26 g (0.1 mol) of 1,3-di-methanesulfonyloxy-2,2-dimethylpropane in 120 mL of THF was added dropwise. The resulting viscous solution was mechanically agitated for 2 h at -40°C before allowing the ammonia to evaporate overnight. Suspension of the solid material in

200 mL ammonium chloride followed by ether extraction (5x 100 mL) and subsequent washing of the combined ether layers with distilled water (3x100 mL) afforded a clear solution which was dried over $MgSO_4$. Reduced pressure removal of the solvent yielded white crystals and an orange oil. An ^1H NMR ($CDCl_3$) of this material indicated it was a mixture of the two starting materials.

1,3-Dibromo-2,2-dimethylpropane. -- Following the procedure of Whitmore, et al.,[16] a 500 mL 3-necked flask fitted with an addition funnel and a reflux condenser was charged with 104.15 g (1.0 mol) of 2,2-dimethyl-1,3-propanediol (Aldrich) and chilled to 0°C by immersion in an ice bath. The addition funnel was charged with 271 g (1.0 mol) of PBr_3 (Matheson, Coleman and Bell) and added slowly over a 2 h period. The addition was accompanied by the evolution of large amounts of HBr. The resulting solution was stirred for 20 h at room temperature followed by heating to 140°C for 18 h. Upon cooling, the tarry material was poured onto 200 mL of crushed ice. Steam distillation afforded 90 mL of crude material which was fractionally distilled through a 1 cm x 25 cm jacketed column. The desired product was collected at 63-66°C/10 Torr (lit.[16] 84°/28 Torr) as a colorless liquid. Yield 79.2 g, 34.4%; ^1H NMR ($CDCl_3$): δ 3.40 (s, 4H, CH_2), 1.17 (s, 6H, CH_3).

10,10-Dimethyl-cis-bicyclo[6.3.0]undeca-2,4,6-triene, 18. -- Under an Ar atmosphere, 2.1 g (0.30 mol) of lithium wire (1% sodium) was added to ca. 300 mL of anhydrous liquid ammonia in

a 500 mL round bottom flask. To this deep blue solution was added 15.6 g (0.15 mol) of cyclooctatetraene (BASF as supplied) at -40°C via syringe. The resulting yellow suspension of dianion was stirred for 0.5 h at -40°C followed by the dropwise addition of 34.5 g (0.15 mol) of 1,3-dibromo-2,2-dimethylpropane in 20 mL of ether. The reaction mixture was stirred for 4.5 h at ca. -40°C followed by overnight evaporation of the ammonia affording a brown solid which was suspended in 200 mL of saturated ammonium chloride and extracted with ether (3x100 mL). The ether extracts were washed with water (3x100 mL) and dried over $MgSO_4$. Removal of solvent followed by two vacuum distillations (40-46°C/0.3 Torr) yielded 15.4 g (58.9%) of a pale yellow oil; mass spectrum parent peak m/e = 174 (5%); ^{1}H NMR ($CDCl_3$): δ 5.77 and 5.60 (6H, vinyl), 2.65 (br m, 4H, bridgehead), 1.58 (br t, 4H, methylene), 1.13 and 0.78 (s, 6H, methyl). See text for ^{13}C NMR.

Anal. Calcd for $C_{13}H_{16}$: C, 89.59; H, 10.41

Found: C, 89.34; H, 10.53

10,10-Dimethyl bicyclo[6.3.0]undeca-1,3,5,7-tetraene potassium, 13. -- Following the procedure for the preparation of 12, reaction of 4.8 g (0.028 mol) of 18 afforded 6.89 g of the crude dianion as a highly air sensitive brown solid; ^{1}H NMR (THF-d_8): δ 5.58, 3.35, 1.20 broad singlets; ^{13}C NMR (THF-d_8): δ 98.9 (quaternary), 90.8, 90.1, 87.6 (ring), 61.0 (α-methylene), 30.0 (methyl). No attempt was made to purify this material).

Bis(dimethylcyclopenteno)uranocene, 11. -- In the glove box, a solution of 2.58 g (6.8 mmol) of UCl_4 in 15 mL THF was slowly added to 3.41 g (13.6 mmol) of 13 in 150 mL of THF in a 500 mL uranocene reactor. After stirring for 3 days, the solvent was removed by vacuum transfer affording a silver grey powder which was washed with hot hexane. The green extract was centrifuged and stripped of solvent to give 0.277 g (7%) of an emerald green solid. See text for characterization.

REFERENCES

1) J. A. Elix, M. V. Sargent and F. Sondheimer, J. Am. Chem. Soc., 89, 160 (1967).

2) J. A. Elix, M. V. Sargent and F. Sondheimer, J. Am. Chem. Soc., 92, 962 (1970).

3) S. W. Staley, G. M. Cramer and A. W. Orvedal, J. Am. Chem. Soc., 96, 7433 (1974).

4) S. W. Staley and T. J. Henry, J. Am. Chem. Soc., 92, 7612 (1970).

5) S. P. Berryhill, Ph.D. Thesis, UC Berkeley (1977).

6) A. Streitwieser, Jr. and C. A. Harmon, Inorg. Chem., 12, 1102 (1973).

7) W. T. Scroggins, M. F. Rettig and R. M. Wing, Inorg. Chem., 15, 1381 (1976).

8) A. Streitwieser, Jr., D. Dempf, G. N. La Mar, D. G. Karraker and N. Edelstein, J. Am. Chem. Soc., 93, 7343 (1971).

9) L. A. Paquette, R. E. Wingard, Jr. and R. H. Meisinger, J. Am. Chem. Soc., 93, 1047 (1971).

10) L. A. Paquette and R. E. Wingard, Jr., J. Am. Chem. Soc., 94, 4398 (1972).

11) L. A. Paquette, J. M. Photis, J. Fayos and J. Clardy, J. Am. Chem. Soc., 96, 1217 (1974).

12) L. A. Paquette, R. E. Wingard, Jr. and J. M. Photis, J. Am. Chem. Soc., 96, 5801 (1974).

13) L. A. Paquette, S. V. Ley, R. H. Meisinger, R. K. Russel and M. Oku, J. Am. Chem. Soc., 96, 5806 (1974).

14) L. A. Paquette, R. H. Meisinger and R. E. Wingard, Jr., J. Am. Chem. Soc., 95, 2230 (1973).

15) F. A. Cotton and G. Deganello, J. Am. Chem. Soc., 94, 2142 (1972).

16) "Reduction Techniques and Applications in Organic Synthesis", R. L. Augustine, Ed., Marcel Decker, Inc., New York (1968).

17) F. C. Whitmore, A. H. Popkin, H. J. Bernstein and J. P. Wilkins, J. Am. Chem. Soc., 63, 124 (1941).

18) D. G. Karraker, J. A. Stone, E. R. Jones, Jr. and N. Edelstein, J. Am. Chem. Soc., 92, 4841 (1970).

19) J. F. Monthony and W. H. Okamura, Tet., 28, 4273 (1972).

20) A. Zalkin, D. H. Templeton, S. R. Berryhill and W. D. Luke, Inorg. Chem., in press.

21) A. Zalkin, D. H. Templeton, W. D. Luke and A. Streitwieser, Jr., submitted for publication.

22) K. O. Hodgson and K. N. Raymond, Inorg. Chem., 12, 458 (1973).

23) L. K. Templeton, D. H. Templeton and R. Walker, Inorg. Chem., 15, 3000 (1976).

24) A. Zalkin and K. N. Raymond, J. Am. Chem. Soc., 91, 5667 (1969).

25) A. Haaland, Fortschitt der Forchung, 53, 1 (1975) and references therein.

26) M. Elian, M. M. L. Chen, D. M. P. Mingos and R. Hoffman, Inorg. Chem., 15, 1148 (1976).

27) N. Rösch and A. Streitwieser, Jr., J. Organomet. Chem., 145, 195 (1978).

28) N. Edelstein, A. Streitwieser, Jr., D. G. Morrell and R. Walker, Inorg. Chem., 15, 1397 (1976).

29) L. Hocks, J. Goffart, G. Duyckaerts and P. Teyssié, Spectrochimica. Acta., 30A, 907 (1974).

Chapter 3 THE NMR OF ALKYL SUBSTITUTED URANOCENES

I. INTRODUCTION AND HISTORICAL BACKGROUND

In the past several years a substantial amount of work has been devoted toward evaluation of the contact and pseudo-contact contributions to the observed isotropic shifts in the ^1H nuclear magnetic resonance (NMR) spectra of uranium(IV) organometallic compounds.[1-14,58] One reason for interest in this area arises from using the presence of contact shifts as a probe for covalent character in the uranium carbon bonds in these compounds. Several extensive ^1H NMR studies on Cp_3U-X compounds[10-13] and less extensive studies on uranocenes have been reported.[5,6,14,58] Interpretation of these results suggests that contact shifts contribute significantly to the observed isotropic shifts. Their presence has been taken as indicative of covalent character of metal carbon bonds in these systems, but agreement is not complete.[2] In this paper we shall critically review the work reported on uranocenes in the light of recent results and report recent work on attempted separation of the observed isotropic shifts in alkyluranocenes into contact and pseudo-contact components.

A) THEORY

A detailed derivation of the theory behind paramagnetic

shifts in the NMR of paramagnetic compounds, or a complete review of the literature concerning separation of observed isotropic shifts into contact and pseudocontact components is well beyond the scope of this paper. Several books and reviews of these subjects are available.[15-20] Instead, to provide the reader with a sufficient understanding of this area to follow the analysis in the following sections, we shall briefly outline the basic principles which give rise to the contact and pseudocontact components of the isotropic shift.

Comparison of different theoretical and experimental work in the literature is somewhat confusing for three reasons: 1)the use of two different systems for defining the sign of NMR shifts relative to the absolute reference standard tetramethylsilane (TMS); 2)the use of different symbols and different nomenclature by different authors; 3)a tendency by European authors, in reporting the temperature dependence of isotropic shifts, to plot isotropic shift^{-1} vs T while other workers plot the inverse, isotropic shift vs T^{-1}.

To alleviate some of these problems, we shall use the modern system for defining the sign of ^{1}H and ^{13}C NMR shifts which defines all shifts upfield from TMS as negative and all shifts downfield from TMS as positive, rather than the older system which assigns the ^{1}H NMR shifts exactly opposite. All of the equations reported will reflect this sign convention. Further, the same symbols will be used for the same terms in all equations, and thus, some of the equations

may not appear as they do in the literature.

The presence of a paramagnetic metal in organometallic compounds significantly influences the NMR spectrum of ligand nuclei. Changes in nuclear relaxation times and changes in resonance frequency are the two principal effects arising from interaction between the unpaired electrons on the metal and ligand nuclei. Nuclear relaxation times are shortened due to increased spin-spin relaxation and result in increased linewidths of the resonance signals. In some compounds this broadening of the resonance signals is large enough to preclude their observation.

Shifts in the resonance frequency of nuclei in a paramagnetic environment from where they normally occur in a corresponding diamagnetic environment, are generally of greater chemical interest. These shifts arise from changes in the effective magnetic field at the resonating nuclei. Unpaired electrons interact with nuclei through magnetic coupling. To a first approximation, one can imagine that by such coupling the electron produces an effective magnetic field at the nucleus. This field is composed of two distinct components which can be qualitatively understood by viewing the electron separately as a classical dipole and as a wave. One magnetic field is generated by a classical dipole-dipole interaction between the electron magnetic moment and the nuclear magnetic moment. This field is geometry dependent and averages to zero if one averages the direction between the electron and the nucleus over a sphere. The second

field is directly proportional to the probability of finding the electron, or excess electron spin density, at the nucleus, and has no angular dependence. For a given nucleus, the observed shift in resonance frequency resulting from the combination of these induced magnetic fields is called the hyperfine isotropic or isotropic shift. We shall refer to it as the isotropic shift.

In the absence of a magnetic field, the unpaired electron(s) in a paramagnetic compound point in all directions with equal probability and the average magnetic moment at the nucleus is zero. However, in the presence of a strong magnetic field, the electron magnetic moment is constrained to exist in either of two states; a lower energy state where the moment is aligned with the applied field and a higher energy state where it is opposed to the applied field. If the electron oscillates rapidly between the states, the average magnetic moment will not be zero since the two states are not equal in energy. The lower energy state will have a slightly greater population and the electronic system is said to be magnetized. Likewise, the average electron-induced magnetic field at a nucleus is non-zero but proportional to the applied field, and thus, contributes to the chemical shift. This induced field can either be aligned or opposed to the applied field depending upon how the spin density is transferred from the metal to the nucleus. Hence, it decreases or reinforces the applied field at the nucleus and shifts the resonance frequency. This shift is called the hyperfine contact, Fermi contact, or contact shift. We shall refer

to it as the contact shift.

In normal NMR experiments with liquids or solutions where the observed molecules tumble rapidly, the magnetic field due to the dipole-dipole interaction would average to zero if the electronic moment was due entirely to electron spin. However, both orbital angular momentum and the spin moment contribute to the total electronic moment. Thus, the electron magnetic moment may depend upon the angle the applied field makes with fixed directions in the molecule. As the molecule tumbles, the magnetization of the electronic system may vary and hence, the dipolar contribution to the induced magnetic field at a given nucleus will no longer average to zero. Like the contact component this induced field is proportional to the applied field and causes a shift in the resonance frequency. This shift is called the dipolar or pseudocontact shift from its similar behavior to the contact shift. We shall refer to it as the pseudocontact shift.

1) CONTACT SHIFT

In paramagnetic organometallic systems where ligand exchange does not occur, NMR spectra can be observed when $T_{1e} >> A_i$, where T_{1e} is the electronic relaxation time, and A_i is the hyperfine coupling constant. Under such conditions, McConnell and Chestnut[21] derived an expression for the contact shift Hamiltonian, which shows that the average

induced field at each nucleus is proportional to $A_i\langle S_z\rangle$, where $\langle S_z\rangle$ is the expectation value of the z component of the total electron spin. Expressions for the contact shift derived using this Hamiltonian operator vary depending upon what assumptions are used in evaluating $\langle S_z\rangle$. The most common form is

$$\delta_{CONTACT} = \frac{A_i g_e^2 \beta_e^2 S(S+1)}{3 g_N \beta_N kT} \qquad (1)$$

where g_e is the rotationally averaged electronic g value, β_e is the Bohr magneton, g_N and β_N are the corresponding nuclear constants and S is the spin of the unpaired electrons. McConnell and Chestnut[21] derived eq. 1 by assuming: a) neglect of orbital contributions to the electronic moment; b) only population of the ground state; c) the magnetic behavior of the complex follows the Curie Law, which permitted evaluation of $\langle S_z\rangle$ using the high temperature limit approximation.

For many organometallic complexes, orbital effects cannot be neglected. Golding[22] has included such spin-orbit coupling in deriving expressions for the contact shift in octahedral complexes.

The further restriction of only one populated state, the ground state, has been removed in a comprehensive derivation of a general expression for the contact shift by Kurland and McGarvey.[19] The contact shift averaged over all

molecular conformations is

$$\delta_{CONTACT} = \frac{\sum_{\alpha=x,y,z} \sum_{n} \left(\frac{b^{\circ}_{n\alpha} E^{(1)}_{n\alpha}}{kT} - b^{(1)}_{n\alpha} \right) \exp\left(\frac{-E_n^{\circ}}{kT} \right)}{3 g_N \beta_N \sum_{n} \exp \frac{-E_n^{\circ}}{kT} - 1} \tag{2}$$

where

$$E^{(1)}_{n\alpha} = \beta \langle \psi_n^{\circ} | (L_\alpha + g S_\alpha) | \psi_n^{\circ} \rangle \tag{3}$$

$$b^{\circ}_{n\alpha} = \langle \psi_n^{\circ} | \hat{H}_F(\alpha) | \psi_n^{\circ} \rangle \tag{4}$$

$$b^{(1)}_{n\alpha} = \beta \sum_{m \neq n} [\langle \psi_n^{\circ} | \hat{H}_F(\alpha) | \psi_m^{\circ} \rangle \langle \psi_m^{\circ} | (L_\alpha + g S_\alpha) | \psi_n^{\circ} \rangle + \langle \psi_o^{n} | (L_\alpha + g S_\alpha) | \psi_m^{\circ} \rangle \langle \psi_m^{\circ} \hat{H}_F(\alpha) | \psi_n^{\circ} \rangle] (E_n^{\circ} - E_m^{\circ})^{-1} \tag{5}$$

$$\hat{H}_F = \frac{8\pi}{3} g_e \beta_e g_N \beta_N \sum_i \hat{\delta}(\hat{r}_i) S_i \tag{6}$$

and ψ is the wave function governing the distribution of the unpaired electrons at the nucleus, $\hat{i}(\hat{r}_i)$ expresses the probability density for the electron at the i^{th} nucleus and L and S have their usual meaning in terms of orbital and spin angular momentum. McGarvey[23] has shown that eq. 2 can be expressed as the sum of two terms, one first order and the other second order in T^{-1}. In most instances this latter term is sufficiently small that it can be neglected. However, the contact shift may not necessarily display a linear dependence (i.e., Curie Law behavior) on T^{-1} as implied by eq. 1.

Since eq. 2 is a general expression, it contains more parameters than are usually necessary to describe the contact shift in most paramagnetic systems. Consequently, several simplified forms more suited to individual systems are encountered in the literature. For molecules where all of the thermally accessible states belong to the same spin level, eq. 2 reduces to

$$\delta_{CONTACT} = \frac{A_i g_e}{3 g_N \beta_N} \left[\frac{X_x}{g_x} + \frac{X_y}{g_y} + \frac{X_z}{g_z} \right] \qquad (7)$$

where X_z, X_y, X_x are the principal components of the magnetic susceptibility tensor and g_z, g_y, and g_x are the principal components of the g tensor. Equation 7 reduces to eq. 1 in the absence of zero field splitting and ground state orbital angular momentum.

In axially symmetric systems where the zero field

splitting tensor, D, is isotropic and small relative to kT, Kurland and McGarvey[19] have shown that the contact shift will not differ significantly from that predicted by eq. 1. This apparently accounts for the behavior of a large number of transition metal complexes.

For lanthanide and actinide complexes where the crystal field splitting is much smaller than the separation between states, and hence J is a good quantum number, the form eq. 2 reduces to depends upon the relative separation of the crystal field levels and kT. If the separation between crystal field levels is less than kT, as for the lanthanides,[24,25] eq. 2 becomes

$$\delta_{CONTACT} = \frac{A_i(g_J-1)g_J\beta_e J(J+1)}{3g_N\beta_N kT} \qquad (8)$$

For actinides,[12] where this separation is large relative to kT, eq. 2 becomes

$$\delta_{CONTACT} = \frac{A_i(g_J-1)X}{Ng_J\beta_e g_N\beta_N} \qquad (9)$$

2) PSEUDOCONTACT SHIFTS

The possibility of pseudocontact contributions to the total isotropic shift was originally proposed by Bloembergen and Dickinson.[26] Assuming that the distance between the observed nucleus and the paramagnetic center is sufficiently

large, the interaction between the electronic moment and the nuclear spin can be approximated as a point-dipole interaction (i.e., point dipole approximation). Thus, McConnell and Robertson[27] showed that the pseudocontact shift at the i^{th} nucleus can be expressed as

$$\delta_{PSEUDOCONTACT} = DG_i + D'G_i' \qquad (10)$$

where G_i and G'_i are geometry factors relating the spatial arrangement of the paramagnetic center and the i^{th} nucleus, and D and D' are algebraic terms which are functions of the magnetic properties of the complex. The two geometric factors, G_i and G'_i, are independent of the symmetry of the complex and are given by

$$G_i = \frac{3\cos^2\theta - 1}{R^3} \qquad (11)$$

$$G'_i = \frac{\sin^2\theta\cos 2\psi}{R^3} \qquad (12)$$

where R, θ, and ψ are the spherical coordinates of the i^{th} nucleus in a coordinate system centered at the metal atom with the z axis colinear with the principal molecular axis (Fig. 3-1).

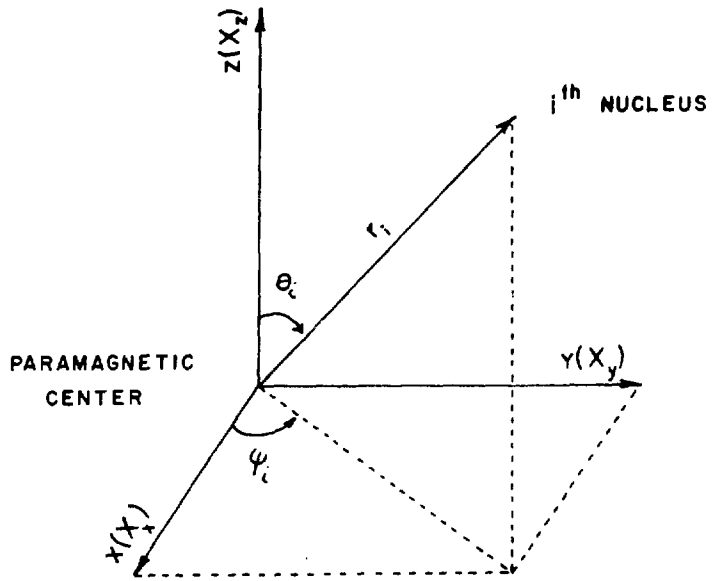

Fig. 3-1 Coordinates R_i, θ_i, and ψ_i of a nucleus i in the coordinate system x, y, z, with the three principal components X_x, X_y, X_z of the magnetic susceptibility.

In their original work, McConnell and Robertson considered only axially symmetric systems where, by symmetry, D' is zero, and thus, the second term in eq. 9 is zero. Originally, D was assumed to be a function of the correlation time for molecular tumbling, t_c, the electron relaxation time, T_{1e}, and the symmetry of the compound. Assuming: a)the g tensor is always axially symmetric; b)only the ground state is populated; c)zero field splitting can be ignored; d)orbital contributions can be accounted for through the use of g tensor components; e)$T_{1e} >> t_c$; the expressions for D in the

the two limiting cases of $1/t_c << |g_{\parallel}-g_{\perp}|bH/\hbar^{-1}$, the solid state case, and $1/t_c >> |g_{\parallel}-g_{\perp}|bH/\hbar^{-1}$, the liquid state, are given by

$$\text{SOLID } D = (g_{\parallel}^2-g_{\perp}^2)\frac{\beta^2 S(S+1)}{9kT} \tag{13}$$

$$\text{LIQUID } D = (g_{\parallel}+2g_{\perp})(g_{\parallel}-g_{\perp})\frac{\beta^2 S(S+1)}{27kT} \tag{14}$$

Since contact shifts are the same regardless of phase, eq. 13 and 14 show that for a given nucleus, the solid/solution ratio of pseudocontact shifts would be $3(g_{\parallel}+g_{\perp})/(g_{\parallel}+2g_{\perp})$. In principle, this provides an experimental criterion for distinguishing between pseudocontact and contact shifts. This criterion has been used by Holm[28] in showing that contact shifts contribute to the isotropic shift in vanadocene.

Jesson,[29] in work on axially distorted octahedral cobalt (II) complexes, extended the initial work of McConnell and Robertson to include axial systems with ground states of well separated Kramer's doublets. Four possible limiting cases were considered: a) $1/t_c << |g_{\parallel}-g_{\perp}|bH/\hbar^{-1}$, $T_{1e} << t_c$; b) $1/t_c << |g_{\parallel}-g_{\perp}|bH/\hbar^{-1}$, $T_{1e} >> t_c$; c) $1/t_c >> |g_{\parallel}-g_{\perp}|bH/\hbar^{-1}$, $T_{1e} << t_c$; d) $1/t_c >> |g_{\parallel}-g_{\perp}|bH/\hbar^{-1}$, $T_{1e} >> t_c$; and expressions for D were derived for each case. Subsequently, Vega and Fiat[30] have shown that the pseudocontact shift is independent of t_c and T_{ie}, and D is accurately given by eq. 13.

Horrocks[31-33] has pointed out that treatment of systems

with several populated energy levels using g tensors is inaccurate, since it neglects Van Vleck paramagnetism arising from second order Zeeman terms. In terms of principal magnetic susceptibility components

$$D = \frac{1}{3N} [X_x - 1/2\ X_y - 1/2\ X_z] \qquad (15)$$

$$D' = \frac{1}{2N} [X_x - X_y] \qquad (16)$$

Kurland and McGarvey[19] have shown that the total pseudocontact interaction consists of two components, one resulting from unpaired electrons in orbitals centered on the metal, and the other from unpaired electrons in orbitals centered on the nucleus under observation. The general expression for the total pseudocontact shift is similar in form to eq. 6 where $\hat{H}_F$ is replaced by the Hamiltonian operators which account for the interaction between the unpaired electrons and the nuclear spin, and the operator which accounts for the electron orbital angular momentum interaction.

For ^1H NMR shifts, where the unpaired spin density at the observed nucleus resides in a s orbital, contributions to the pseudocontact shift rising from unpaired electrons in ligand orbitals are essentially zero and can be neglected.

Using the point dipole approximation, the contribution to the pseudocontact shifts arising from unpaired electrons on the metal is given by

$$\delta_{PSEUDOCONTACT} = \frac{(X_z - 1/2(X_x+X_y))}{3N}\left[\frac{3\cos^2\theta-1}{R^3}\right] + \frac{(X_x-X_y)}{2N}\left[\frac{\sin^2\theta\cos 2\psi}{R^3}\right] \quad (17)$$

which is identical to the expression derived by Horricks (i.e., eq. 11,12,15,16). Since X does not necessarily display Curie Law dependence, the pseudocontact shift may not be a linear function of T^{-1}.

If only one thermally populated multiplet with spin S is considered and zero field splitting is ignored, then susceptibility components can be replaced by the corresponding g factors

$$X_\alpha = \frac{g_\alpha^2 \beta_e^2 S(S+1)}{3kT} \quad (18)$$

For small zero field splitting relative to kT ($D \gg kT$), Kurland and McGarvey[19] have shown that the pseudocontact shift expression, eq. 17, can be expanded in terms of g factors into first and second order terms. The first order term has the form of eq. 17, and the second order term is a function of T^{-2}. The contribution of this second order term will be much larger than the second order term for contact shifts, and thus, nonlinearity in the temperature dependence of isotropic shifts is expected to arise principally from pseudocontact interactions.

In work on lanthanide complexes, Bleaney[34] has developed an expression for the pseudocontact shift in terms of the zero field tensor D.

$$\delta_{PSEUDOCONTACT} = K[D_z \frac{3\cos^2\theta-1}{R^3} + (D_x-D_y) \frac{\sin^2\theta\cos 2\psi}{R^3} \quad (19)$$

$$K = \frac{g_e^2\beta_e^2 J(J+1)(2J-1)(2J+3)}{60(kT)^2} \quad (20)$$

These equations predict a T^{-2} dependence for the shift, which a variety of experimental studies have verified.[18] However, Bleaney's work has been criticized by several authors[35,36] who suggest the temperature dependence of isotropic shifts in lanthanide complexes should be more complex than just first or second order.

Recently, McGarvey[37] has extended Bleaney's analysis to include a T^{-3} term. Using crystal field parameters reported in the literature, McGarvey showed that the magnitude of the T^{-3} term is no more than 10% of the magnitude of the T^{-2} term at room temperature for all systems where Bleaney's theory is applicable, and thus, the T^{-3} term can be effectively neglected in calculating shifts at room temperature.

Buckingham and Stiles[38,39] have discussed the effects of nuclear multipoles on the pseudocontact shift. They conclude that a quadrupolar contribution to the pseudocontact shift may be on the order of 10% at a distance of 5 A in a complex lacking a center of inversion but only ca. 1% in centrosymmetric complexes.

For complexes where eq. 17 is applicable, both Huber[40] and Briggs and co-workers[41] have shown that the pseudocontact shift is given by

$$\delta_{PSEUDOCONTACT} = K \frac{3\cos^2\theta - 1}{R^3} \qquad (21)$$

where K is a function of D and D', even if $X_{||}$ is not colinear with the metal substituent bond axis, provided that the barrier to rotation about the bond is 3-fold or greater.

3) FACTORING OF ISOTROPIC SHIFTS

Interest in the NMR of paramagnetic organometallic complexes centers around the information derivable from the contact and pseudocontact components of the isotropic shift. Ideally, if contact shifts are lacking, the observed isotropic shift will be solely geometric dependent and can be used in structural and conformational studies. This is the basic principle behind the use of lanthanide shift reagents. The presence or lack of contact shifts provides information on ligand-metal bonding. If contact shifts are lacking, this implies no ligand metal orbital overlap or a totally ionic bond. Similarly, the presence of contact shifts is indicative of ligand metal orbital overlap and some degree of covalency in ligand metal bonds.

The methods employed in factoring observed isotropic shifts into contact and pseudocontact components can be classified into two broad categories: ratio methods and computational methods.

a.) RATIO METHODS

Several types of ratio method studies have been reported. Horrocks, et al.,[32] have proposed the following approach for determining pseudocontact shifts. If two series of isomorphous compounds exist which have identical modes of spin delocalization, but differ in their central metal ions, one magnetically isotropic (i.e., no pseudocontact shift) and the other magnetically anisotropic, the ratio of contact shifts between two nuclei in one series should equal the ratio of contact shifts between the same nuclei in the second series. This is expressed in eq. 22 where x is the isotropic species and y is the anisotropic species.

$$\frac{\delta_{y\ \mathrm{CONTACT(i)}}}{\delta_{y\ \mathrm{CONTACT(j)}}} = \frac{\delta_{x\ \mathrm{CONTACT(i)}}}{\delta_{x\ \mathrm{CONTACT(j)}}} = \frac{\delta_{y\ \mathrm{ISOTROPIC(i)}} - \delta_{y\ \mathrm{PSEUDOCONTACT(i)}}}{\delta_{y\ \mathrm{ISOTROPIC(j)}} - \delta_{y\ \mathrm{PSEUDOCONTACT(j)}}} \qquad (22)$$

Thus, the pseudocontact shift in a given complex can be expressed in terms of the shift for a particular nucleus and the known ratio of geometry factors, between the i^{th} and j^{th} nucleus. This approach has been applied to a parallel series of magnetically isotropic six-coordinate nickel (II) and magnetically anisotropic cobalt (II) complexes.[42,43]

Both Pinkerton, et al.,[44] and Dobson, et al.,[45] have employed a similar approach in analysis of contact shifts in lanthanide complexes. Using isomorphous lanthanide complexes, the ratio of shifts for two different protons was compared while changing the lanthanide ion. If no

contact shifts were present, the ratio should remain constant regardless of the metal ion.

b.) COMPUTATIONAL METHODS

For most systems of interest, two series of isomorphous compounds which fulfill the requirements implicit in the ratio method are not available. Thus, factoring of the observed isotropic shift is achieved by calculating either the contact or the pseudocontact shift from magnetic or spectroscopic data and one of the equations presented previously. Generally, one is interested in deducing the presence of contact shifts, and thus, the pseudocontact shift is calculated. Such calculation requires solution structure geometric data and magnetic anisotropy data. Geometric data can usually be estimated with a high degree of accuracy from solid state x-ray diffraction data. On the other hand, magnetic susceptibility data along ordered axes in single crystals are rare. In most cases, values for X_x, X_y, and X_z are derived from crystal field models for the electronic structure of the complex, which model the readily available bulk susceptibility data. Most of the literature reports on factoring of isotropic shifts involve use of the computational method. Several comparisons of the two methods have appeared and the agreement appears to be quite good.[18,43]

B) NMR OF URANIUM (IV) ORGANOMETALLIC COMPOUNDS

Current interest in the NMR of U(IV) organometallic compounds has been concerned with the relative contributions of contact and pseudocontact shifts to the observed isotropic shifts. Much of this interest arises from the possible presence, and relative role of covalency in ligand metal bonds in organoactinide compounds. Ideally, if the isotropic shifts in U(IV) compounds can be factored into contact and pseudocontact components, the contact shift can be correlated with electron delocalization and bond covalency.

From an experimental point of view, the ^1H NMR spectra of U(IV) compounds are ideally suited to such analysis. In general, the isotropic shifts are less than ± 100 ppm, which is small compared to shifts observed in many transition metal complexes. The linewidths for protons on carbons directly bonded to uranium are less than 50 Hz and rapidly decrease for protons on carbons not directly bonded to the metal atom, so that J-J coupling is often observed. A review of early work on the ^1H NMR spectra of U(IV) compounds appeared in 1971.[7]

1) TRISCYCLOPENTADIENYL URANIUM (IV) COMPOUNDS

The ^1H NMR resonance of the cyclopentadienyl ligand in Cp_4U is shifted -19.27 ppm upfield from the corresponding resonance in diamagnetic Cp_4Th at room temperature. Interpretation of unpublished data on the temperature dependence

of the magnetic moment led Fischer, von Amnon, and Kanellakopulos[1] to propose that the observed paramagnetism of Cp_4U arises from a low lying triplet state slightly above a diamagnetic ground state. If in both states the unpaired electrons are strongly localized on the metal and if the complex is of tetrahedral symmetry, then by symmetry the magnetic susceptibility must be isotropic. Thus, they proposed that the observed isotropic shift in the ^1H NMR spectrum arises from a purely contact type interaction.

Siddall, Stewart and Karraker[2] have objected to this proposal, arguing that both the magnitude and the sign of isotropic shifts in uranium (IV) acetylacetonate complexes can only be accounted for by substantial pseudocontact contributions to the isotropic shift. By inference, pseudocontact shifts were suggested to be present in Cp_4U.

In rebuttal, Fischer, von Amnon, and Kanellakopulos[4] have pointed out that if, from the point of view of the f-electrons, the complex is tetrahedral, then the g tensor and the magnetic susceptibility must be isotropic. A subsequent x-ray crystal structure has confirmed the tetrahedral structure of Cp_4U.[49,50]

The temperature dependent behavior of the isotropic shift of Cp_4U is a linear function of T^{-1} from -106°C to 153°C.[4,10] Unfortunately, the data are reported in a plot of the inverse of the isotropic shift vs. T. Extrapolation of T to infinity leads to an intercept of ca. $-0.0025\ ppm^{-1}$. While Curie Law behavior predicts an intercept of zero, the significance of this difference cannot be as easily accounted

for in this type of plot as in plots of shift vs T^{-1}. The linear inverse temperature dependence implies that the compound possesses high symmetry with no low lying excited states. This is in direct contrast to the original report of Fischer et al.,[1] on the magnetic properties of this complex, and one is forced to believe that the earlier work is in error.

Since this initial analysis, a wide variety of Cp_3U-X compounds have been prepared and extensive studies on their ^1H NMR spectra have been reported. Some confusion exists in comparing the isotropic shifts reported in the literature. Some shifts are reported referenced relative to various solvents while others are referenced relative to the corresponding thorium compound instead of the universal standard TMS. To facilitate comparison the reported shifts have been referenced to TMS and are recorded in Table 3-1.

Table 3-1

The ^1H NMR Resonances of Cp_3U-X Compounds

δ ppm from TMS

	X		Temp	Solvent	Ref.
1	Cp	-13.96	25	THF	10,1,7
2	F	-6.46	25	Benzene	10,46,7
3	Cl	-3.40	25	Benzene	10,46,13,7
4	Br	-3.65	25	Benzene	10,46,7
5	I	-4.28	25	Benzene	10,46,7
6	BH_4	-6.53	25	Benzene	3,7

	X		Temp	Solvent	Ref.
7	C_6H_5	-3.26	25	Benzene	47,12
8	CH_3	-2.76 -194.76(CH_3)	25	Benzene	12
9	n-C_4H_9	-3.06 -11.46(CH_3) -20.36(γ) -26.36(β) -192.76(α)	25	Benzene	12
10	i-C_3H_7	-3.66 -12.06(CH_3) -182.76(H)	25	Benzene	12
11	t-C_4H_9	-4.16 -15.96(CH_3)	25	Benzene	12
12	neopentyl	-4.36 -14.86(CH_3) -184.76(CH_2)	25	Benzene	12
13	allyl	-2.76 -30.96(CH) -118.76(CH_2)	25	Benzene	12
14	vinyl	-2.06 31.64(β-trans) -9.76 (β-cis) -156.36(α)	25	Benzene	12
15	cis-2-butenyl	-3.36 -12.56(α-CH_3) -15.36(H) -35.06(β-CH_3)	25	Benzene	12
16	trans-2-butenyl	-3.46 30.74(H) -25.76(β-CH_3) -26.36(α-CH_3)	25	Benzene	12
17	C_6F_5	-3.66	25	Benzene	12
18	OCH_3	-17.06 52.54(CH_3)	RT	Benzene	48,7
19	OC_2H_5	-18.36 59.04(OCH_2) 16.84(CH_3)	RT	Benzene	48,7
20	O-n-C_4H_9	-17.86 57.84(OCH_2) 17.04(δ) 8.94(γ) 4.58(CH_3)	RT	Benzene	48,7
21	O-i-C_3H_7	-18.56 121.94(OCH_2) 17.84(CH_3)	RT	Benzene	48,7
22	O-t-C_4H_9	-19.36 19.64(CH_3)	RT	Benzene	48,7
23	n-hexyloxy	-17.0 56.9(α) 16.69(β) 8.80(γ) 5.08(δ) 2.57(ε) 1.67(ρ)	RT	Benzene	11
24	cyclohexyloxy	-18.3[a] 122.0(α) 19.0(β) 17.0(β) 10.2(γ) 9.8(γ) 7.5(δ)	30	Benzene	11
25	cholesteryloxy	-17.7[a,b]	30	Benzene	11

[a]extrapolated from spectrum reported in re 11. [b]See ref. 11 for substituent proton resonances

Assuming axial symmetry along the U-X bond, the isotropic shifts for compounds 3, 7-16 and 25- have been factored into contact and pseudocontact components. In the rigid cholesteryloxy ligand, 25, Fischer and co-workers[11] showed the ratio of the geometry factors $(3\cos^2-1)/R^3$ for the A-ring protons in the β and γ-positions to be equal to the ratio of the isotropic shifts, whereas gross deviations occurred when the α-positions were compared. This implies that all of the isotropic shifts except those in the α-position arise purely from pseudocontact-type interactions, whereas both pseudocontact and contact interactions contribute to the α-proton isotropic shifts. From eq. 23-25 the isotropic

$$\delta(\gamma) \approx \delta_{\text{PSEUDOCONTACT}}(\gamma) \tag{23}$$

$$\delta_{\text{PSEUDOCONTACT}}(\alpha) = \delta_{\text{ISOTROPIC}}(\gamma) \frac{G(\alpha)}{G(\gamma)} \tag{24}$$

$$\delta_{\text{CONTACT}}(\alpha) = \delta_{\text{ISOTROPIC}}(\alpha) - \delta_{\text{PSEUDOCONTACT}}(\alpha) \tag{25}$$

shifts were factored into contact and pseudocontact components. Taking the average geometry factor, (G_r), for the ring protons as -5.49×10^{-22} cm^{-3}, the calculated pseudocontact and contact shifts at room temperature are -6.4 ppm and -17.6 ppm, respectively. The approximate invariance of the ring proton isotropic shifts in all of the alkoxy substituted compounds suggests that there is no great fluctuation in the molecular anisotropy throughout this series.

Marks and co-workers[12] have studied the alkyl substituted compounds 7-16. Assuming that INDO/2 molecular orbital calculations on alkyl radicals can reasonably predict experimental electron-nuclear hyperfine coupling constants, a_i, they have calculated the a_i values for each of the alkyl substituents. Taking the ratio of the contact shifts of the ortho positions in 7 and vinylic position in 16 as equal to the ratio of calculated a_i values, and the ratio of the geometry factors as equal to the ratio of pseudocontact shifts, Marks and co-workers could solve for the contact and pseudocontact shifts in 7 and 16. Factoring the isotropic shifts in the remaining members of the series was effected by assuming that the pseudocontact shifts are all proportional to the corresponding geometry factors. Agreement between the calculated shifts and a_i values was fair, and, in general, the contact shifts were less than 50 ppm. For the ring protons an average geometry factor of -7.97×10^{-22} cm^{-3} was used to calculate a pseudocontact shift of 19.1 ppm and a contact shift of -28 ppm. While this contact shift is similar in magnitude to that calculated for the alkoxy compounds, the calculated pseudocontact shifts for the two series are opposite in sign. This implies that the replacement of -OR by -R caused a reversal of sign in the magnetic anisotropy term of eq. 17, (i.e., $X_{\parallel}-X_{\perp}$).

Recently, Amberger[13] has assigned the bands in the absorption spectrum of 3. In this analysis a set of first-order crystal field functions was derived which models the known temperature dependence of the magnetic susceptibility.

From these parameters, the isotropic ^1H NMR shifts of the ring protons were factored into contact and pseudocontact components. Using the geometry factor of Marks (-7.97×10^{-22} cm^{-3}) or that of Fischer (-5.49×10^{-22} cm^{-3}) the calculated pseudocontact shifts at 25°C are 2.38 and 1.64 ppm and the calculated contact shifts are -11.58 and -10.84 ppm, respectively.

Interestingly, all of the calculated contact shifts for the ring protons in these Cp_3U-X compounds are of the same sign and of the same order of magnitude as the isotropic shift in Cp_4U, suggesting that the ring metal bonding in all of these compounds is quite similar. Replacement of one Cp in Cp_4U by any other ligand lowers the symmetry of the complex leading to magnetic anisotropy and pseudocontact contributions to the isotropic ^1H NMR shifts. Lower symmetry alone does not completely control the magnetic anisotropy. The substituent has a profound effect which can serve to change the sign of the magnetic anisotropy term in eq. 17, and hence, the sign of the pseudocontact shift.

The temperature dependent behavior of the ring proton isotropic shifts also reflects the effects of lower symmetry. While the ring proton shift in Cp_4U shows a linear dependence on T^{-1} from -106°C to 133°C, the ring proton shifts of Cp_3U-X compounds 2-5, 8-10, 12, 17-18, and 23-25 all show marked deviations from linearity. The alkyl-substituted systems show linear behavior from ca. -150°C to room temperature but deviate from linearity above room temperature. The alkoxy compounds show apparent linearity from ca. 200°C to 400°C

but deviations from linearity below 200°C. All of the halides except for the fluoride display a slight curvature from 200°C to 400°C. The variable temperature behavior of the fluoride is solvent dependent and reflects the formation of dimers, although it is monomeric in the solid state.

The presence of the paramagnetic center in Cp_3U-X compounds also serves as an internal shift reagent and as such has been used as a conformational probe. In a variable temperature ^1H NMR study, Marks and co-workers[51] have observed line broadening of the borohydride proton resonances in 6. The broadening was not a result of temperature dependent changes in boron quadrupolar relaxation but instead was interpreted as indicative of slowing of the chemical exchange process between bridging and terminal protons. Estimation of the coalescence temperature as -140 ± 20°C leads to a calculated $\Delta G^{\neq}$ for the process of 5.0 ± 0.6 kcal mole^{-1}. Similarly, the energy barrier to rotation of the isopropyl group in Cp_3U-i-C_3H_7 has been estimated to be E_a = 10.5 ± 0.5 kcal mole^{-1} from computer simulated line shape analysis of variable temperature spectra.[12] From the coalescence temperature for fluxionality between monohapto- and trihapto-bonding of the allyl group in Cp_3U-allyl of 43°C, a value of 8.0 kcal mole^{-1} for $\Delta G^{\neq}$ for the process was calculated,[12] while in cyclohexyloxy-UCp_3, a lower limit for $\Delta G^{\neq}$ for ring inversion of the cyclohexyl ring has been estimated to be 2.3 kcal mole^{-1}.[11]

2) URANOCENES

Edelstein and co-workers[5] have proposed that the ^1H isotropic shift in uranocene can be approximated by

$$\delta_{ISOTROPIC} = \frac{X_{\parallel}-X_{\perp}}{3} \quad \frac{3\cos^2\psi-1}{R^3} \quad + \quad \frac{A_i}{3} \quad \frac{16g'J^6e}{5kT} \qquad (26)$$

The pseudocontact term is simply the axially symmetric form of eq. 17, which is valid for non-axially symmetric systems provided that they possess a 3-fold or greater rotational axis. The contact term is eq. 9, where X and g_J have been evaluated using a crystal field model for bis-cyclooctatetraene-actinide sandwich compounds proposed by Karraker.[52]

The ground term for U^{+4} is $^3H_4$. In a crystal field of D_{8h} symmetry this ninefold degenerate state is split into four doublets (J_z = ±4, ±3, ±2, ±1) and one singlet (J_z = 0). Analysis of bulk magnetic susceptibility data led to selection of the ground state as J_z = ±4, provided that an effective orbital reduction factor of k = 0.8, which corrects for reduction of orbital size caused by covalent contributions to metal ligand bonding, was included in the crystal field calculations.[53] This model successfully predicts the magnetic behavior of uranocene, neptunocene, and plutonocene assuming: 1)only the lowest crystal field state is populated in the temperature range T < 400°K; 2)there is no mixing of J states by the crystal field; 3)the effects of intermediate coupling are small and can therefore be

neglected.[52]

A direct result of the $J_z = \pm 4$ ground state is in the limit of $kT << D$, the total crystal field splitting, $X_{\parallel} = 3X_{av}$ and $X_{\perp} = 0$ where

$$X_{av} = 1/3\ X_{\parallel} + 2/3\ X_{\perp} \qquad (27)$$

Thus, the magnetic susceptibility component of the pseudocontact shift was evaluated from bulk susceptibility measurements. Using geometric data from the x-ray structure of Raymond and Zalkin,[54] and a magnetic moment of 2.4 B.M., Edelstein and co-workers calculated the pseudocontact shift for uranocene ring protons, (entry 1, Table 3-2). Interestingly, these authors used the Curie Law to relate X and μ_{eff}, while the magnetic data obeyed the Curie-Weiss Law, with μ_{eff} = 2.4 B.M. and $\theta = 9.6°K$. Neglect of the Weiss constant, (i.e., the Curie Law instead of the Curie-Weiss Law) underestimates the value of X_{av} resulting in smaller values for the pseudocontact shift. This underestimation amounts to about 3.5% for the ring ^1H resonances in uranocene (entry 2, Table 3-2).

Since the calculated pseudocontact shifts are smaller in magnitude than the observed isotropic shift, Edelstein, et al., concluded that an upfield contact component contributes to the total isotropic shift, indicative of covalency in the ligand metal bonds of uranocene.

Table 3-2

Earlier Analysis of Isotropic ^1H Shifts of Uranocene

Proton	$3\cos^2\theta-1/R^3$ x 10^{21} cm^{-3}	Temp °C	μ_{eff} B.M.	Isotropic shift (ppm)	Pseudo-contact shift(ppm)	Contact shift(ppm)
uranocene ring	-3.55	23	2.4	-41.4	-14.0	-27.4
uranocene ring	-3.55	7	2.4	-41.4	-14.0	-27.4
octamethyl ring	-2.0	25	2.38	-41.3	-7.9	-33.4
octamethyl ring	-5.9	25	2.38	-41.0	-23.6	+17.6
uranocene ring	-2.0	25	2.38	-42.6	-7.9	-34.7

The plot of shift vs T^{-1} was linear in accord with Curie-Weiss magnetic behavior and in agreement with the linearity predicted by eq. 26. The intercept, however, was ca. 7 ppm instead of zero as predicted by eq. 26. Edelstein and co-workers suggested that the non-zero intercept was due to some population of the $J_z = \pm 3$ level, approximately 400-600 cm^{-1} above the ground state, over the temperature range observed.

Subsequently, the ^1H NMR of 1,1',3,3',5,5',7,7'-octamethyluranocene was analyzed in a similar manner.[6] The contact shifts for the ring and α-protons were found to be similar in magnitude, but opposite in sign, implying spin density in a π-MO, and transfer of spin density via a spin polarization type mechanism (entries 3 and 4, Table 2-3). In this paper, a new, significantly smaller, value for the pseudocontact shift in uranocene was reported (entry 5, Table 2). This value was calculated using better geometric data from the

refined x-ray structure of uranocene by Raymond and co-workers.[55] The values of μ_{eff} used are not reported; however, geometry factors are given which show that μ_{eff} = 2.38 B.M. was used in calculating shifts for both compounds.

Plots of shift vs T^{-1} for both the methyl and ring protons were reported to be linear, with the ring protons similar to those in uranocene. No mention is made of the intercepts at $T^{-1} = 0$, except that the methyl proton intercept is non-zero and larger than that of the ring protons. No explanation was given for this observation.

These results have led to a proposed model for the contact shifts in uranocenes shown in Fig. 3-2.[56] In the ground state, orbital angular momentum dominates so the two f-electrons on the metal have their magnetic moments opposed to the applied field. Electron density, donated from filled ligand molecular orbitals to vacant metal orbitals, will be spin-polarized so the net spin density in the ligand π-MO gives rise to a magnetic moment aligned with the applied field, which should shift the ring ^{13}C resonances downfield. Relay of spin density via a spin polarization mechanism affords an upfield shift to the ring protons, and via hyperconjugation, a downfield shift to the α-carbons. Subsequent spin transfer results in an alternating upfield, downfield shift pattern, which decreases substantially the greater the number of sigma bonds between the observed nucleus and the ring carbons.

Separation of the isotropic shifts in uranocenes into pseudocontact and contact components is certainly an appealing

Fig. 3-2 Spin-polarization in uranocenes. Arrows shown refer to magnetic moments.

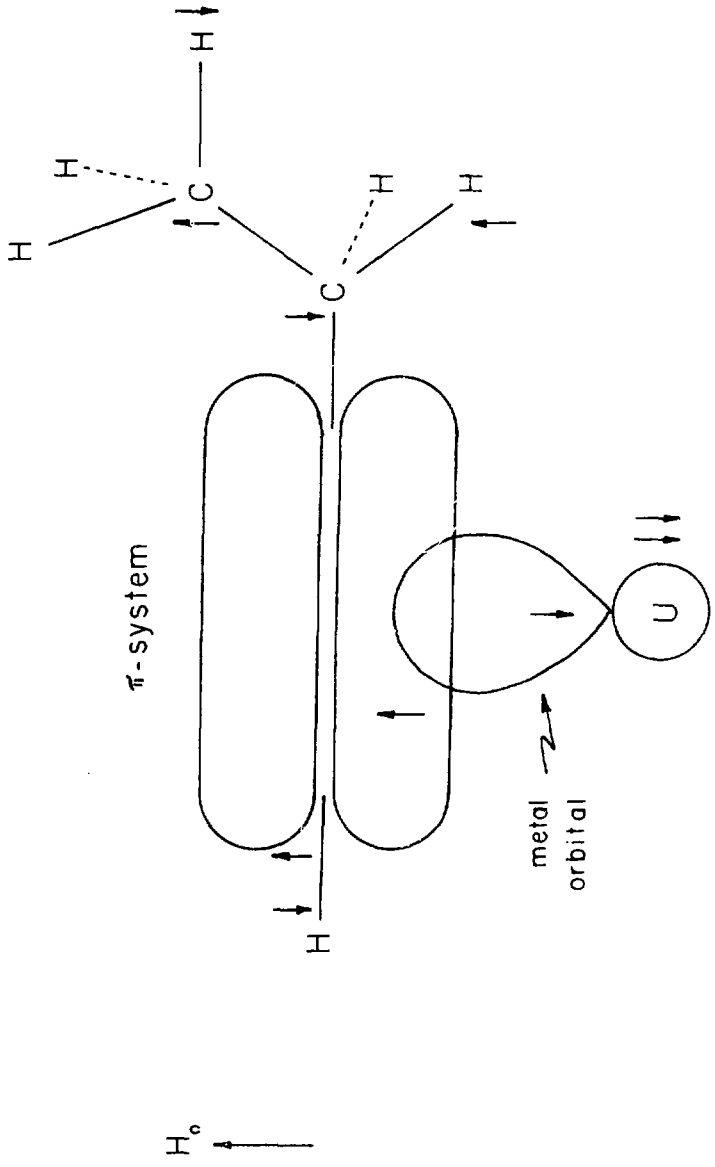
H
H
C
H
C
H
H
H
π-system
U
metal
orbital
H_o

method of attributing covalent character to bonding in uranocene. However, Hayes and Thomas[7] have advised caution in making deductions about covalency from NMR data on actinide complexes. In these compounds J is assumed to be a good quantum number, and thus, both spin and orbital angular momentum contribute to the observed magnetic moment. In actinide complexes, the spin magnetic moment may not be parallel to the net magnetic moment, which is aligned with the applied field. In fact, it is opposed if the 5-f shell is less than half full as in uranocene. Hence, direct transfer of spin density to a ring proton will give rise to a downfield shift.

Second and more importantly, the ligand metal interaction in organometallic complexes involves only certain orbitals on both the ligand and the metal. The electronic states giving rise to shifts in an NMR experiment may not involve these orbitals. Hence, little if any direct information on covalency can be derived from NMR experiments. In general, one must consider the occupancy of the relevant orbitals in the crystal field states populated over the temperature range of the NMR experiment in attempted correlation of contact shifts with specific modes of bonding.

From Streitwieser's model for the bonding in uranocene, Hayes and Thomas originally suggested that the major contribution to the contact shift should arise from spin density in the $m_l \pm 2$ metal orbital. The spin in this orbital is negative, leading to negative spin density in the ligand orbitals and affording a downfield shift to the ring

protons. That is, this model involves direct spin transfer by direct donation of metal f-electrons to ligand orbitals. Experimental evidence requires an upfield shift, and thus, direct spin transfer cannot account for the observed shifts.

The alternative model of spin polarization of ligand electrons donated to empty metal orbitals gives rise to positive spin density in the ligand system and the observed upfield shift to the ring protons.

Regardless of how they arise, it appears that contact shifts contribute to both the ring and α-proton isotropic shifts in uranocene and 1,1',3,3',5,5',7,7'-octamethyluranocene. Because both ring and α-positions experience contact and pseudocontact shifts, it is impossible to test if the assumptions used in factoring the observed shifts are valid. Of particular interest are the assumptions concerning the magnetic anisotropy term ($X_{||} - X_{\perp}$). Typically contact shifts are effectively zero if at least three atoms (i.e., four sigma bonds) separate the observed nucleus from the paramagnetic center.[57,58] Ideally, in a 1,1',3,3',5,5',7,7'-octaalkyluranocene, where the alkyl groups have β or γ protons, the observed isotropic shifts for these positions would be solely pseudocontact in nature. Provided that the geometry factor could be evaluated, use of equations 23-25 would permit calculation of the pseudocontact and contact shifts in the α and ring positions and would provide a test for the assumptions used in deriving $X_{||}$ and $X_{\perp}$. Unfortunately, none of these systems is known and attempts to prepare the t-butyl compound have not been successful.[59]

Numerous 1,1'-dialkyluranocenes are known and could potentially serve as test systems. However, three important factors limit analysis of these compounds. One, the symmetry of these systems is lower (i.e., they lack a 3-fold or greater rotation axis), and thus, the second term in eq. 17 is no longer constrained to zero by symmetry. Two, as in the Cp_3U-X compounds, not only the lower symmetry but also the substituent may have a profound effect on the magnetic anisotropy of these uranocenes. Three, the analysis of the substituent ^1H resonances in these molecules requires rigorous knowledge of the conformation(s) of the substituent in solution.

If the magnetic moment of a paramagnetic molecule obeys the Curie or Curie-Weiss Law, variable temperature ^1H NMR can serve as a conformational probe. Conformationally rigid nuclei or those rapidly oscillating between conformations of equal energy, will exhibit a linear shift dependence on T^{-1} while those which undergo exchange between conformations differing in energy will show a non-linear dependence. Equation 17 shows that the slope of these plots will depend upon the sign of A_i and the sign of the geometry factor.

Berryhill[14] has attempted analysis of the ^1H NMR resonances in 1,1'-diethyl-, 1,1'-diisopropyl-, 1,1'-dineopentyl-, and 1,1'-di-t-butyluranocene. The temperature dependence of the substituent proton resonances from ca. -100°C to 100°C are all linear except for the methyl group in 1,1-diethyluranocene. Using the corresponding cycloocta-

tetraene dianions as diamagnetic references, extrapolation of the linear plots to $T^{-1} = 0$ leads to a zero intercept for the t-butyl group in 1,1'-dineopentyluranocene and positive values less than 15 ppm for the other resonances. The positive intercepts do not appear to result from extrapolation errors and are similar to the reported intercept for 1,1',3,3',5,5', 7,7'-octamethyluranocene.[6] Assuming that the linearity implies Curie or Curie-Weiss Law magnetic behavior, the results suggest: 1)rapid rotation of the substituent between conformations of equal energy in 1,1'-di-t-butyluranocene (i.e., single resonance for the t-butyl group); 2)either rapid or no rotation of the substituent in 1,1'-diisopropyl-uranocene and 1,1'-dineopentyluranocene; 3)rapid rotation of the substituent between conformations of unequal energy in 1,1'-diethyluranocene. The linearity of the methylene proton resonances in 1,1'-diethyluranocene is surprising. If the ethyl group is rotating between conformations of unequal energy, as evidenced by the methyl group resonances, why don't the methylene protons show a similar non-linearity?

Similar behavior has been observed for the methyl and methylene protons of paramagnetic 1,1'-diisopropylcobalticene in variable temperature ^{1}H and ^{13}C NMR studies. Kohler[60] has proposed that this behavior results from rapid equilibration between two structures of unequal energy: a more stable symmetrical sandwich structure and a less stable slipped sandwich where the substituent carbon of the 5-membered ring has slid away from the metal. While a similar process in 1,1'-diethyluranocene is highly unlikely,

it cannot be ruled out based on Berryhill's data alone.

Attempted simulation of the curvature in the methyl group resonance by assuming that the geometry factor is given by

$$\frac{3\cos^2\theta-1}{R^3} = \frac{\int_0^{2\pi} \frac{3\cos^2\Omega-1}{R^3} e^{\frac{-\varepsilon(1-\cos\phi)}{kT}}}{\int_0^{2\pi} e^{\frac{-\varepsilon(1-\cos\phi)}{kT}}} d\phi \qquad (27)$$

where ϕ is the angle of rotation about the α-carbon bond, failed to reproduce the curvature for a variety of values of ε. Undoubtedly due to instrumental limitations, Berryhill did not record the resonances of the ring protons, and thus, one cannot rigorously establish if the non-linearity results from conformational changes or changes in the magnetic moment.

If, however, the data for 1,1'-diethyluranocene reflect rotation between conformations unequal in energy whose population ratio changes over the temperature range of the experiment, then the larger size of the neopentyl group coupled with the linear temperature dependence of the t-butyl resonance in 1,1'-dineopentyluranocene strongly suggest that the neopentyl group is locked in a single conformation.

For reasonable conformations of the substituents in these compounds, Berryhill calculated the pseudocontact shift for each assuming: 1)the geometric parameters in Table 3-3; 2)the compounds are effectively axially symmetric, and thus,

the second term in eq. 17 can be neglected; 3)the ground state and electronic properties are identical to uranocene, and thus, $X_{||} = 3X_{av}$, with $X_{\perp} = 0$ where $\mu_{eff} = 2.4$ B.M. Neglecting conformations where the methyl groups are in the plane of the 8-membered ring, the analysis of 1,1'-di-t-butyl- and 1,1'-diisopropyluranocene led to a substantial contact shift of ca. 10 ppm for the β-protons. This is quite surprising in light of the ca. -30 ppm contact shift for ring protons and the calculated contact shifts of 10.0 ppm and 5.3 ppm for the α-protons in 1,1'-diethyl- and 1,1'-diisopropyl-uranocene. Minor changes in geometry had little effect on the factored values.

The sign of the contact shift at the β-position precludes spin transfer by spin polarization and led to a proposed direct spin transfer via overlap between the β-hydrogen 1s orbitals and in-plane f or d uranium orbitals at the position of closest approach (ca. 2.6 A).

Table 3-3

Bond Lengths Used by Berryhill in Calculating Uranocene Geometry Factors

ring center - U	1.92
$C_{ring} - C_{ring}$	1.42
$C_{ring} - C_{\alpha}$	1.54
$C_{sp^2} - H$	1.08
$C_{sp^3} - H$	1.09
$C_{sp^3} - C_{sp^2}$	1.54

magic angle 54.7356°

A similar interaction has been proposed by Fischer to account for the temperature dependent change in linewidth of the t-butyl resonance in 1,1'-bis(di-t-butylphosphino)-uranocene.[58] At low temperature, rotation about the C_{ring}-P bond is 'frozen out' and the substituent is locked in a conformation where the 8-membered ring bisects the C_b - P - C_b bond angle. Below the coalescence temperature of 40°C, the linewidth of the exo t-butyl resonance remains relatively constant while that of the endo t-butyl resonance rapidly increases. Fischer suggested that this broadening could result from direct interaction of the endo t-butyl protons with metal orbitals. An alternative and more likely explanation is that the increase in linewidth reflects the onset of coalescence resulting from slowing of rotation about the $C_{b\text{-endo}}$ - P bond. The proximity of the metal should increase the energy barrier for rotation about the $C_{b\text{-endo}}$ - P bond over that for the $C_{b\text{-exo}}$ -P bond.

Further, direct overlap cannot account for the result of Hillard[104] which showed that the calculated pseudocontact shift for the t-butyl protons of 1,1'-dineopentyluranocene is at least four times larger than the observed isotropic shift. From this initial work it appears that the calculated pseudocontact shifts are of the right sign but systematically too large in magnitude to consistently account for the observed shifts.

During the preparation of this paper, Fischer[58] reported an alternative approach to factoring the isotropic shifts in

uranocene where the anisotropy term $X_{\parallel} - X_{\perp}$ is derived from the geometry factor and isotropic shift of protons sufficiently insulated from the uranium to preclude contact contributions to their isotropic shift. Fischer selected 1,1'-bis(trimethylsilyl)uranocene as a reference compound and assumed: 1)substitution has a negligible effect on the magnetic anisotropy in uranocene, and thus, $X_x \approx X_y$, 2)both the silicon atom and the number of bonds between the methyl protons and the 8-membered ring serve as effective insulators preventing transmission of spin to the β-protons; thus, the contact shift for these protons is effectively zero. These assumptions and selection of an appropriate geometry factor and the isotropic shift for the methyl protons led to $X_{\parallel} - X_{\perp}$ and $\mu_{\parallel}^2 - \mu_{\perp}^2 = 8.78$ at 30°C.

Values of $\mu_{\parallel}$ and $\mu_{\perp}$ derived from $X_{\parallel} - X_{\perp}$ and the known value of X_{av} were found to vary inversely with temperature. Thus, Fischer proposed an alternative electronic structure for uranocene with a ground state of $J_z = \pm 3$ and an excited state of $J_z = \pm 2$ approximately 300 ± 50 cm^{-1} above the ground state.

At 30°C, the value of $X_{\parallel} - X_{\perp}$ is substantially smaller than that assumed by Edelstein, et al., and leads to smaller calculated pseudocontact and larger contact shifts. The calculated pseudocontact shifts for an α-methyl group and a ring proton are respectively -12.5 ppm and -4.5 ppm and the corresponding contact shifts are 3.5 ppm and -38.1 ppm.

Two observations were presented in support of the assumption that substitution has little effect on the magnetic anisotropy of uranocene. One, monosubstitution has little

effect on the near IR of uranocene. Two, the temperature dependence of the ^1H NMR resonance of the unsubstituted ring in $(C_8H_8)(C_8H_7R)U$, R = $P(C_2H_5)_2$ and $P(t\text{-}C_4H_9)_2$ is similar to that of uranocene.

II. THE VARIABLE TEMPERATURE ^1H NMR OF URANOCENE AND SUBSTITUTED URANOCENES

The initial work on factoring isotropic shifts in uranocene and substituted uranocenes suggested that this was a fruitful area for additional study. In the following section we shall discuss work devoted to extending the contact - pseudocontact analysis of isotropic shifts to the ^1H NMR spectra of alkyl-substituted uranocenes. Extending such analysis to the isotropic shifts in 1,1'-dialkyluranocenes requires knowing: a)what is the temperature dependent behavior of the ^1H isotropic shift in uranocene? b)what effect does alkyl substitution have on the magnetic properties of uranocene and how does this effect the ^1H NMR shifts? c)what are the conformation(s) of the substituent in solution and what is their rate of interconversion relative to the NMR time scale?

Table 3-4

Uranocenes Analyzed by Variable Temperature ^1H NMR

26	Uranocene
27	1,1'-Dimethyl-
28	1,1'-Diethyl-
29	1,1'-Di-*n*-butyl-
30	1,1'-Diisopropyl

31	1,1'-Dineopentyl-
32	Mono-t-butyl
33	1,1'-Di-t-butyl
34	1,1',4,4'-Tetra-t-butyl-
35	1,1',3,3',5,5',7,7'-Octamethyl-
36	1,1'-Diphenyl-
37	1,1'-Bis(p-dimethylaminophenyl)-
38	Dicyclobuteno-
39	Dicyclopenteno-
40	Bis(dimethylcyclopenteno)-
41	1,1'-Di(t-butoxycarbonyl)-
42	Mono-(t-butoxycarbonyl)-
43	1,1'-Di(1,3,5,7-cyclooctatetraenyl)-

In an effort to answer these questions, we have measured the variable temperature ^1H NMR of a wide variety of uranocenes listed in Table 3-4.

The recent availability of a 180 MHz FT NMR spectrometer equipped with a variable temperature probe has greatly simplified studies by permitting easy simultaneous observation of all of the ^1H resonances in uranocenes. All spectra were run in toluene-d_8. In general, spectra were taken in 10° intervals from at least the range -80°C to 70°C. The temperature of the probe was monitored by a pre-calibrated thermocouple 5 mm from the sample tube, and could be held to ±0.3°C over the dynamic temperature range. Shifts were measured relative to the methyl group of toluene rather than stopcock grease; the latter shifted ca. 0.2 ppm over the temperature range. The shifts are reported relative to TMS by assigning the toluene methyl resonance as 2.09 ppm. This resonance differs from that in protio-toluene (2.31 ppm). Often this resonance

is erroneously assigned the same value as in the protio-compound; however, we have experimentally verified the difference which is a recognized secondary deuterium isotope effect in ^{1}H NMR spectroscopy.[61,62]

A) DIAMAGNETIC REFERENCE COMPOUNDS

Analysis of the isotropic shifts requires referencing the observed shifts to their positions in the spectrum of a corresponding hypothetical diamagnetic uranocene. The diamagnetic thorocenes are probably the closest analogy to such a model uranocene; however, only a meager number of these systems have been reported.[63,64] The difference between the ^{1}H resonances in the thorocenes and the corresponding cyclooctatetraene dianions is small (Table 3-5) and thus, the isotropic shifts in all the uranocenes discussed in this chapter have been references to the ^{1}H shifts in the corresponding cyclooctatetraene dianions. For those cyclooctatetraenes where the dianion has not been isolated and characterized by ^{1}H NMR the shifts have been estimated by comparison with other cyclooctatetraene dianions. The error resulting from such reference is probably less than 1-2 ppm.

Table 3-5

The ^{1}H NMR Resonances of Cyclooctatetraene Dianions and Thorocenes in THF

δ ppm from TMS

	ring	substituent		
COT$^{=a}$	5.9			
thorocene	6.5			
n-butylCOT$^{=a}$	5.7	2.9	1.3	0.9
1,1'-di-n-butylthorocene	6.5	3.2	1.6	1.0
methylCOT$^{=a}$	5.6	2.8		
1,1'-dimethylthorocene	6.5	3.1		
t-butylCOT$^{=a}$	5.7	1.5		
1,1'-di-t-butylthorocene	6.5	1.7		

^{a}the dipotassium salt

B) THE TEMPERATURE DEPENDENT ^{1}H NMR OF URANOCENE

Our initial interest was in verifying the temperature dependence of the ^{1}H isotropic shift in uranocene. The reported non-zero intercept at $T^{-1} = 0$ could result from extrapolation errors or it may reflect population of a low-lying excited state as Edelstein, et al.,[5] proposed. Recent laser Raman studies by Spiro and co-workers[65] have established that the first excited state in uranocene is 466 cm^{-1} above the ground state. Thus, the isotropic shift may not vary linearly with the inverse of temperature from -100°C to 100°C. Indeed, below 100°K some controversy exists concerning the temperature dependence of the magnetic moment in uranocene.[52,66,67]

The temperature dependence of the isotropic shift in uranocene was measured on two independent samples from -80°C

to 100°C. At the same nominal temperature slight differences in the shift between the two samples are undoubtedly due to slight differences in the true temperature of the samples and provide an estimate of the error in temperature measurement or measurement of the resonance frequency in this study.

The plot of shift vs T^{-1} (Fig. 3-3, Table 3-6) is strictly linear with an extrapolated intercept at $T^{-1} = 0$ of zero within experimental error. The difference between this result and that report by Edelstein et al.,[5] arises from uncertainty in measurement of the temperature. In the earlier work the uncertainty in the temperature at both the high and low extremes was +3.0°C while in this study it is +0.3°C. In fact, if one takes into account the reported error in the temperature measurements in the earlier work, the data can be fitted with a straight line which intercepts zero at $T^{-1} = 0$.

Table 3-6

Least Squares Linear Regression Analysis of VT ^{1}H NMR Data For Ring Protons in Uranocene, Octamethyluranocene[a] and the Unsubstituted Ring in Monosubstituted Uranocenes

Compound	Slope	Intercept	r^2
Uranocene Run #1	-12.83 ± 0.07	-0.32 ± 0.32	0.9992
Uranocene Run #2	-12.94 ± 0.06	0.21 ± 0.21	0.9997
Uranocene Edelstein Data[6]	-14.70 ± 0.17	6.96 ± 0.64	0.9991
Mono-t-butyl[b]	-12.62 ± 0.04	-0.32 ± 0.19	0.9998
Mono-t-butoxycarbonyl[b]	-13.54 ± 0.12	1.88 ± 0.47	0.9989
Octamethyl[a]	-13.12 ± 0.03	-2.45 ± 0.14	0.9999

[a]The 1,1',3,3',5,5',7,7' isomer [b]Unsubstituted ring, substituted ring data in Table 3-12

Fig. 3-3 Isotropic shift vs T^{-1} for uranocene.

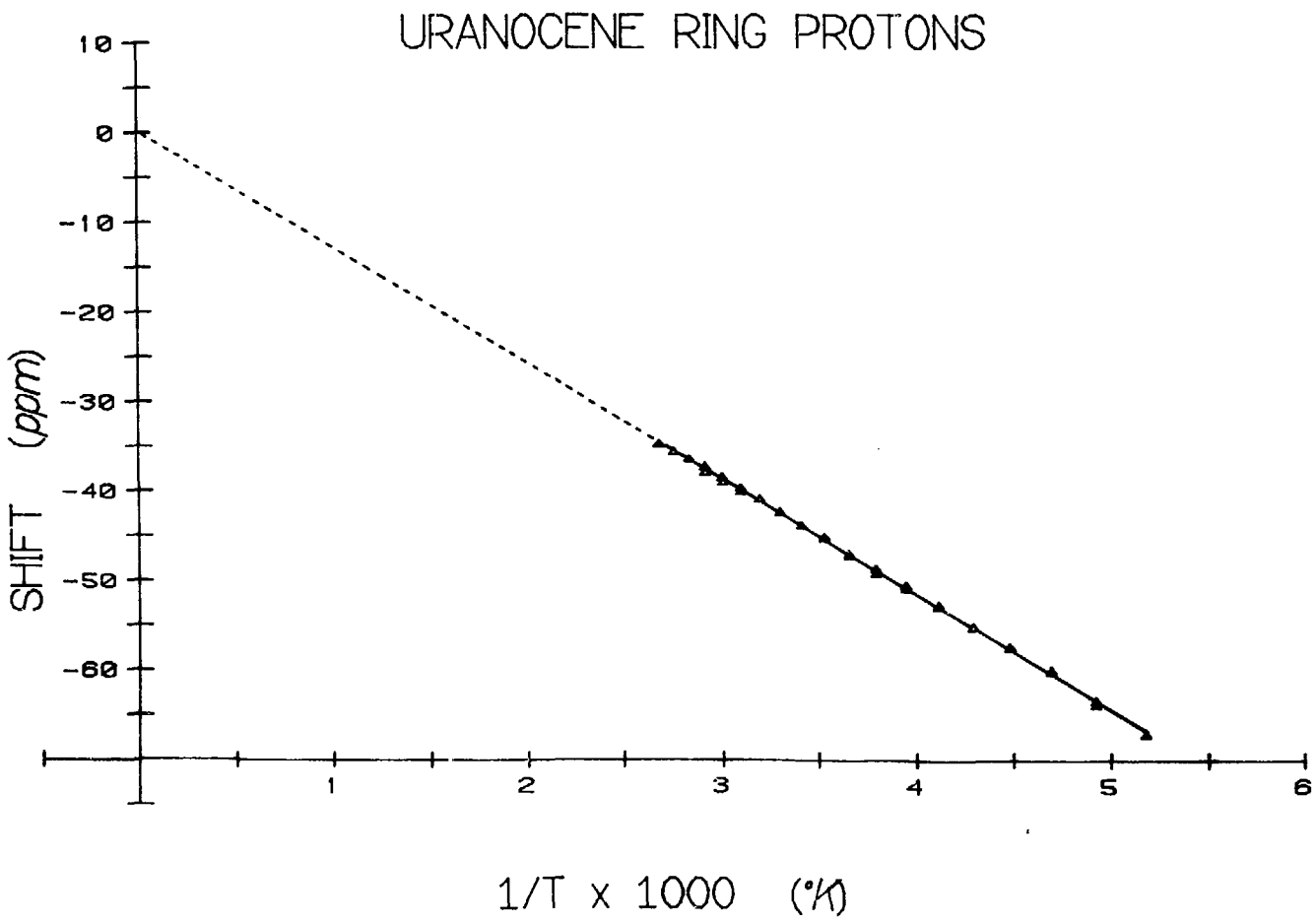
URANOCENE RING PROTONS
10
0
-10
-20
-30
-40
-50
-60
SHIFT (ppm)
1
2
3
4
5
6
1/T x 1000 (°K)

C) THE EFFECT OF SUBSTITUTION ON THE ^1H NMR OF URANOCENE

Substitution of the uranocene skeleton effectively lowers the symmetry of the complex, and in crystal field terms, the crystal field surrounding the U(IV) ion. Depending upon the magnitude of this change, the electronic structure and the magnetic properties of the complex can experience very large or very small changes. Such changes would then be reflected in the isotropic ^1H NMR shifts.

Inspection of Table 3-7, which lists the ^1H NMR shifts at 30°C of a wide variety of substituted uranocenes, suggests that the effects of substitution are minimal on the total isotropic shift. Indeed, the frequency and temperature dependence of the ring proton resonance in 1,1',3,3',5,5',7,7'-octamethyluranocene is virtually identical with that of the parent system indicating that $X_{\parallel} - X_{\perp}$ is identical in these two compounds. However, for 1,1'-disubstituted uranocenes, the two components of the magnetic susceptibility tensor perpendicular to the principal molecular axis (z-axis), X_x and X_y, are no longer constrained to be equal by symmetry as in uranocene. Thus, there may be additional components to the pseudocontact shift such as the second term in eq. 17. If, however, population of the various rotomeric confomers in such uranocenes is nearly equal, and rotation of the rings is rapid on the NMR time scale, then the anisotropy in the xy plane perpendicular to the principal axis will average to zero and the complex can be viewed as having effective axial symmetry.

TABLE 3-7

^{1}H NMR Resonances of Substituted Uranocenes

δ ppm from TMS

	Substituent[a]	Shift[b] at 30°C
26,	H	-36.63
35,	1,3,5,7-tetramethyl	-35.15, -4.21 (CH_3)
27,	CH_3	-31.70, -33.67 (H5), -36.10,-40.39 -7.20 (CH_3)
28,	CH_2CH_3	-32.89, -34.45 (H5), -36.33, -39.7 -7.47 (CH_2), -1.20 (CH_3)
30,	i-C_3H_7	-35.50, -35.98, -36.00 (H5), -36.40 -14.47 (CH), -9.89(CH_3,d,J=4.4 Hz)
29,	n-C_4H_9	-32.64, -34.10 (H5), -36.22, -39.74 -19.03 (α-CH_2), 0.22 (ß-CH_2) 0.98 (γ-CH_2,m), 0.36 (CH_3,t,J= 6.3 Hz)
33,	t-C_4H_9	-33.43, -33.80, -37.30, -40.54 (H5) -11.49 (CH_3)
32,	t-C_4H_9	-33.41, -34.74, -39.81, -43.37 (H5) -36.02 (8H, unsubstituted ring), -10.82 (CH_3)
34,	1,4-di-t-butyl	-25.23, -39.66, -42.23 -10.25 (CH_3)
31,	neo-C_5H_{11}	-32.84, -33.42 (H5), -36.26, -41.07 -23.97 (CH_2), 3.86 (CH_3)
	$(CH_2)_3N(CH_3)_2$[d]	-31.5, -32.9 (H5), -34.9, -38.1, -18.3 (α-CH_2,t,J=7.5 Hz) 0.63 (ß-CH_2,m), 113 (CH_3) 2.80 (γ-CH_2,t,J=7.0 Hz)
36,	C_6H_5	-34.29, -36.15, -36.45, -37.13 (H5) 0.76 (p,d,J=7.2 Hz) 0.85 (m,t,J=7.6 Hz) -13.95 (o,d,J=7.3 Hz)
37,	p-$(CH_3)_2NC_6H_4$	-34.29, -36.15, -36.46, -37.13 (H5) -14.10 (o,d,J=7.6 Hz) 0.13 (m,d,J=7.6 Hz), -0.04 (CH_3)
38,	cyclobuteno	-27.70, -35.90, -43.80 -26.75 (α_{endo}) 19.65 (α_{exo}) (J=9.64 Hz)

	Substituent[a]	Shift[b] at 30°C
39,	cyclopenteno	-32.12, -34.20, -41.15 -32.58 (β_{endo},m) -8.28 (β_{exo},m) -18.78 (α_{endo},m) 24.43 (α_{exo},m)
40,	dimethyl cyclopenteno	-32.43, -33.26, -39.83 -12.91 (CH_{3endo}) 5.39 (CH_{3exo}) -22.90 (α_{endo}) 8.28 (α_{exo}) (J=14.5 Hz)
44,	cyclohexeno	-30.64, -32.53, -38.70 -22.35 (β_{endo},m) -2.94 (β_{exo},m) -16.42 (α_{endo},m) 6.56 (α_{exo},m)
	$C(C_6H_5)_3$[e]	-21.35, -34.87, -49.50, -52.01(H5) 4.88 (o,d,J=6.8 Hz) 4.95 (m,t,J=6.6 Hz) 5.44 (p,t,J=6.6 Hz)
	OCH_3[d]	-27.5, -30.2 (H5), -35.6, -43.7 -3.73 (CH_3)
	o-t-C_4H_9[d]	-28.1, -28.7 (H5), -36.2, -45.7 2.08 (CH_3)
	$OCH_2CH\ CH_2$[d]	-27.9, -30.5 (H5), -35.5, -43.5 -0.33 (α-CH_2,d,J=5.0 Hz) 0.70 (trans-H, d,J=17.5 Hz) 1.75 (β-CH,m), 2.60 (cis-H,d,J=10.5 Hz)
41,	CO_2-t-C_4H_9	-30.51, -32.65, -36.01 (H5),-42.45 -6.07 (CH_3)
42,	CO_2-t-C_4H_9[c]	-29.42, -33.69, -36.0 (H5), -40.06 -37.06 (8H, unsubstituted ring) -6.27 (CH_3)
	$CO_2CH_2C_6H_5$	-29.81, -32.08, -36.23 (H5),-43.16 -2.98 (CH_2), -0.56 (o) 4.09 (m) 5.20 (p)
	$CO_2CH_2C_6H_5$[c]	-28.51, -32.40, -32.98 (H5),-40.63 -2.99 (CH_2), -36.06 (8H, unsubstituted ring) -1.16 (o) 3.94 (m) 5.30 (p)

Substituent[a]	Shift[b] at 30°C
$CO_2CH_2CH_3$	-29.93, -32.69, -35.78 (H5), -42.14 -6.05 (CH_3), -4.23 (CH_2)
$CO_2CH_2CH_3$[c]	-28.84, -32.93, -36.14 (H5), -40.27 -6.57 (CH_3), -4.45 (CH_2), -37.07 (8H, unsubstituted ring)

(a) Substituent on each 8-membered ring.

(b) In monosubstituted cyclooctatetraene ligands the ring H5 could be identified by integration relative to the other ring proton resonances.

(c) Monosubstituted.

(d) Data from ref. 51 at 39°C.

(e) At 26°.

1) THE ENERGY BARRIER TO RING ROTATION IN 1,1',4,4'-TETRA-t-BUTYLURANOCENE

The energy barrier to ring rotation in sandwich organometallic complexes has generally been assumed to be very low. The barrier to ring rotation in ferrocene has been measured by gas phase electron diffraction (1.1 ± 0.1 kcal mole^{-1})[69,70] and by second moment measurements using wideline ^{1}H NMR (1.8 ± 0.2 kcal mole^{-1}).[71] Similarly the energy barrier to ring rotation in nickelocene and chromocene have been measured by gas phase electron diffraction (1.8 ± 0.2 kcal mole^{-1}).[70,72] Considering that the ring-ring distance in uranocene is 0.52 A longer than that in ferrocene and that the ring rotation barrier is 8-fold rather than 5-fold, the energy barrier to ring rotation in uranocene is expected to be lower. Second moment wideline ^{1}H NMR studies on solid uranocene samples estimate the ring rotation energy barrier to be 0 kcal mole^{-1}.[71] Appropriate substitution of the rings should raise this barrier. Wideline ^{1}H NMR study of second moments has shown that monosubstitution of ferrocene raises the barrier to ring rotation to ca. 10-11 kcal mole^{-1}.[73]

Quite unexpectedly in measuring the variable temperature ^{1}H NMR of 1,1',4,4'-tetra-t-butyluranocene, we were successful in 'freezing out' ring rotation on the NMR time scale (Fig. 3-4, 3-5). Above -30°C where ring rotation is rapid, the spectrum consists of four singlets with an area ratio of 18:2:2:2, corresponding to the t-butyl protons and three

sets of non-equivalent ring protons. In the low temperature spectrum below -80°C, where the compound is conformationally rigid on the NMR time scale, the spectrum consists of eight singlets with an area ratio of 9:9:1:1:1:1:1:1, corresponding to two kinds of t-butyl groups and six dintinct sets of ring protons. Labeling the three ring proton resonances in the high temperature spectrum A-C, from low field to high field, the B resonance coalesces first, followed by virtual simultaneous coalescence of the A and C resonances and eventual coalescence of the t-butyl group as the lowered (Table 3-8).

The coalescence temperature is directly proportional to the difference in frequency of the resonance signals in the low temperature spectrum of the conformationally 'frozen' molecule. As eq. 28 shows, the larger the difference in frequency, ν, the higher the coalescence temperature. Due

At Coalescence Temperature $$k_C = \frac{\pi(\Delta\nu)}{\sqrt{2}} \qquad (28)$$

to the temperature dependence of the isotropic shifts resulting from the paramagnetic uranium, the resonances of the conformationally 'frozen' molecule vary as a function of temperature. Fortunately, the temperature dependence of the shifts in the conformationally 'frozen' molecule is linear in T^{-1} (Fig. 3-6, 3-7) and thus, the resonance frequencies at the coalescence temperatures were obtained by linear extrapolation (Table 3-9). As expected, the frequency

Fig. 3-4 The temperature dependent ^{1}H NMR spectra of the ring protons in 1,1',4,4'-tetra-t-butyluranocene.

Fig. 3-5 The temperature dependent ^{1}H NMR spectra of 1,1',4,4'-tetra-t-butyluranocene.

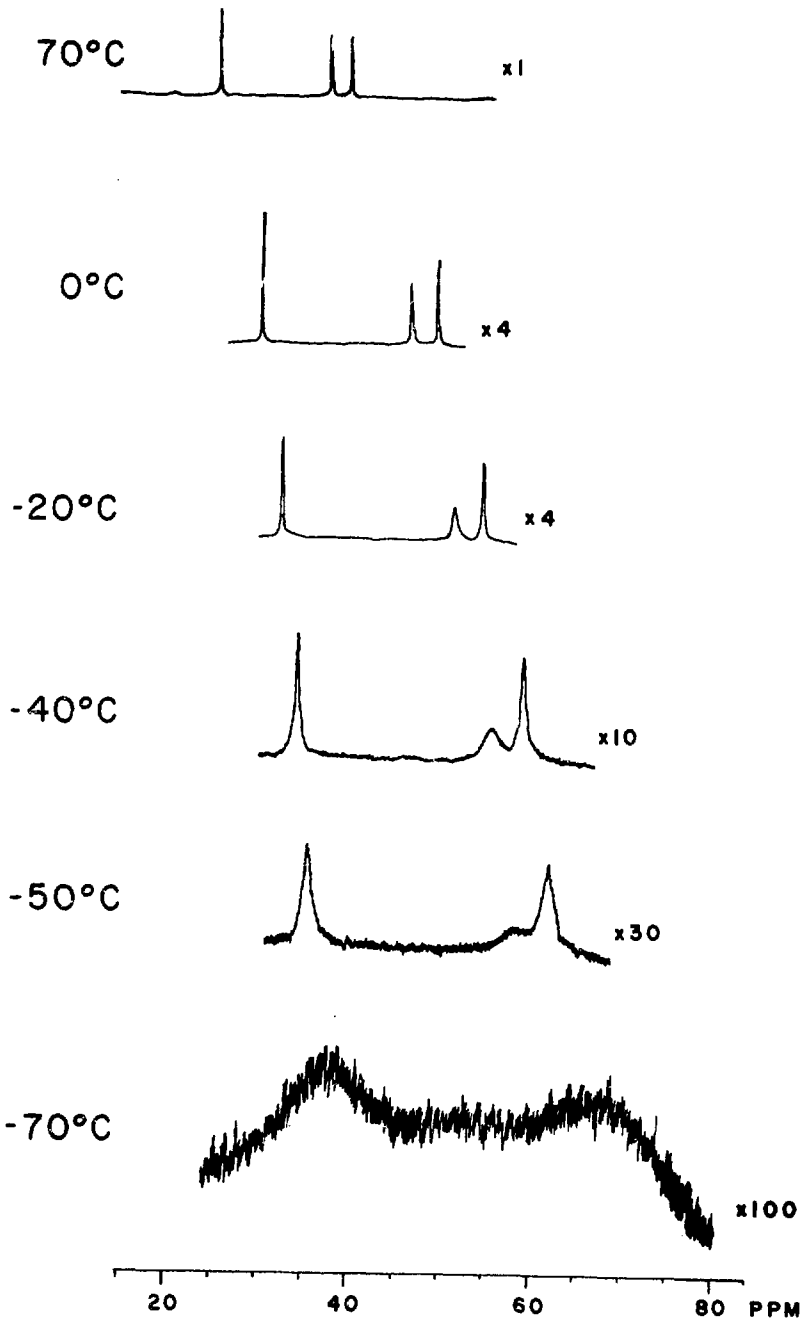
70°C
x1
0°C
x4
-20°C
x4
-40°C
x10
-50°C
x30
-70°C
x100
20
40
60
80
PPM

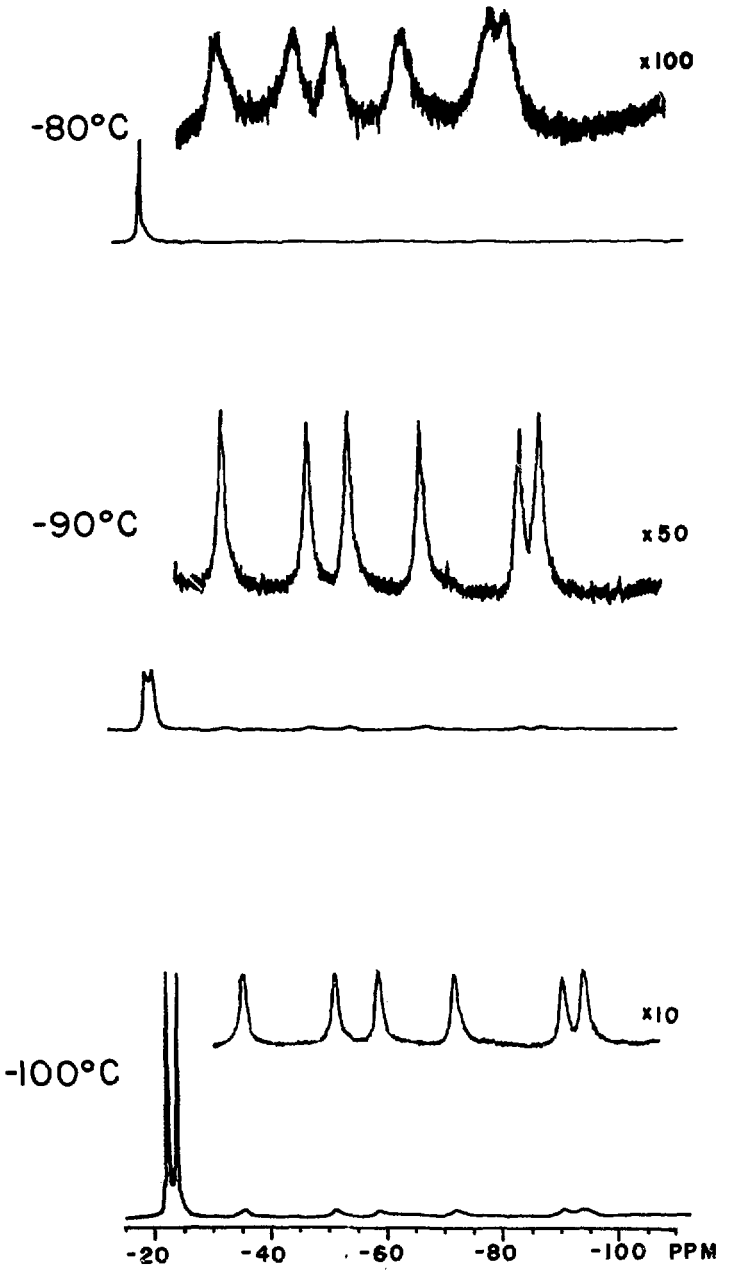
-80°C
x100
-90°C
x50
-100°C
x10
-20
-40
-60
-80
-100
PPM

difference of the B' and B'' resonances in the low temperature spectrum, which coalesce to the B resonance in the high temperature spectrum, is larger than that for the A, C and t-butyl resonances. From these data, values for $\Delta G^{\neq}$ for ring rotation were calculated using eq. 28, and are recorded in Table 3-8.

Observation of six ring proton resonances at low temperature eliminates 44a as the structure of the conformationally 'frozen' form of 1,1',4,4'-tetra-t-butyluranocene, since it contains a symmetry plane. Inspection of molecular models suggest that 44b is the most reasonable conformation of the two rings and

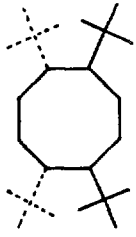

44a

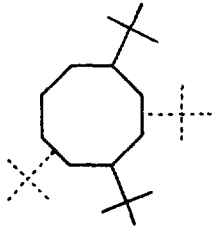

44b

undoubtedly corresponds to the low temperature conformation. From the pattern of the ring proton resonances at high temperature and the coalescence temperatures, the various ring proton positions can be tentatively assigned. In the high temperature spectrum, resonances B and C are quite close in frequency and are at substantially higher field than the A resonance. With free rotation of the rings the four protons of the 8-membered ring adjacent to the t-butyl groups (i.e., protons 2,3,5,8) are similar, and different from protons 6 and 7. Thus, the A resonance can be assigned to the 6 and 7 protons. Of the B and C resonances, B coalesces faster

Table 3-8

VT ^{1}H NMR Data for 1,1',4,4'-Tetra-t-Butyluranocene

Proton	Coalescence Temp. °C	Isotropic Shift* ppm		$G^{\neq}$ kcal $mole^{-1}$
t-butyl	-85	-20.37	-21.33	8.61
ring A	-70	-32.03	-44.10	8.30
ring B	-65	-48.30	-71.49	8.58
ring C	-70	-61.52	-77.76	8.58

Ave. $G^{\neq}$ 8.42 0.5 kcal $mole^{-1}$

* extrapolated from shifts of the conformationally 'frozen' molecule

Table 3-9

Least Squares Linear Regression Analysis of 1,1',4,4'-Tetra-t-Butyluranocene VT ^{1}H NMR Data

Resonance	Slope	Intercept	r^2
Ring A	-7.72±0.08	-5.49±0.30	0.9985
Ring B	-14.73±0.22	3.26±0.81	0.9970
Ring C	-15.42±0.16	2.95±0.62	0.9983
t-Butyl	-5.09±0.06	5.04±0.22	0.9980
Ring A'	-13.65±0.51	-3.73±0.09	0.9981
Ring A''	-8.18±0.25	-3.82±1.36	0.9972
Ring B'	-9.42±0.02	-4.12±0.13	0.9999
Ring B''	-11.89±0.08	-3.01±0.42	0.9998
Ring C'	-17.43±0.46	10.29±2.53	0.9979
Ring C''	-19.33±0.61	17.42±3.33	0.9970
t-Butyl'	-3.87±0.0	0.20±0.0	1.0000
t-Butyl''	-5.77±0.0	9.36±0.0	1.0000

Fig. 3-6 and 3-7 Isotropic shift vs T^{-1} for the ring protons in 1,1',4,4'-tetra-t-butyluranocene

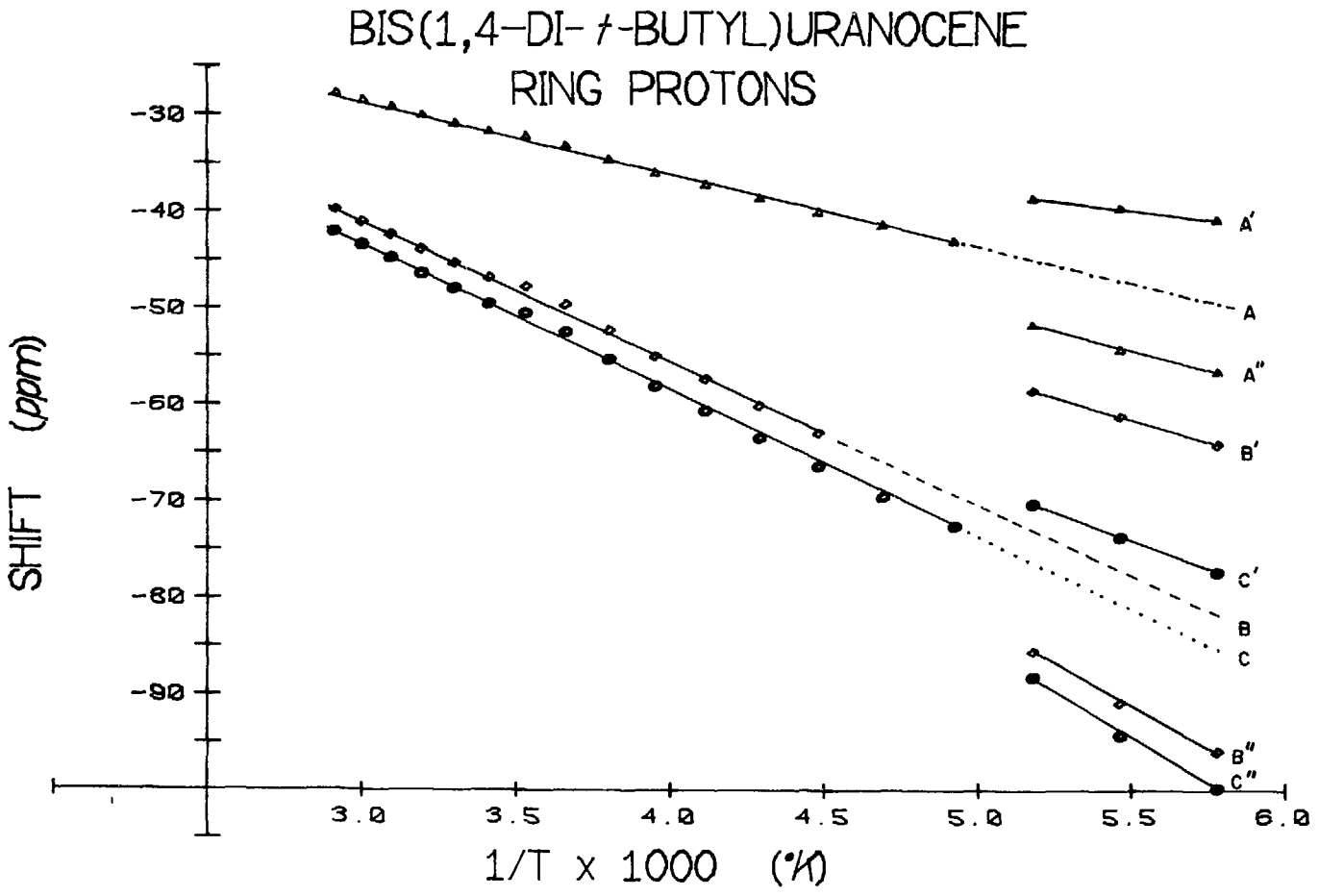
BIS(1,4-DI-t-BUTYL)URANOCENE
RING PROTONS
SHIFT (ppm)
-30
-40
-50
-60
-70
-80
-90
3.0
3.5
4.0
4.5
5.0
5.5
6.0
1/T x 1000 (°K)
A'
A
A"
B'
C'
B
C
B"
C"

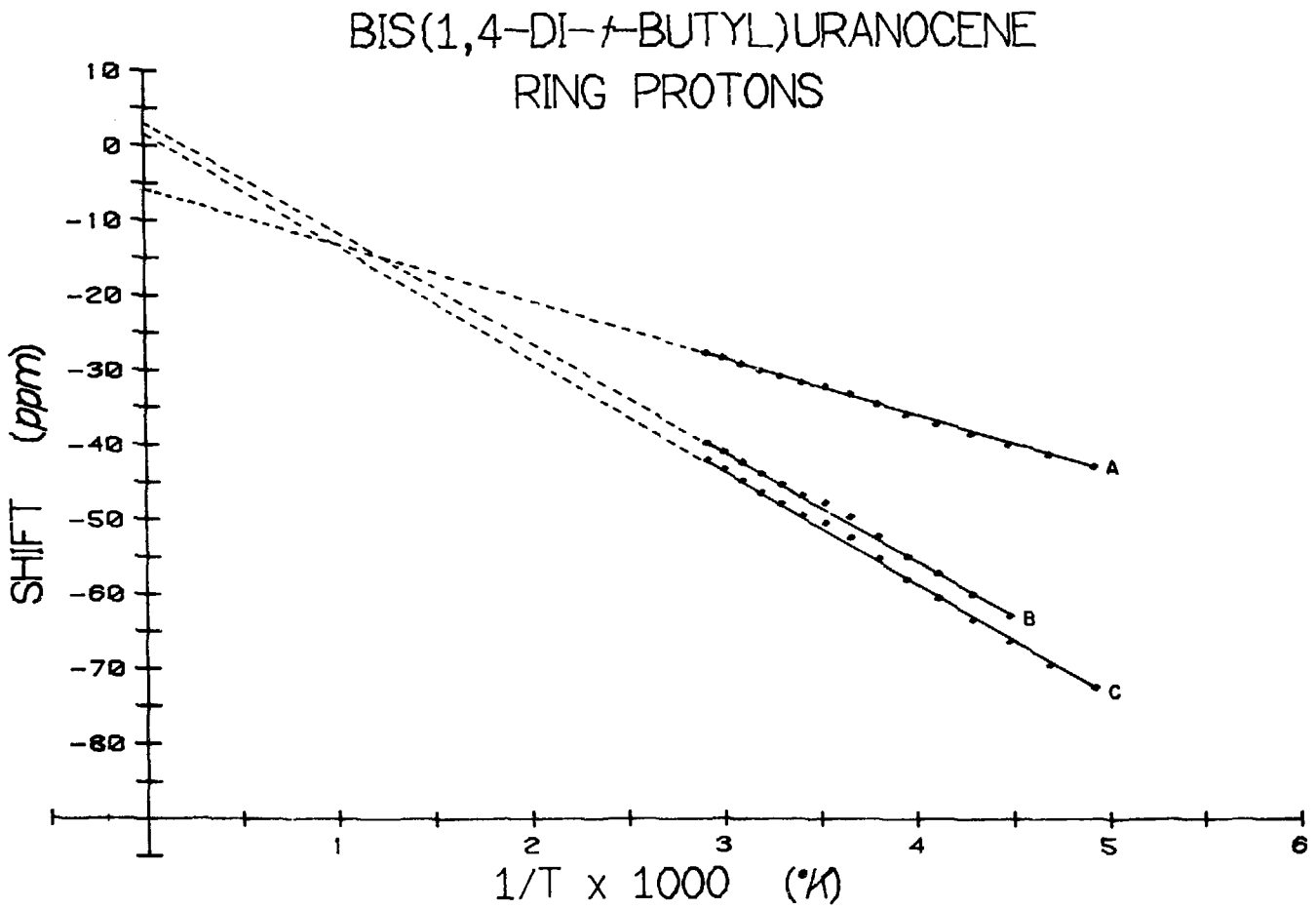
BIS(1,4-DI-t-BUTYL)URANOCENE
RING PROTONS
SHIFT (ppm)
10
0
-10
-20
-30
-40
-50
-60
-70
-80
1
2
3
4
5
6
1/T x 1000 (°K)
A
B
C

than C and hence, the environment of the B protons experiences a greater change than that of the C protons in going from the conformationally frozen to the freely rotating molecule.

Inspection of 44b shows that the difference between the environment of the 5 and 8 protons is significantly greater than the difference between the environments of the 6 and 7 or the 2 and 3 protons. As such, the 5 and 8 proton resonances should coalesce at a higher temperature than the resonances of the other two sets of protons. Thus, we can tentatively assign the B resonance to the 5 and 8 positions. Correspondingly, the C resonance can be assigned to the 2 and 3 protons. While this assignment is certainly not rigorously conclusive, it represents the first attempt at assigning the non-equivalent ring proton resonances in substituted uranocenes. In Chapter 4, we will discuss assignment of ring proton resonances in 1,1'-dialkyluranocenes using deuterium labeling.

2) THE ENERGY BARRIER TO RING ROTATION IN 1,1',3,3'-TETRA-t-BUTYLFERROCENE

The rather serendipitous success in measuring the rotational barrier in 1,1',4,4'-tetra-t-butyluranocene suggested that the rotational barrier in the ferrocene analog 1,1',3,3'-tetra-t-butylferrocene could be measured in a similar manner. Surprisingly, although 1,1',3,3'-tetra-t-butylferrocene has been prepared several times,[74-76] and its structure has been elucidated by single crystal x-ray

diffraction,[77] the ring rotational barrier has not been reported. In fact, the literature is void of any reports concerning the determination of ring rotational energy barriers of substituted ferrocenes in solution by variable temperature ^1H NMR.

In analogy with the synthesis of 1,1',3,3'-tetra-t-butyl ferrocene by Leigh,[74] treatment of ferrocene with 4 eq. of t-butyl chloride and 4 eq. of $BF_3 \cdot Et_2O$ in refluxing hexane for 24 hr yielded a mixture of 1,1',3-tri-t-butyl- and 1,1',3,3'-tetra-t-butyl ferrocene. Removal of the tri-alkylated species by reduced pressure short path distillation followed by two recrystallizations of the pot residue from CH_2Cl_2 afforded the desired tetra-substituted ferrocene in 23% yield.

At 30°C, in $CDCl_3$, the ^1H NMR spectrum of 1,1',3,3'-tetra-t-butyl ferrocene consists of one t-butyl resonance (1.218 ppm, s, 18H) and two ring proton resonances; (3.822 ppm, t, 2H, J = 2.45 Hz, 3.097 ppm, d, 4H, J = 1.46 Hz), indicating rapid ring rotation relative to the NMR time scale. Interestingly, the non-equivalent ring protons are coupled via 1,3 coupling. Upon lowering the temperature this coupling disappears and the t-butyl resonance slowly broadens. Below -35°C two distinct t-butyl resonances are observed: (1.231 ppm and 1.206 ppm), Fig. 3-8. Unfortunately, the resonances of the non-equivalent ring proton in the conformationally 'frozen' molecule could not be resolved. At -60°C the high field ring proton resonance is a broad singlet while the low field resonance is a broad doublet and thus, only the t-butyl resonance can be used to calculate $\Delta G^{\neq}$.

Fig. 3-8 The temperature dependent ^{1}H NMR spectra of 1,1',3,3'-tetra-t-butylferrocene.

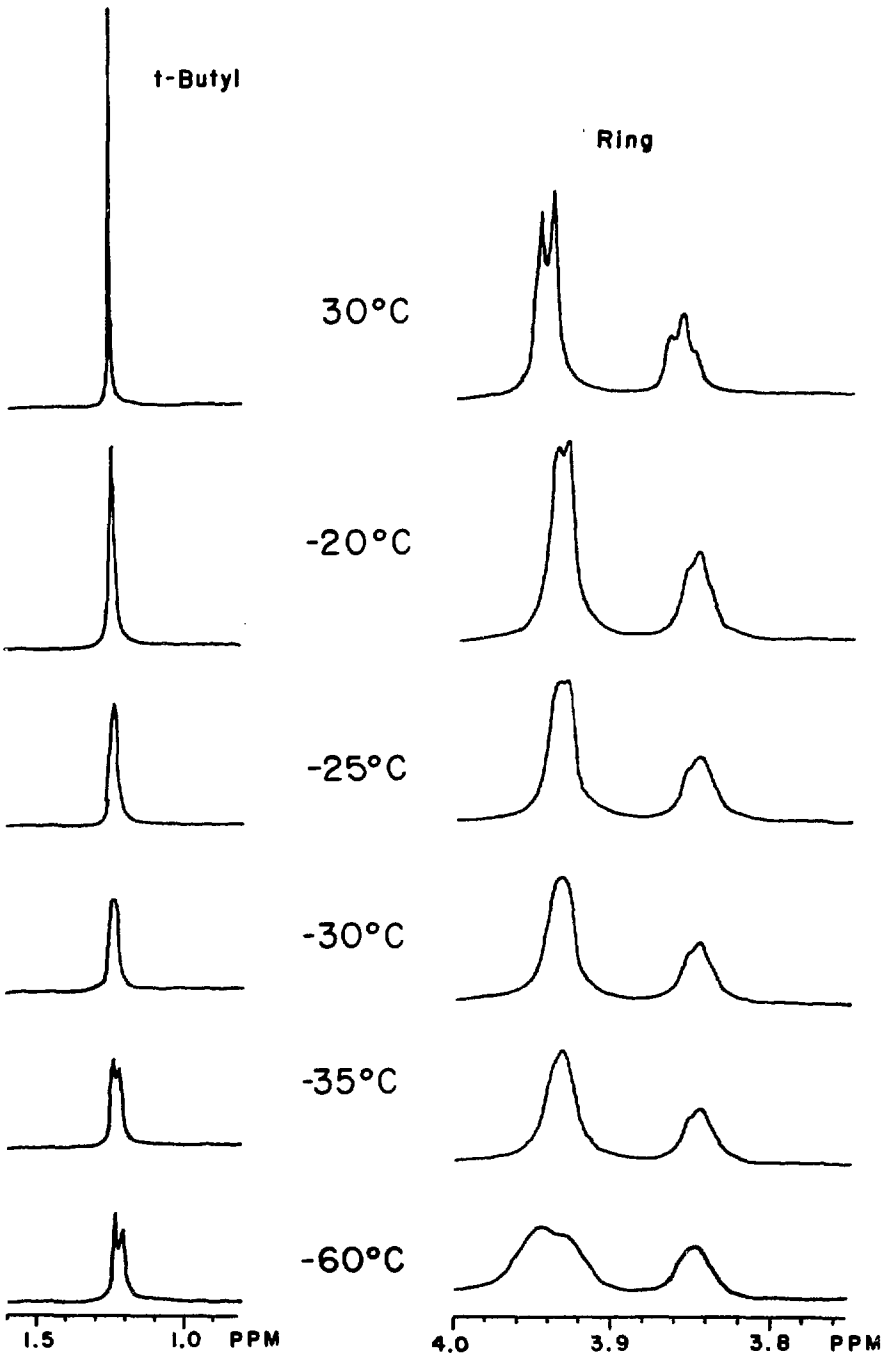
t-Butyl
Ring
30°C
-20°C
-25°C
-30°C
-35°C
-60°C
1.5
1.0
PPM
4.0
3.9
3.8
PPM

Taking its coalescence temperature as -27.5°C, the calculated $\Delta G^{\neq}$ for ring rotation is 13.1 kcal $mole^{-1}$. As expected, both the coalescence temperature is higher, and the corresponding $\Delta G^{\neq}$ is larger in the ferrocene, than in the corresponding uranocene.

3) THE ENERGY BARRIER TO RING ROTATION IN MONOSUBSTITUTED URANOCENES

Reaction of 1 eq. of a substituted cyclooctatetraene dianion and 1 eq. of cyclooctatetraene dianion with 1 equivalent of UCl_4 is known to lead to a mixture of uranocene, the 1,1'-disubstituted and the monosubstituted uranocene. Except for alkoxycarbonyluranocenes, where the 1,1'-disubstituted compound is less stable than the monosubstituted compound, and can be selectively decomposed, no attempt has been made to isolate monosubstituted uranocenes.

From an NMR point of view, the unsubstituted ring in monosubstituted uranocenes offers a unique probe into the effects of substitution on the uranocene skeleton. High field ^1H NMR established that the NMR resonances of a monosubstituted uranocene are differentiable from those of the corresponding 1,1'-disubstituted uranocene. Thus, we measured the temperature dependent ^1H NMR spectra of two monosubstituted uranocenes; mono-t-butoxycarbonyl and mono-t-butyl.

The ester had been prepared by Burghardt[82] while the t-butyl compound was prepared by the reaction of 1 eq. each of the potassium salts of t-butylcyclooctatetraene dianion

and cyclooctatetraene dianion. Soxhlet extraction of the crude reaction product with hexane until the extract was light green effectively separated the uranocene from a mixture of the mono- and disubstituted uranocenes. Analysis by ^{1}H NMR showed the ratio of mono- to disubstitution was 1.8 : 1.

In both of the monosubstituted uranocenes investigated, the proton resonance of the unsubstituted ring is a singlet. Table 3-7 shows that at 30°C, the protons of the unsubstituted ring in mono-t-butyluranocene resonate at 0.51 ppm lower field, while those in the mono ester resonate at 0.43 ppm higher field, than the ring protons in uranocene. These differences are real and were independently established by observing the spectrum of mixtures of these compounds.

The temperature dependence of the unsubstituted ring proton resonances are linear functions of T^{-1} and the slopes of shift vs T^{-1} are identical within experimental error to that of uranocene (Fig. 3-9, 3-10, Table 3-6). The slight difference in intercepts at $T^{-1} = 0$ undoubtedly results from using the proton resonance of cyclooctatetraene dianion as a diamagnetic reference for all the compounds. In a variety of monosubstituted ferrocenes the proton resonances of the unsubstituted rings are not identical with the resonance in the parent compound.[78]

Changes in the linewidths at half height of the unsubstituted ring resonances as a function of temperature parallels that of uranocene and results from the known change in paramagnetic relaxation times as a function of temperature rather than the onset of coalescence (Table 3-10).[18] This implies that ring rotation in monosubstituted uranocenes is

rapid on the NMR time scale or that rotation is slow and the differences between the resonance frequency of the non-equivalent protons is smaller than the linewidths of the observed signals. In light of the energy barrier to rotation in 1,1',4,4'-tetra-t-butyluranocene, the energy barrier to rotation in these compounds must be small, and free rotation is occurring.

Table 3-10

Linewidth at Half Height of ^{1}H NMR Resonances of Uranocene (Hz)

	-70°C	30°C	70°C
uranocene	102	90	76
mono-t-butyl-[a]	45	33	30
mono-t-butoxycarbonyl-	50	38	32

[a]unsubstituted ring

The behavior of these two monosubstituted uranocenes implies that both the magnetic anisotropy (i.e., $X_{\parallel} - X_{\perp}$) and the contact shift in the monosubstituted uranocene and uranocene must be identical within the experimental error of the NMR experiment. Furthermore, both the ring and the substituent proton resonances in the substituted ring of these compounds parallels the behavior of the proton resonances in the corresponding 1,1'-disubstituted uranocene (Fig. 3-42, 3-47).

Recently, Fischer[58] has independently arrived at the same conclusion based on the temperature dependent behavior of the ^{1}H NMR resonances of the two monosubstituted uranocenes, $(C_8H_8)(C_8H_7R)U$, R = $P(t\text{-}C_4H_9)_2$ and $Sn(t\text{-}C_4H_9)_2$. In both of

Fig. 3-9 Isotropic shift vs T^{-1} for uranocene and the ring protons in the unsubstituted ring of mono-t-butyl and mono-t-butoxycarbonyluranocene.

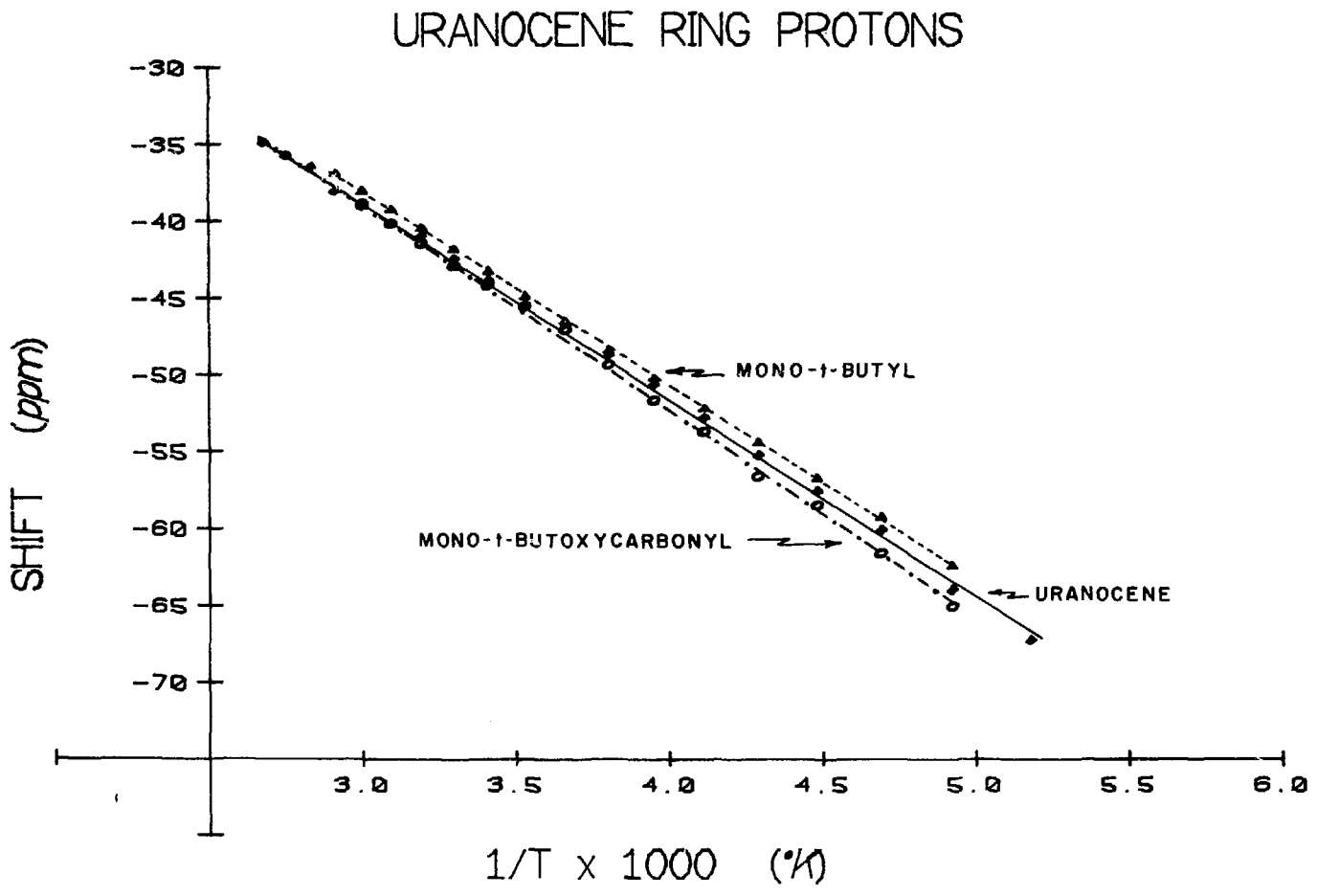
URANOCENE RING PROTONS
SHIFT (ppm)
-30
-35
-40
-45
-50
-55
-60
-65
-70
MONO-t-BUTYL
MONO-t-BUTOXYCARBONYL
URANOCENE
3.0
3.5
4.0
4.5
5.0
5.5
6.0
1/T x 1000 (°K)

Fig. 3-10 Isotropic shift vs T^{-1} for uranocene and the ring protons in 1,1',3,3',5,5',7,7'-octamethyluranocene.

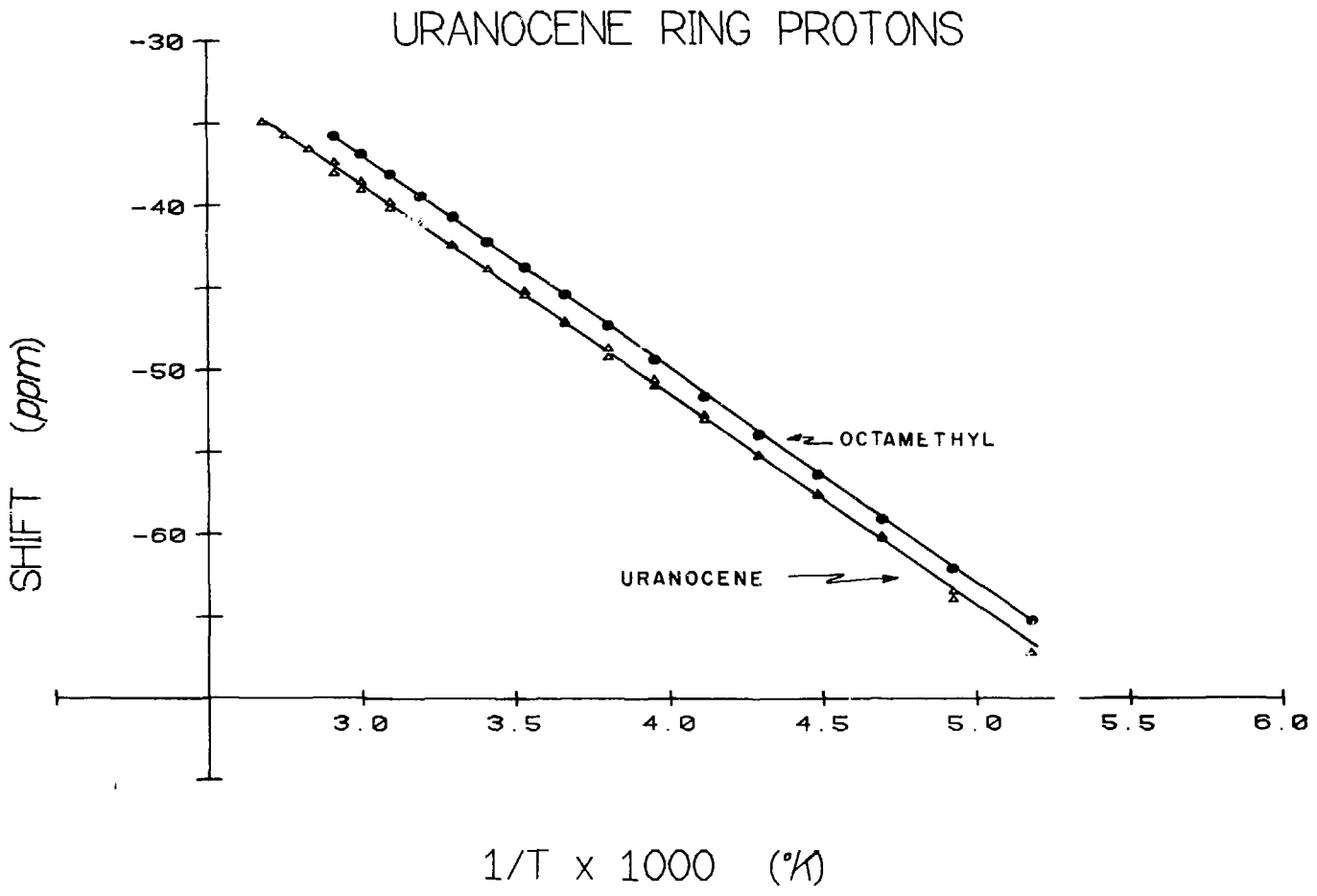
URANOCENE RING PROTONS
-30
-40
-50
-60
SHIFT (ppm)
OCTAMETHYL
URANOCENE
3.0
3.5
4.0
4.5
5.0
5.5
6.0
1/T x 1000 (°K)

these compounds the unsubstituted ring resonance is reported to be identical with that in uranocene.

4) THE RING ROTATION ENERGY BARRIER IN 1,1'-DIALKYLURANOCENES

In 1,1'-disubstituted uranocenes steric considerations suggest that the preferred conformation will possess an inversion center at the uranium. Because of this, the number of non-equivalent ring protons will remain unchanged regardless of whether the rings freely rotate or are conformationally 'frozen', and thus, variable temperature ^{1}H NMR cannot be used to measure the energy barrier to ring rotation.

In light of the two crystal structures reported in Chapter 2, and the previous crystal structure of 1,1',3,3', 5,5',7,7'-octamethyluranocene, it appears that at least in the solid state, the energy barrier to rotation in alkylated uranocenes is small. Consideration of Dreiding models suggests that the rotational energy barrier in 1,1',4,4'-tetra-t-butyluranocene should be larger than the rotational energy barrier in any 1,1'-dialkyl-substituted uranocene. Thus, we can set an upper limit for $\Delta G^{\neq}$ for ring rotation in 1,1'-dialkyluranocenes as 8.42 ± 0.21 kcal mole^{-1} and hence, over the temperature range -70°C to 100°C the rings in 1,1'-dialkyluranocenes are freely rotating.

D) THE EFFECT OF SUBSTITUTION ON THE MAGNETIC SUSCEPTIBILITY OF URANOCENE

If substitution significantly changes the electronic structure and the magnetic anisotropy of uranocene then the resonance frequency and temperature dependence of the ^{1}H NMR resonances will not be similar to that in uranocene. Further, the temperature dependent behavior of the isotropic shifts in substituted uranocenes may vary depending upon the rate of ring rotation relative to the NMR time scale. In the limit of rapid ring rotation and effective axial symmetry, $X_x = X_y$, while in the limit of 'frozen' rotation X_x may not equal X_y.

In the case of rapid rotation the resonance frequency and temperature dependent behavior of the unsubstituted rings in the two monosubstituted uranocenes require that both the magnetic anisotropy (i.e., $X_{||} - X_{\perp}$) and the contact shift be identical within the experimental error of the NMR experiment, with that of uranocene. The ^{1}H NMR data on 1,1',4,4'-tetra-t-butyluranocene permit evaluation of the effects of the population distribution of rotomeric conformers and the rate of ring rotation on the magnetic anisotropy term. All of the ^{1}H NMR resonances in this compound are linear functions of T^{-1} both in the limit of free and 'frozen' rotation (Fig. 3-6). In the region of 'frozen' rotation, the average of each of the pairs of resonances (i.e., A'A''; B'B''; etc.) is very close to the value extrapolated from the linear dependence of the shift after coalescence, where ring rotation is now occurring.

Thus, to a good first approximation, $(X_{\parallel} - X_{\perp})$, in the limit of free rotation, is identical to $(X_z - 1/2)(X_x - X_y)$ in the limit of 'frozen' rotation or $X_x = X_y$. This implies that substitution of the uranocene skeleton, while formally lowering the symmetry of the complex, only exerts a small perturbation on the crystal field around the uranium. Intuitively this is not surprising since substitution does not directly change any of the 16 carbon atoms in the immediate coordination sphere of the uranium (IV) ion. Evidentally, from the point of view of the uranium atom, it still experiences a C_{8v} crystal field as in uranocene. Thus, to a good first approximation substituted uranocenes can be viewed as having effective axial symmetry regardless of the rate of ring rotation.

Is this consistent with other physical properties of uranocenes? Bulk magnetic susceptibility measurements at low temperature on several substituted uranocenes appear to suggest that within experimental error the magnetic properties of all uranocenes are identical and equal to 2.4 ± 0.2 B.M. (Table 3-11). Again this is not surprising in light of the Streitwieser model for bonding in uranocene. If the magnetic properties of uranocenes are principally determined by the two unpaired electrons, this model predicts they should reside primarily in the metal $m_l \pm 3$ orbital. Either symmetry, or energy difference restricts significant interaction of this orbital with other orbitals, so it remains essentially metal in character even when the rings are substituted. This point has recently been substantiated by X_α and qualitative Hückel molecular orbital calculations on uranocene and substituted

Table 3-11

Magnetic Properties of Uranocenes

Substituent	Temp. Range °K	μ_{eff} B.M.	Weiss Constant °K	Ref.
H	4.2-45	2.43	9.56	66
H	4-10	3.33	9.4	52
H	10-42	2.3	0.9	52
H	12-72	2.42	2.9	67
H	180-300	2.62	3	67
H	10-300	2.6		5
CH_3	14.5-81.5	2.26±0.2	17	83
CH_2CH_3	3-8	2.86	14.9	52
CH_2CH_3	10-27	1.9	0.4	52
CH_2CH_3	14.7-79.6	2.13±0.2	-7	83
$(CH_2)_3CH_3$	3-10	2.85	5.8	52
$(CH_2)_3CH_3$	10-50	2.3	2.6	52
C_6H_5	14-100	2.65±0.2	12.2±3	81
cyclobuteno	15-100	2.35±0.2	8.5	14
cyclopenteno	15-95.6	2.4±0.2	16.1	
cyclohexeno	14.4-97.8	2.65±0.2	23	
1,3,5,7-tetramethyl	1.9-73.7	2.2±0.2	11.3±3	81
1,3,5,7-tetraphenyl	4.2-100	2.5±0.1	6.7±1	81
CO_2-t-C_4H_9	30-100	2.64±0.2	10.4	82

uranocenes.[79,80]

E) THE TEMPERATURE DEPENDENCE OF RING PROTON RESONANCES IN SUBSTITUTED URANOCENES

In substituted cyclooctatetraene dianions where substitution lifts the symmetry imposed equivalency of the ring protons, the difference in resonance frequency of the magnetically non-equivalent protons is sufficiently small that the observed resonances appear as a broadened singlet even in high field NMR experiments. Likewise in corresponding substituted thorocenes, the non-equivalent ring proton resonances appear as a broadened signal with no assignable features. However, in substituted uranocenes the non-equivalent ring proton resonances all appear as well resolved singlets for all of the uranocenes whose ^{1}H NMR has been reported.

The structure of a sufficient number of substituted uranocenes has been determined by single crystal X-ray diffraction to establish that both the uranium-ring distance and the C_{ring}-C_{ring} bond distance are invarient, within experimental error, regardless of substituents on the uranocene skeleton. From the discussion in Chapter 2, it appears that the substituents, and most likely the ring protons in substituted uranocenes, are tipped slightly out of the plane of the 8-membered ring toward the uranium atom. Assuming that the geometry factor for all of the ring protons is the same, and if $X_x = X_y$ as we have shown in the preceding section,

then the pseudocontact shift for each will be the same and the observed differences in resonance frequency must arise from differences in the contact shift at the magnetically non-equivalent ring positions. Similarly, differences in the isotropic shifts of the non-equivalent ring protons in substituted bisarenechromium complexes have been attributed to differences in the contact shift.[84]

For purposes of discussion in this chapter, the ring proton resonances in the spectra of substituted uranocenes will be alphabetically labeled starting with the lowest field resonance. This does not imply that the "A" resonance in two different uranocenes corresponds to the same ring position. In Chapter 4, we shall discuss assignment of the individual ring proton resonances.

The temperature dependence of the ring proton resonances of the uranocenes listed in Table 3-4 are plotted as shift vs. T^{-1} in Fig. 3-11 to 3-38. In all, 60 individual ring proton resonances in 17 different uranocenes were observed. Three general features are immediately apparent. One, in all cases except one position in dicyclobutenouranocene, the shifts are linear functions of T^{-1} from at least the range -70°C to 70°C. The non-linearity of the one position in dicyclobutenouranocene (Fig. 3-25,26) probably reflects a temperature dependent geometry change of the ring proton resulting from conformational changes in the fused ring which will be discussed in a subsequent section. Two, the total difference between the highest and lowest field resonance of the non-equivalent ring protons in all the uranocenes increases

as the temperature decreases. Three, the relative pattern of the ring proton resonances in each uranocene remains constant as a function of temperature except for the two phenyl-substituted uranocenes and 1,1-biscyclooctatetraenyluranocene.

Above 0°C the pattern for 1,1'-diphenyluranocene is 2:2:2:1, by integration. The temperature dependent shift in the C resonance is greater than that for the D resonance and thus, below 0°C the pattern becomes 2:2:1:2. Similarly for 1,1'-bis(p-dimethylaminophenyl)uranocene, the pattern above -50°C is 2:2:1:2, but changes to 2:1:2:2 below -50°C. These changes may reflect temperature dependent changes in the rate of rotation about the C_{ring}-C_{α} bond, which affect conjugation between the 6 and 8-membered rings in these compounds. The temperature dependent changes in the ring proton resonances of 1,1'-dicyclooctatetraenyluranocene are indicative of slowing of some conformational exchange process(es) relative to the NMR time scale, and will be discussed in a subsequent section along with the behavior of the substituent proton resonances.

The high degree of linearity in the temperature dependence of the ring proton shifts is evident from the correlation coefficients of the least squares regression lines (Table 3-12). The slopes of the lines are all negative and similar in magnitude to that of uranocene. However, the standard deviations of the extrapolated intercepts at $T^{-1} = 0$ indicate that a number of the intercepts are non-zero. Ideally, eq. 17 predicts that all of the intercepts should be zero at $T^{-1} = 0$.

Considering all of the ring proton resonances together, there is no apparent correlation between the non-zero intercepts

Table 3-12

Least Squares Linear Regression Lines For
Alkyl Uranocene Ring Proton Data

Fig. #	Substituent	Proton Resonance	Slope	Intercept	r^2
3-11,12	methyl	A	-10.89±0.05	-1.35±0.19	0.9997
		B	-11.20±0.05	-2.30±0.18	0.9997
		C	-12.80±0.06	0.57±0.24	0.9996
		D	-15.59±0.09	5.48±0.36	0.9994
3-13,14	t-butyl[a]	A	-12.12±0.04	0.75±0.17	0.9998
		B	-12.08±0.04	0.71±0.16	0.9998
		C	-14.03±0.04	0.92±0.17	0.9999
		D	-15.22±0.05	1.00±0.18	0.9999
3-15,16	t-butyl	A	-11.80±0.03	-0.37±0.12	0.9999
		B	-11.89±0.05	-0.51±0.18	0.9998
		C	-14.24±0.08	3.77±0.32	0.9995
		D	-15.59±0.11	4.96±0.41	0.9993
3-17,18	ethyl	A	-10.95±0.06	-2.43±0.20	0.9994
		B	-10.85±0.06	-4.31±0.20	0.9994
		C	-13.12±0.08	1.17±0.31	0.9991
		D	-16.04±0.13	7.25±0.46	0.9986
3-19,20	n-butyl	A	-10.78±0.02	-2.77±0.08	0.9999
		B	-10.73±0.02	-4.37±0.08	0.9999
		C	-12.85±0.03	0.39±0.11	0.9999
		D	-15.69±0.07	6.14±0.25	0.9996
3-21,22	neopentyl	A	-11.27±0.05	-1.68±0.17	0.9998
		B	-11.15±0.05	-2.68±0.19	0.9997
		C	-13.01±0.05	0.58±0.19	0.9998
		D	-15.93±0.07	5.31±0.25	0.9998
3-23,24	isopropyl	A	-13.06±0.05	1.68±0.19	0.9999
		B	-12.79±0.05	0.39±0.19	0.9998
		C	-13.12±0.05	1.40±0.19	0.9998
		D	-13.44±0.08	2.04±0.30	0.9995

Fig. #	Substituent	Proton Resonance	Slope	Intercept	r^2
3-25,26	cyclobuteno	A	non-linear		
		B	-12.81±0.12	0.65±0.48	0.9984
		C	-17.58±0.20	8.45±0.77	0.9979
3-27,28	cyclopenteno	A	-11.07±0.25	-1.50±1.02	0.9912
		B	-13.20±0.08	3.67±0.31	0.9994
		C	-16.84±0.23	9.02±1.04	0.9960
3-29,30	dimethylcyclo-cyclopenteno	A	-10.29±0.05	-4.11±0.21	0.9996
		B	-12.26±0.06	1.52±0.22	0.9997
		C	-16.80±0.11	9.93±0.45	0.9993
3-31,32	phenyl	A	-12.04±0.08	-0.71±0.32	0.9992
		B	-12.03±0.10	-2.58±0.38	0.9989
		C	-13.95±0.09	3.41±0.34	0.9994
		D	-12.05±0.10	-3.52±0.40	0.9988
3-33,34	p-dimethylamino-phenyl-	A	-11.23±0.10	-3.49±0.41	0.9985
		B	-12.20±0.13	-0.49±0.53	0.9979
		C	-11.17±0.09	-5.21±0.38	0.9987
		D	-14.93±0.19	5.74±0.76	0.9971
3-35,36	t-butoxy-carbonyl[a]	A	-11.02±0.08	0.19±0.31	0.9993
		B	-12.47±0.12	2.89±0.47	0.9987
		C	-13.01±0.08	1.30±0.31	0.9995
		D	-14.62±0.09	0.19±0.36	0.9994
3-37,38	t-butoxy-carbonyl	A	-4.63±0.02	1.16±0.08	0.9997
		B	-10.52±0.07	-0.37±0.29	0.9993
		C	-12.60±0.12	2.36±0.47	0.9987
		D	-14.05±0.11	0.73±0.43	0.9991

[a]substituted ring of monosubstituted uranocene

Fig. 3-11 and 3-12 Isotropic shift vs T^{-1} for the ring protons in 1,1'-dimethyluranocene.

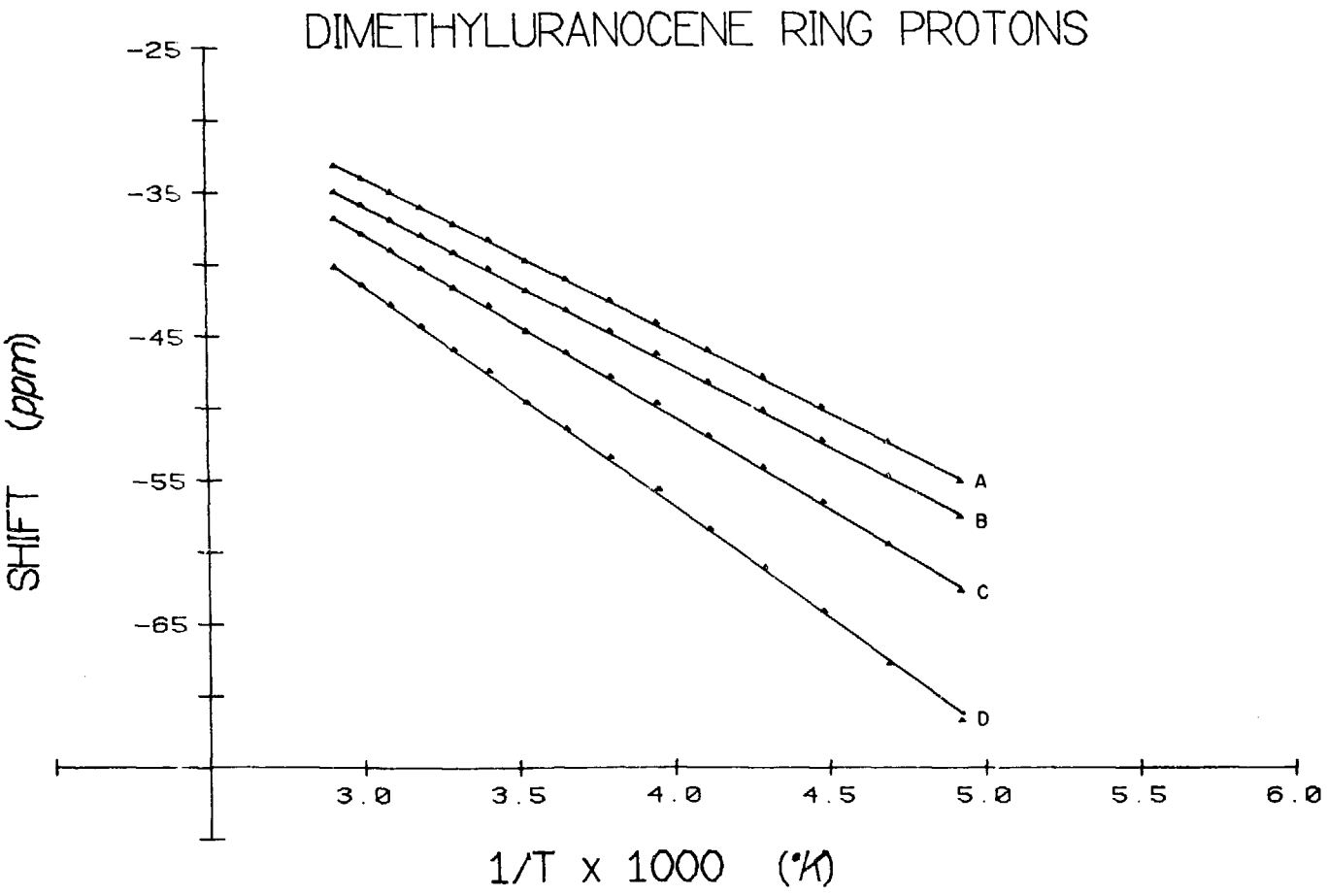
DIMETHYLURANOCENE RING PROTONS
SHIFT (ppm)
-25
-35
-45
-55
-65
A
B
C
D
3.0
3.5
4.0
4.5
5.0
5.5
6.0
1/T x 1000 (°K)

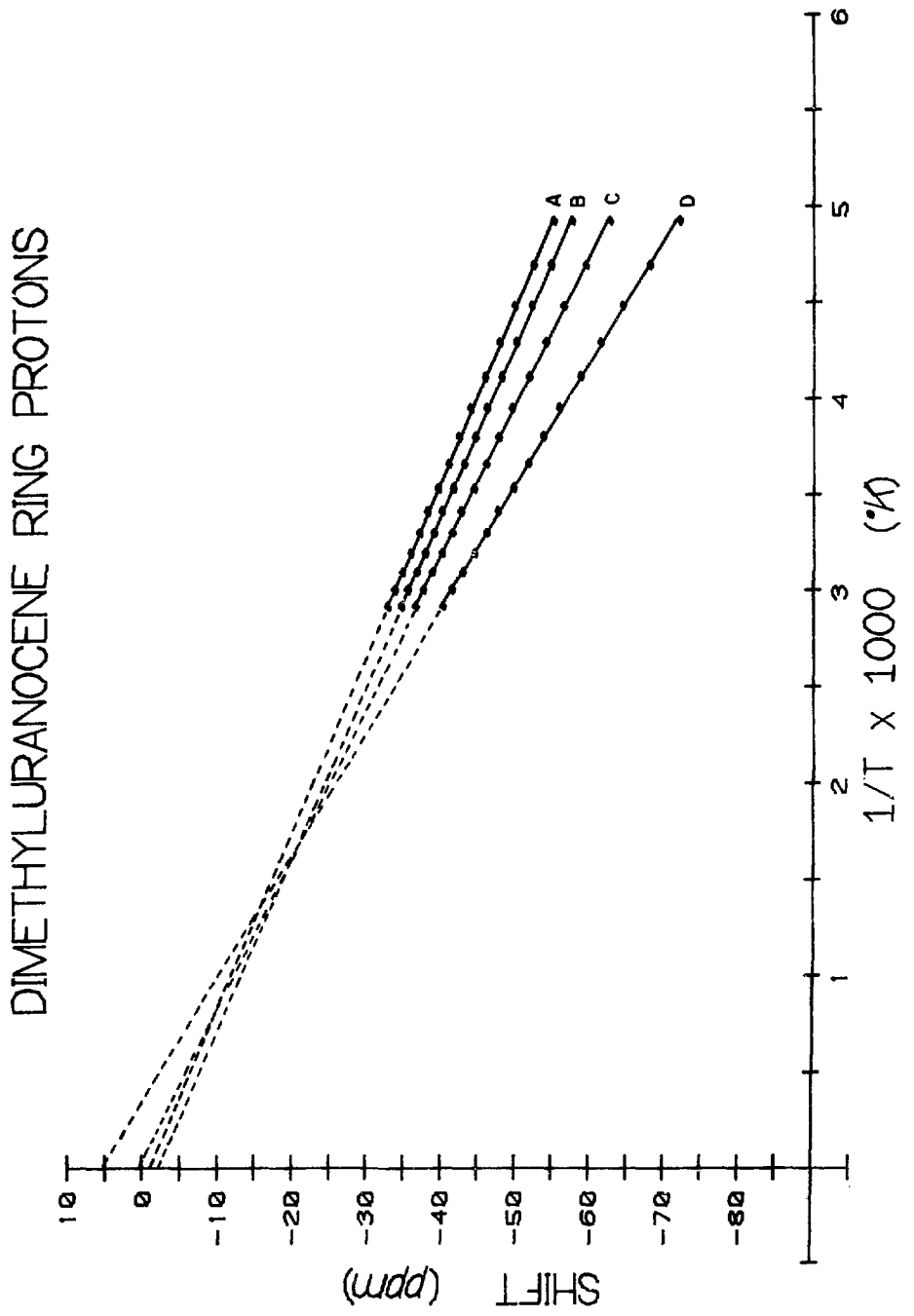
DIMETHYLURANOCENE RING PROTONS
SHIFT (ppm)
10
0
-10
-20
-30
-40
-50
-60
-70
-80
1/T x 1000 (°K)
1
2
3
4
5
6
A
B
C
D

Fig. 3-13 and 3-14 Isotropic shift vs T^{-1} for the ring protons in the substituted ring of mono-t-butyluranocene.

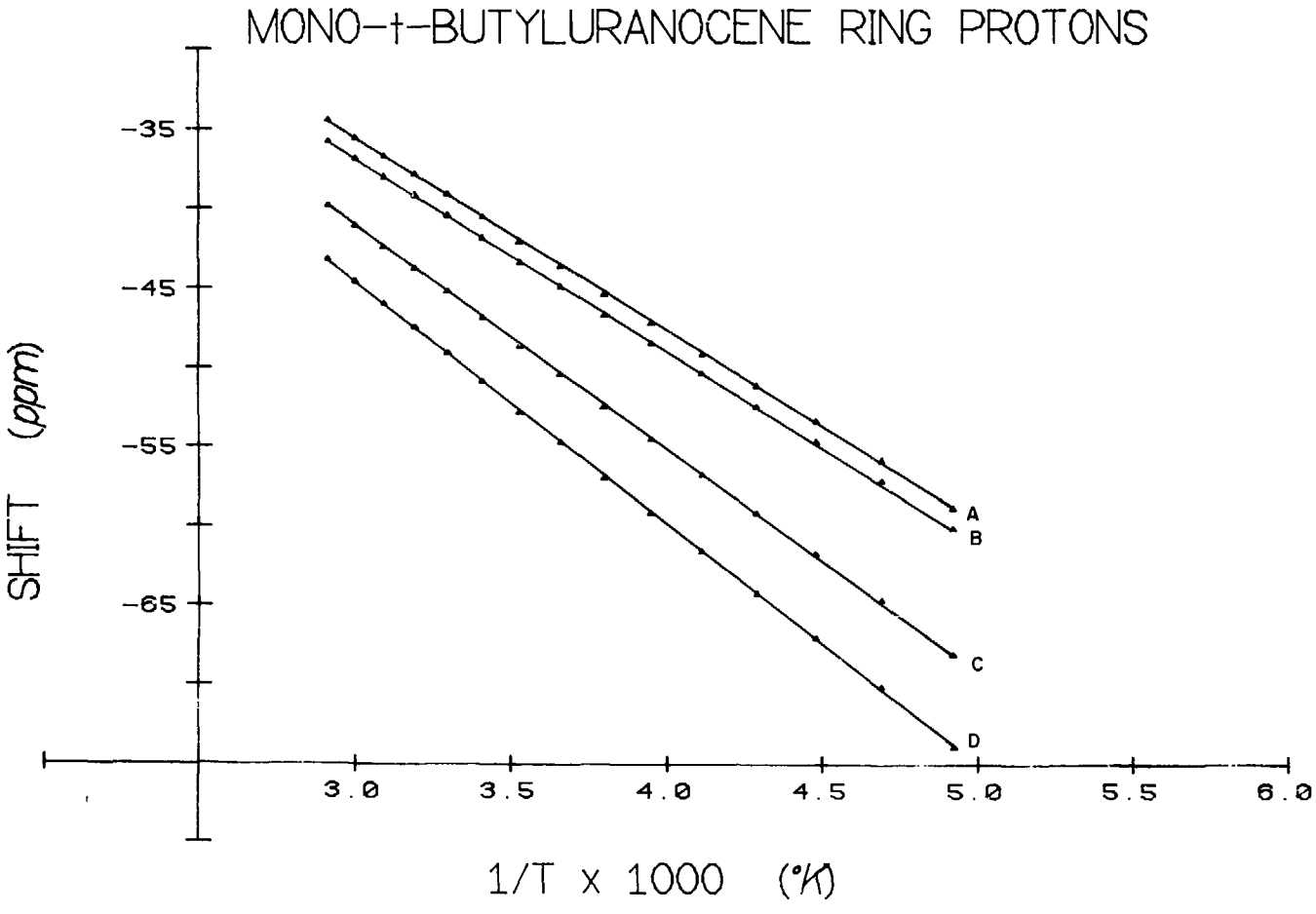
MONO-t-BUTYLURANOCENE RING PROTONS
SHIFT (ppm)
-35
-45
-55
-65
A
B
C
D
3.0
3.5
4.0
4.5
5.0
5.5
6.0
1/T x 1000 (°K)

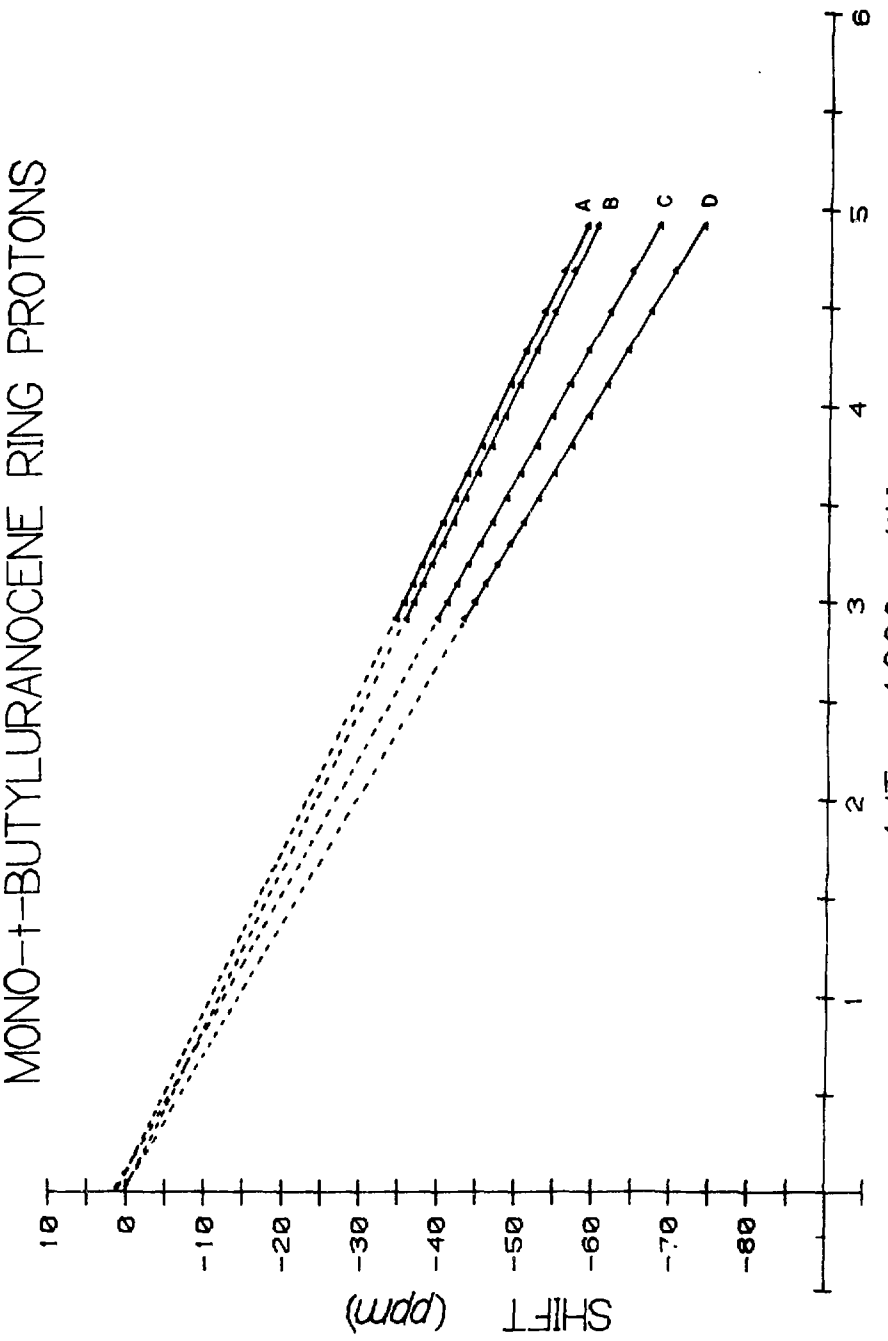
MONO-t-BUTYLURANOCENE RING PROTONS
SHIFT (ppm)
10
0
-10
-20
-30
-40
-50
-60
-70
-80
1/T x 1000 (°K)
1
2
3
4
5
6
A
B
C
D

Fig. 3-15 and 3-16 Isotropic shift vs T^{-1} for the ring protons in 1,1'-di-t-butyluranocene.

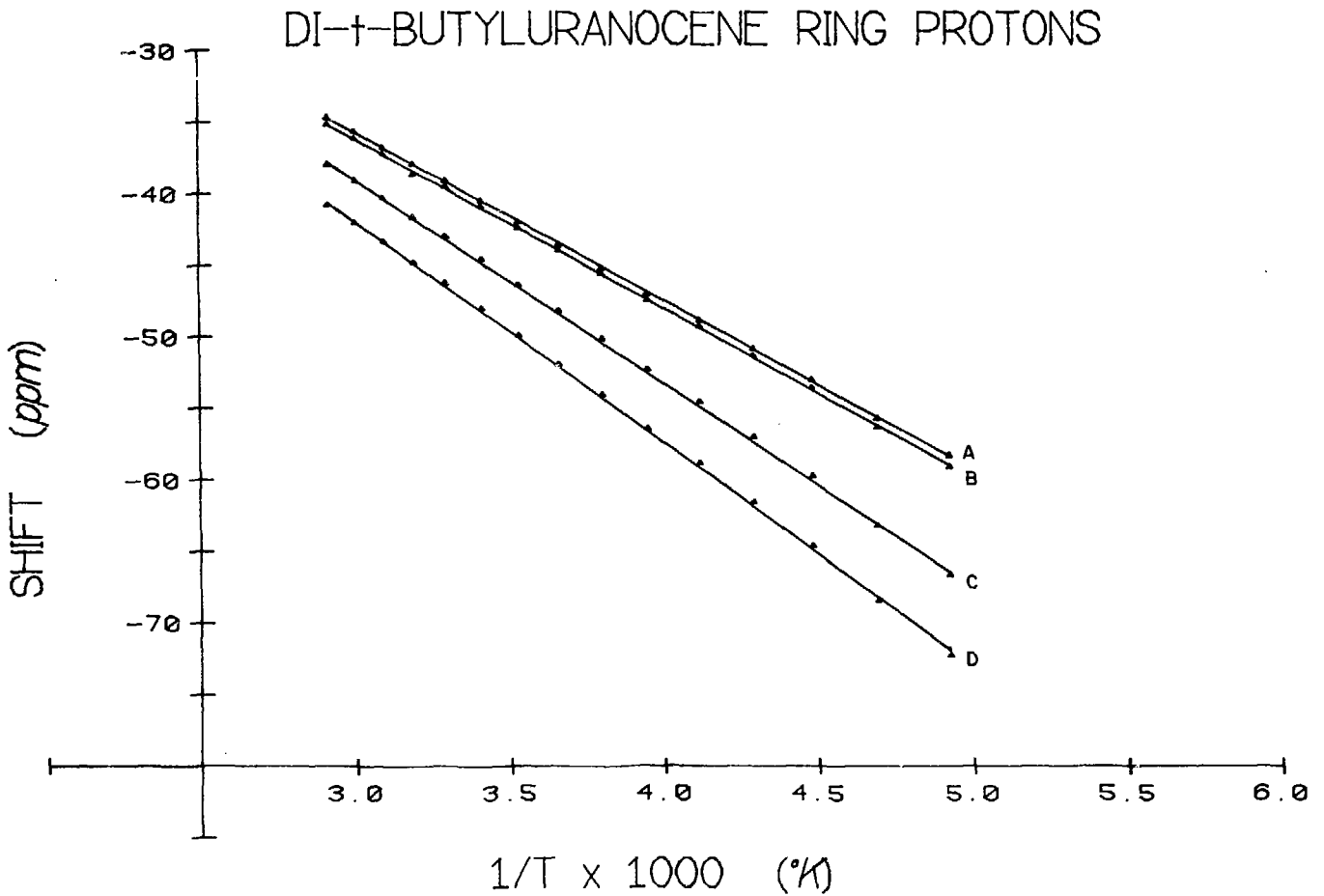
DI-t-BUTYLURANOCENE RING PROTONS
SHIFT (ppm)
-30
-40
-50
-60
-70
A
B
C
D
3.0
3.5
4.0
4.5
5.0
5.5
6.0
1/T x 1000 (°K)

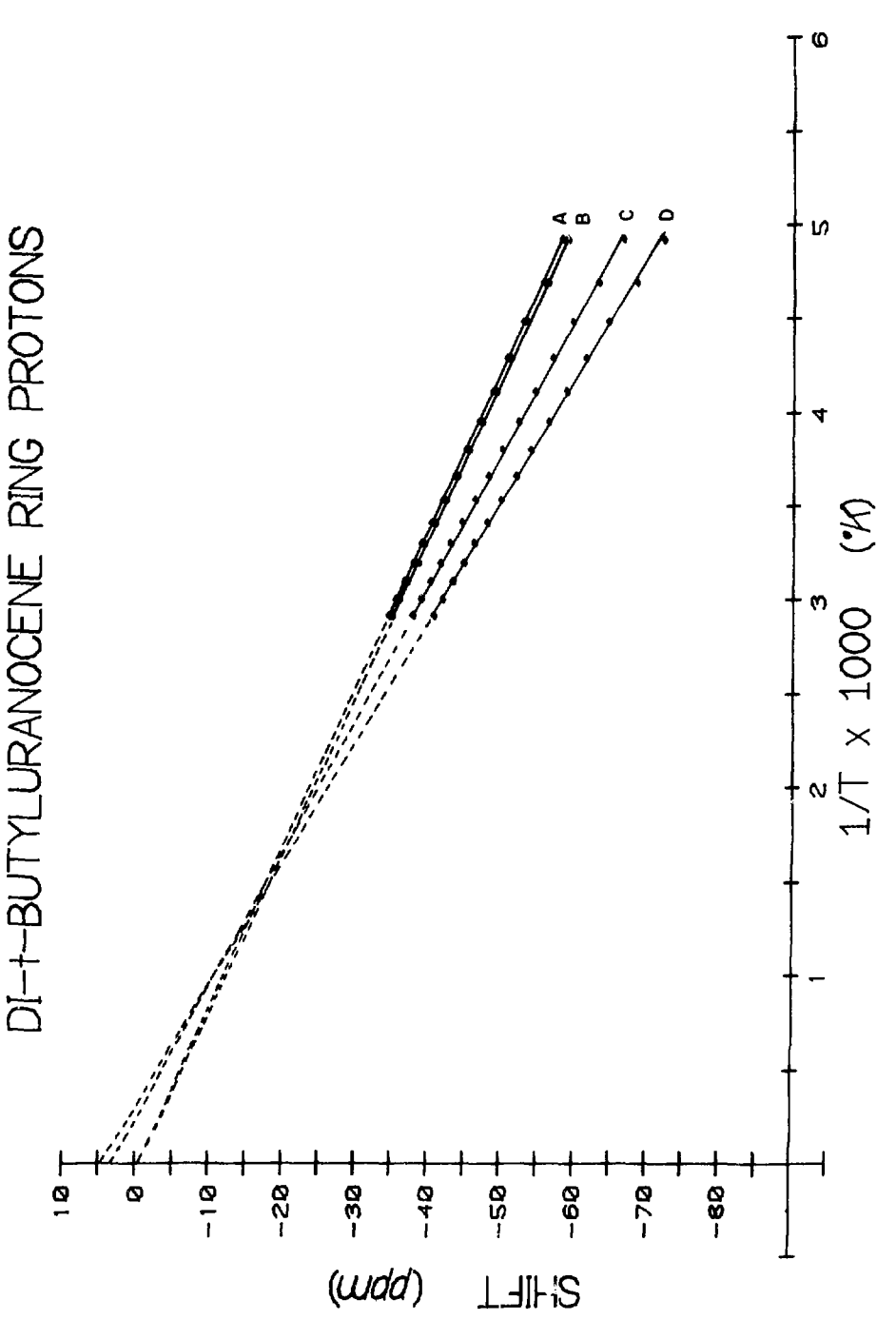
DI-t-BUTYLURANOCENE RING PROTONS
SHIFT (ppm)
10
0
-10
-20
-30
-40
-50
-60
-70
-80
1
2
3
4
5
6
1/T x 1000 (°K)
A
B
C
D

Fig. 3-17 and 3-18 Isotropic shift vs T^{-1} for the ring protons in 1,1'-diethyluranocene.

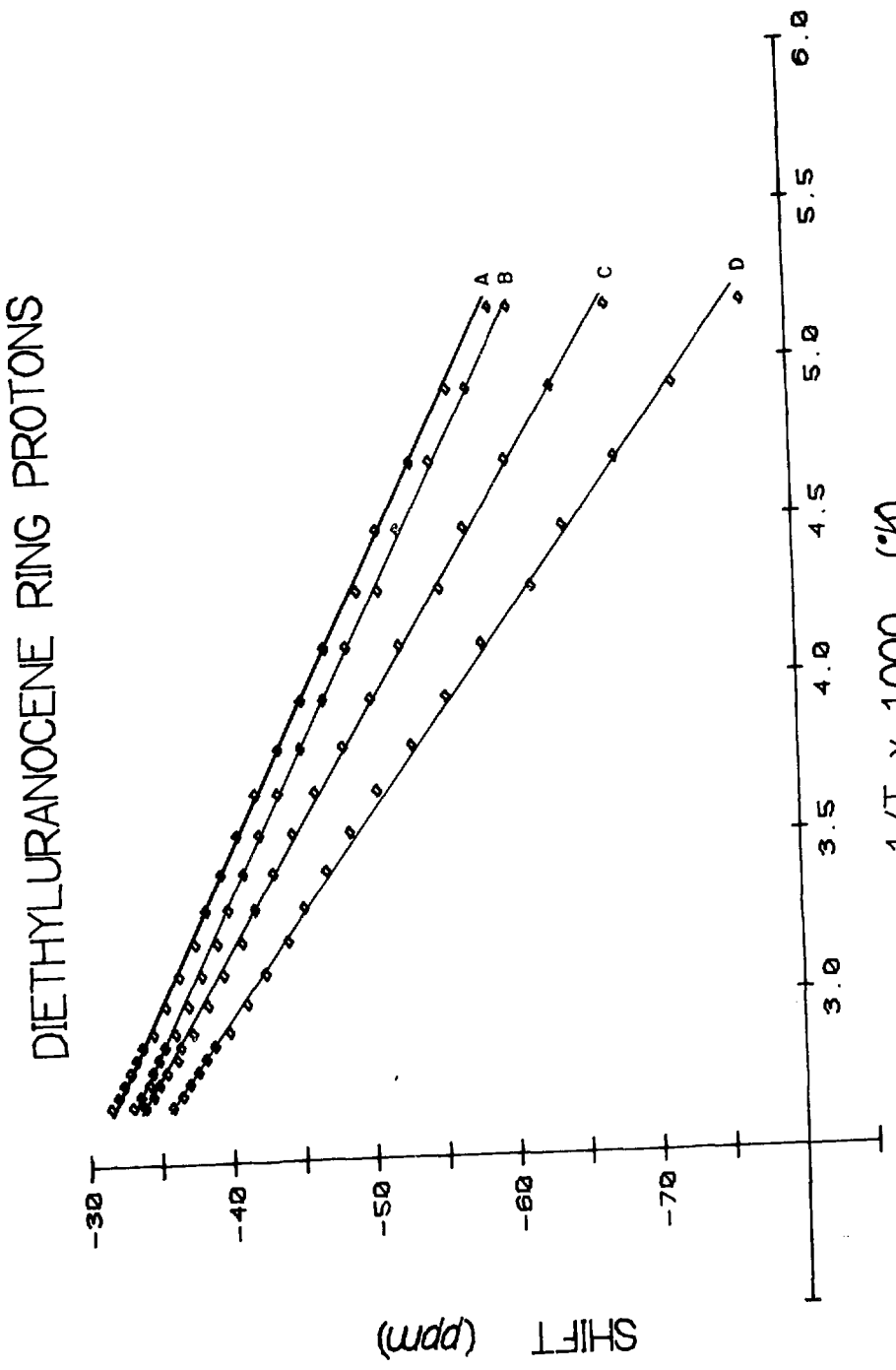
DIETHYLURANOCENE RING PROTONS
SHIFT (ppm)
-30
-40
-50
-60
-70
1/T x 1000 (°K)
3.0
3.5
4.0
4.5
5.0
5.5
6.0
A
B
C
D

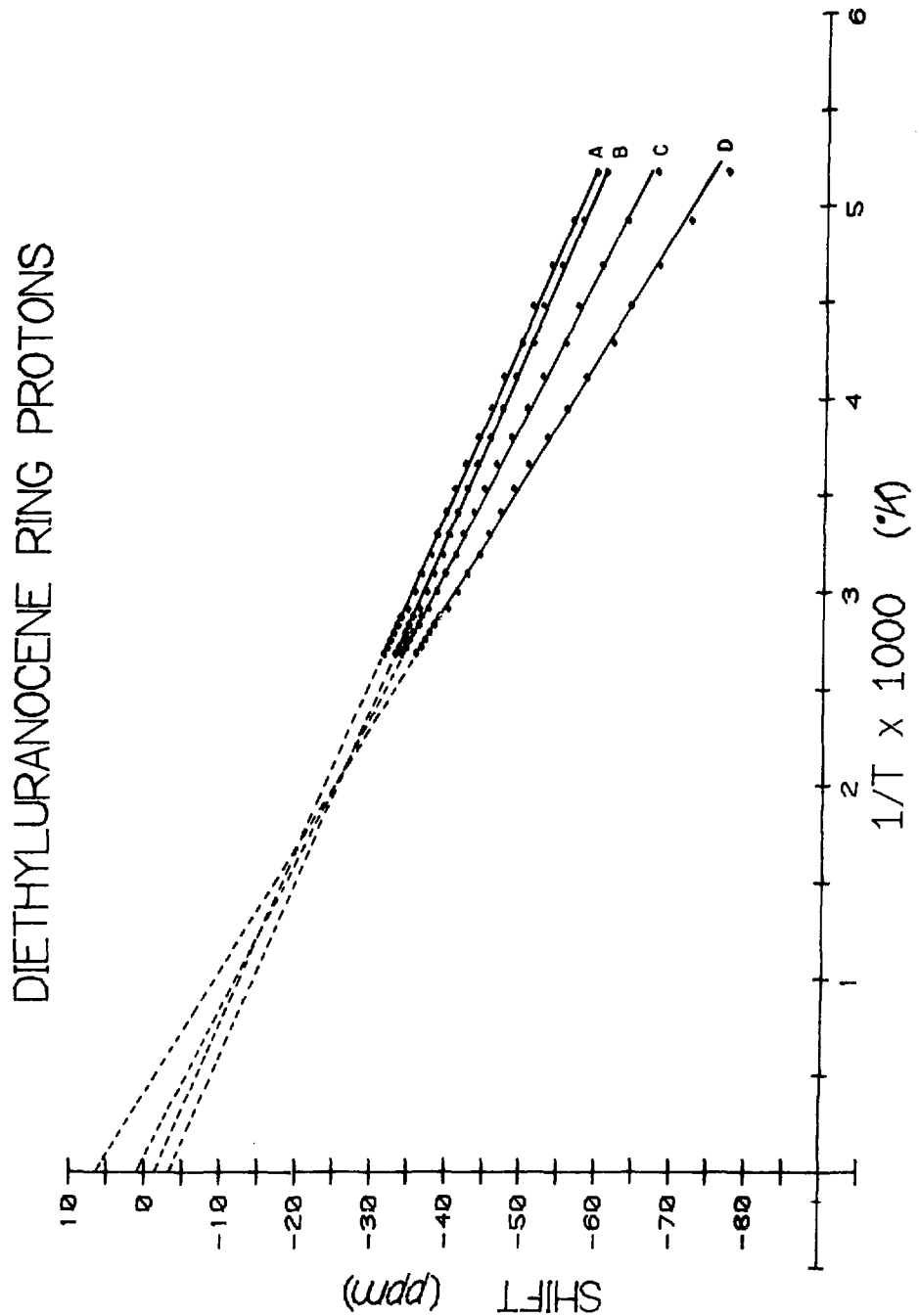
DIETHYLURANOCENE RING PROTONS
SHIFT (ppm)
10
0
-10
-20
-30
-40
-50
-60
-70
-80
1/T x 1000 (°K)
1
2
3
4
5
6
A
B
C
D

Fig. 3-19 and 3-20 Isotropic shift vs T^{-1} for the ring protons in 1,1'-di-n-butyluranocene.

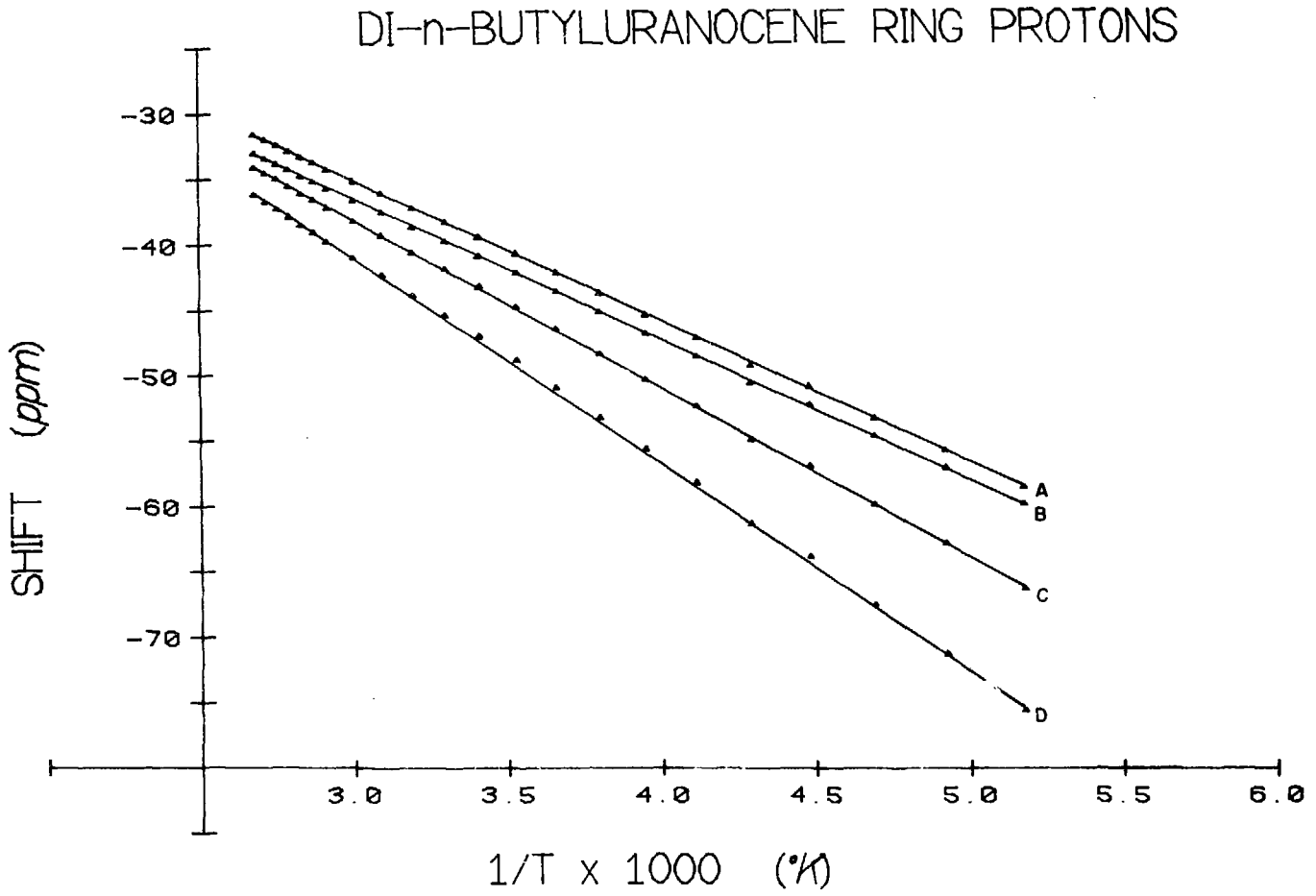
DI-n-BUTYLURANOCENE RING PROTONS
SHIFT (ppm)
-30
-40
-50
-60
-70
A
B
C
D
3.0
3.5
4.0
4.5
5.0
5.5
6.0
1/T x 1000 (°K)

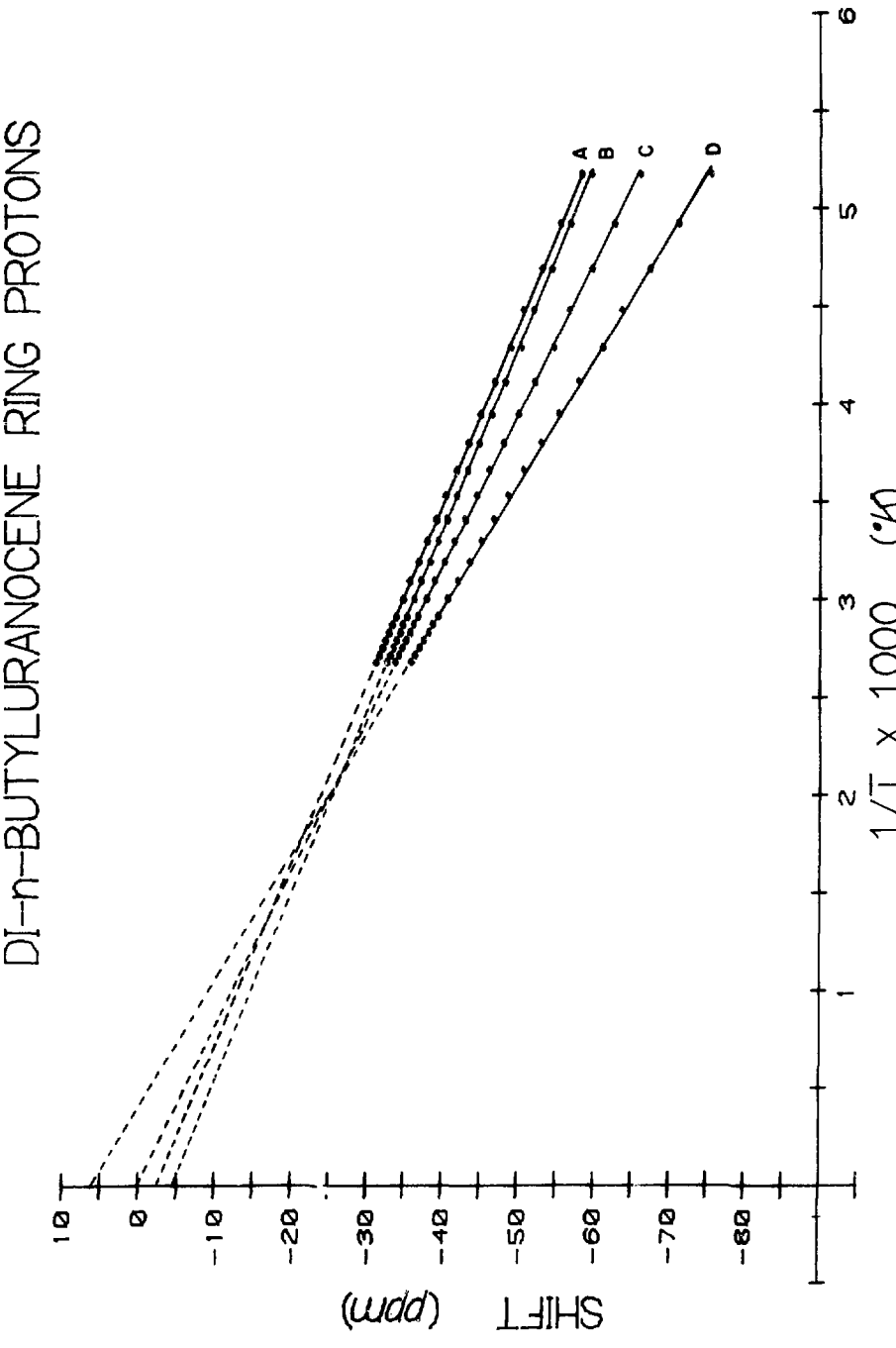
DI-n-BUTYLURANOCENE RING PROTONS
SHIFT (ppm)
10
0
-10
-20
-30
-40
-50
-60
-70
-80
1
2
3
4
5
6
1/T x 1000 (°K)
A
B
C
D

Fig. 3-21 and 3-22 Isotropic shift vs T^{-1} for the ring protons in 1,1'-dineopentyluranocene.

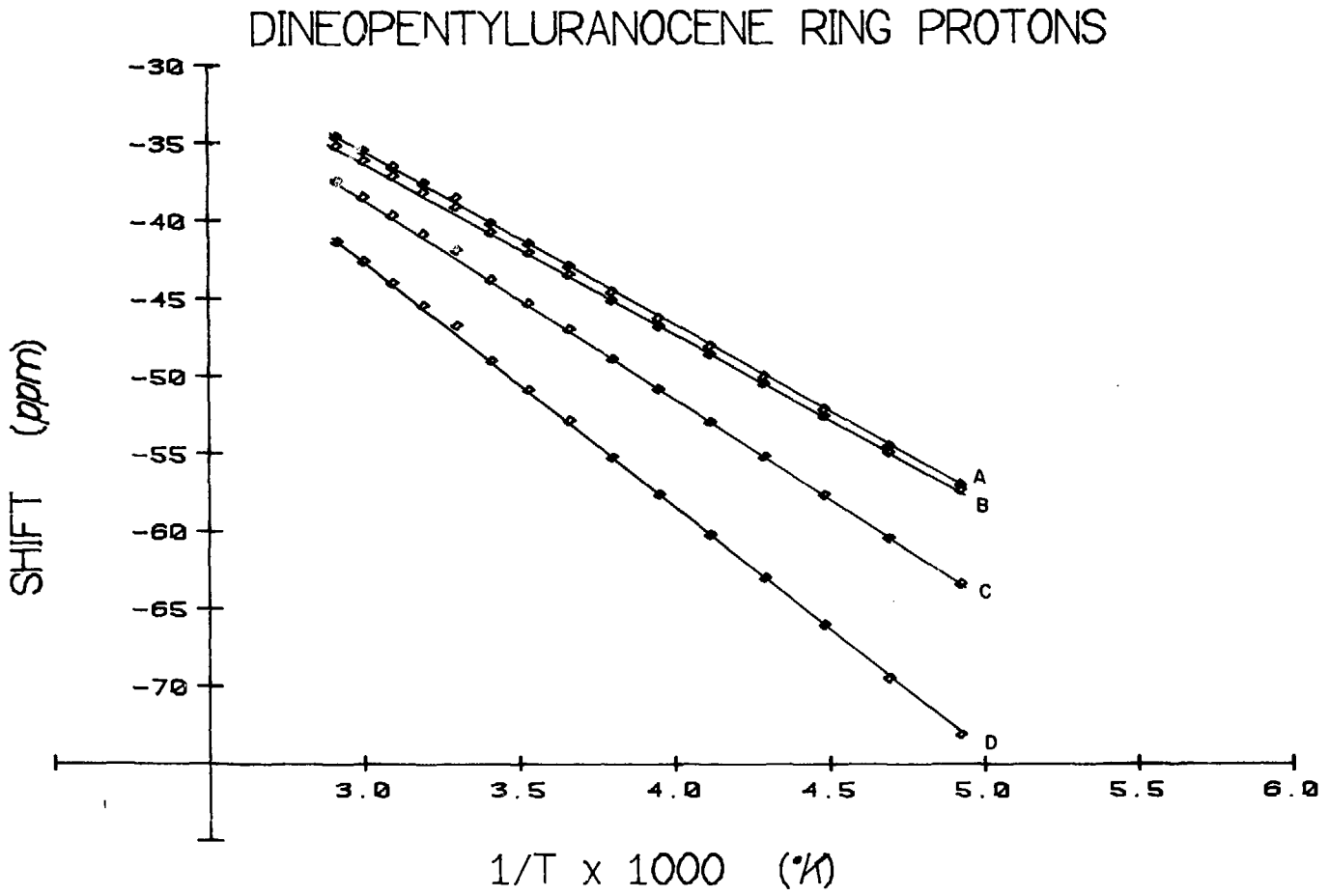
DINEOPENTYLURANOCENE RING PROTONS
SHIFT (ppm)
-30
-35
-40
-45
-50
-55
-60
-65
-70
3.0
3.5
4.0
4.5
5.0
5.5
6.0
1/T x 1000 (°K)
A
B
C
D

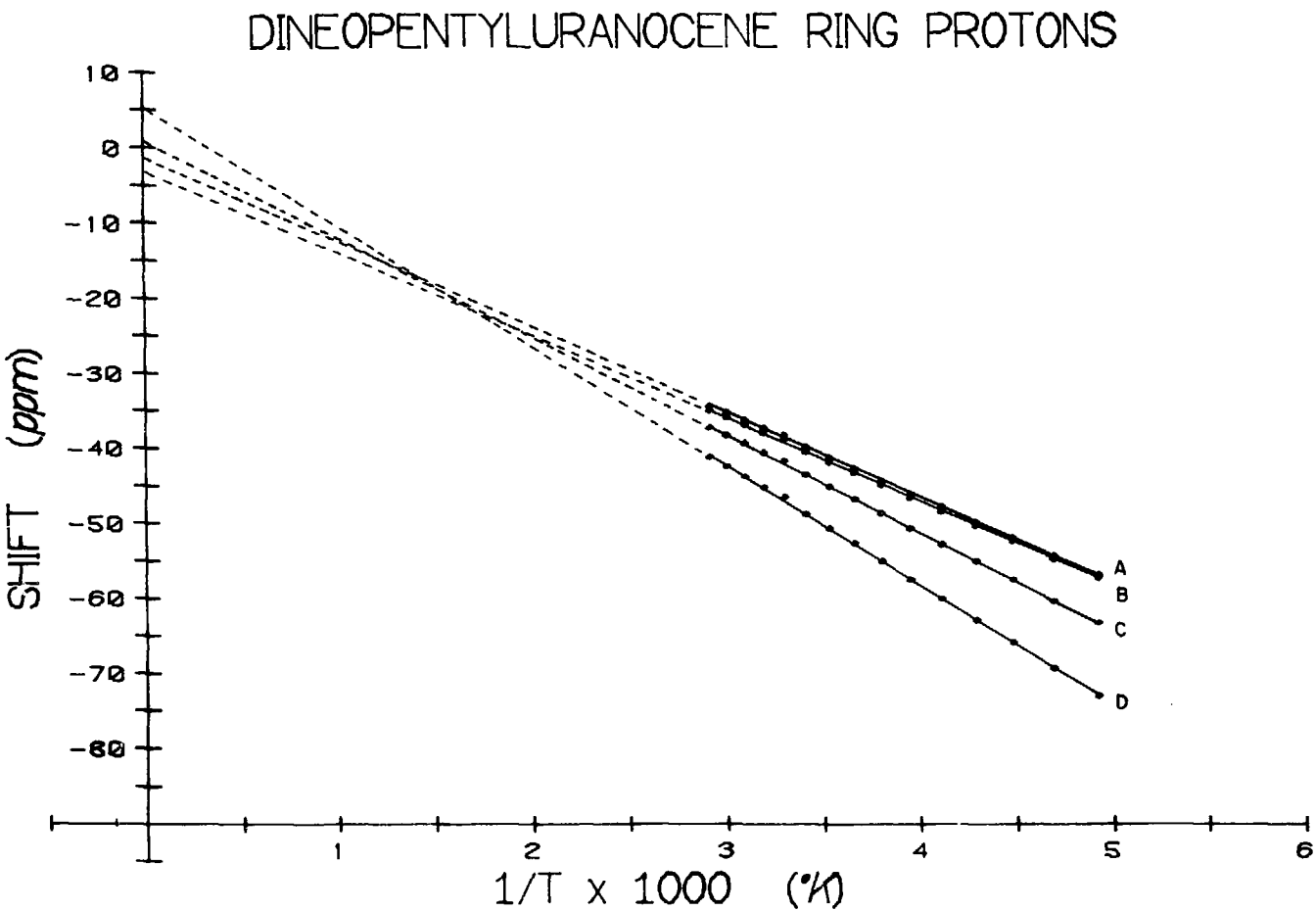
DINEOPENTYLURANOCENE RING PROTONS
SHIFT (ppm)
10
0
-10
-20
-30
-40
-50
-60
-70
-80
1
2
3
4
5
6
1/T x 1000 (°K)
A
B
C
D

Fig. 3-23 and 3-24 Isotropic shift vs T^{-1} for the ring protons in 1,1'-diisopropyluranocene

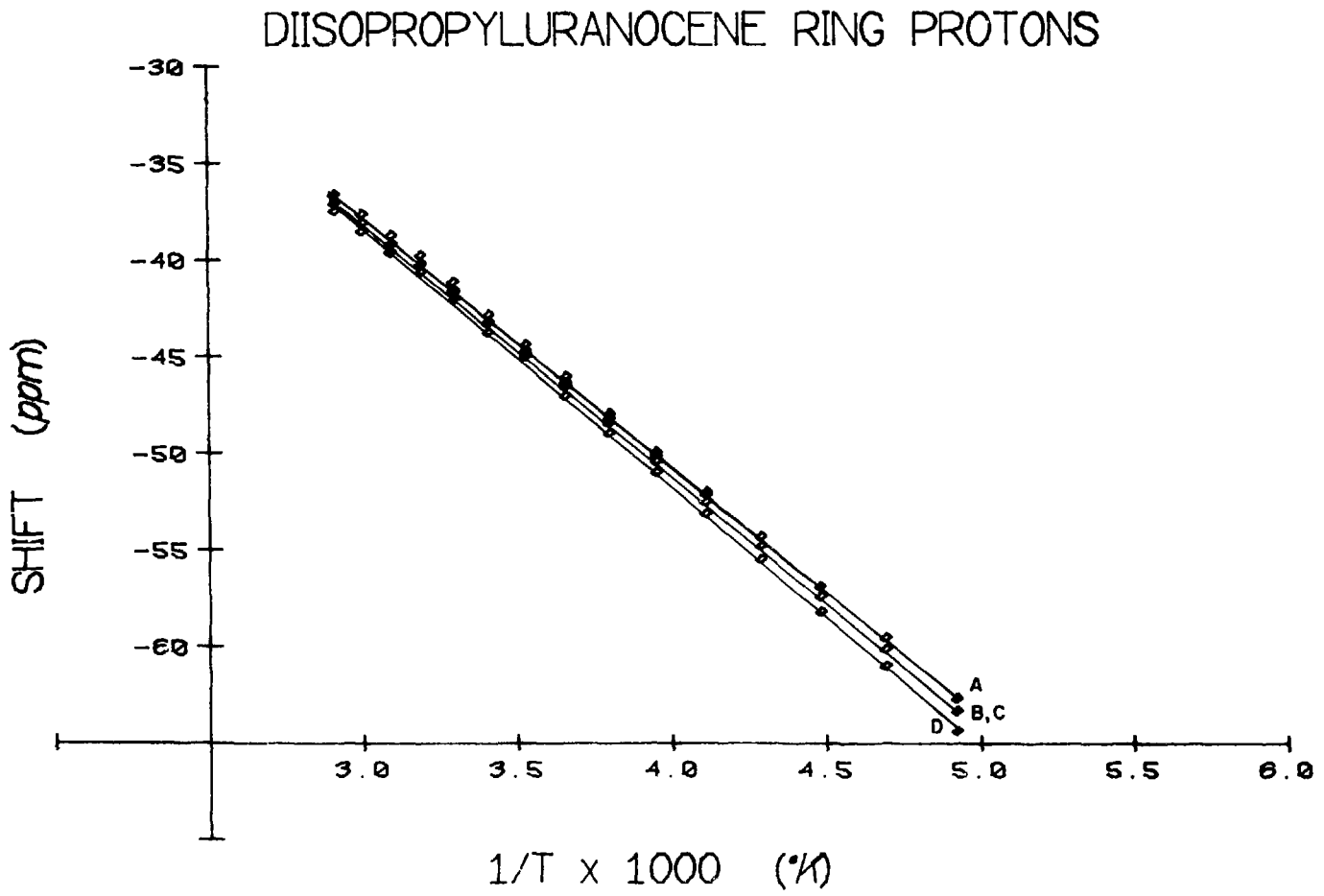
DIISOPROPYLURANOCENE RING PROTONS
SHIFT (ppm)
-30
-35
-40
-45
-50
-55
-60
3.0
3.5
4.0
4.5
5.0
5.5
6.0
A
B,C
D
1/T x 1000 (°/K)

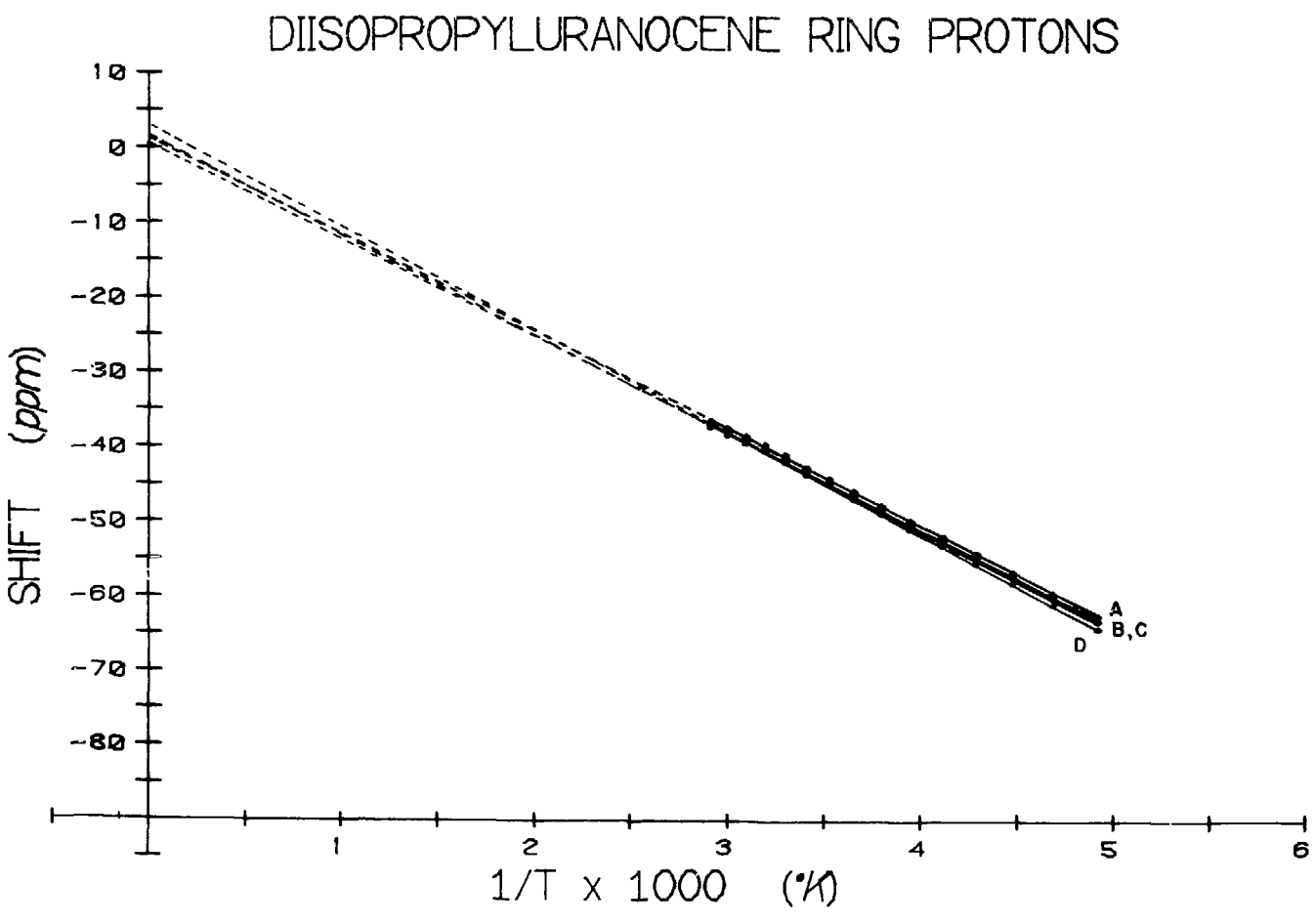
DIISOPROPYLURANOCENE RING PROTONS
SHIFT (ppm)
10
0
-10
-20
-30
-40
-50
-60
-70
-80
1
2
3
4
5
6
1/T x 1000 (°K)
A
B,C
D

Fig. 3-25 and 3-26 Isotropic shift vs T^{-1} for the ring protons in dicyclobutenouranocene.

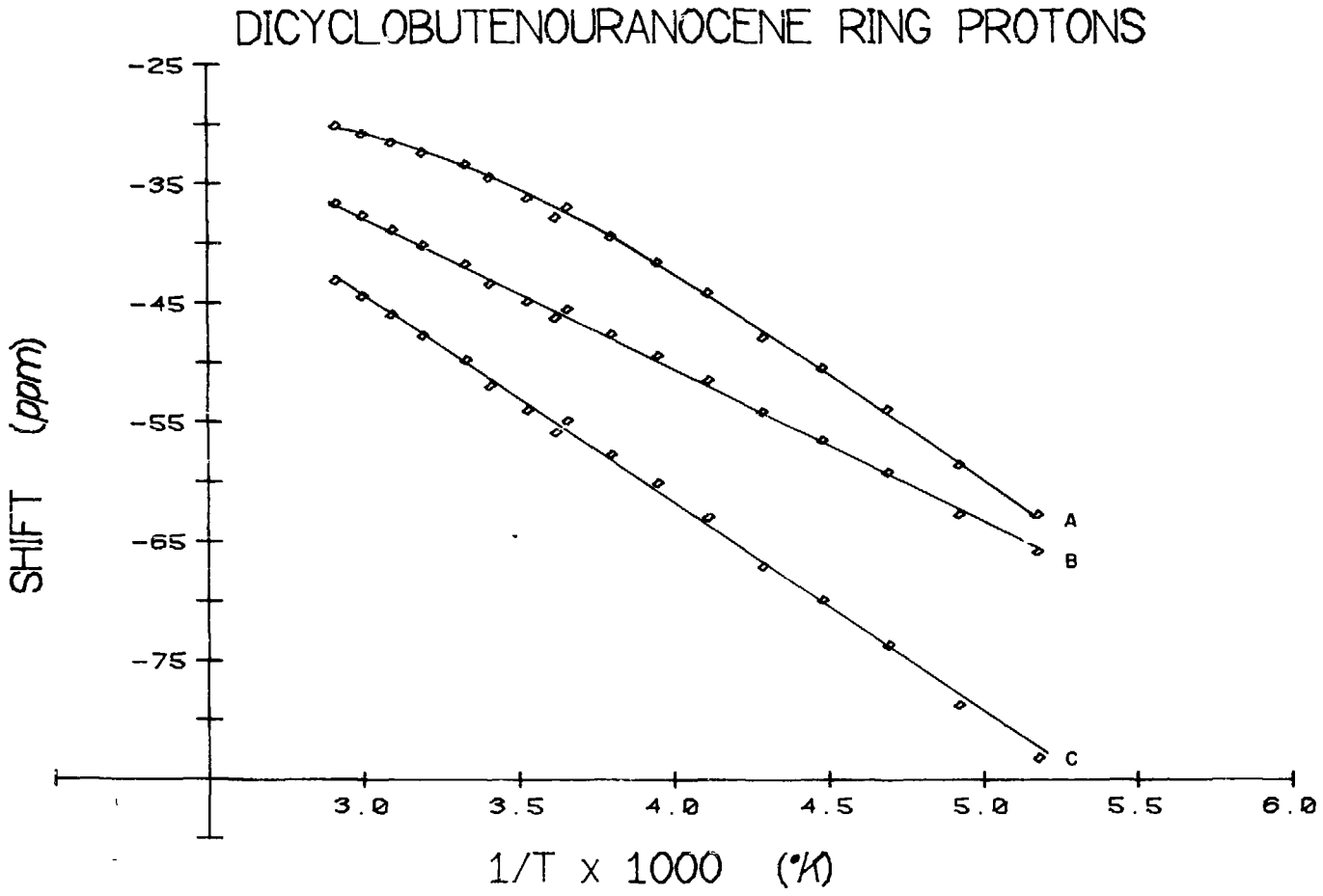
DICYCLOBUTENOURANOCENE RING PROTONS
SHIFT (ppm)
-25
-35
-45
-55
-65
-75
3.0
3.5
4.0
4.5
5.0
5.5
6.0
1/T x 1000 (°K)
A
B
C

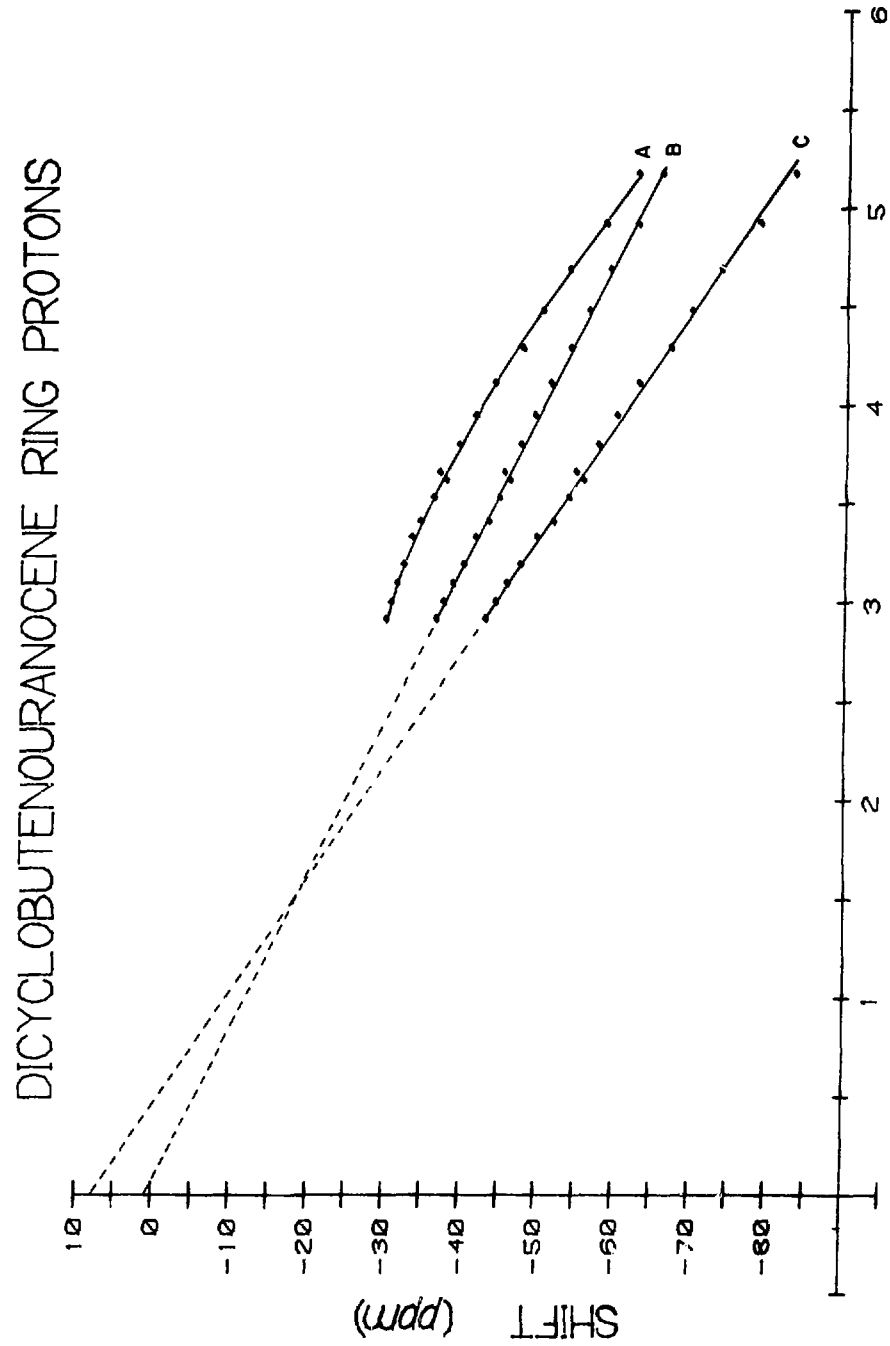
DICYCLOBUTENOURANOCENE RING PROTONS
SHIFT (ppm)
10
0
-10
-20
-30
-40
-50
-60
-70
-80
1
2
3
4
5
6
1/T x 1000 (°K)
A
B
C

Fig. 3-27 and 3-28 Isotropic shift vs T^{-1} for the ring protons in dicyclopentenouranocene.

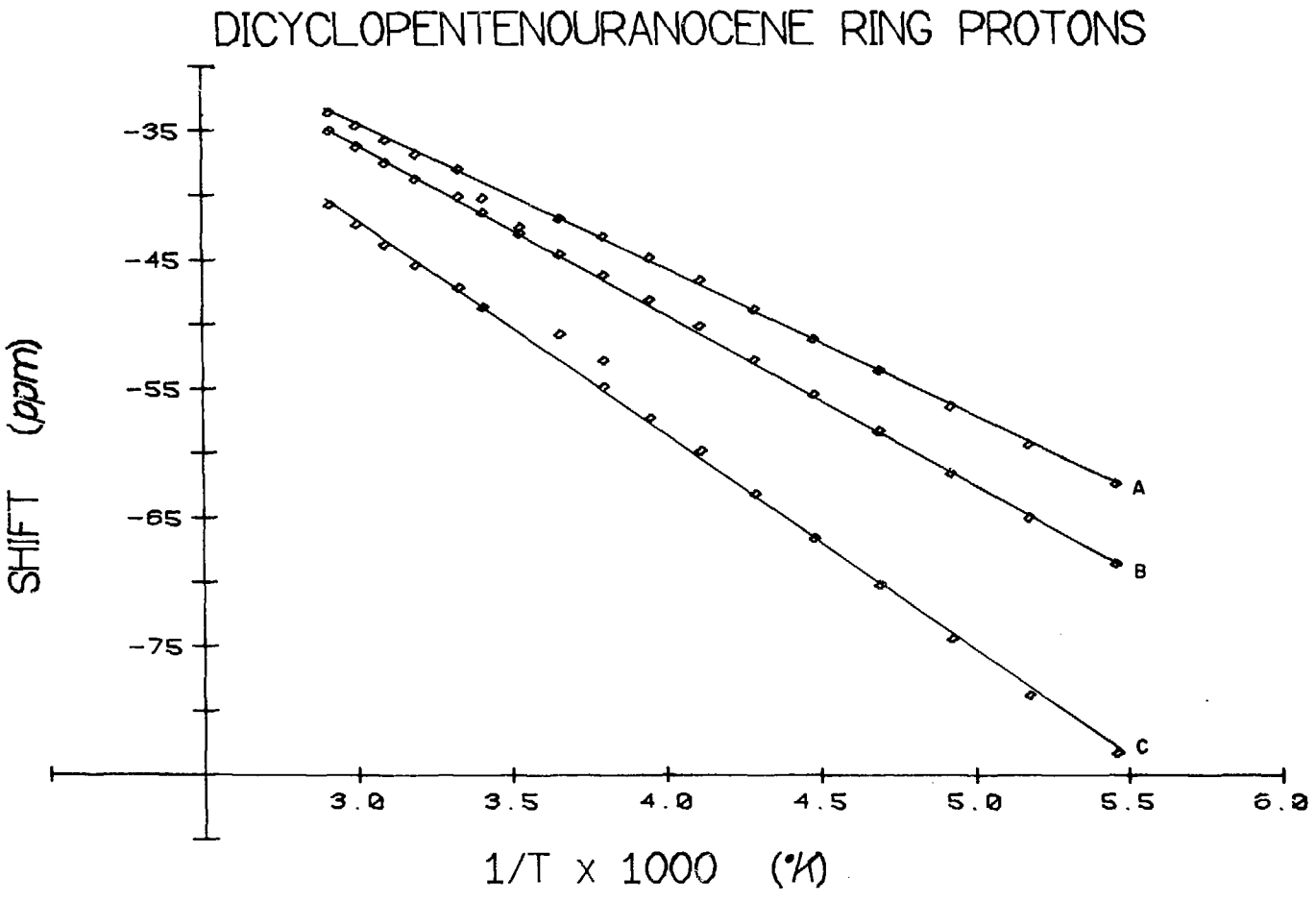
DICYCLOPENTENOURANOCENE RING PROTONS
SHIFT (ppm)
-35
-45
-55
-65
-75
A
B
C
3.0
3.5
4.0
4.5
5.0
5.5
6.0
1/T x 1000 (°K)

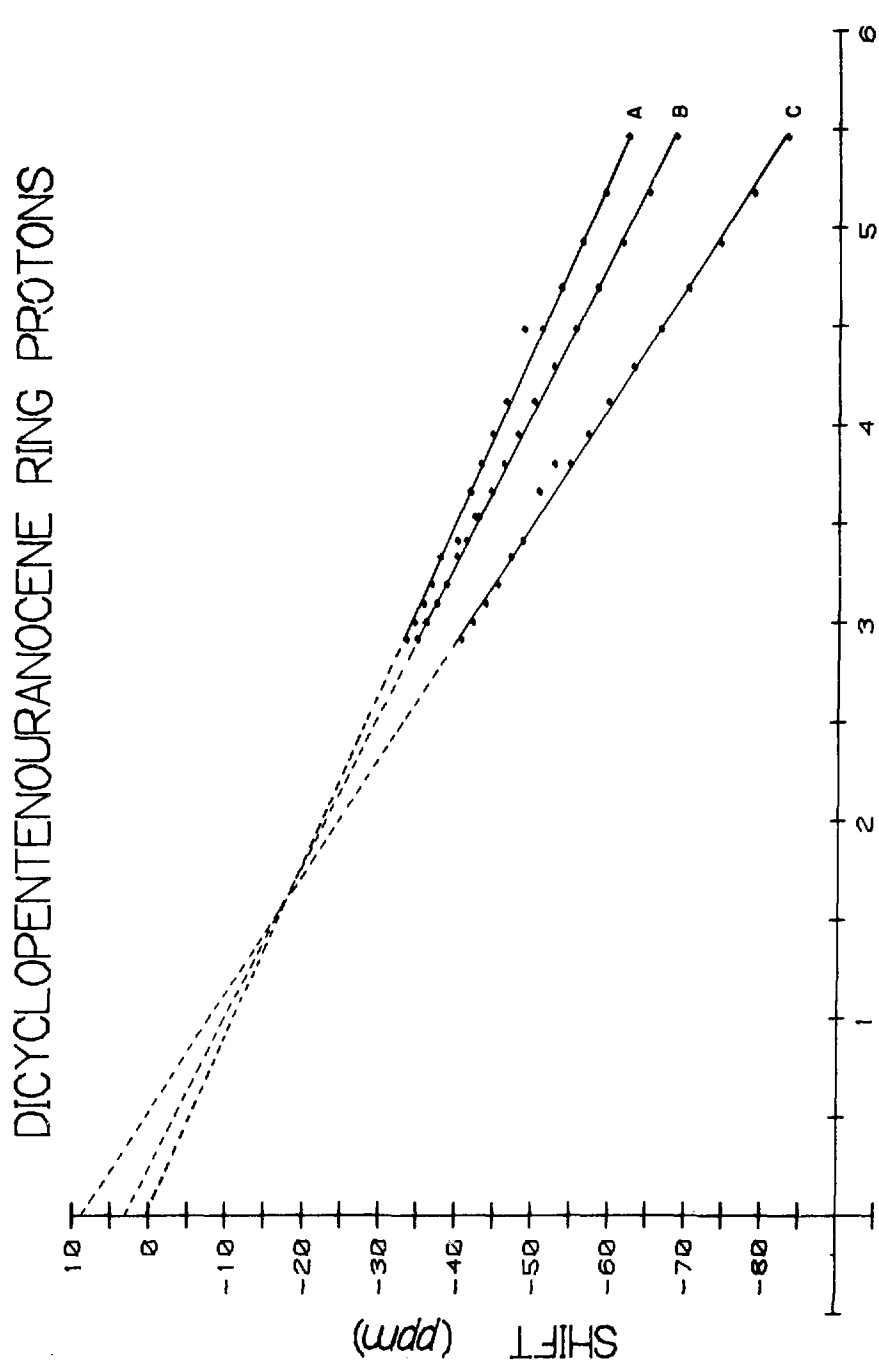
DICYCLOPENTENOURANOCENE RING PROTONS
SHIFT (ppm)
10
0
-10
-20
-30
-40
-50
-60
-70
-80
1/T x 1000 (°K)
1
2
3
4
5
6
A
B
C

Fig. 3-29 and 3-30 Isotropic shift vs T^{-1} for the ring protons in bis(dimethylcyclopenteno)uranocene.

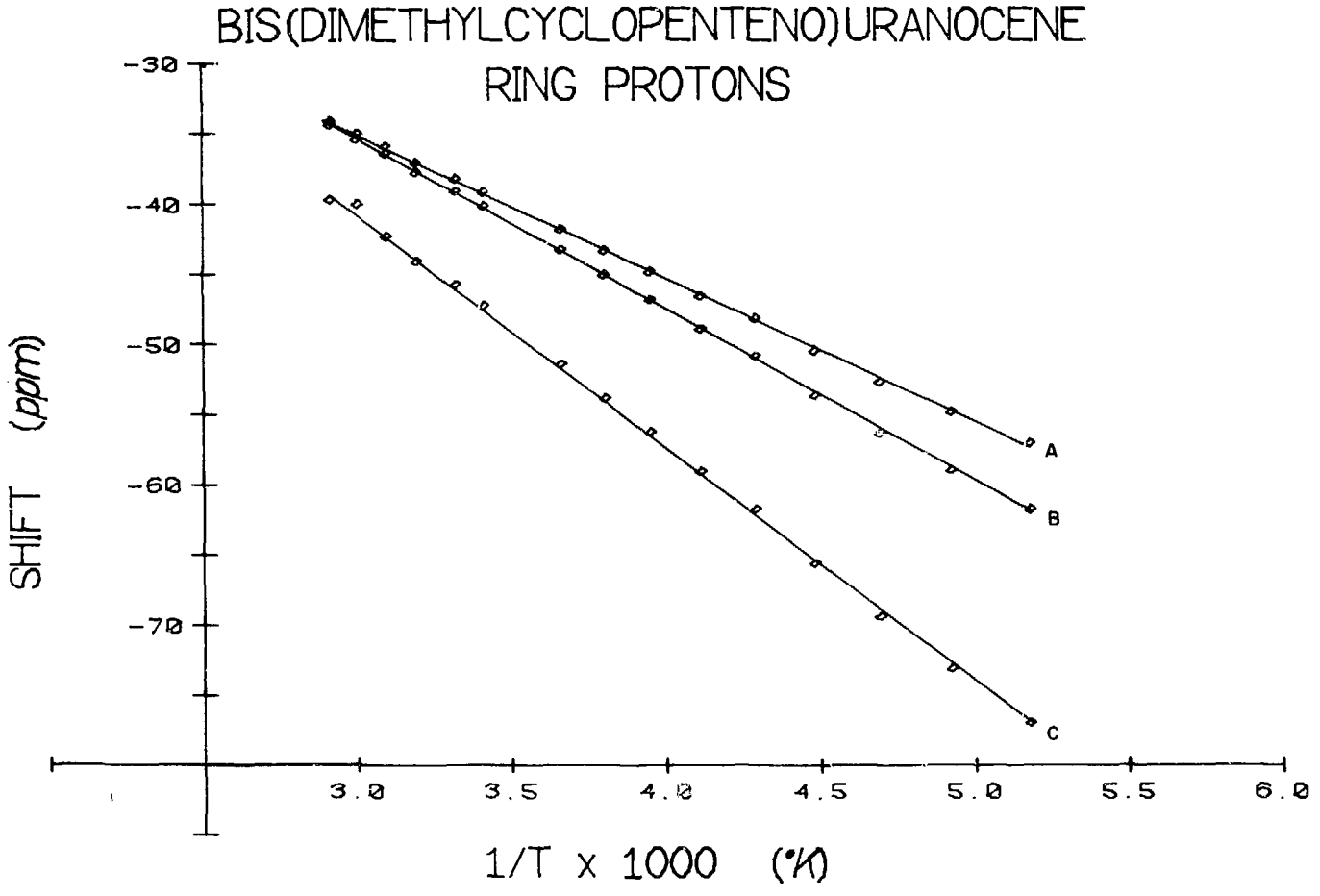
BIS(DIMETHYLCYCLOPENTENO)URANOCENE
RING PROTONS
-30
-40
-50
-60
-70
SHIFT (ppm)
A
B
C
3.0
3.5
4.0
4.5
5.0
5.5
6.0
1/T x 1000 (°K)

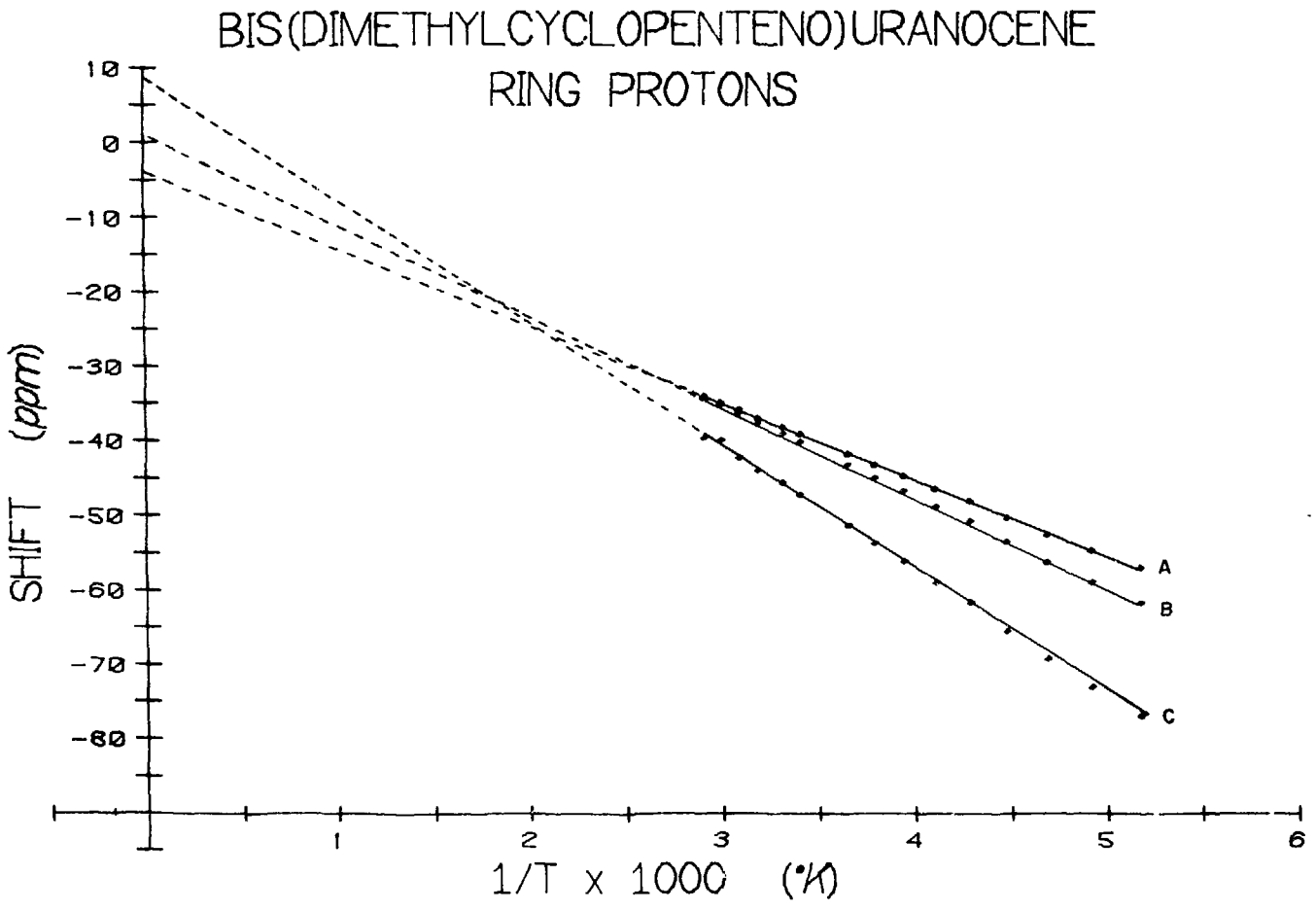
BIS(DIMETHYLCYCLOPENTENO)URANOCENE
RING PROTONS
SHIFT (ppm)
10
0
-10
-20
-30
-40
-50
-60
-70
-80
1
2
3
4
5
6
1/T x 1000 (°K)
A
B
C

Fig. 3-31 and 3-32 Isotropic shift vs T^{-1} for the ring protons in 1,1'-diphenyluranocene.

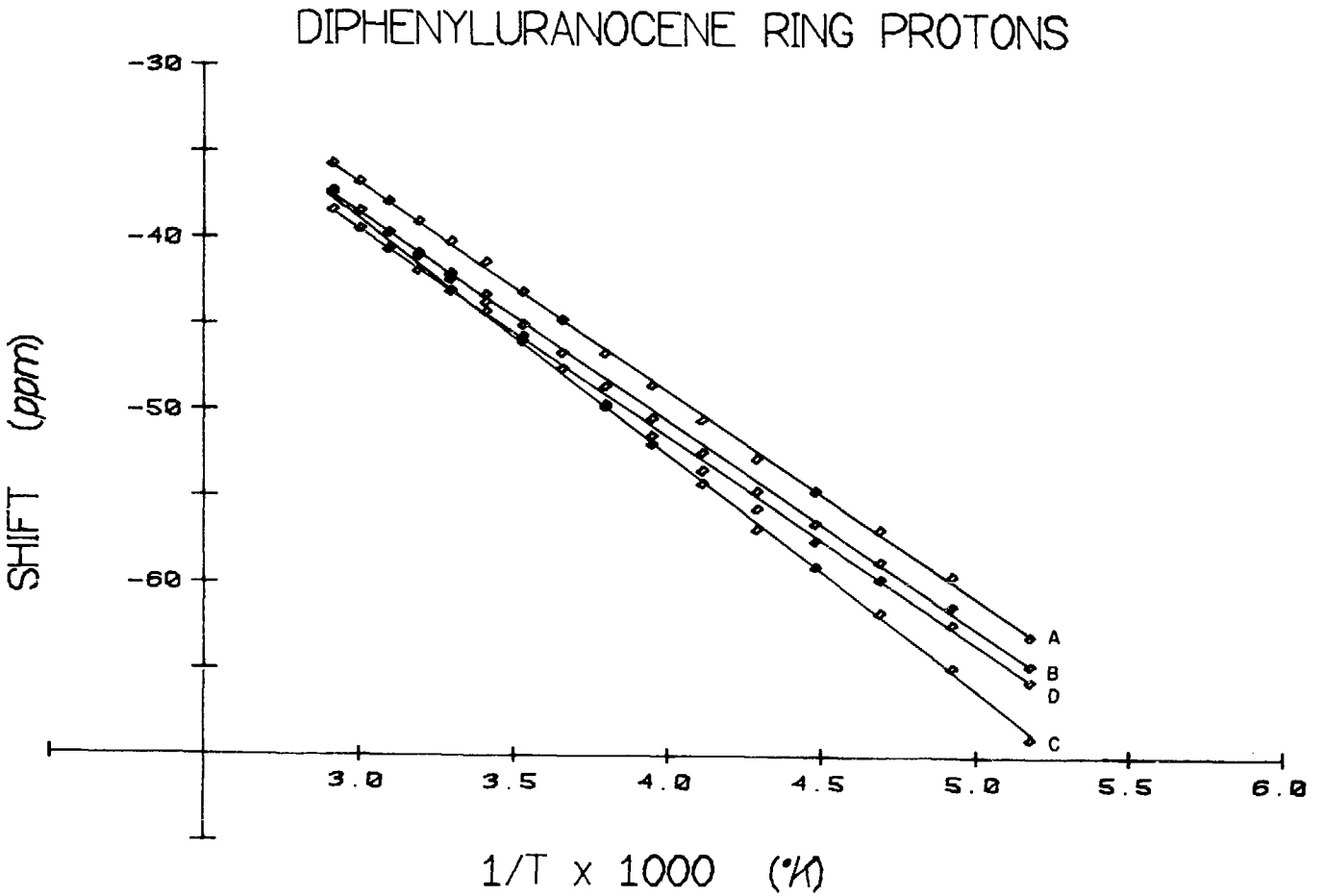
DIPHENYLURANOCENE RING PROTONS
SHIFT (ppm)
-30
-40
-50
-60
3.0
3.5
4.0
4.5
5.0
5.5
6.0
1/T x 1000 (°K)
A
B
D
C

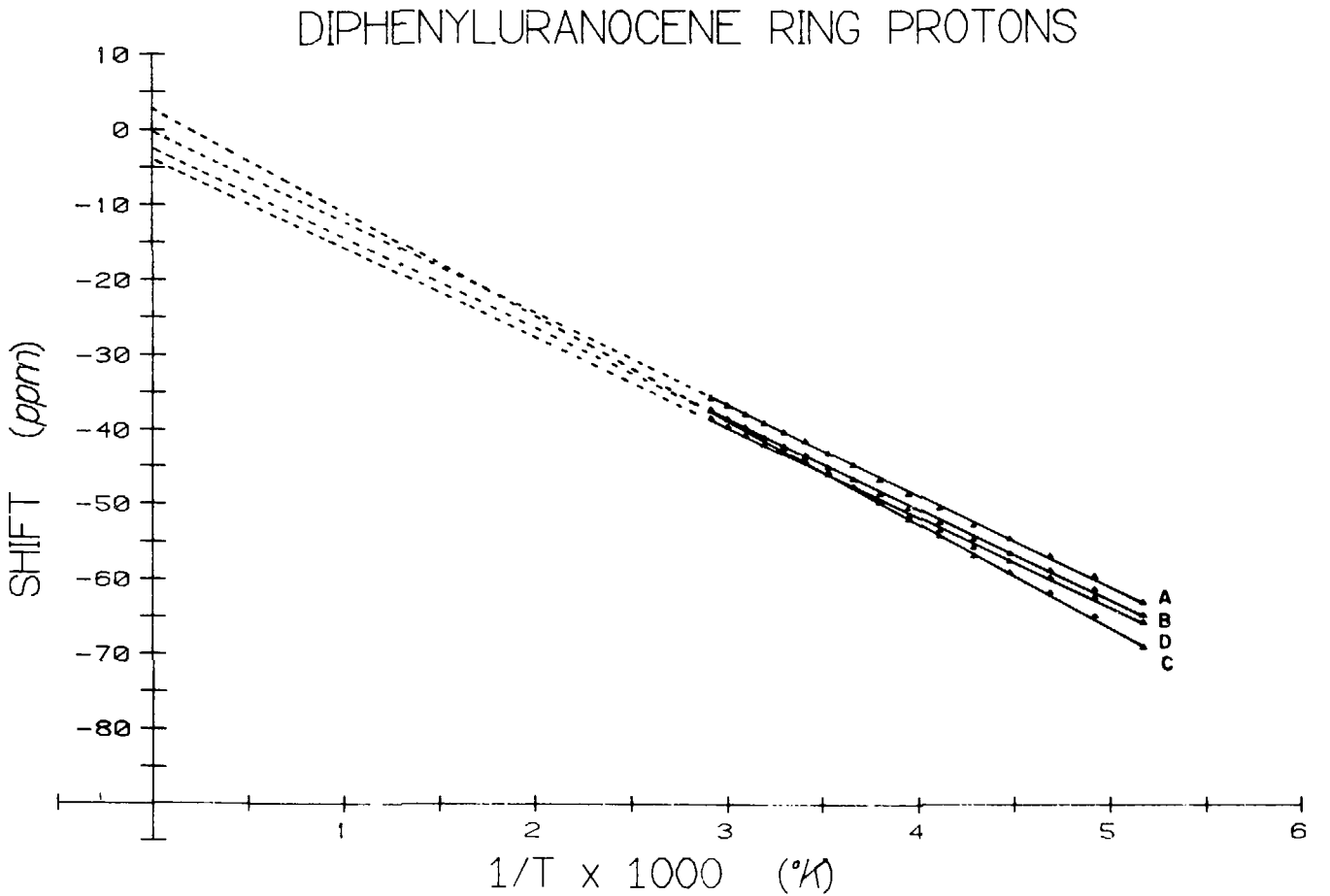
DIPHENYLURANOCENE RING PROTONS
SHIFT (ppm)
10
0
-10
-20
-30
-40
-50
-60
-70
-80
1
2
3
4
5
6
1/T x 1000 (°K)
A
B
D
C

Fig. 3-33 and 3-34 Isotropic shift vs T^{-1} for the ring protons in 1,1'-bis(p-dimethylaminophenyl)uranocene.

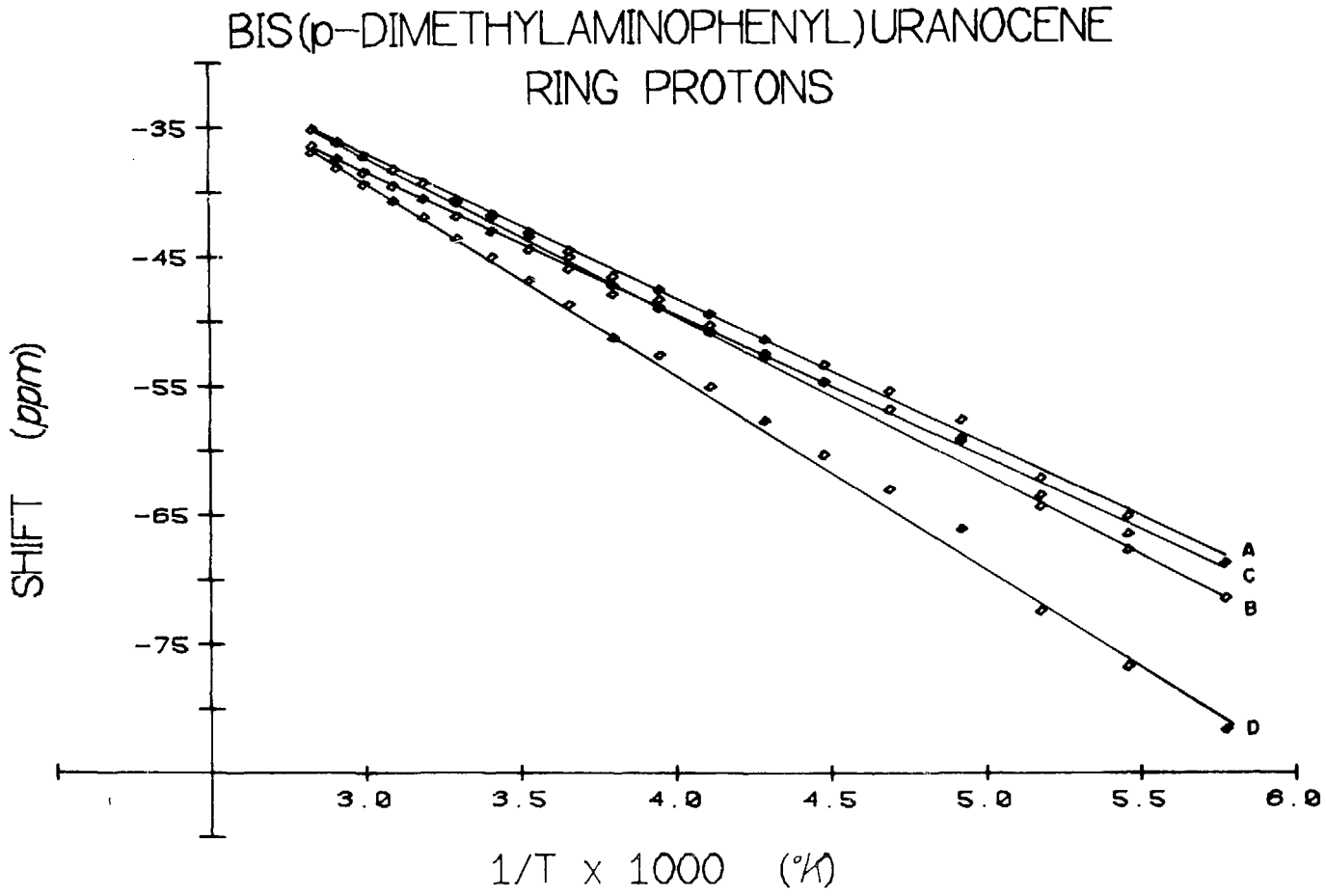
BIS(p-DIMETHYLAMINOPHENYL)URANOCENE
RING PROTONS
SHIFT (ppm)
-35
-45
-55
-65
-75
3.0
3.5
4.0
4.5
5.0
5.5
6.0
1/T x 1000 (°K)
A
C
B
D

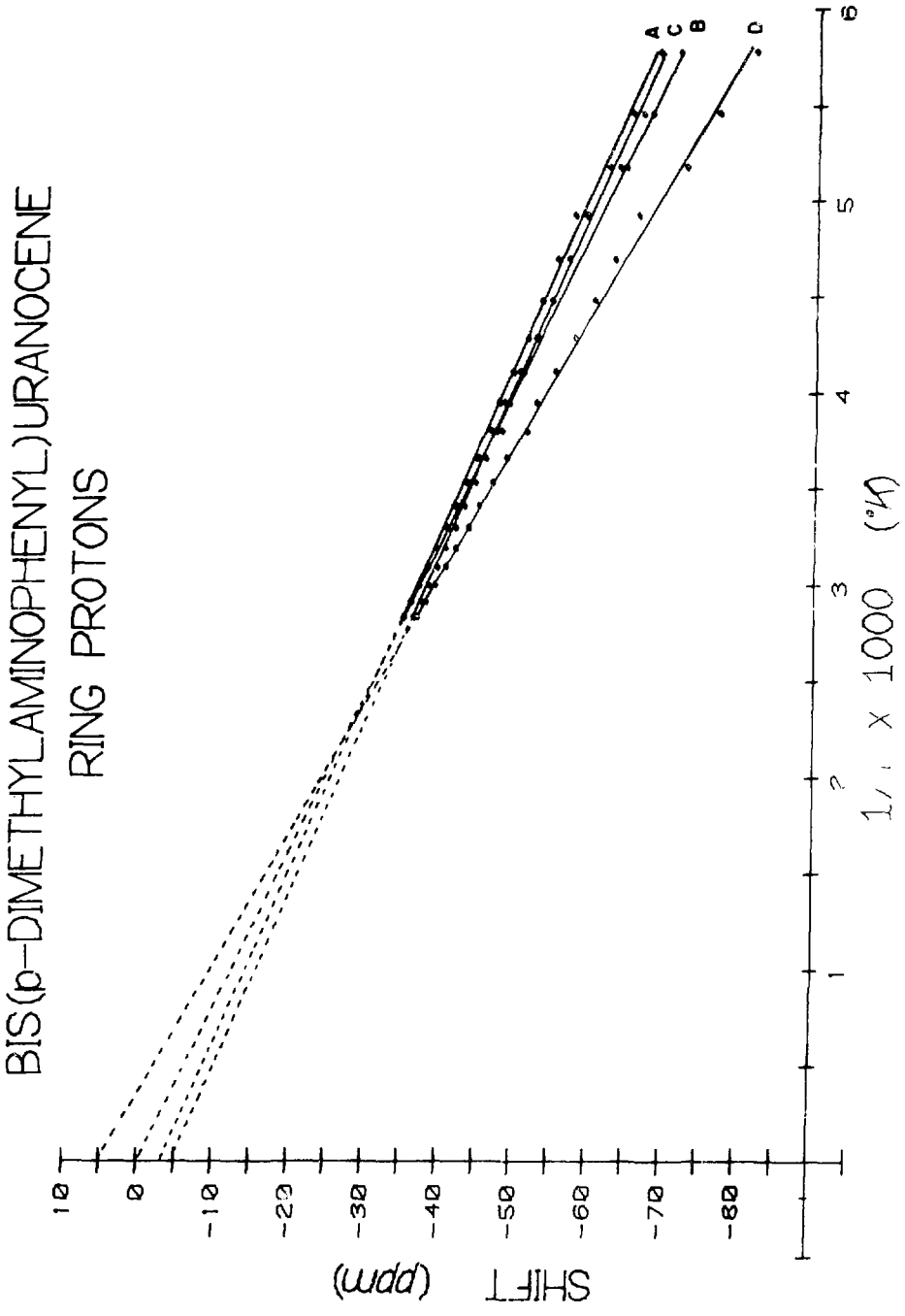
BIS(p-DIMETHYLAMINOPHENYL)URANOCENE
RING PROTONS
SHIFT (ppm)
10
0
-10
-20
-30
-40
-50
-60
-70
-80
1
2
3
4
5
6
A
C
B
D

Fig. 3-35 and 3-36 Isotropic shift vs T^{-1} for the ring protons of the substituted ring in mono-t-butoxycarbonyl-uranocene.

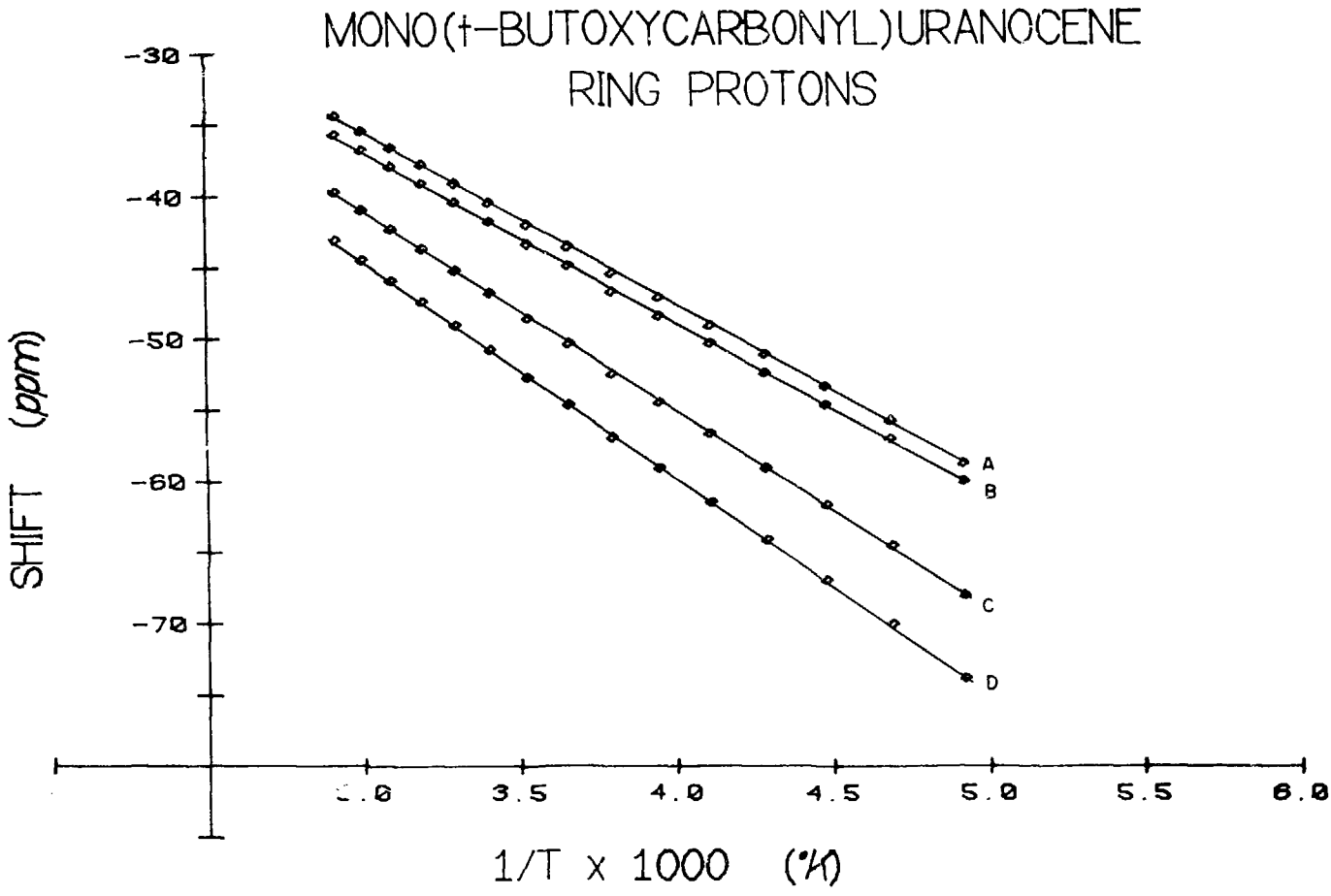
MONO(t-BUTOXYCARBONYL)URANOCENE
RING PROTONS
SHIFT (ppm)
-30
-40
-50
-60
-70
3.0
3.5
4.0
4.5
5.0
5.5
6.0
1/T x 1000 (°K)
A
B
C
D

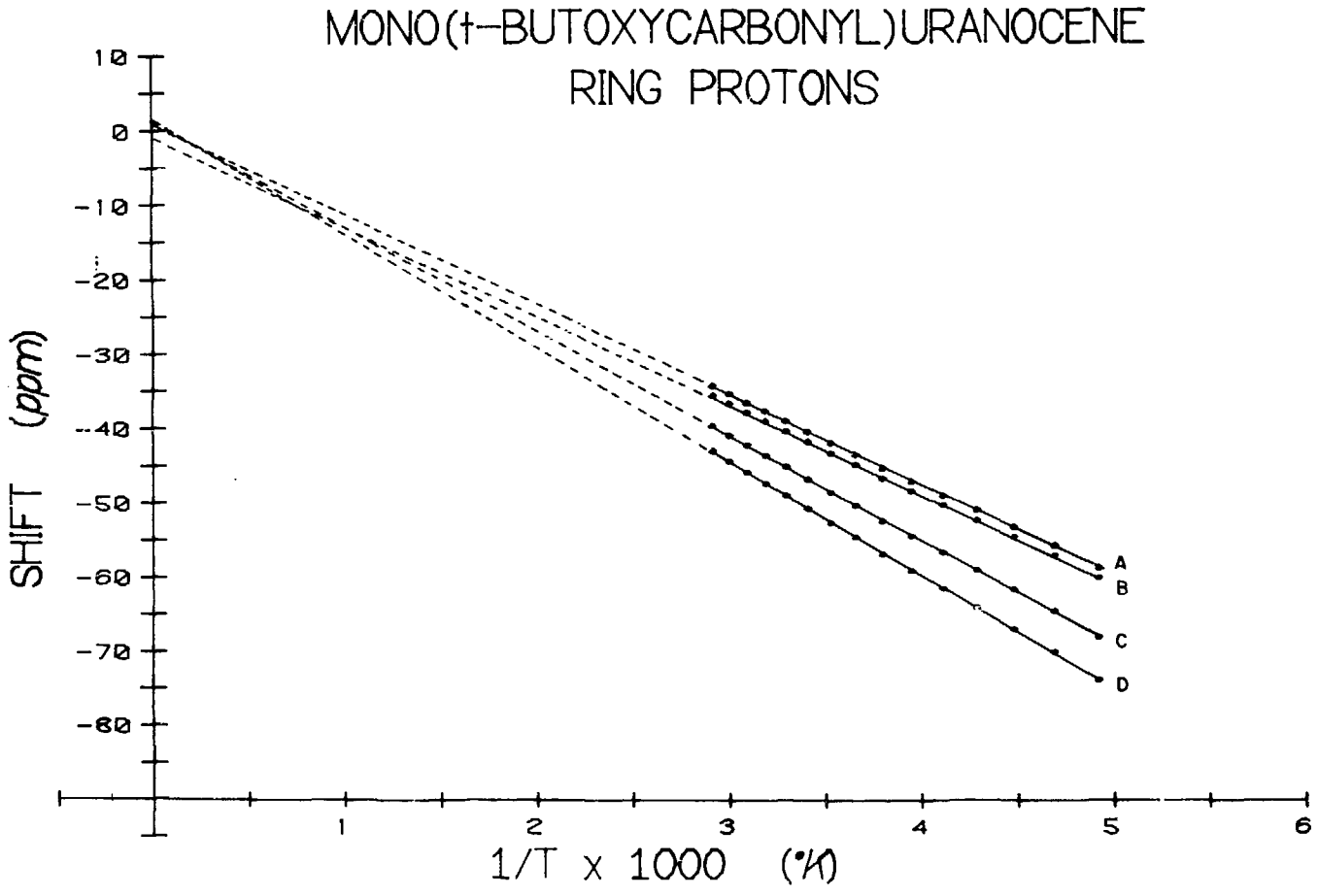
MONO(t-BUTOXYCARBONYL)URANOCENE
RING PROTONS
SHIFT (ppm)
10
0
-10
-20
-30
-40
-50
-60
-70
-80
1
2
3
4
5
6
1/T x 1000 (°K)
A
B
C
D

Fig. 3-37 and 3-38 Isotropic shift vs T^{-1} for the ring protons in 1,1'-di-t-butoxycarbonyluranocene.

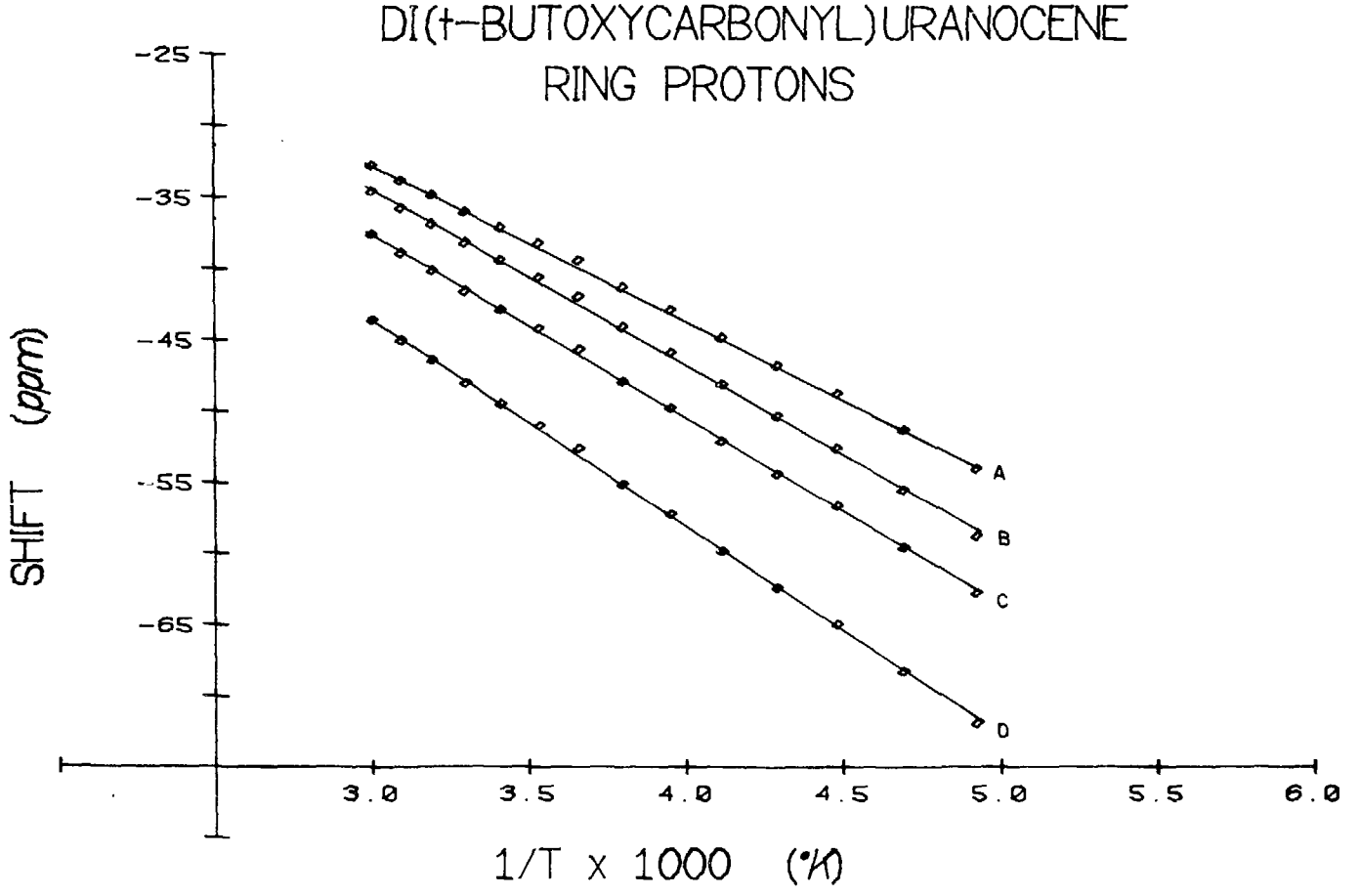
DI(t-BUTOXYCARBONYL)URANOCENE
RING PROTONS
SHIFT (ppm)
-25
-35
-45
-55
-65
A
B
C
D
3.0
3.5
4.0
4.5
5.0
5.5
6.0
1/T x 1000 (°K)

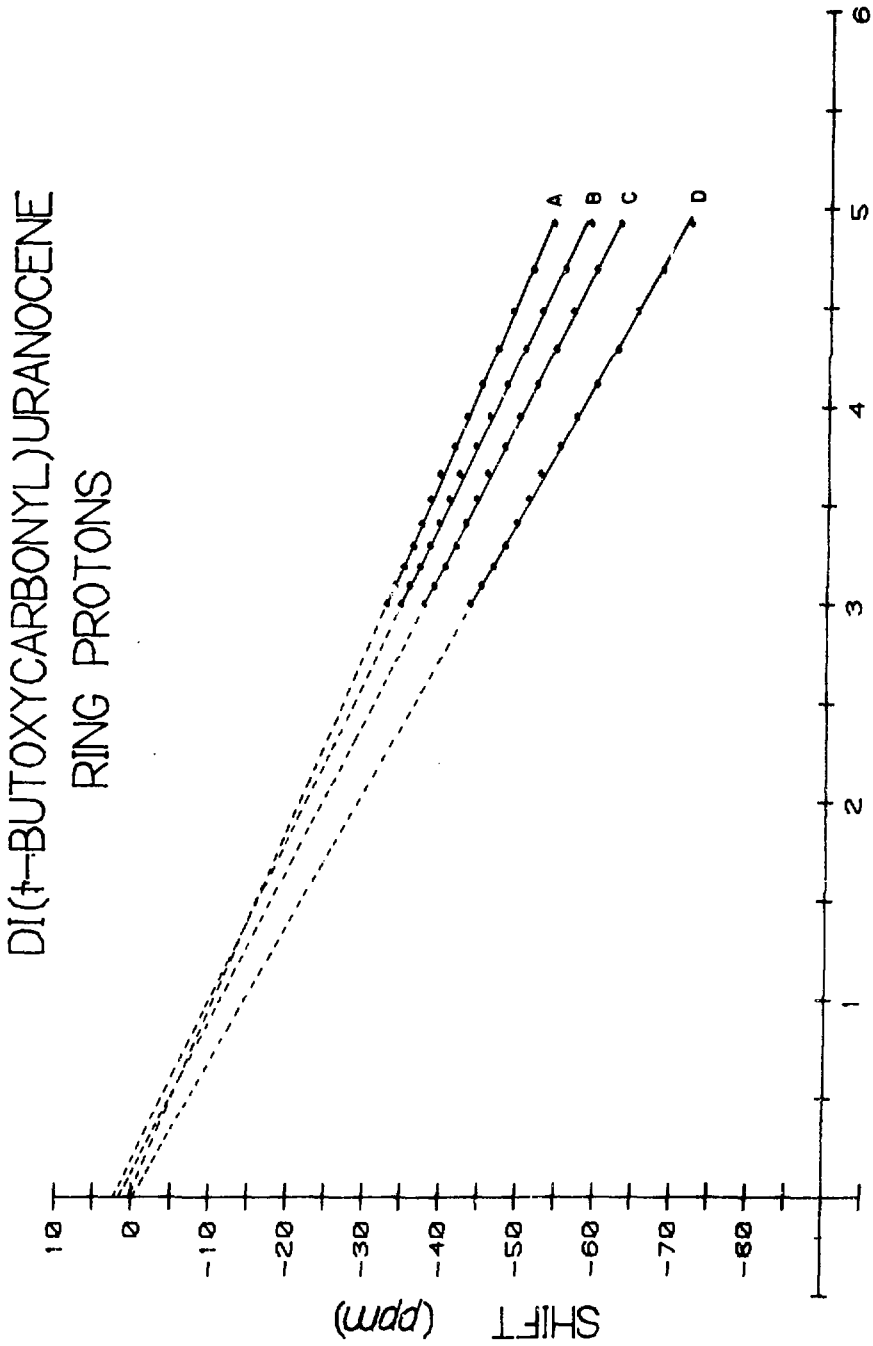
DI(t-BUTOXYCARBONYL)URANOCENE
RING PROTONS
SHIFT (ppm)
10
0
-10
-20
-30
-40
-50
-60
-70
-80
1/T x 1000 (K)
1
2
3
4
5
6
A
B
C
D

and the magnitude of the isotropic shifts at a given temperature, say 30°C. However, for some individual uranocenes, it appears that a correlation does exist such that the intercept increases the larger the isotropic shift at a given temperature. This seems to suggest that the non-zero intercepts are in some way associated with the contact shift.

The linear dependence of the isotropic shifts on T^{-1} over the observed temperature range can imply one of two things: 1)both the contact and pseudocontact shifts are linear functions of T^{-1}; 2)the contact shift is a linear function of T^{-1} while the pseudocontact shift is a function of both T^{-1} and higher orders of T^{-1}, where the combined contact and pseudocontact T^{-1} dependence is large relative to the higher order terms of the pseudocontact shift. In principle, these two possibilities can be differentiated by observing the temperature dependence of α and β protons whose geometry factor is invarient with temperature. The contact shift for α and particularly for β-protons should be substantially smaller than for ring protons. Hence, their temperature dependence should be linear in T^{-1} if the former is true, but non-linear if the latter is true.

F) THE TEMPERATURE DEPENDENCE OF SUBSTITUENT PROTON RESONANCES IN SUBSTITUTED URANOCENES

The temperature dependence of the substituent proton resonances of the uranocenes listed in Table 3-4 are shown in Fig. 3-40-57. Two general features are immediately apparent. One, the temperature dependence of most of the protons in α,

β and γ-positions is not linear in T^{-1}. Two, for all of the proton resonances which do display a linear or near linear T^{-1} dependence, extrapolation to $T^{-1} = 0$ leads to significantly non-zero and positive intercepts (Table 3-13).

Non-zero intercepts upon extrapolation to $T^{-1} = 0$ are observed for a large number of paramagnetic organometallic complexes. Drago[85] has summarized several principal causes of non-zero intercepts: 1)extrapolation errors; 2)large values of the Weiss constant in the Curie-Weiss equation describing the magnetic behavior of the complex; 3)temperature dependent conformational changes; 4)non-Curie or Curie-Weiss magnetic behavior of the complex.

Considering both the Weiss constants in Table 3-11 and the standard derivations in the slopes and intercepts for the ring proton data, it appears doubtful that extrapolation errors, or errors due to neglect of the Weiss constant can account for the non-zero intercepts. Further, if the intercepts were due to extrapolation errors one would more likely expect a spread of both positive and negative values rather than all positive values. Thus, the latter two possibilities more likely account for the observed intercepts.

To facilitate analysis of the ^{1}H NMR data, the geometry factors (i.e., eq. 11) for the substituent protons have been calculated. Taking the average U-ring distance and the C_{ring} - C_{ring} distance from the X-ray structural data reported for uranocene[55] and several substituted uranocenes,[86-88] and standard bond lengths and angles for the substituent (Table 3-14), the calculated geometry factors for α, β and γ protons for the

Table 3-13

Least Squares Regression Data for Alkyl Uranocene Substituent Proton Data

Fig. #	Proton Resonance	Slope	Intercept	r^2
α-Protons				
3-39	methyl	non-linear		
3-39	octamethyl	-5.53 ± 0.04	11.19 ± 0.14	0.9993
3-39	ethyl	-12.65 ± 0.17	21.84 ± 0.61	0.9962
3-39	n-butyl	-12.22 ± 0.10	18.10 ± 0.37	0.9984
3-39	neopentyl	-12.5 ± 0.73	14.02 ± 0.28	0.9995
3-39	isopropyl	-8.58 ± 0.05	11.47 ± 0.20	0.9994
3-40	cyclobuteno exo	non-linear		
3-41	cyclobuteno endo	non-linear		
3-40	cyclopenteno exo	non-linear		
3-41	cyclopentono endo	non-linear		
3-40	dimethylcyclo-penteno exo	non-linear		
3-41	dimethylcyclo-penteno endo	non-linear		
β-Protons				
3-42	mono-t-butyl	-5.42 ± 0.03	4.42 ± 0.10	0.9996
3-42	t-butyl	-5.60 ± 0.07	5.32 ± 0.25	0.9979
3-42	tetra-t-butyl	-5.09 ± 0.06	5.03 ± 0.22	0.9980
3-43,44	n-butyl	non-linear		
3-43,44	ethyl	non-linear		
3-42	isopropyl	-4.69 ± 0.04	4.51 ± 0.14	0.9991
3-45	cyclopenteno exo	non-linear		
3-45	cyclopenteno endo	non-linear		
γ and δ Protons				
3-46	neopentyl t-butyl	1.14 ± 0.01	-0.97 ± 0.03	0.9992
3-46	dimethylcyclo-penteno CH_3 exo	non-linear		
3-45	dimethylcyclo-penteno CH_3 endo	non-linear		

Fig. #	Proton Resonance	Slope	Intercept	r^2
3-46	n-butyl γ-CH_2	non-linear		
3-46	n-butyl CH_3	non-linear		
Aryl Protons				
3-47	phenyl ortho	-8.75 ± 0.06	7.53 ± 0.22	0.9993
3-48	phenyl meta	2.77 ± 0.02	2.81 ± 0.09	0.9988
3-48	phenyl para	-2.52 ± 0.02	1.85 ± 0.08	0.9990
3-47	dimethylaminophenyl ortho	-8.84 ± 0.03	7.86 ± 0.09	0.9999
3-48	dimethylaminophenyl meta	-3.03 ± 0.05	3.68 ± 0.19	0.9955
3-48	dimethylaminophenyl CH_3	-1.44 ± 0.02	1.41 ± 0.08	0.9963
Ester Protons				
3-47	mono-t-butyl	-3.47 ± 0.04	3.73 ± 0.16	0.9980
3-47	t-butyl	-3.41 ± 0.04	4.72 ± 0.16	0.9980

Fig. 3-39 Isotropic shift vs T^{-1} for the α-protons in 1,1'-dimethyl-, 1,1-diethyl-, 1,1-di-n-butyl-, 1,1'-diisopropyl-, 1,1'-dineopentyl-, and 1,1',3,3',5,5',7,7,'-octamethyluranocene.

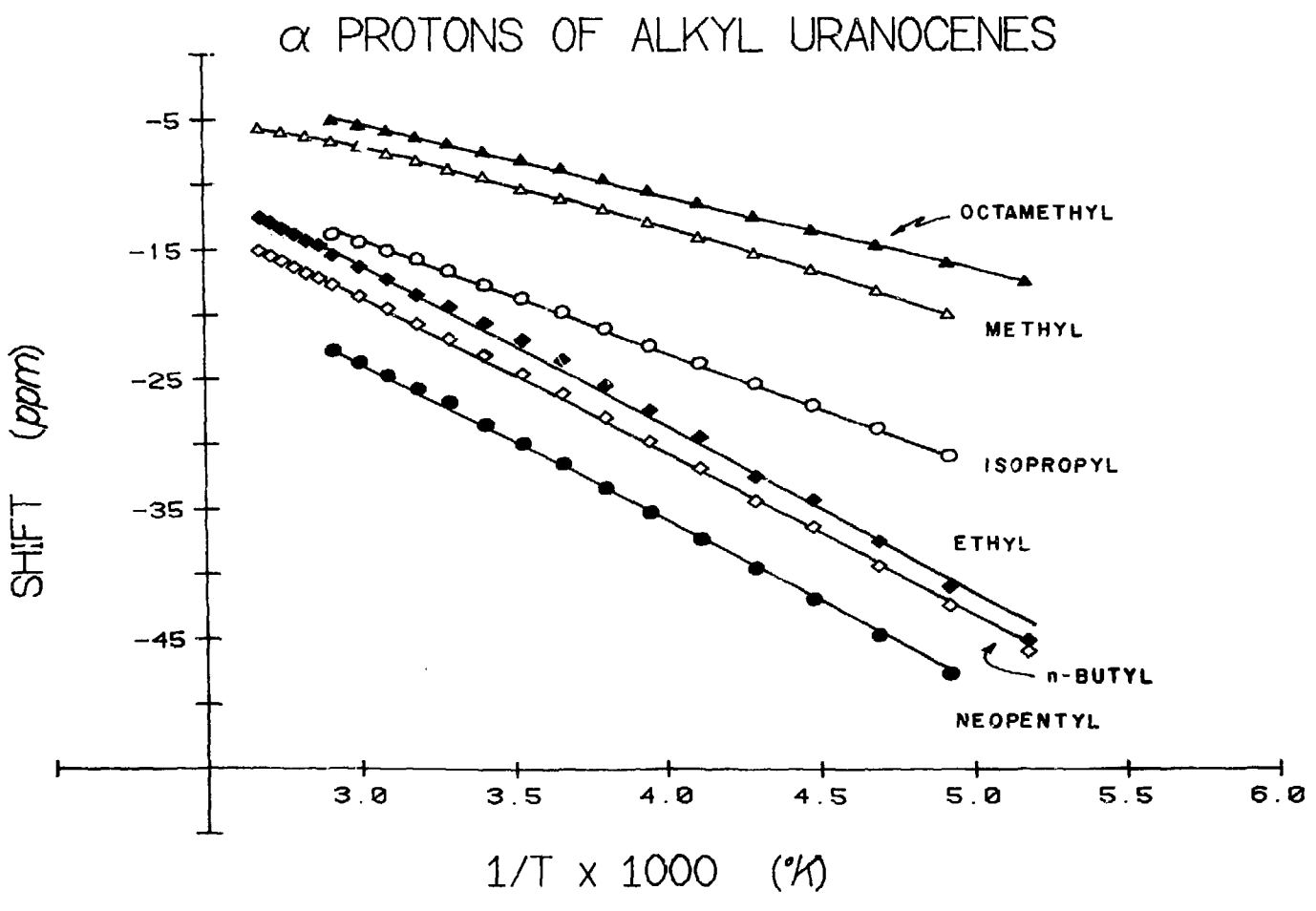
α PROTONS OF ALKYL URANOCENES
SHIFT (ppm)
-5
-15
-25
-35
-45
OCTAMETHYL
METHYL
ISOPROPYL
ETHYL
n-BUTYL
NEOPENTYL
3.0
3.5
4.0
4.5
5.0
5.5
6.0
1/T x 1000 (°K)

Fig. 3-40 Isotropic shift vs T^{-1} for the α_{exo} protons in annulated uranocenes.

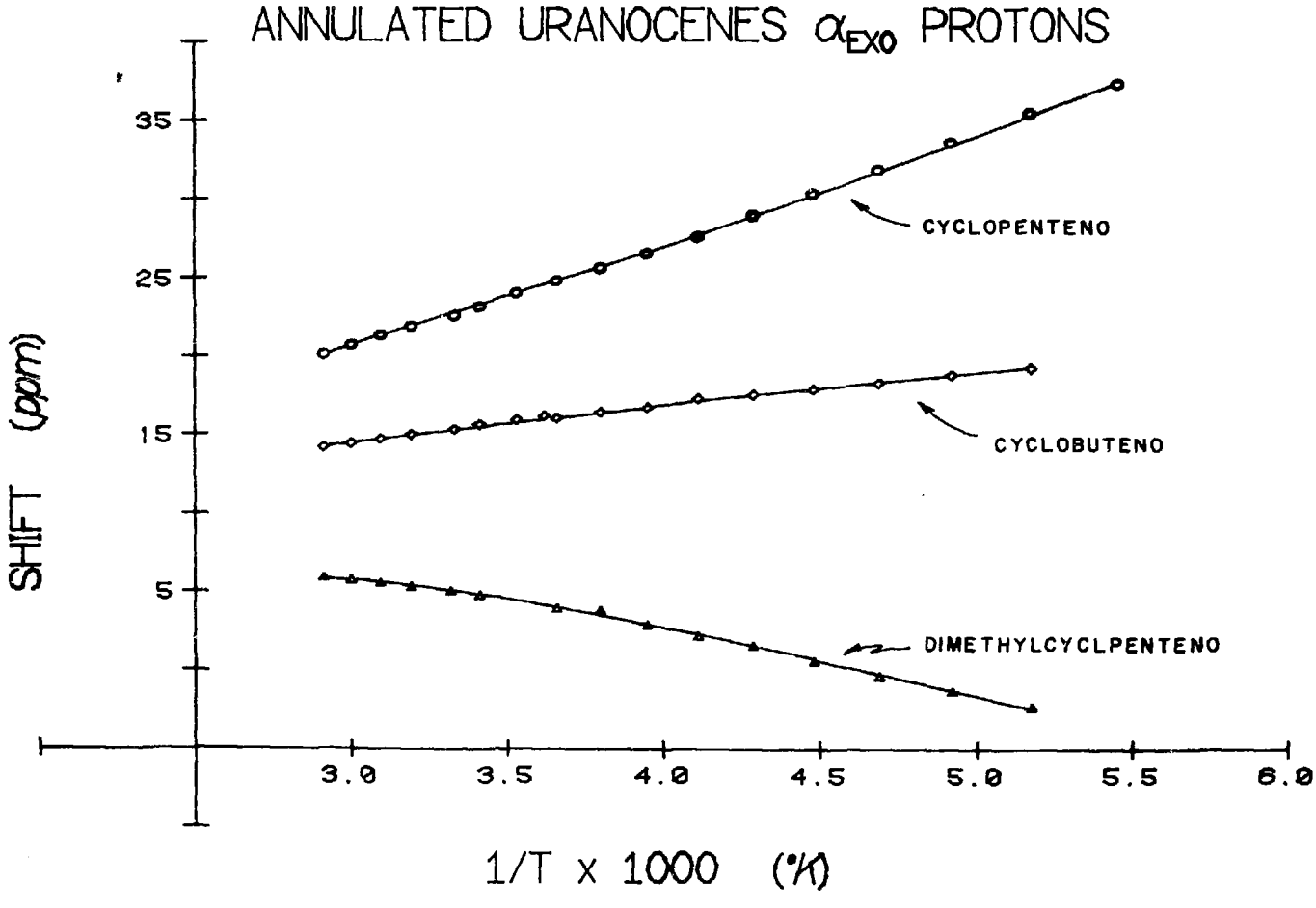
ANNULATED URANOCENES α_{EXO} PROTONS
SHIFT (ppm)
35
25
15
5
CYCLOPENTENO
CYCLOBUTENO
DIMETHYLCYCLPENTENO
3.0
3.5
4.0
4.5
5.0
5.5
6.0
1/T x 1000 (°K)

Fig. 3-41 Isotropic shift vs T^{-1} for the α_{endo} protons in annulated uranocenes.

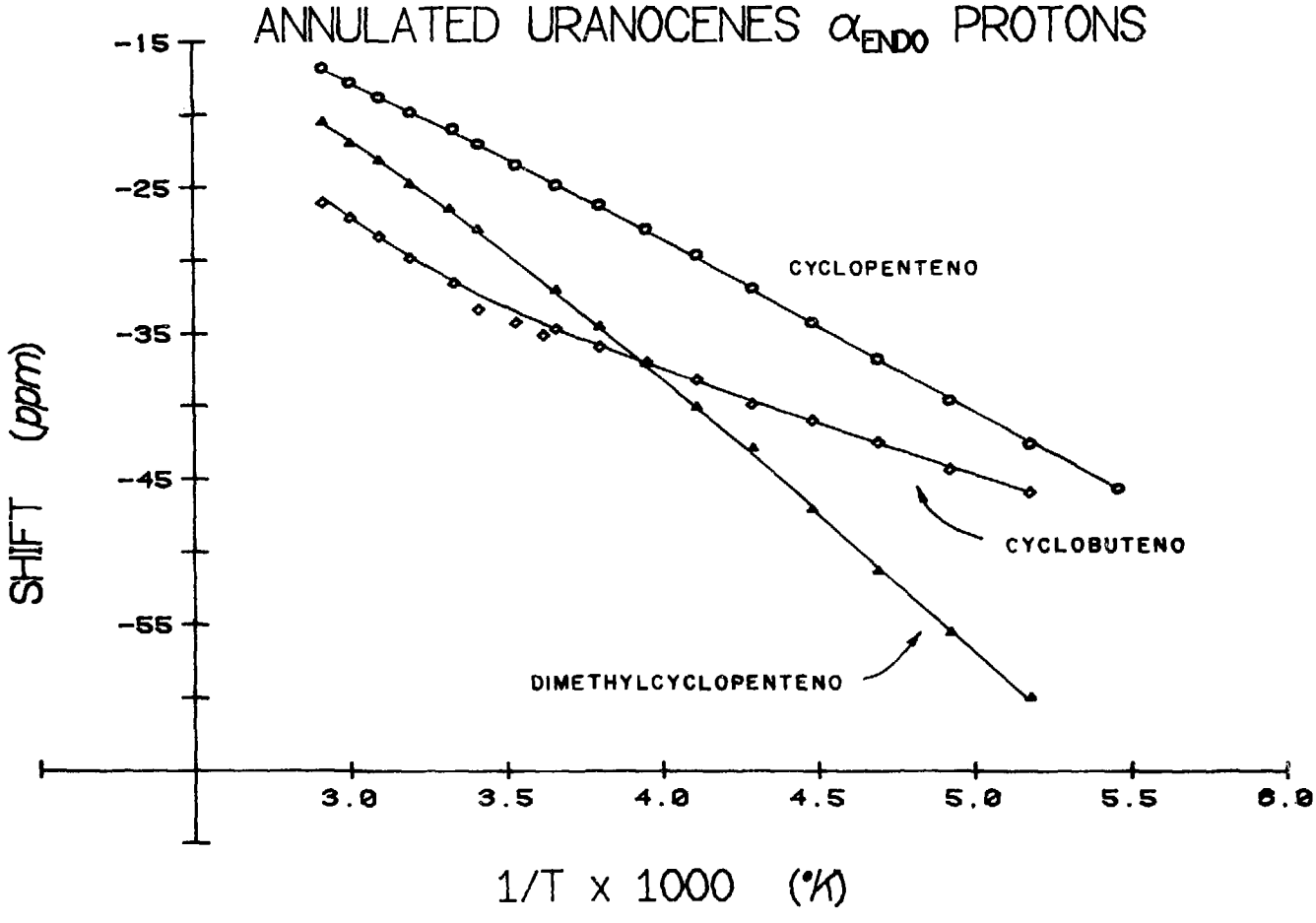
ANNULATED URANOCENES α_{ENDO} PROTONS
SHIFT (ppm)
-15
-25
-35
-45
-55
3.0
3.5
4.0
4.5
5.0
5.5
6.0
1/T x 1000 (°K)
CYCLOPENTENO
CYCLOBUTENO
DIMETHYLCYCLOPENTENO

Fig. 3-42 Isotropic shift vs T^{-1} for the β-protons in 1,1'-diisopropyl- and the t-butyl substituted uranocenes.

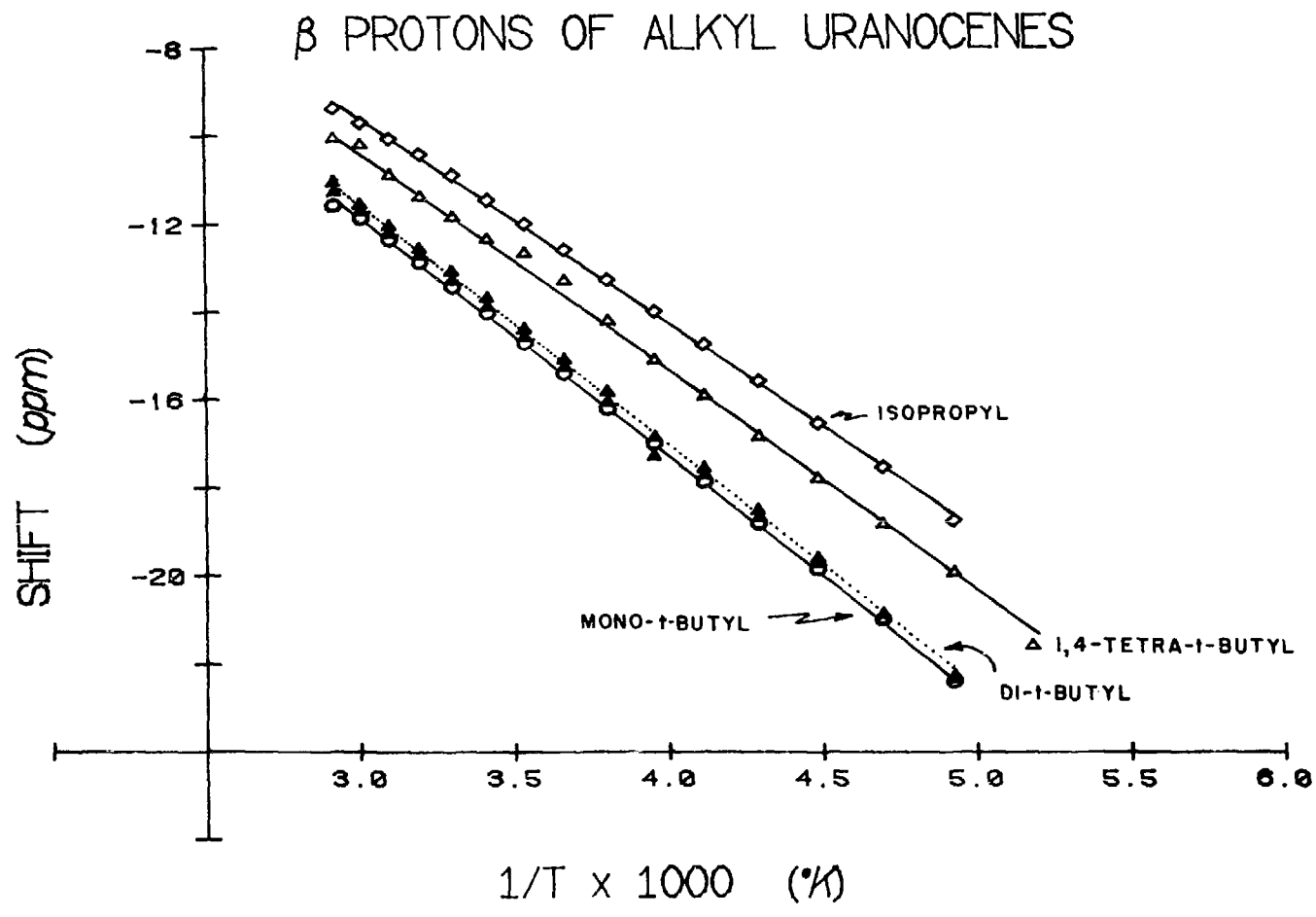
β PROTONS OF ALKYL URANOCENES
SHIFT (ppm)
-8
-12
-16
-20
3.0
3.5
4.0
4.5
5.0
5.5
6.0
1/T x 1000 (°K)
ISOPROPYL
MONO-t-BUTYL
1,4-TETRA-t-BUTYL
DI-t-BUTYL

Fig. 3-43 and 3-44 Isotropic shift vs T^{-1} for the β-protons in 1,1'-diethyl- and 1,1'-di-n-butyluranocene. The calculated simulation of the data for 1,1'-diethyluranocene, assuming a Boltzmann population of two conformations where C_L = 3.0 x 10^3 ppm T, C_H = -4.2 x 10^3 ppm T and ε = 0.395 kcal $mole^{-1}$ is given by the solid line.

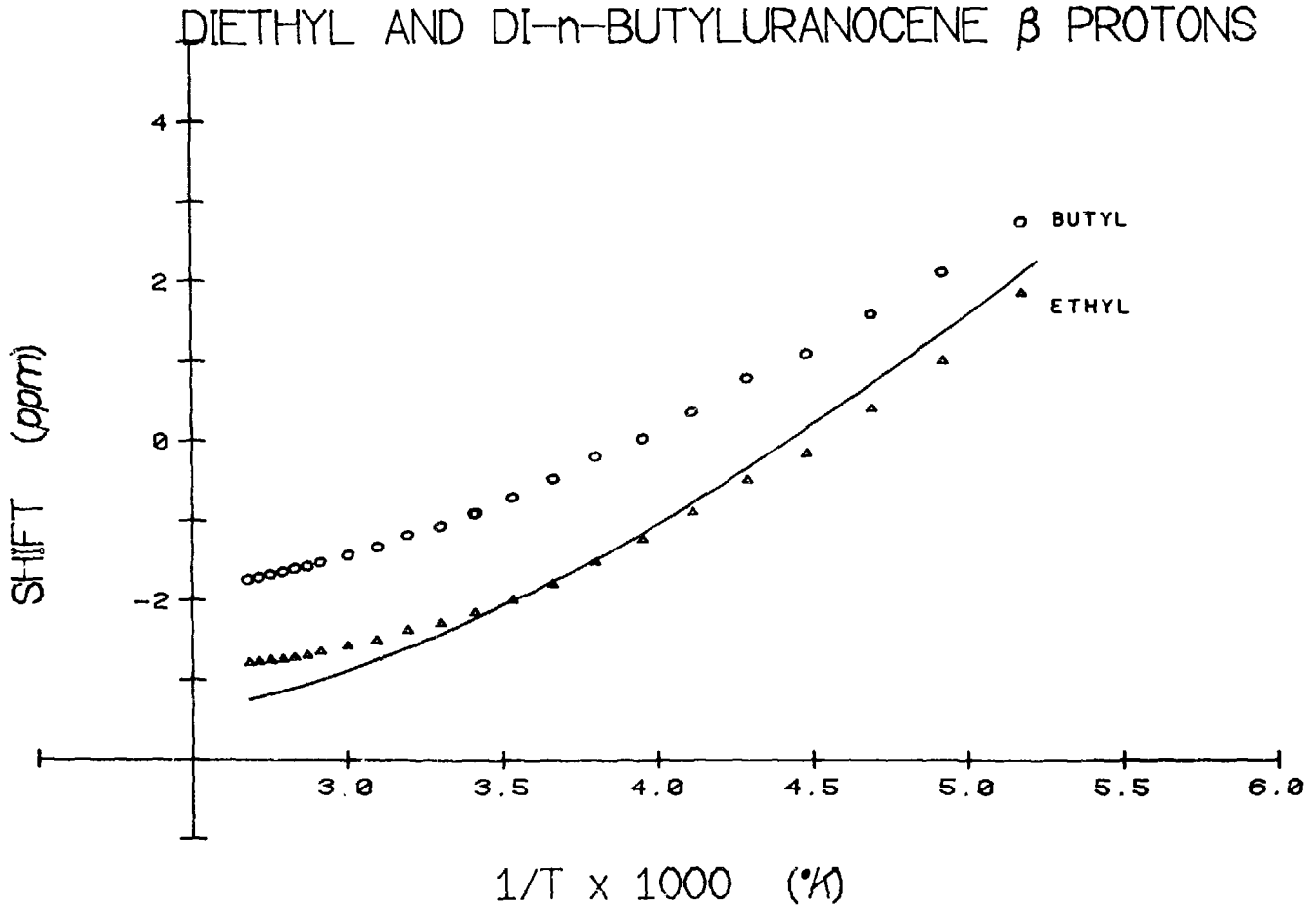
DIETHYL AND DI-n-BUTYLURANOCENE β PROTONS
SHIFT (ppm)
4
2
0
-2
BUTYL
ETHYL
3.0
3.5
4.0
4.5
5.0
5.5
6.0
1/T x 1000 (°K)

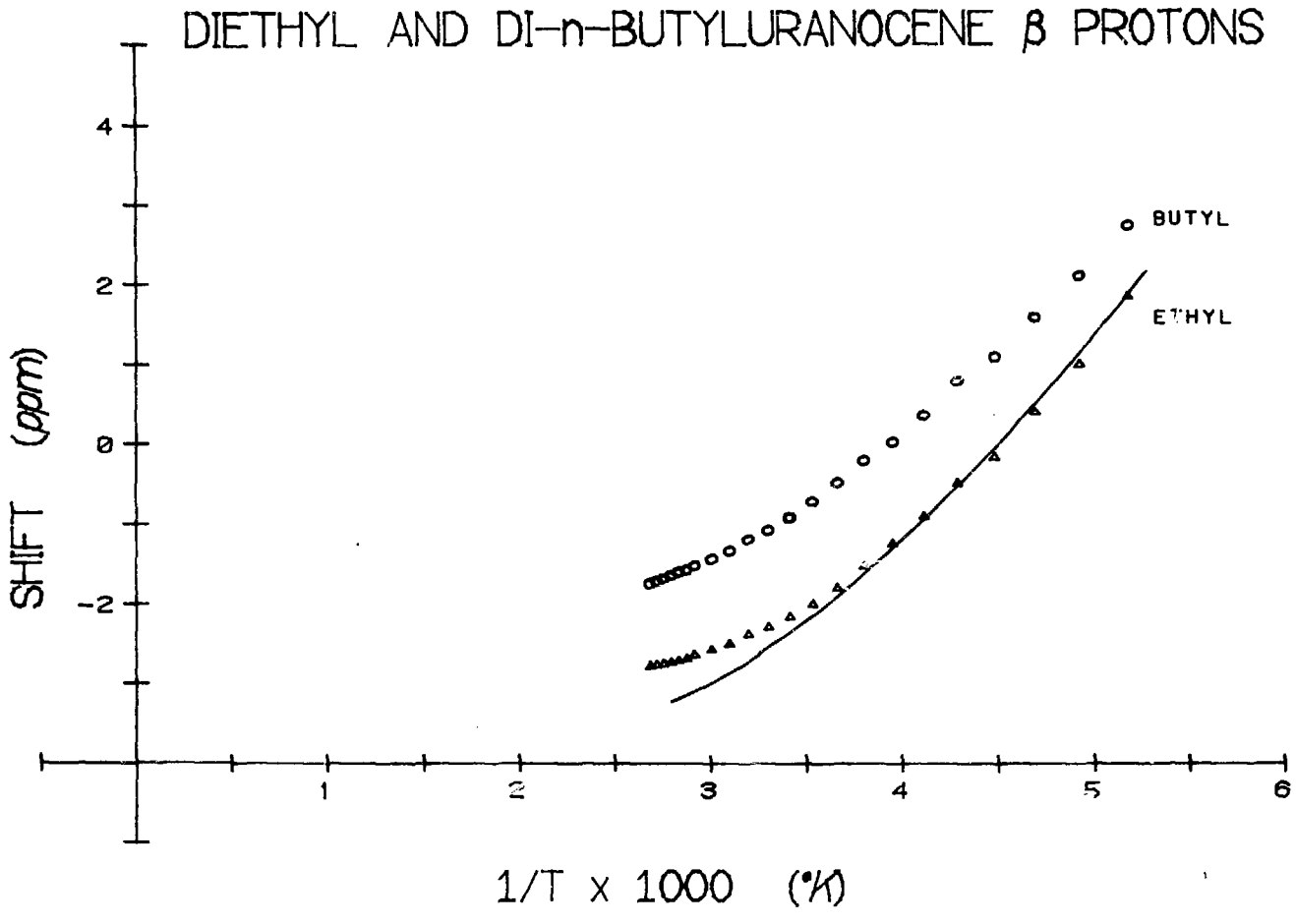
DIETHYL AND DI-n-BUTYLURANOCENE β PROTONS
SHIFT (ppm)
4
2
0
-2
1
2
3
4
5
6
1/T x 1000 (°K)
BUTYL
ETHYL

Fig. 3-45 Isotropic shift vs T^{-1} for the β_{exo} and β_{endo} protons in dicyclopentenouranocene and the endo methyl group in bis(dimethylcyclopenteno)uranocene.

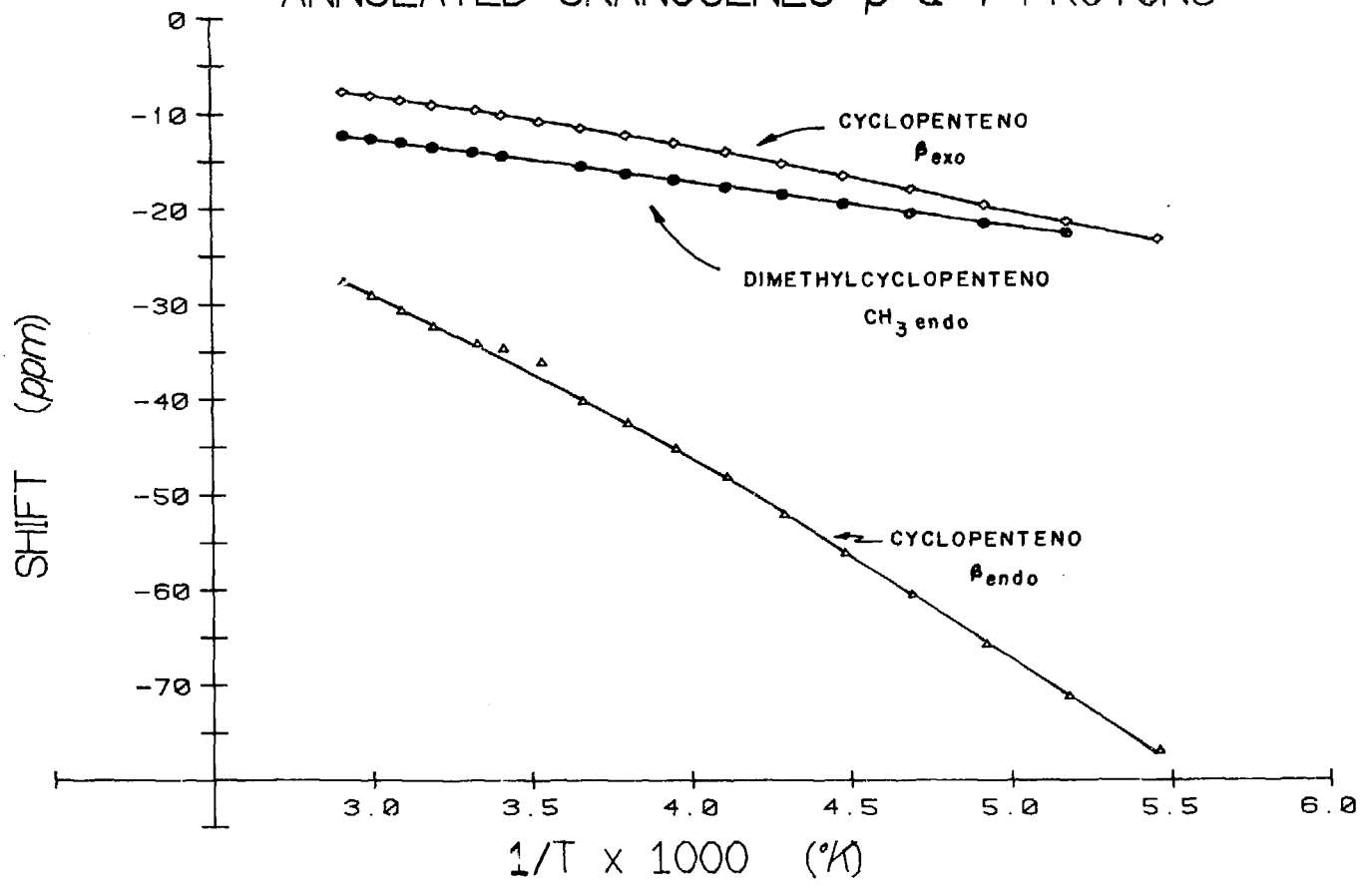
ANNULATED URANOCENES β & γ PROTONS
SHIFT (ppm)
0
-10
-20
-30
-40
-50
-60
-70
3.0
3.5
4.0
4.5
5.0
5.5
6.0
1/T x 1000 (°K)
CYCLOPENTENO
β exo
DIMETHYLCYCLOPENTENO
CH3 endo
CYCLOPENTENO
β endo

Fig. 3-46 Isotropic shift vs T^{-1} for the t-butyl group in 1,1'-dineopentyluranocene, the γ and δ protons in 1,1'-di-n-butyluranocene and the exo methyl group in bis(dimethyl-cyclopenteno)uranocene.

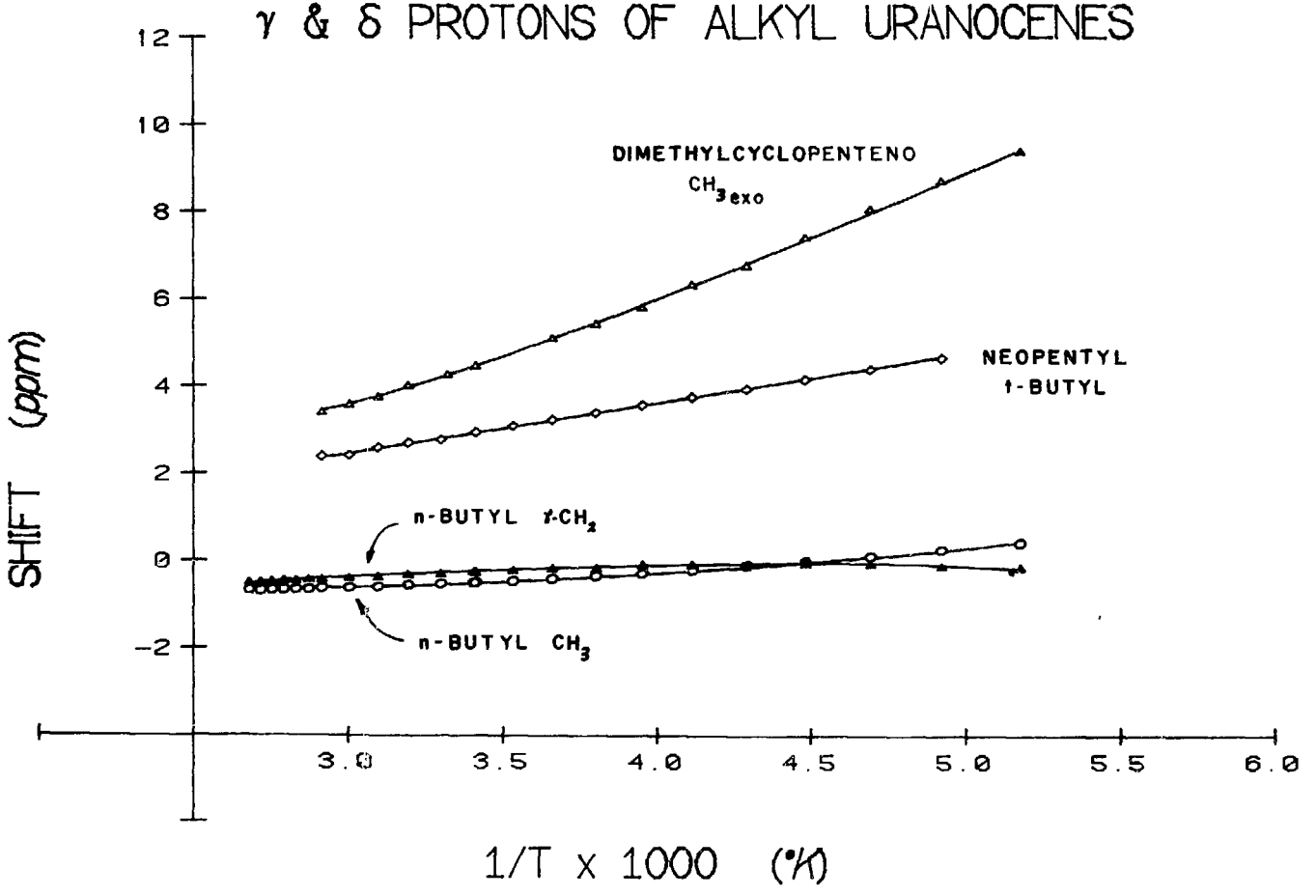
γ & δ PROTONS OF ALKYL URANOCENES
SHIFT (ppm)
12
10
8
6
4
2
0
-2
DIMETHYLCYCLOPENTENO
CH3exo
NEOPENTYL
t-BUTYL
n-BUTYL γ-CH2
n-BUTYL CH3
3.0
3.5
4.0
4.5
5.0
5.5
6.0
1/T x 1000 (°K)

Fig. 3-47 Isotropic shift vs T^{-1} for the ortho protons in 1,1'-diphenyl- and 1,1'-bis(p-dimethylaminophenyl)uranocene.

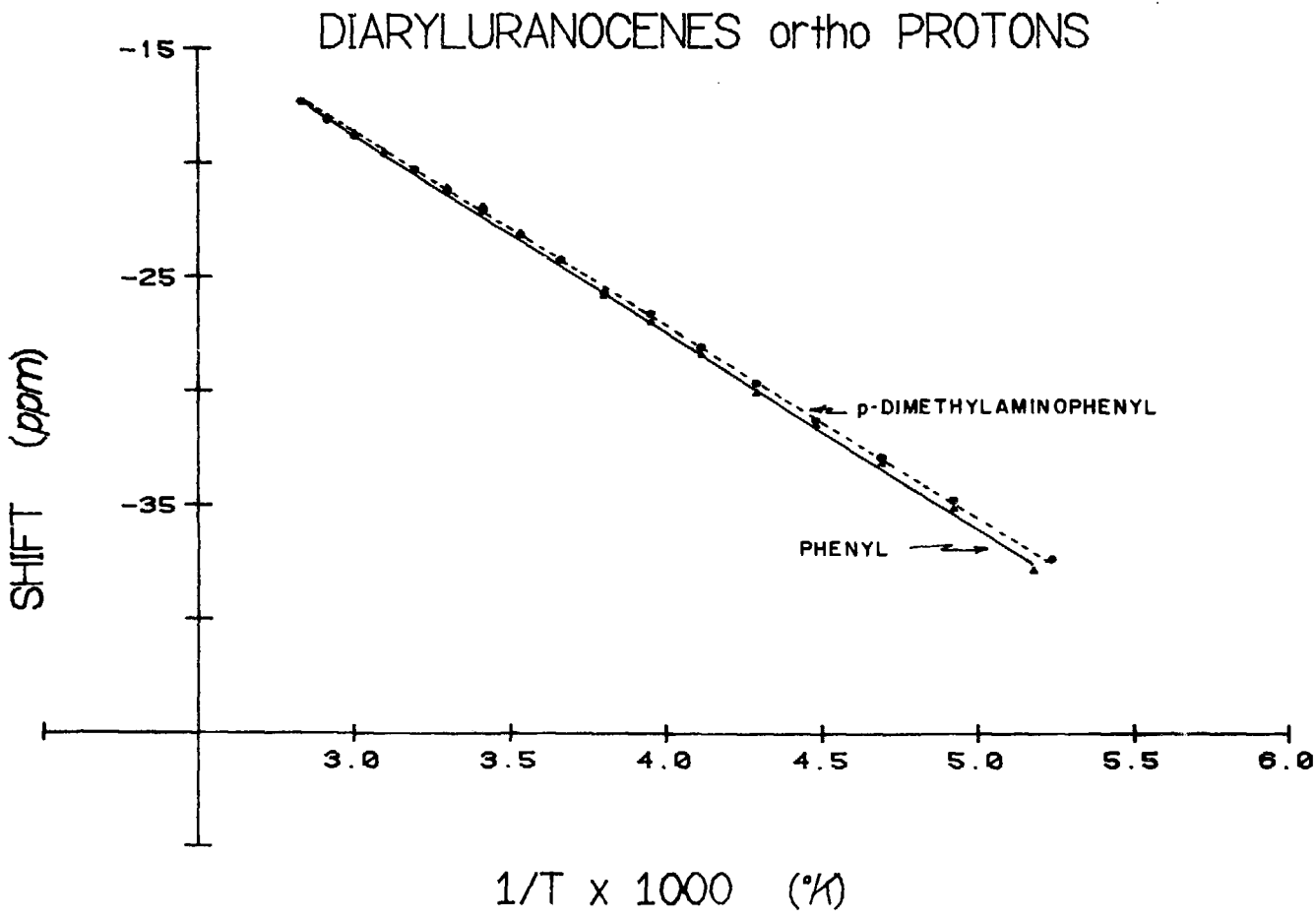
DIARYLURANOCENES ortho PROTONS
-15
-25
-35
SHIFT (ppm)
p-DIMETHYLAMINOPHENYL
PHENYL
3.0
3.5
4.0
4.5
5.0
5.5
6.0
1/T x 1000 (°K)

Fig. 3-48 Isotropic shift vs T^{-1} for the meta, para, and methyl protons in 1,1'-diphenyl- and 1,1'-bis(p-dimethylaminophenyl)uranocene.

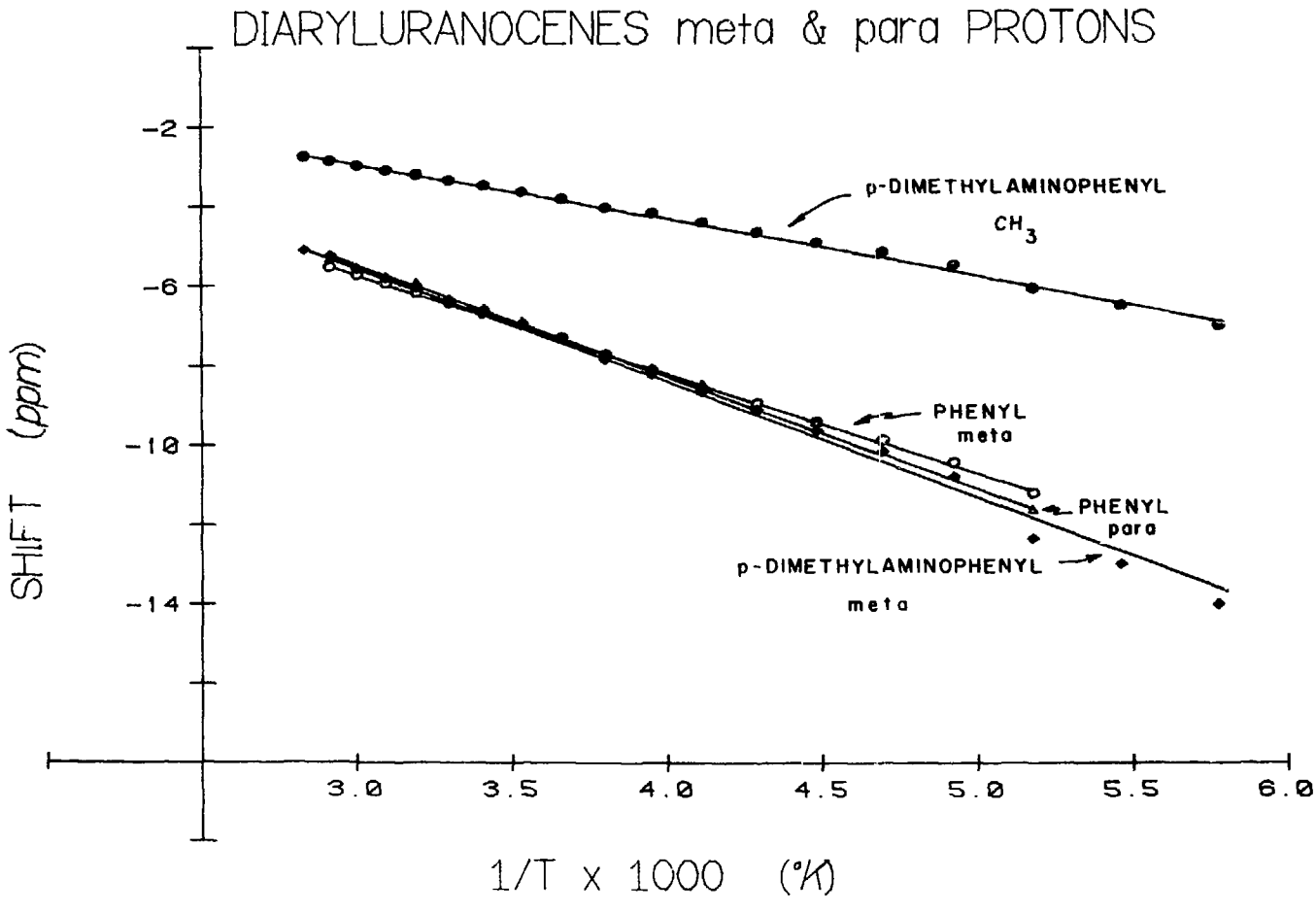
DIARYLURANOCENES meta & para PROTONS
SHIFT (ppm)
-2
-6
-10
-14
3.0
3.5
4.0
4.5
5.0
5.5
6.0
1/T x 1000 (°K)
p-DIMETHYLAMINOPHENYL
CH3
PHENYL
meta
PHENYL
para
p-DIMETHYLAMINOPHENYL
meta

Fig. 3-49 Isotropic shift vs T^{-1} for the t-butyl groups in mono- and 1,1'-t-butoxycarbonyluranocene.

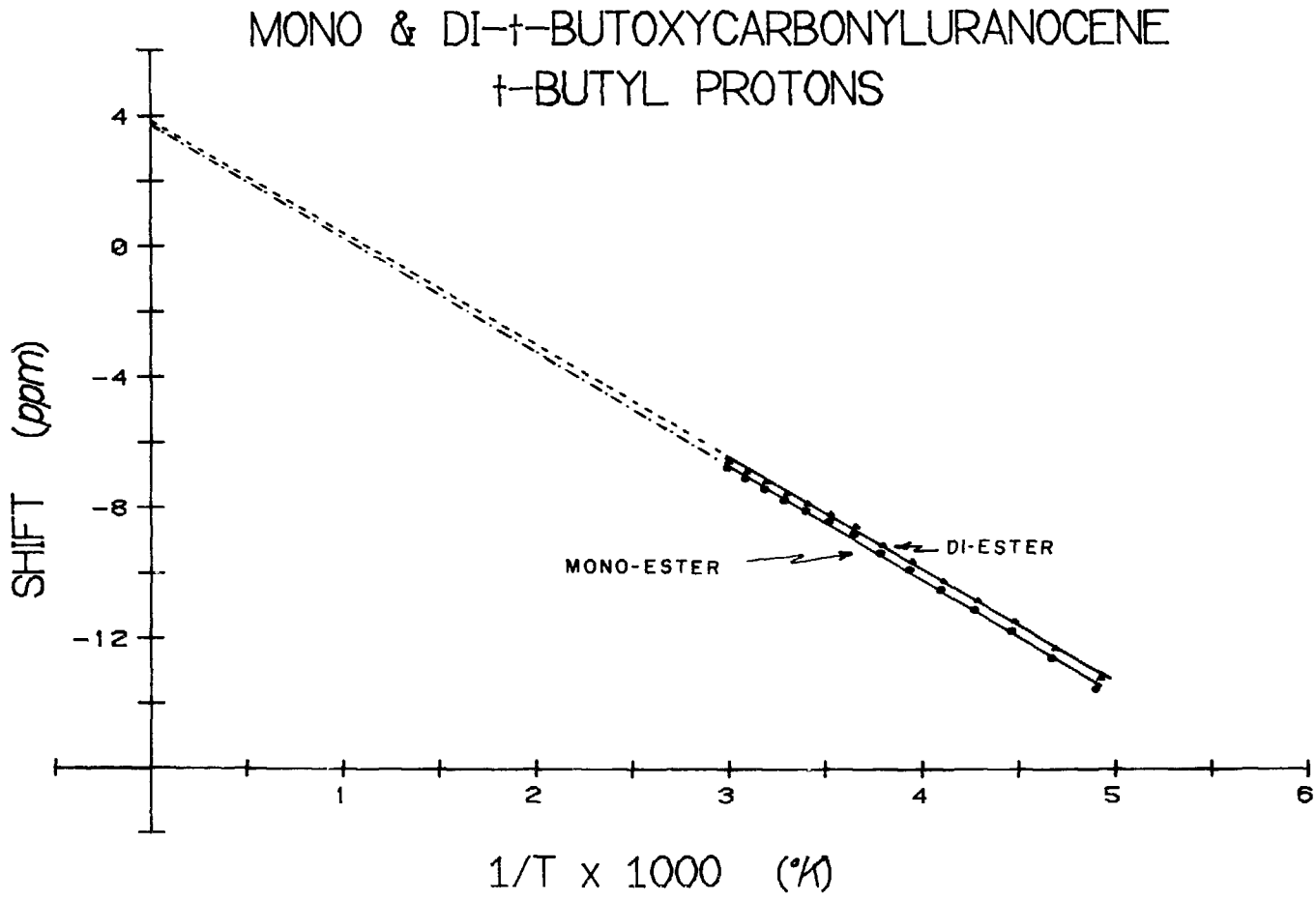
MONO & DI-t-BUTOXYCARBONYLURANOCENE
t-BUTYL PROTONS
SHIFT (ppm)
4
0
-4
-8
-12
1
2
3
4
5
6
1/T x 1000 (°K)
MONO-ESTER
DI-ESTER

conformations shown in Fig. 3-48 are listed in Tables 3-15-17. Calculations are listed assuming that the C_{ring} - C_{α} bond is both coplanar and tipped 5° down toward the uranium atom from the plane of the 8-membered ring. The major difference between the values in Table 3-14 and those used by Berryhill, Table 3-3, is the C_{ring} - C_{α} bond length assumed to be 1.52 A in this work, rather than 1.54 A in the former.

Table 3-14

Bond Lengths Used in Calculating Uranocene Geometry Factors

ring center - U	1.92
C_{ring} - C_{ring}	1.42
C_{ring} - C_{α}	1.52
C_{sp^2} - H	1.08
C_{sp^3} - H	1.09
C_{sp^3} - C_{sp^2}	1.54

1) METHYL AND t-BUTYL SUBSTITUTED URANOCENES

Focusing first on the methyl and t-butyl substituted uranocenes 27, 32, 33 and 35, the substituent resonances in these compounds remains a sharp singlet at low temperature implying free rotation about the C_{ring} - C_{α} bond. Neglecting high energy conformations, where bonds in the substituent eclipse the ring plane, and assuming equal population of the remaining conformations, the geometry factor for the substituent protons is constant and temperature independent. Thus, the

Fig. 3-50 Conformations of the substituent in substituted uranocenes. The uranium atom is assumed to be below the plane of the ring in each figure.

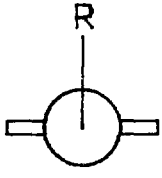

A

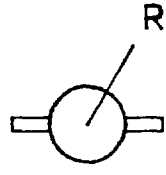

B

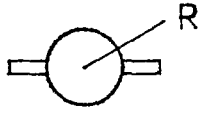

C

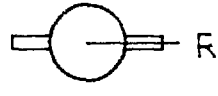

D

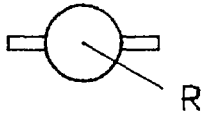

E

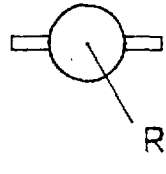

F

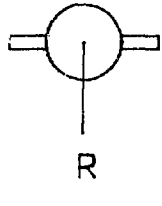

G

Table 3-15

Calculated Geometry Factors $\frac{3\cos^2\theta-1}{R^3}$ For α Protons

(R = H in Fig. 3-50)

Conformation	Planar Gi x 10^{21} cm^{-3}	5° Tip Gi x 10^{21} cm^{-3}
A	1.388	0.3599
B	0.6717	-0.3653
C	-1.503	-2.604
D	-5.053	-6.357
E	-9.424	-11.14
F	-13.23	-15.46
G	-14.76	-15.55

Table 3-16

Calculated Geometry Factors $\frac{3\cos^2\theta-1}{R^3}$

For β Methyl Group

(R = CH_3 in Fig. 3-50)

Conformation	Planar Gi x $10^{21}cm^{-3}$	5° Tip Gi x $19^{21}cm^{-3}$
A	2.563	1.793
B	1.756	0.9977
C	-0.7736	-1.557
D	-5.081	-6.082
E	-10.32	-11.83
F	-14.64	-16.65
G	-16.45	-18.74

Table 3-17

Calculated Geometry Factors $\frac{3\cos^2\theta-1}{R^3}$

for t-Butyl Group of Neopentyl
Substituent Staggered Conformation

(R = t-Butyl in Fig. 3-50)

Conformation	Planar $G_i \times 10^{21} cm^{-3}$	5° Tip $G_i \times 10^{21} cm^{-3}$
A	3.148	1.608
B	2.056	1.417
C	-0.6594	-1.271
D	-5.423	-6.17
E	-11.35	-13.49
F	-15.66	-17.81
G	-18.43	-19.82

linearity or non-linearity of the variable temperature data is controlled solely by the susceptibility term in eq. 17.

The temperature dependences of the substituted proton resonances in 1,1',3,3',5,5',7,7'-octamethyl-, mono-t-butyl- and 1,1'-di-t-butyluranocene are all linear while that of 1,1'-dimethyluranocene is distinctly non-linear in T^{-1}. The possibility that this non-linearity arises from experimental errors in spectral acquisition was eliminated by reexamination of the spectra from 40°C to 100°C.

The non-linearity could reflect a higher order dependence of the magnetic susceptibility on T^{-1} over the temperature range -100°C to 100°C, which could also account for the non-zero intercepts. Fitting the data with a second order polynomial regression leads to a smaller extrapolated intercept. However, if this were true, then 1,1',3,3',5,5',7,7'-octamethyl- and the two t-butyluranocenes should show similar non-linearity. The fits of the parameters for the second order polynomial to the experimental data (Table 3-18) show that the second order term is effectively zero for these compounds. Potentially, this could imply that the excited state(s) which gives rise to the non-linear behavior is closer to the ground state in 1,1'-dimethyluranocene than in the other three uranocenes. However, there is no compelling reason why this should be the case.

Similarly, no obvious conformational changes can account for the observed non-linearity. Consider the possibility of unequal population of two principal conformations. Taking the conformations as E-A-E and C-G-C (Table 3-15), with the substituent either coplanar or tipped 5° toward the uranium,

Table 3-18

Second Order Regression Analysis Data for
Alkyl Uranocene Substituent Proton Data

Proton Resonance	A_0	A_1	A_2	r^2
α Protons				
methyl	6.47	-2.35	-0.54	0.9999
octamethyl	7.99	-3.91	-0.20	0.9998
ethyl	11.47	-6.30	-1.04	0.9972
n-butyl	11.40	-6.96	-0.69	0.9999
isopropyl	9.28	-6.25	-0.30	0.9998
neopentyl	11.27	-9.52	-0.38	0.9998
β & γ Protons				
mono-t-butyl	4.27	-4.50	-0.12	0.9998
t-butyl	5.49	-4.85	-0.10	0.9980
isopropyl	2.24	-2.96	-0.22	0.9998
tetra-t-butyl	3.32	-3.39	-0.21	0.9987
neopentyl	-0.15	1.29	0.01	0.9993

both molecular models and extended Hückel calculations[80] show that E-A-E is lower in energy. Neglecting contact shifts, increasing the temperature will lead to a more positive shift as the population of C-G-C increases, in exact opposition to what is observed experimentally. Inclusion of a positive contact shift for an α-proton also fails to account for the experimental data. If the substituent is coplanar with the 8-membered ring, hyperconjugation and the contact shift for both conformations are equal and the contact shift has no effect. Tipping the substituent will slightly increase hyperconjugation and the contact shift for C-G-C over that for E-A-E. Thus, an increase in temperature will increase the contact shift. The net effect is that the total isotropic shift will be more positive with increasing temperature rather than more negative as observed.

Thus, it is not clear what factors give rise to the observed non-linearity.

2) 1,1'-DIETHYLURANOCENE

The temperature dependence of the substituent proton resonances in 1,1'-diethyluranocene is identical with that reported by Berryhill. At room temperature, the isotropic shifts measured in toluene-d_8 solution in this study are identical within experimental error with those measured in THF-d_8 solution by Berryhill, indicating that solvation has no apparent effect on the properties of uranocene and in agreement with the general observation that solvent has little effect on the visible spectrum of uranocene.

The apparent linear dependence on T^{-1} of the methylene proton resonance and the marked deviation from linearity at high temperature of the methyl group resonance was verified by measuring the ^1H NMR spectrum at 10°C intervals from -80°C to 70°C and in 5°C intervals from 70°C to 100°C (Fig. 3-43, 3-44). In light of the linear T^{-1} dependence of the ring proton resonances, we believe that this non-linear behavior results from rapid exchange between conformations of unequal energy whose population ratio changes as a function of temperature.

Fig. 3-43 shows that at low temperature, the temperature dependence of the methyl group resonance approaches linearity with a positive slope. The slope in a shift vs. T^{-1} plot is composed of two components, a pseudocontact component and a contact component. For a β-proton, the sign of the contact shift is negative and hence, the sign of the contact component of the slope is negative. The sign of the pseudocontact shift and its slope component depend upon the sign of the anisotropy term and the geometry factor. Both the large upfield isotropic shift of the ring protons and the smaller upfield shift of the α-protons require that the sign of the anisotropy term $X_{\parallel} - X_{\perp}$ be positive in uranocenes; otherwise, the contact shift at the α-position would be substantially larger than at a ring position. This requirement is in total agreement with all of the proposed models for the electronic structure of uranocene. Therefore, the sign of the pseudocontact shift, and its slope component, is determined solely by the sign of the geometry factor.

Thus, the positive slope at low temperature requires that

the pseudocontact shift be positive and larger than the contact shift for the methyl group protons and that the geometry factor for the methyl group be positive at low temperature. Table 3-16 shows that the geometry factor is positive only for conformations A and B, where the methyl group lies above the plane of the 8-membered ring, and away from the uranium atom. The negative deviation from linearity at high temperature implies population of a conformation(s) where the geometry factor is negative.

In an attempt to model this behavior, we have assumed population of two conformations: a low energy conformation with a positive geometry factor and isotropic shift, and a higher energy conformation with a negative geometry factor and isotropic shift. The non-inverse temperature terms of the isotropic shift in the axial form of eq. 17 were obtained from the experimental data in the following manner. Assuming that the linear T^{-1} dependence at low temperature reflects exclusive population of the low energy conformation, these terms C_L, for the low energy conformation were given by the slope of the shift vs T^{-1} plot from -50°C to -80°C; $C_L = 2.8 \times 10^3$ ppm T. At high temperature, both conformations were assumed to be equally populated and thus, the slope of the shift vs T^{-1} plot from 90°C to 100°C was taken as the average of C_L and C_H for both conformations which yields a value of $C_H = -2.06 \times 10^3$ ppm T for the high energy conformation.

The total isotropic shift was calculated from -100°C to 100°C assuming a Boltzmann distribution and a variety of values for ϵ, the energy difference between the two conformations (eq. 29). While the calculated shifts are approximately 10 ppm

$$\delta_{ISOTROPIC} = [C_L(1-e^{-\varepsilon/kT}) + C_H(e^{-\varepsilon/kT})]T \qquad (29)$$

too large, deviations from linearity result when ε is less than 0.7 kcal mole^{-1}. Both the positive isotropic shift and slope of the T^{-1} dependence at low temperature, coupled with the small magnitude of the negative isotropic shift at high temperature, require that contact shift is small if not zero for the -protons. If the contact shift is zero, then division of C_L and C_H by $[(\mu_{\parallel}^2 - \mu_{\perp}^2)\beta_N^2/9k] \times 10^6$ leads to the geometry factors for the two conformations. Assuming $\mu_{\parallel}^2 - \mu_{\perp}^2 = 3\mu_{av}^2 = 17.28$ B.M.^{2} the calculated geometry factors are: (low) 2.34×10^{21}cm^{-3}, (high) -1.72×10^{21}cm^{-3}. While the value for the low energy conformation is similar to the geometry factors for conformations A and B, the value for the high energy conformation is significantly smaller than the negative geometry factors in Table 3-16.

The value of C_H could be larger in magnitude if the assumption of equal population of both conformations from 90-100°C is relaxed. The solid line in Fig. 3-43, 3-44 shows that the experimental data can be closely approximated using values of $C_L = 3.0 \times 10^3$ ppm T, $C_H = -4.2 \times 10^3$ ppm T and $\varepsilon = 0.395$ kcal mole^{-1}. The corresponding geometry factors are entirely reasonable in light of the calculated values in Table 3-16. However, is this energy difference realistic? This energy quantity is not the energy barrier for bond rotation, but the energy difference between two conformations; it is of the same order of magnitude, and only slightly smaller, than energy barriers for rotation about carbon-carbon bonds in molecules such as ethane and substituted ethanes.[72] Further, small bond rotational energies have been observed by ^{1}H NMR.

In geometrically rigid magnetically isotropic nickel (II) complexes, Knor and co-workers have used deviations in linear T^{-1} dependence of isotropic shifts to measure 1-3 kcal $mole^{-1}$ energy differences between conformations of substituents in substituted benzenes.[89,90] Thus, it would appear that this energy difference is reasonable, and that to a good first approximation the non-linear behavior of the isotropic shift of the methyl group results from changes in the population of two conformations of unequal energy, where the lower energy conformation corresponds to conformation A or B in Fig. 3-48. Inclusion of additional conformations particularly at high temperature should result in a better fit to the experimental data and lead to slight differences in this energy.

If the non-linear behavior of the methyl group resonance reflects population of more than one conformation, why is the α-proton resonance virtually linear in T^{-1}? Table 3-15 shows that the geometry factors for all of the possible conformations of the α-protons are negative. Since the isotropic shift for the α-protons is negative and the contact shift is positive, the pseudocontact shift component must dominate. Assuming population of any two conformations, the isotropic shift for both will be negative. Taking the energy difference between the two as 0.395 kcal $mole^{-1}$, selection of a wide variety of negative values for C_L and C_H results in virtually straight lines over the temperature range -100°C to 100°C. Curvature is only apparent if the difference between C_L and C_H is greater than an order of magnitude, or the energy difference between the two conformations is substantially increased. Thus, any

non-linearity in the temperature dependence of the α-proton resonance, will be small over the observed temperature range and close to the limits of experimental error.

The temperature dependent change in population ratio of conformations in 1,1'-diethyluranocene suggests that similar behavior should be observed in other 1,1'-disubstituted uranocenes where the α-carbon bears a single substituent. Two such uranocenes were investigated, 1,1'-di-n-butyl- and 1,1'-dineopentyluranocene.

3) 1,1'-DI-n-BUTYLURANOCENE

Over the temperature range -80°C to 100°C the corresponding proton resonances of 1,1'-di-n-butyl- and 1,1'-diethyluranocene are virtually superimposable. Thus, the α-proton resonance displays a linear T^{-1} dependence while the β-proton resonance displays virtually identical non-linearity (Fig. 3-43, 3-44). The proposed temperature dependent change in conformational populations is further supported by the temperature dependence of the γ and δ-proton resonances which show gross deviations from linearity (Fig. 3-46). Unambiguous assignment of individual resonances could be verified at low temperature where all the resonances are resolved and display J-J coupling.

4) 1,1'-DINEOPENTYLURANOCENE

The temperature dependence of the substituent proton resonances in 1,1'-dineopentyluranocene are both linear in T^{-1}

implying that the substituent is locked in one conformation. Further, the slope of the shift vs T^{-1} plot for the t-butyl resonance is positive and the extrapolated intercept at $T^{-1} = 0$ is zero. Table 3-17 shows that the average geometry factor for the t-butyl protons is positive only in conformation A and B, which are identical to the proposed low energy conformations of the substituent in 1,1'-diethyl- and 1,1'-di-n-butyluranocene. This argument provides compelling evidence that the substituent must be locked in conformation A. Intuitively, this is the conformation one would predict based on steric considerations.

Interestingly, the extrapolated intercept at $T^{-1} = 0$ for the α-proton resonance is significantly non-zero. If the substituent is strictly locked in one conformation, the extrapolated intercept should be zero and thus, the observed non-zero value cannot be attributed to temperature dependent conformational changes. We shall return to this point in our discussions on factoring isotropic shifts in 1,1'dialkyluranocenes.

5) 1,1'-DIISOPROPYLURANOCENE

In 1,1'-diisopropyluranocene where the α-carbon is disubstituted, the substituent proton resonances are also linear functions of T^{-1}. Of the seven principal conformations of the isopropyl group in Fig. 3-51, steric interactions predict BD and DF will be the highest in energy. Ordering of the remaining conformations is not intuitively obvious. In isopropylbenzene, the preferred conformation is BF where the α-proton is in the plane of the ring.[91] Relief of steric

Fig. 3-51 Conformations of an isopropyl group attached to a planar carbocyclic ring system. In metallocenes the metal atom is assumed to be below the plane of the ring in each figure.

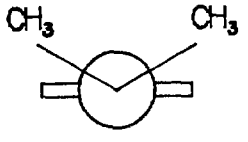

CC

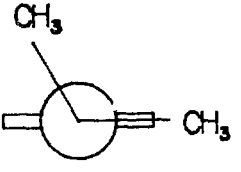

BD

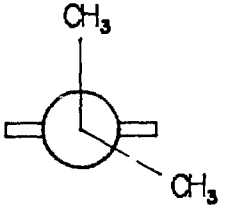

AE

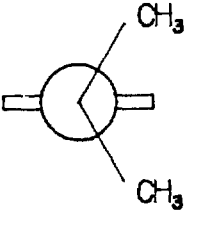

BF

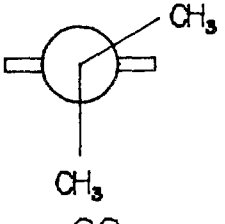

CG

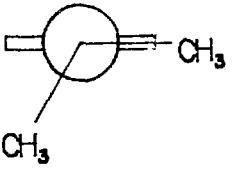

DF

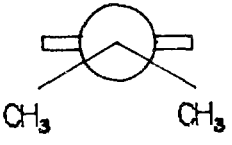

EE

strain between the methyl groups and the ortho protons upon increasing the dihedral angle from 30° in CC, AE, CG, and EE is greater than the strain introduced by the eclipsing of the methine and ortho protons. Extended Hückel calculations by Schilling[80] predict the ordering of conformations in isopropylbenzene and isopropylcyclooctatetraene dianion is BF < AE = GC < BD = DF << CC = EE, while in 1,1'-diisopropyluranocene the calculated order is BF < AE < GC << BD < DF << CC << EE. In the preferred conformations, BF, AE and GC, the two methyl groups are non-equivalent and thus, bond rotation must be fast relative to the NMR time scale since a single methyl resonance is observed.

Conformational preferences of secondary alkyl groups attached to planar carbocyclic ligands in organometallic complexes have been studied by other authors using variable temperature ^{1}H NMR. In 1,1'-dialkyl nickelocenes, $(RC_5H_4)_2Ni$, where R = $CH(CH_3)_2$ and $CH(CH_2CH_3)_2$, Rettig and co-workers[92] have found a linear T^{-1} dependence for the methine resonance when R = $CH(CH_3)_2$ but non-linear when R = $CH(CH_2CH_3)_2$ indicating that the energy barrier to rotation about the C_{ring} - C_α bond increases with increasingly bulky substituents. In both cases, the preferred conformation was shown to be one where the dihedral angle between the ring plane and the methine bond was close to zero.

In paramagnetic nickel (II) complexes with alkyl groups attached to a 6-membered ring, Knor and co-workers[89] have found that both the $CH(CH_3)_2$ and $CH(CH_2CH_3)_2$ have similar steric requirements and a rotation energy barrier of 4.5 ± 0.03 kcal

mole^{-1}. The increase in rotational energy barrier on changing from a 5 to a 6-membered ring parallels the enhanced buttressing effect of ortho protons on the larger carbocyclic ring and suggests that one should expect a still larger barrier upon attachment to the 8-membered ring in 1,1'-diisopropyluranocene. However, such extrapolation is not strictly valid. Knor's work involved a system where both faces of the six-membered ring are equivalent, while in both the nickelocene and the uranocene, complexation of the metal to one face of the carbocyclic ligand will destabilize all conformations in which the methyl groups are on the same side as the metal and thus, should serve to lower the energy barrier to rotation.

Analysis of geometry factors for conformations of the isopropyl group in Fig. 3-51 show that similar to the α-protons in 1,1'-diethyluranocene, the average geometry factor for the methyl groups in each of these conformations is negative and thus, deviations from linear dependence on T^{-1} resulting from changes in conformational population ratios, will be small and of the same order of magnitude as experimental errors.

6) 1,1'-BIS(TRIPHENYLMETHYL)URANOCENE

The ^{1}H NMR spectrum of 1,1'-bis(triphenylmethyl)uranocene was measured at 30°C and -80°C to see if trisubstitution of the α-carbon with large bulky groups would appreciably raise the energy barrier for rotation about the C_{ring} - C_α bond. However, at both temperatures, the spectrum consists of four sharp ring proton resonances and three substituent resonances

corresponding to the ortho, meta, and para positions, indicating that rotation is rapid.

7) 1,1'-DIARYLURANOCENES

Phenyl-substituted uranocenes were investigated to see if the buttressing effect of the ortho protons would effectively raise the energy barrier to substituent rotation. In our discussion of the ring proton resonances we suggested that the change in pattern of the non-equivalent ring proton resonances in these compounds may result from temperature dependent changes in the rate of substituent rotation.

All of the substituent proton resonances are linear in T^{-1}, in both of the 1,1'-diaryluranocenes studied. The extrapolated intercepts at $T^{-1} = 0$ for the ortho protons is non-zero and positive while those of the other resonances are close to zero. At low temperature, the linewidth of the ortho resonance in both systems is appreciably broadened indicating the onset of coalescence. For 1,1'-diphenyluranocene coalescence could not be reached at the lowest attainable temperature of -80°C. However, for 1,1'-bis(p-dimethylaminophenyl)uranocene, the ortho resonance completely coalesces into the baseline at -100°C and at -110°C the ring protons begin to coalesce. Comparison of the temperature dependent changes in linewidth of the ortho resonance for the two compounds suggest that coalescence of the ortho proton resonance in 1,1'-diphenyluranocene will occur at -125 to -135°C.

The lower coalescence temperature of the phenyl substituent

implies that the energy barrier to substituent rotation is larger in 1,1'-bis(p-dimethylaminophenyl)uranocene than in 1,1'-diphenyluranocene. This may result from the electron donating character of the dimethylamino group. The cyclooctatetraene ligands in uranocene are electron rich so that conjugation with a coplanar phenyl ring bearing a π-electron donor will be unfavorable. Hence, the coplanar conformation of the ring will be destabilized, and thus, the energy barrier to rotation will be larger.

Thus, while the buttressing effect of the ortho protons in arylsubstituted uranocenes does raise the energy barrier to substituent rotation, the energy barrier is still slightly lower than the lowest energy barriers readily measureable by variable temperature ^{1}H NMR. However, observation of temperature dependent changes in the rate of substituent rotation in these arylsubstituted uranocenes may also account for the temperature dependent changes in the pattern of the ring proton resonances, a point which we shall explore in greater detail in Chapter 4.

8) 1,1'-DI(CYCLOOCTATETRAENYL)URANOCENE

Both Miller[59] and, recently, Fischer and co-workers[93] have reported that the number of substituent and ring proton resonances of 1,1'-di(cyclooctatetraenyl)uranocene vary as a function of temperature indicative of a dynamic process which is slow on the NMR time scale. Above 90°C, the spectrum consists of 4 ring proton resonances in an

area ratio of 2:2:2:1, similar to that of other 1,1'-disubstituted uranocenes. At 30°C, six broad ring proton resonances are present and determination of relative areas is extremely difficult. Initially, we had hoped that monitoring coalescence of the ring protons in this system would provide a method of assigning individual ring proton resonances. However, interpretation of the temperature dependent changes was not straightforward and no assignment could be made.

Initially, the B ring resonance begins to broaden at 80°C, followed by the A resonance at ca. 70°C, and both merge into a single peak at 50°C. Below this temperature, they rapidly separate into three broad peaks at 40°C and to at least six peaks at 30°C. At 40°C, the C resonance also begins to coalesce followed by the D resonance at ca. 30°C. Below 30°C, it is not clear which of the peaks in the 'low temperature' spectrum are associated with peaks in the 'high temperature' spectrum. From 0°C to -80°C, eleven ring proton resonances are discernible; however, relative peak areas indicate that not all of the individual resonances are resolved.

Similar temperature dependent behavior is observed for the substituent proton resonances. At 90°C, all of the resonances have coalesced into the baseline, while at 80°C, a resonance appears at 1.8 ppm, followed at 70°C, by the appearance of two broad resonances at -9.0 ppm and -14.9 ppm and a sharper resonance at ca. 0.0 ppm. Labeling these resonances as K (1.8 ppm), L (0.0 ppm), M (-9.0 ppm) and N (-14.9 ppm), the L resonance separates into two peaks at ca. 50°C, while the other resonances remain fairly sharp. At 30°C, the N resonance

begins to broaden and separates into two peaks at 20°C, followed by broadening of the M resonance. At 10°C, the M and N regions each consist of two resonances while the two resonances of the L region are broadened. The behavior of the K resonance is obscured by the TMS/grease signal. At 0°C, the L region consists of four resonances. At -80°C, the M and N signals are both well separated sets of two resonances each while the K and L regions consist, respectively, of four and five sets of double resonances of essentially equal area.

Of the substituent resonances, only the M and N signals can be definitively assigned to the α position of the uncomplexed ring. At low temperature, the α position protons are equally distributed in four magnetically different environments.

A combination of slowing or effective stopping of several dynamic exchange processes could give rise to the observed changes in the spectrum: 1)tub tub interconversion of the uncomplexed cyclooctatetraene ring; 2)double bond reorganization in the uncomplexed cyclooctatetraene ring; 3)rotation about the C_{ring} - C_{α} bond; 4)ring-ring rotation in the uranocene moiety. The presence of four different α position resonances in the 'low temperature' spectrum requires that double bond reorganization be slow relative to the NMR time scale. This implies that in the 'high temperature' spectra where double bond reorganization is rapid, four rather than seven substituent resonances should be observed. Unfortunately, due to solvent and instrumental limitations, we could not obtain spectra above 100°C to confirm this. The data do not permit further differentiation between the other possible dynamic exchange

processes.

9) DIANNULATED URANOCENES

Initially, we had hoped that the fused ring in the annulated uranocenes would prevent, or at least restrict conformational mobility of the substituent. However, as Fig. 3-40,41, 3-45,46 indicate, the temperature dependences of all of the substituent proton resonances in these compounds are non-linear in T^{-1} indicative of conformational mobility. In the crystalline state, the X-ray crystal structure of dicyclobutenouranocene shows that the two methylene groups are non-equivalent.[86] In solution, however, they are equivalent on the NMR time scale. Taking the average position of the methylene groups from the X-ray structure, the sign of the geometry factor for both the exo and endo protons is negative. The slope in the shift vs T^{-1} plot for the exo proton resonance is positive and thus, the contact component must be positive and larger than the pseudocontact component of the exo proton isotropic shift.

The deviations in linear dependence on T^{-1} for both resonances are correlated. At both temperature extremes, the deviation is negative for the exo resonance and positive for the endo resonance. This clearly implies that the non-linearity arises from conformational mobility and not a second or higher order dependence on temperature of the contact or pseudocontact shift.

The conformational changes of the fused ring also appear

to affect the 8-membered ring. One ring proton resonance is at significantly lower field than the other two and is not linear in T^{-1}. Perturbations in the 8-membered ring resulting from conformational changes in the 4-membered ring are probably largest for protons adjacent to the ring juncture, and those furthest removed, where distortion of the 8-membered ring is most pronounced. Thus, this resonance can be tentatively assigned to the 3 and 8 protons although it could also be the 5 and 6 proton resonance. This assignment is in apparent contrast to the ring proton assignment in 1,1',4,4'-tetra-t-butyluranocene, where the ring proton most removed from the substituent resonates at lowest field.

Both the resonance frequency and the temperature dependence of the α-protons in dicyclopentenouranocene and bis(dimethylcyclopenteno)uranocene indicate that introduction of the two methyl groups changes the conformation of the 5-membered ring in these compounds. Similar to dicyclobutenouranocene, the slope in the shift vs T^{-1} plots for the α-protons in dicyclopentenouranocene is positive for the exo protons and negative for the endo protons. Deviations in linear dependence for the two positions are also correlated but exactly opposite that in dicyclobutenouranocene. The exo resonance deviation is positive while that of the endo is negative at the two temperature extremes. In bis(dimethylcyclopenteno)uranocene the shift dependence on T^{-1} is negative for both the α exo and endo protons, with the exo resonance showing a pronounced deviation from linearity. The shift dependence on T^{-1} is positive for the exo and negative for the endo methyl groups

indicating that the average geometry factor for the two groups is opposite in sign. Undoubtedly, the non-linear dependence on T^{-1} of the substituent proton resonances in the two cyclopentenouranocenes results from temperature dependent puckering of the 5-membered rings.

III. FACTORING THE ^1H ISOTROPIC SHIFTS IN ALKYL SUBSTITUTED URANOCENES

The preceeding discussion has shown that the pseudocontact component of the isotropic shift in 1,1'-dialkyluranocenes is accurately given by the axially symmetric form of eq. 17, and thus, these systems can be used in evaluating both the assumptions employed in deriving, and the value of the anisotropy term $(X_{\parallel} - X_{\perp})$, used, by previous workers in factoring isotropic shifts in uranocenes. In the following section we present such an analysis comparing pseudocontact shifts calculated assuming $X_{\parallel} - X_{\perp} = 3X_{av}$ and assuming values of $X_{\parallel} - X_{\perp}$ derived from isotropic shift and geometric data for protons which experience little or no contact shift. However, prior to such analysis it is important to be cognizant of the accuracy of calculated pseudocontact and contact shifts. Irrespective of the method or the equation(s) used to calculate pseudocontact shifts, three factors limit their accuracy: a)errors in measurement of the isotropic shift; b)errors in the assumed geometry; c)errors in the magnetic anisotropy. For uranocenes, the uncertainty associated with the isotropic shifts is small, larger for the

assumed geometries and largest for the assumed anisotropy difference. In calculating shifts assuming $X_{||} - X_{\perp} = 3X_{av}$, Table 3-11 shows that to a good first approximation, μ_{av} = 2.4 ± 0.2 B.M. for all uranocenes. As a result of the 10% uncertainty in this value, calculated pseudocontact shifts will have an uncertainty of at least 10%. Similarly, in using a value of $X_{||} - X_{\perp}$ derived from isotropic shift and geometric data, the uncertainty associated with calculated pseudocontact shifts will depend upon the reference compound chosen and will undoubtedly be of the same order of magnitude. Thus, the factored shifts in the following section will have an error of at least 10%.

In the following discussion, all calculated shifts are derived assuming a temperature of 30°C. For numerical convenience, the anisotropy term $X_{||} - X_{\perp}$ will be expressed in terms of $\mu_{||}^2 - \mu_{\perp}^2$.

Three alkyl uranocenes, 1,1'-di-t-butyl-, 1,1'-dineopentyl- and dicyclobutenouranocene are ideally suited test systems, since they contain α, β and γ-protons constrained in known geometric configurations relative to the uranium center. In the former two compounds, contact contributions to the t-butyl isotropic shift must be vanishingly small, while in the latter compound, the fixed geometric relationship of the methylene group relative to the 8-membered ring requires that both hyperconjugation and the contact shift must be effectively the same for the exo and endo protons, if the contact shift results from hyperconjugative transfer of spin density.

The average geometry factor for the t-butyl group in

1,1'-di-t-butyluranocene was taken as 1/6(A + 2C + 2E + G) in Table 3-16 and for the t-butyl group in the neopentyl substituent it was taken as conformation A (Table 3-17). While the methylene protons in dicyclobutenouranocene are conformationally mobile, as evidenced by their temperature dependent ^1H NMR spectra, we believe their average position in solution is adequately given by the average position of the two methylene groups in the X-ray crystal structure. Although atomic coordinates are reported for all of the atoms in the X-ray structure, geometry factors calculated from these data are probably in error for two reasons: 1)the reported coordinates are not thermally corrected, and thus, they reflect an average $C_{ring} - C_{ring}$ bond length of 1.39 A rather than a thermally corrected value of 1.41 A; 2)the two reported $H_{exo} - C_{\alpha} - H_{endo}$ bond angles of 104° and 106° are certainly too small and reflect the large uncertainty associated with the location of hydrogen atoms by X-ray diffraction.

Formally, the fused 4-membered ring is similar to the 4-membered ring of cyclobutene or benzocyclobutene, and the methylene bond angle should be similar to the methylene bond angle in these compounds. Gas phase electron diffraction of cyclobutene gives this angle as 110°,[94] while of $J_{^{13}C-H}$ coupling constants yield a value of 114°.[95] Similarly, $J_{^{13}C-H}$ coupling constant analysis predict a bond angle of 112° in benzocyclobutene.[96] Thus, 112° is certainly a more realistic value for the $H_{exo} - C_{\alpha} - H_{endo}$ bond angle. In calculating geometry factors for the exo and endo protons, we have used the idealized geometry in 45, which more accurately describes the location of the methylene protons,

rather than the coordinates of the atoms from the published X-ray crystal structure.

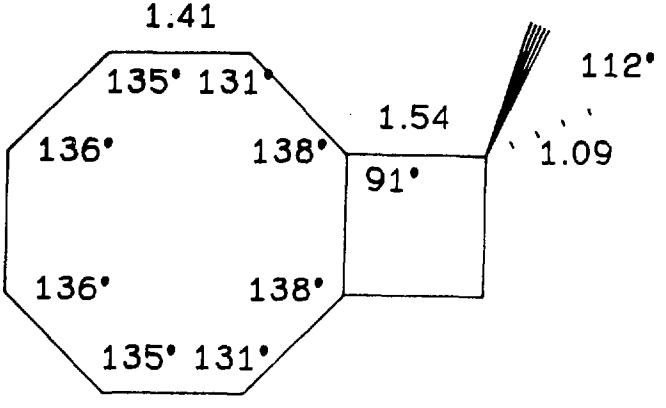

The geometry factors for the exo and endo protons calculated with these data are -0.7097×10^{21} cm^{-3} and -16.97×10^{21} cm^{-1}, respectively.

Considering first the Edelstein, et al.,[5] proposal that $X_{\parallel} - X_{\perp} = 3X_{av}$, the average μ_{eff} of 2.4 ± 0.2 B.M. for uranocene and substituted uranocenes affords a value of 17.28 B.M.^{2} for μ_{av}^2. The calculated pseudocontact shifts for a t-butyl group, and the t-butyl protons in a neopentyl group, assuming coplanarity of the $C_{ring} - C_{\alpha}$ bond and the 8-membered ring are -23.7 ppm and 14.3 ppm, respectively, With a tipped substituent the values are respectively -28.8 ppm and 6.35 ppm. Comparison with the experimental isotropic shifts of -13.29 ppm and 2.76 ppm shows that the calculated values overestimate the magnitude of the pseudocontact shift. Factoring the isotropic shifts of the methylene protons in the cyclobuteno group further reinforces this result. The calculated pseudocontact shifts are: exo

-2.80 ppm, endo -67.0 ppm. By difference from the isotropic shifts of 15.19 ppm (exo) and -31.20 ppm (endo), the corresponding contact shifts are 17.-9 ppm (exo) and 35.8 ppm (endo). The large difference in the contact shifts cannot result from slight differences in hyperconjugation, which may arise from the ca. 6° decrease in the 180° dihedral angle between the 4 and 8-membered rings, but clearly results from overestimation of the pseudocontact shift.

Reducing the magnitude of the calculated pseudocontact shifts requires small values of the anisotropy term $X_{\parallel} - X_{\perp}$, which can only result if $X_{\perp} \neq 0$. Both the electronic structure of uranocene proposed by Warren,[97] assuming a $J_z = \pm 4$ ground state, and the more recent model proposed by Fischer,[58] assuming a $J_z = \pm 3$ ground state, show that $X_{\perp}$ will be non-zero, and less than $X_{\parallel}$, at 30°C.

During this study, Fischer[58] reported factoring the isotropic shifts in uranocene, 1,1',3,3',5,5',7,7'-octamethyluranocene, and 1,1'-bis(trimethylsilyl)uranocene using a non-zero value of $X_{\parallel}$. Fischer arrived at values of $\mu_{\parallel}^2$ and $\mu_{\perp}^2$, at several temperatures, from the ratio of the geometry factor and the isotropic shift for methyl protons in bis(trimethylsilyl)-uranocene, and bulk magnetic susceptibility data, assuming no contact contributions to the isotropic shift of the methyl protons. From the published data of Fischer, the value of $\mu_{\parallel}^2 - \mu_{\perp}^2$, at 30°C, is 8.78 B.M.^{2}

Using this value, the calculated pseudocontact shifts for the t-butyl groups in 1,1'-di-t-butyl- and 1,1'-dineopentyl uranocene are -12.1 ppm and 7.28 ppm, respectively, for a

coplanar substituent, and -14.6 ppm and 3.22 ppm for a tipped substituent. Agreement between the calculated pseudocontact shifts and the observed isotropic shifts is extremely good. Calculation of the pseudocontact shifts for the cyclobuteno substituent afford values of -1.42 ppm (exo) and -34.0 ppm (endo) with corresponding contact shifts of 16.6 ppm (exo) and 2.80 ppm (endo). Again the difference in contact shifts for the two positions is not reasonable or theoretically justifiable. It does not arise from the difference between the reported atomic coordinates from the X-ray crystal structure data and our 'idealized' geometry for cyclobutenouranocene. The calculated pseudocontact shifts using geometry factors derived from the average position of the methylene groups in the X-ray structure are -2.36 ppm (exo) and -28.5 ppm (endo), with contact shifts of 17.5 ppm (exo) and -2 7 ppm (endo). Moreover, increasing the dihedral angle between the fused rings in the cyclobuteno ligand from 173° to 180° results in a larger discrepancy between the calculated contact shifts for the two positions.

The value of the contact shift for the exo and endo protons can be derived indirectly from the calculated contact shift for the methyl groups in 1,1'-dimethyluranocene. Assuming a geometry factor for the methyl group as 1/6(A + 2C + 2E + G) and $\mu_{||}^2 - \mu_{\perp}^2 = 8.78$ B.M.^{2}, the calculated pseudocontact shifts for the coplanar and tipped substituent are -11.8 ppm and -12.8 ppm, respectively. From the isotropic shift of -10.00 ppm, the corresponding contact shifts are 1.8 ppm and 2.8 ppm. Contact shifts for α-protons are assumed to arise

from hyperconjugative transfer of spin. Hyperconjugation between a carbon p orbital and a carbon hydrogen bond is a function of the dihedral angle between the two. When unpaired spin is transferred by hyperconjugation, the magnitude of both the hyperfine coupling constant in ESR, and the contact shift in NMR, can be expressed by

$$B = B_o \cos^2(\phi) \qquad (30)$$

where ϕ is the dihedral angle, and B_o is the magnitude of the hyperfine coupling constant or the contact shift when $\phi = 0$.[90,91,92,98] Evaluation of B_o from the contact shift for the methyl group affords values of 3.54 ppm and 5.54 ppm respectively, for a planar and a tipped substituent.

The fixed dihedral angle between the p-orbitals of the 8-membered ring and the methylene C-H bonds in the cyclobutene substituent permit evaluation of the contact shift for the exo and endo protons from B_o. In our idealized structure of the ligand, the dihedral angle is 25° which compares favorably with the average value of 22° from the X-ray data. With $\phi = 25°$, the calculated contact shift is 2.91 ppm when $B° = 3.54$ ppm and 4.5 ppm when $B° = 5.54$ ppm. These values are significantly different than those obtained by difference, from the isotropic shifts for the exo and endo protons and the calculated pseudo-contact shifts assuming $\mu_{||}^2 - \mu_{\perp}^2 = 8.78$ B.M.^{2} The discrepancy between the calculated contact shifts for the exo and endo protons in 1,1'-dicyclobutenouranocene using Fischer's value of $\mu_{||}^2 - \mu_{\perp}^2$ can only arise from underestimation of the pseudo-

contact shifts resulting from underestimation of $\mu_{\parallel}^2 - \mu_{\perp}^2$.

The known geometry of the methylene protons in the cyclobuteno substituent permit calculation of $\mu_{\parallel}^2 - \mu_{\perp}^2$. Assuming that the contact shift for both methylene protons is equal, the relationship between $X_{\parallel} - X_{\perp}$, the isotropic shift δ, and the geometry factor G for the exo and endo protons is given by

$$\frac{X_{\parallel} - X_{\perp}}{3} = \frac{\delta_{exo} - \delta_{endo}}{G_{exo} - G_{endo}} \qquad (31)$$

Equation 31 leads to a value of 12.5 B.M.^{2} for $\mu_{\parallel}^2 - \mu_{\perp}^2$ with corresponding pseudocontact shifts of -2.03 (exo), -48.5 ppm (endo) and a contact shift of 17.2 ppm.

This value of $\mu_{\parallel}^2 - \mu_{\perp}^2$ yields pseudocontact shifts of -17.2 ppm and 10.4 ppm for the t-butyl groups in 1,1'-di-t-butyl- and 1,1'-dineopentyluranocene, assuming coplanar substituents, and -20.8 ppm and 4.59 ppm, assuming tipped substituents. Although agreement between the calculated and experimental shifts for the neopentyl t-butyl group, assuming a tipped substituent is good, agreement between the t-butyl calculated and experimental data is poor for the coplanar and worse for the tipped substituent. If we assume the difference in the observed and the calculated shifts for the t-butyl substituent is contact in nature, neither its sign nor its magnitude are consistent with the predicted sign based on transfer of spin by spin polarization, or the magnitude limits established from analysis of the temperature dependence of the methyl resonance in 1,1-diethyluranocene. Thus, if the difference in calculated

and observed shift does not arise from the anisotropy term, it must result from inaccuracies in the assumed geometry factor.

Inspection of Table 3-7 shows that the pattern of the non-equivalent ring protons in 1,1'-dialkyluranocenes varies depending upon the substituent. In Chapter 4, we show that the pattern is directly related to the degree of substitution of the α-carbon. Molecular models show that changes in the pattern as substitution on the α-carbon increases from mono- to di- to trisubstituted, result from non-bonding interactions between β-hydrogens on the substituent and both 2 position ring proton on the ring of attachment, and ring protons of the second cyclo-octatetraene ring, which change the spacial location and geometry of the 2 and possibly the 3 position ring protons.

Such non-bonding interactions should also induce geometric distortions in the substituent. Further, the proximity of the β-hydrogens to the second cyclooctatetraene ring protons in conformation D-A-D should prevent the substituent from tipping down toward the uranium as it appears to do in alkyluranocenes with primary substituents. In fact, this latter interaction may be sufficient to force the substituent out of the plane of the 8-membered ring and away from the uranium. Indeed, regardless of the value of $X_{\parallel} - X_{\perp}$ tipping the substituent away from the uranium center leads to better agreement between the calculated and observed shift for the t-butyl group in 1,1'-di-t-butyluranocene. With $\mu_{\parallel}^2 - \mu_{\perp}^2 = 12.5$ B.M.^{2}, a tip of 5° affords a calculated pseudocontact shift of -13.7 ppm, in excellent agreement with the isotropic shift of -13.29 ppm. Thus, geometry changes can account for the discrepancy between

the calculated pseudocontact shift and the observed isotropic shift for the t-butyl substituent in 1,1'-di-t-butyluranocene.

The similarity between a t-butyl group and a trimethylsilyl group suggests that similar, sterically induced geometric distortions should occur in 1,1'-bis(trimethylsilyl)uranocene. The pattern of the ring proton resonances, and the frequency and temperature dependence of the substituted proton resonance, are all similar in both 1,1'-di-t-butyl- and 1,1'-bis(trimethylsilyl)uranocene. Assuming a coplanar substituent, as Fischer has, the ratio of the isotropic shift and geometry factor for the t-butyl group in 1,1'-di-t-butyluranocene is virtually identical with that of the trimethylsilyl group in 1,1'-bis(trimethylsilyl)uranocene, reported by Fischer.[58] Thus, it appears that the trimethylsilyl substituent experiences the same sterically induced geometric distortions as the t-butyl substituent. Failure to account for this geometric distortion in calculating $\mu_{\parallel}^2 - \mu_{\perp}^2$ from geometric and isotropic shift data, from either 1,1'-di-t-butyluranocene or 1,1'-bis(trimethylsilyl)uranocene, results in underestimation of $\mu_{\parallel}^2 - \mu_{\perp}^2$.

To further demonstrate the difficulties associated with selecting an appropriate reference compound from which $\mu_{\parallel}^2 - \mu_{\perp}^2$ can be derived, we shall derive $\mu_{\parallel}^2 - \mu_{\perp}^2$ from the geometry factor and the isotropic shift of the t-butyl group in 1,1'-dineopentyluranocene. Our conformational analysis showed that the substituent is locked in conformation A. For a coplanar substituent, the derived value of $\mu_{\parallel}^2 - \mu_{\perp}^2$ is 3.33 B.M.^{2}, while tipping the substituent 5° toward the uranium leads to a value of 7.51 B.M.^{2} However, relaxing the restriction of exclusive

population of conformation A, and assuming an extremely small population of any other conformation where the geometry factor and the pseudocontact shift are negative, will greatly increase the derived value of $\mu_{\parallel}^2 - \mu_{\perp}^2$.

Thus, evaluation of the geometry factor is extremely important in deriving a value of $\mu_{\parallel}^2 - \mu_{\perp}^2$ from geometric and isotropic shift data. Two factors favor our approach to deriving a value of $\mu_{\parallel}^2 - \mu_{\perp}^2$ from the methylene protons in dicyclobutenouranocene: 1) the single crystal X-ray data and the variable temperature ^{1}H NMR data provide an excellent estimate for the geometry factors for the two methylene protons, 2) calculation involves using the isotropic shift and geometry factor of two magnetically non-equivalent protons rather than one.

From the contact shift of the exo and endo protons in dicyclobutenouranocene, derived using $\mu_{\parallel}^2 - \mu_{\perp}^2 = 12.5$ B.M.^{2}, a value of B_o, the maximum contact shift for an α-proton, can be calculated from eq. 30. Taking $\Phi = 25°$ leads to a value of 20.9 ppm for B_o.

Assuming a geometry factor of 1/6(A + 2B + 2D + C) for the methyl group in 1,1'-dimethyluranocene, the calculated pseudocontact shifts are -16.8 ppm and -18.2 ppm, respectively, for a coplanar and a tipped substituent. By difference from the isotropic shift, the contact shifts are 6.76 ppm and 8.17 ppm, while calculation of the contact shift from B_o affords a value of 8.71 ppm. Agreement between the contact shifts calculated by both methods is excellent, particularly for the tipped substituent.

Considering the α-protons in 1,1'-dineopentyluranocene, if A is the only populated conformation of the neopentyl substituent, then the conformation of the α-protons is EE. The calculated pseudocontact shift is -26.9 ppm (coplanar), -31.8 (tipped) and by difference from the experimental isotropic shift of -23.97 ppm the contact shifts are 2.93 ppm (coplanar), and 7.83 ppm (tipped). Calculation of the contact shift from B_o affords a value of 5.23 ppm.

Comparison of the calculated pseudocontact shifts for the neopentyl t-butyl resonances with the isotropic shift showed the tipped geometry afforded better agreement between the two values, but still the value of calculated shift was approximately twice that of the experimental isotropic shift. However, an extremely small population of any conformation other than A will readily decrease the magnitude of the calculated pseudocontact shift for the t-butyl resonance. Assuming an extremely small population of conformations other than A, how does this affect the factored shifts of the α-protons?

From the geometry factors in Table 3-15 and eq. 30, the pseudocontact shift for any conformation other than EE will be less negative than that for EE, while the contact shift will be smallest in magnitude for EE and larger for any other conformation. The magnitude of these changes is such that the isotropic shift will be less negative as the population of conformations other than EE increase. Thus, assuming a tipped substituent, and an extremely small population of conformations other than A for the neopentyl substituent in 1,1'-dineopentyluranocene, leads to better agreement between the calculated

pseudocontact and contact shifts for both the α and t-butyl resonance, than assuming either exclusive population of conformation A or a coplanar substituent.

This analysis also accounts for the observed trend in the isotropic shift of the α-protons in 1,1'-diethyl-, 1,1'-di-n-butyl-, and 1,1'-dineopentyluranocene, respectively, -17.47 ppm, -19.03 ppm, and -23.97 ppm. The increase in magnitude of the isotropic shift directly parallels the increasing stability of the preferred conformation of the substituent, (i.e., conformation A).

In modeling the temperature dependence of the methyl group isotropic shift in 1,1'-diethyluranocene, we have proposed that the data could be fit assuming population of only two principal conformations. From C_L and C_H, the calculated isotropic shifts for these two conformations at 30°C is 9.90 ppm (low) and -13.9 ppm (high). The low temperature data showed that the low temperature conformation corresponds to conformation A. The calculated pseudocontact shift for conformation A is 7.32 ppm for a coplanar substituent and 5.11 ppm for a tipped substituent, which are both close to the proposed shift for the low temperature conformation, considering the uncertainty associated with the calculated value of 9.90 ppm. The calculated pseudocontact shifts of -47.0 ppm (coplanar), -53.5 ppm (tipped) and -41.7 ppm (coplanar), -47.5 ppm (tipped), respectively, for conformations F and G which should correspond to the high energy conformation, show that the assumption of only one high temperature conformation is obviously too restrictive.

Conformational analysis of 1,1'-diisopropyluranocene showed

the preferred conformations of the substituent to be AE, BF and CG. Comparison of the calculated pseudocontact shifts for conformations AE and BF, of -11.1 ppm and -18.4 ppm, respectively, assuming a coplanar substituent, and -14.4 ppm and -22.3 ppm, respectively, assuming a tipped substituent, with the experimental isotropic shift of -10.89 ppm shows that the agreement between the calculated and experimental values is better assuming a coplanar substituent, but still poor. The disparity between the calculated and experimental shifts undoubtedly results from two factors: 1)unequal population of more than one conformation of the substituent; 2)sterically induced geometric distortions in the substituent as evidenced by the pattern of the non-equivalent ring proton resonances (see Chapter 4).

Assuming the conformation of the isopropyl group is AE, BF, or CG, the methine proton will reside in conformations C, D or E. The calculated pseudocontact shifts for these conformations are -4.29 ppm, -14.4 ppm, and -26.9 ppm, respectively, for a coplanar substituent, and -7.43 ppm, -18.1 ppm, and -31.8 ppm, respectively, for a tipped substituent. Further, eq. 30 shows that the contact shift will be zero for conformation D and 5.2 ppm for conformations C and E. Comparison with the isotropic shift of -16.67 ppm indicates that the methine proton is either in conformation D or in a conformation where it is slightly below the plane of the 8-membered ring and on the same side as the uranium, implying that conformation AE is lower in energy than conformation CG. This energy ordering is in total agreement with the results of extended Hückel calculations.

In the two annulated uranocenes with fused 5-membered rings, the isotropic shifts for the β-protons in dicyclopenteno-uranocene and the methyl groups in bis(dimethylcyclopenteno)-uranocene should result from purely pseudocontact interactions. However, calculation of reasonable geometry factors for these protons from modeling of the conformational mobility of the 5-membered rings is extremely difficult, and thus, any correlation between the calculated and experimental shifts is subject to a high degree of uncertainty. Such modeling of the ring in dicyclopentenouranocene showed that the ratio of the geometry factor for the β exo and endo protons was equal to the ratio of the isotropic shifts for two conformations: conformation 1, where the α-carbons are coplanar with the 8-membered ring and the β-carbon is tipped 15° from this plane toward the uranium and conformation 2, where the α-carbons are tipped 5° toward the uranium and the β-carbon is also tipped 5° out of plane of the other four carbons in the 5-membered ring and toward the uranium. The calculated pseudocontact shifts of -7.54 ppm (exo) and -30.2 ppm (endo) for conformation 1, and -7.32 ppm (exo) and -28.5 ppm (endo) for conformation 2 are in reasonable agreement with the experimental isotropic shifts of -9.38 ppm (exo) and -33.58 ppm (endo).

While both of these conformations are reasonable in light of the X-ray crystal structure of dicyclopentenouranocene,[88] it is interesting that we could find no reasonable agreement between the calculated and experimental values assuming that the β-carbon is tipped out of the plane of the other four substituent carbons, and that the two conformations resulting

from tipping the α-carbon both up and down are equally populated.

Modeling of the conformation of the 5-membered ring in bis(dimethylcyclopenteno)uranocene showed that regardless of whether the α-carbons are coplanar with the 8-membered ring, or tipped toward the uranium atom, the β-carbon must be tipped out of the plane defined by the remaining four carbons of the 5-membered ring and away from the uranium, for the average geometry factor of the exo methyl protons to be positive. Assuming coplanarity of the α-carbons and the 8-membered ring, and a 20° tip of the β-carbon, results in good agreement between the calculated pseudocontact shifts of 4.91 ppm (exo) and -13.9 ppm (exo) and the experimental values of 4.39 ppm (exo) and -13.91 ppm (endo). The orientation of the β-carbon in this conformation could also account for the observed differences in the α exo proton resonace in this compound and dicyclopentenouranocene.

IV. DISCUSSION AND SUMMARY

Previous attempts at factoring the isotropic ^{1}H NMR shifts in uranocene and substituted uranocenes have all assumed that these systems can be viewed as having effective axial symmetry. The temperature dependent ^{1}H NMR spectra of uranocene and a variety of substituted uranocenes clearly verify this assumption and show that eq. 32 can be used to evaluate the pseudocontact contribution to the total isotropic shift in uranocenes.

$$\delta_{PSEUDOCONTACT} = \frac{X_{\parallel} - X_{\perp}}{3N} \quad \frac{3\cos^2\theta - 1}{R^3} \qquad (32)$$

Early attempts to factor the isotropic shifts in alkyluranocenes using eq. 32 were unsuccessful for two reasons: a) failure to correctly access the conformation of the substituent in solution; b) overestimation of the value of the anisotropy term $X_{\parallel} - X_{\perp}$.[5,6,14]

In alkyl-substituted uranocenes, our conformational analysis shows that a primary substituent resides principally in a conformation where the dihedral angle between the substituent $C_\alpha - C_\beta$ bond and the ring plane is 90°, and is on the side of the ring away from the metal. For secondary substituents, the preferred conformations are ones where the ring plane bisects the $C_\beta - C_\alpha - C_\beta$ bond angle and the methine proton is near or in the plane of the 8-membered ring. These conformations are similar to the preferred conformation of primary and secondary substituents in alkylcyclooctatetraene radical anions deduced by ESR.[99,100] For both secondary and tertiary substituents, steric interactions between the substituent and ring protons on the ring of attachment, and interaction with ring protons on the other ligand, induce geometrical changes in both the substituent and the ring protons. This proposal is not unique. In modeling the rotation barrier for an isopropyl group appended to a benzene ring, Mannschreck and Ernst[101] found that the experimental potential could only be reproduced if the geometry of the substituent was assumed to be flexible.

The second important contribution from this study is the conclusion that $X_{\perp}$ is not equal to zero in uranocene. Previous

attempts to factor isotropic shifts in uranocene have all assumed that $X_\perp = 0$, which leads to overestimation of the anisotropy term. Recently, Fischer has independently arrived at the same conclusion. A precise value of $X_\perp$ is difficult to access from analysis of the NMR data. We have found that $\mu_\parallel^2 - \mu_\perp^2 = 12.5$ B.M.^{2} leads to the best internal consistency in factored isotropic shifts for a wide variety of 1,1'-dialkylsubstituted uranocenes. Assuming $\mu_{av}^2 = 5.76$ B.M.^{2} and $\mu_\parallel^2 - \mu_\perp^2 = 12.5$ B.M.^{2}, at 30°C, the corresponding values of $\mu_\parallel^2$ and $\mu_\perp^2$ are 14.09 B.M.^{2} and 1.59 B.M.^{2}, respectively. This implies that $X_\parallel / X_\perp \approx 8$ in uranocene, which is larger than Fischer's ratio of $X_\parallel / X_\perp \approx 2.8$.[58]

As a result of $X_\perp \neq 0$, early work on factorization of the isotropic shift of the ring protons in uranocene underestimated the magnitude of the contact shift. Using our value of $\mu_\parallel^2 - \mu_\perp^2 = 12.5$ B.M.^{2} the pseudocontact and contact shifts for uranocene ring protons are -8.30 ppm and -34.2 ppm, ($G_i = -2.34 \times 10^{21}$ cm^{-3}), respectively. Thus, this study clearly shows that both contact and pseudocontact interactions contribute to the observed isotropic shifts in uranocenes. Further, the contact component is dominant for ring protons, but rapidly attenuates the greater the number of σ-bonds between the observed nucleus and the uranium, such that the contact shift is effectively zero for β-protons.

The value of the contact shift for ring protons in uranocene is of the same sign but ca. 10 to 15 ppm larger in magnitude than the contact shift for ring protons in Cp_3U-X compounds. If a linear correlation exists between the magnitude

of the contact shift and the degree of covalency in ligand-metal bonding in these systems then the NMR data suggest a higher degree of covalency in the ligand-metal bonds in uranocene.

V. THE ^{13}C NMR SPECTRA OF URANOCENES

Due to the low solubility of uranocenes, their ^{13}C NMR spectra could not be measured until the availability of FT ^{13}C NMR spectrometers. Bauer[102] originally recorded the ^{13}C NMR spectra of a large number of cyclooctatetraenes, the di-potassium salt of their dianions, and the corresponding uranocenes. Since this initial sutdy, acquisition of ^{13}C NMR spectra has become an integral part of the characterization of new cyclooctatetraenes, their dianions, and uranocenes synthesized by a wide variety of authors. The collected ^{13}C NMR data on neutral cyclooctatetraenes, the di-potassium salts of cyclo-octatetraene dianions, and uranocenes, are recorded in Tables 3-19 through 3-21.

The ^{13}C NMR spectra of cyclooctatetraene consists of a single resonance 131.6 ppm downfield from TMS. In general, the ^{13}C NMR spectra of substituted cyclooctatetraenes consist of a group of resonances in the range of 120-130 ppm, and a single resonance of lower intensity, in the range of 135-150 ppm. Proton coupled spectra have established that the low-field resonance corresponds to the quaternary carbon (C-1), in agreement with the general observation that quaternary carbons resonate at lower field than primary, secondary or tertiary

Table 3-19

The ^{13}C NMR Resonances of Cyclooctatetraenes

δ ppm from TMS

Substituent	Substituent Resonances	Ring Resonances	Ref.
H		131.7	102
Br		121.4(C-R), 130.9, 131.5, 131.9 132.7, 133.1	102
CH_3	24.2(CH_3)	127.6, 132.4(broad), 133.0, 136.2	102
octamethyl	23.9(CH_3)	128.7, 138.7(C-R)	102
CH_2CH_3	13.3(CH_3), 30.6(CH_2)	125.1, 131.0, 131.9, 134.3	102
$CH_2CH_2CH_2CH_3$	13.9(CH_3), 22.2(γCH_2) 30.8(βCH_2), 37.5(αCH_2)	126.0, 131.3, 132.2, 134.4 144.6(C-R)	102
$CH(CH_3)_2$	22.0(CH_3), 35.5(CH)	126.2, 128.8, 130.7, 131.7	102
$CH_2C(CH_3)_3$	30.1(CH_3), 31.5(CH_2), 52.1(βC)	131.6, 131.8, 132.2, 142.2(C-R)	104
1,4-di-t-butyl	29.8(CH_3), 36.2(αC)	121.5, 151,3(C-R)	59
$CH=CH_2$	113.5(CH_2)	131.4, 131.6, 132.7, 133.2, 138.8(C-R)	102
$CO_2CH_2CH_3$	14.3(CH_3), 60.7(CH_2) 163.5(C=O)	131.6, 133.3(broad), 134.2	102
$CO_2CH_2C_6H_5$	66.4(CH_2), 128.4(O), 128.0(m), 128.2(p), 165.3(C=O)	130.0(broad), 131.4, 132.5(broad) 133.5, 136.0	102
$OCH_2CH=CH_2$	68.6(OCH_2), 101.3(CH) 117.1(CH_2)	129.4, 129.6, 130.5, 131.2, 132.6, 133.4, 158.9(C-R)	102
$C(Ph)_3$	125.6(p), 127.2(o), 130.8(m), 65.9(αC)	132.2, 134.4, 131.2, 132.5, 131,8, 135.2, 132.3, 147.7(C-R)	103

Table 3-20

The ^{13}C NMR Spectra of Cyclooctatetraene Dianions[a]

δ ppm from TMS

Substituent	Substituent Resonances	Ring Resonances	Ref.
H		90.1	102
CH_2	33.7(CH_3)	89.2(C5), 89.9, 90.9, 91.9 93.2(C-R)	102
octamethyl	34.7(CH_3)	89.7(C-R), 96.3	102
CH_2CH_3	21.81(CH_3), 42.3(CH_2)	89.6, 90.7, 91.2, 103.1(C-R)	102
$CH_2CH_2CH_2CH_3$	14.9(CH_3, 24.1 (γCH_2)	89.3(C5), 89.5, 90.7(C4)	
	40.7(βCH_2), 49.6(αCH_2)	91.8, 101.0 (C-R)	102
$CH(CH_3)_2$	28.2(CH_3), 44.9(CH)	89.4, 89.6, 90.2(C5), 90.8, 107.2(C-R)	102
$C(CH_3)_3$	35.8(CH_3), 39.0 (αC)	88.2, 89.1, 89.5(C5), 90.2, 108.2(C-R)	102
$CH_2C(CH_3)_3$			104
C_6H_5	118.4(p), 127.6(m), 128.8(o), 158.3(ipso)	90.3, 91.7, 93.3, 94.1(C5) 102.9(C-R)	102
1,4-di-t-butyl	36.0(CH_3), 39.1(αC)	87.7, 87.9, 89.5, 108.3(C-R)	59
$C(Ph)_3$	123.0(o), 126.4(m), 131.2(p), 25.5(αC), 151.9(ipso)	90.3, 91.9, 92.7(C5), 95.2	
cyclobuteno	34.7(CH_2)	87.7, 90.3, 91.5, 103.2(C-R)	

[a] the dipotassium salt

Table 3-21

The ^{13}C NMR Spectra of Uranocenes at 37°C

δ ppm from TMS

Substituent[a]	Substituent Resonances	Ring Resonances	Ref.
H		297	102
CH_3	-52.5(CH_3)	272, 279, 295, 299, 317	102
octamethyl	-53.2(CH_3)	276, 288	102
CH_2CH_3	-35.7(CH_2), 63.6(CH_3)	279, 286, 297, 299, 310	102
$CH_2CH_2CH_2CH_3$	-28.3(αCH_2), 12.8(CH_3) 25.8(γCH_2), 78.2(βCH_2)	280, 283, 296, 299, 309	102
$CH(CH_3)_2$	-22.1(CH), 46.7(CH_3)	274, 286, 295, 300, 304	102
tetra-t-butyl[b]	-22.2(αC), 44.5(CH_3)	276, 281, 307, 331	59
$CH_2(CH_3)_3$	-17.3(CH_2), 74.1(βC) 36.3(CH_3)	278, 288, 293, 305	104
$CH_2CH_2CH_2N(CH_3)_2$	-33.0(αCH_2), 45.2(CH_3) 63.7(γCH_2), 76.9(βCH_2)	282, 286, 298, 302, 312	102
$C(CH_3)_3$	-24.7(αC), 42.6(CH_3)	276, 290, 308	102
OCH_3	100.6(CH_3)	268, 276, 289, 309	102
$OC(CH_3)_3$	1.2(OC), 33.8(CH_3)	260, 283, 296, 299, 330	102
$OCH_2CH{=}CH_2$	112.6(CH_2), 115.0(OCH_2) 132.7(CH)	269, 276, 289, 308, 341	102
$CO_2CH_2CH_3$	8.1(CH_3), 50.2(OCH_2) 75.3(C=O)	201, 257, 298, 312, 332	102
cyclobuteno	-63.7(CH_2)	273, 313, 326	14

[a] 1,1'-disubstituted

[b] 1,1',4,4' isomer

Table 3-22

^{13}C NMR Spectra of Cyclooctatetraenes, Cyclooctatetraene Dianions,[a] Thorocenes and Uranocenes[b]

δ ppm from TMS

Substituent	Compound	Shift
H	COT	131.6
	Dianion	90.1
	Thorocene	89.1
	Uranocene	297
CH_3	COT	24.2(CH_3), 141.8(C-1), 136-128 (ring)
	Dianion	33.7(CH_3), 93.2(C-1), 92-89 (ring)
	Thorocene	33(CH_3), 120(C-1), 109-106 (ring)
	Uranocene	-52.5(CH_3), 272-316 (ring)
nC_4H_9	COT	13.9(CH_3), 22.2(γ), 30.8(β), 37.5(α), 144.6(C-1) 131-134 (ring)
	Dianion	14.9(CH_3), 24.1(γ), 40.7(β), 49.6(α), 101.0(C-1), 89-91 (ring)
	Thorocene	14(CH_3), 23(γ), 38(β), 49(α), 121(C-1), 106-109 (ring)
	Uranocene	12.8(CH_3), 25.8(γ), 78.2(β), -28.3(α), 279-309 (ring)

[a] the di-potassium salt

[b] data from ref. 64

carbons, in ^{13}C NMR spectroscopy. However, as a result of complicated coupling patterns and peak overlap, the proton coupled spectra of mono substituted cyclooctatetraenes do not permit unambiguous identification of the C-5 resonance.

Upon potassium metal reduction to the dianion, the ^{13}C NMR resonance of cyclooctatetraene shifts 41.5 ppm upfield to 90.1 ppm, reflecting both the increased charge, and an appreciable ring current. Likewise, in substituted cyclooctatetraene dianions, the ring carbon resonances are shifted ca. 40-42 ppm upfield, with the quaternary carbon resonance still remaining at lower field relative to the other resonances. In alkyl-substituted cyclooctatetraene dianions, the α-carbon resonance is shifted ca. 10 ppm downfield from its position in the spectrum of the neutral hydrocarbon. Correlations between ^{13}C NMR shifts and ring current effects in cyclic aromatic ions and hydrocarbons have been the topic of several studies[95] and will not be discussed here.

In uranocene, the ring carbon resonance shifts 165.4 ppm downfield from where it occurs in cyclooctatetraene (297.0 ppm). The ring carbon resonances in substituted uranocenes display a similar downfield shift of ca. 155-185 ppm. In alkyl-substitued uranocenes, the α-carbon experiences an upfield shift of ca. 50-70 ppm relative to that in the cyclooctatetraene or the dianion while the ß-carbon is shifted slightly downfield. As in the ^{1}H NMR spectrum, these shifts result from the presence of the paramagnetic metal ion and are composed of contact and pseudocontact components.

Roberts and Doddrell[105] have shown that the contact shift

for a carbon nucleus in the i^{th} position can be related to the contact shift for a proton in the i^{th} position by

$$\frac{^{13}C_{CONTACT}}{^{1}H_{CONTACT}} = \frac{a^{C_i}\gamma_H}{a^{H_i}\gamma_C} \qquad (33)$$

where γ_H and γ_C are, respectively, the magnetogyric ratio of the proton, and of the carbon nucleus, and a^{H_i} and a^{C_i} are respectively, the proton, and the carbon hyperfine coupling constants.

Due to the p-orbitals on carbon, the pseudocontact shift for a carbon nucleus will consist of a term identical to eq. 17, for the metal-centered pseudocontact shift and a second term, similar in form, for the ligand-centered pseudocontact shift, resulting from unpaired spin density in the carbon orbitals which lack spherical symmetry. If this latter term is effectively zero, then the relationship between the i^{th} proton, pseudocontact shift and the i^{th} carbon pseudocontact shift is simply the ratio of their geometry factors.

$$\frac{^{13}C_{PSEUDOCONTACT}}{^{1}H_{PSEUDOCONTACT}} = \frac{G_{C_i}}{G_{H_i}} \qquad (34)$$

Factoring the observed shifts in the ^{13}C NMR spectra of uranocenes requires referencing them to the shifts in a corresponding diamagnetic compound. Taking the thorocenes as a diamagnetic reference, Table 3-22 shows the relationship of the ^{13}C NMR resonances in thorocenes to those in the corresponding

cyclooctatetraene, the dianion and the uranocene. Unlike analysis of ^{1}H isotropic shifts, where the difference in the thorocene resonances and the corresponding dianion resonances was small, and thus, the dianion resonance could serve as diamagnetic references, the difference between the ^{13}C resonances of thorocenes and the resonances of the corresponding dianions are sufficiently large to prevent the latter from being used as diamagnetic reference compounds.

Table 3-22 shows that the ring carbon resonances in uranocenes are shifted ca. 190 ppm downfield, the α-carbon resonances ca. -70 ppm upfield and the β-carbon resonance slightly downfield relative to the carbon resonances in thorocenes. For carbon nuclei further removed, the isotropic shifts are effectively zero. This pattern is exactly opposite that observed in the proton spectra and precisely that predicted by the proposed model for spin delocalization in uranocenes. However, this agreement may be completely artifactual, since this model only predicts the sign and relative magnitude of contact shifts, without regard for pseudocontact contributions to the isotropic shift.

Fischer[58] has factored the ^{13}C isotropic shifts of the ring carbons in uranocene and the methyl carbon of 1,1'-dimethyl-uranocene by calculating the metal-centered pseudocontact shift using the axially symmetric form of eq. 17, and assuming that the difference between the isotropic shift and the calculated pseudocontact shift is the contact shift. Assuming an isotropic shift of 207.9 ppm for the ring carbons in uranocene, the factored shifts are 140.8 ppm (contact) and 67.1 ppm (pseuso-

contact), while for an isotropic shift of -71.0 ppm for the methyl group the factored values are -61.6 ppm (contact) and -9.4 ppm (pseudocontact). However, this analysis neglects the presence of ligand-centered contributions to the pseudocontact shift. The presence of pseudocontact shifts, and in particular, the presence of ligand-centered contributions to the pseudocontact shift can be ascertained in the following manner.

Roberts and Doddell[105] have shown that if hyperconjugation is the dominant mechanism for spin delocalization into a methyl group, then

$$\frac{a^{C}_{CH_3}}{a^{H}_{CH_3}} \approx -1/2 \qquad (35)$$

a result which has been confirmed both theoretically from SCF calculations[106] and experimentally by ESR measurements on the ethyl radical.[107,108] The sign dependence has also been confirmed by NMR studies. From eq. 33, it follows that

$$\frac{C_{CONTACT}}{H_{CONTACT}} \approx -1/2 \quad \frac{\gamma_H}{\gamma_e} \approx -2 \qquad (36)$$

Taking the ^1H contact shift for a methyl group as 8.71 ppm, the calculated contact shift for the α-carbon in 1,1'-dimethyluranocene is -17.4 ppm. By difference from the experimental isotropic shift of -85.5 ppm, (i.e., referenced to 1,1'-dimethylthorocene), the pseudocontact shift is -68.1 ppm. If the ligand-centered contribution to the pseudocontact shift is zero, then

eq. 33 shows that this value will be equal to the ^{1}H pseudocontact shift for the methyl group (-18.2 ppm) times the ratio of the geometry factors (0.7747) or -14.1 ppm. Clearly, the large discrepancy implies that ligand-centered pseudocontact shifts are significant in the ^{13}C NMR of uranocenes.

Bauer[102] has assigned the ^{13}C ring resonances in 1,1'-disubstituted uranocenes as C-1, C-2,8, C-3,7, C-4,6 and C-5 from high field to low field. However, this assignment is extremely tenuous if not completely in error. Although comparison of peak areas shows that the lowest field resonance is usually somewhat smaller than the higher field resonances, and thus, may correspond to the C-1 or C-5 resonance, the highest field resonance is not always smaller also, and even in some cases it is the largest in area. Further, in the ^{13}C NMR spectra of most of these substitued uranocenes, fewer than the five expected resonances are observed, due to overlap of the broad peaks. Comparison of peak areas and even assignment of which peaks correspond to two resonances is extremely difficult and certainly not definitive.

Attempted assignment of the C1 and C5 ring resonances by proton coupling techniques was not definitive due to the low solubility of the uranocenes and the complexed,poorly resolved spectra observed. We have found that this problem could not be overcome using a higher field instrument (45 MHz) with substantially greater sensitivity. Thus, we believe that insufficient evidence exists to assign specific ^{13}C NMR resonances of ring carbons in substituted uranocenes.

EXPERIMENTAL

Purification of solvents, instrumentation, and facilities used in preparation and characterization of compounds are described in Chapter 2. The ^{1}H NMR spectra were run on the UC Berkeley FT-NMR spectrometer designed and built by R. Nunlist. The system employs a superconducting magnet, a deuterium lock system, and modified Nicolet software. For proton operation the instrument operates at 180 MHz, with 5 mm sample tubes. Normally, spectra were run with a sweepwidth of 10,000 Hz where the resolution of the instrument is 0.625 Hz. The temperature control system consisted of passage of an N_2 stream through a lg. N_2 dewar, followed by passage over a dewared preheater and a heater mounted in the probe. The probe temperature was measured by monitoring the N_2 stream ca. 5 mm from the sample tube with a precalibrated thermocouple. Heater operation and probe temperature control were operated by a computer driven feedback control system which could maintain the probe temperature within a range of $\pm$0.2°C from -100°C to 100°C.

Uranocenes were purified by either Soxhlet extraction, recrystallization from hot hexane or sublimation. Spectra were run on dilute solutions (ca. 10^{-5} to 10^{-6} M) to prevent precipitation at low temperatures. In the glove box, samples were prepared by dissolving a small amount of the uranocene in 1.5 to 3 mL of deuterated solvent followed by centrifugation and transfer into 5 mm polished glass NMR tubes attached by a seal-off constriction to a O-ring joint. The joint was fitted with a stopcock and the apparatus was transferred to

the vacuum line where the tube was frozen by immersion in lq. N_2, evacuated to ca. 10^{-3} Torr, and sealed off.

mono-t-Butyluranocene. -- In the glove box, a 50 mL THF solution of 0.5 g (2.74 mmol) of dipotassium cyclooctatetraene and 0.62 g (2.74 mmol) of dipotassium t-butylcyclooctatetraene, was slowly added to a stirred solution of 1.042 g (2.74 mmol) of UCl_4 in 50 mL of THF. The resulting emerald green solution was stirred for 2 h followed by removal of solvent by vacuum transfer. The resulting green solid was Soxhlet extracted with hexane for ca. 1 h until the fresh extract was pale green. The extracted solid and solution were cooled to -78°C and the pale green solution was decanted into the extractor sidearm. The solid was washed once with -78°C hexane and dried at high vacuum. The yield of extracted material was 0.330 g and 1.490 g of green residue were recovered from the extraction thimble. Analysis by ^1H NMR (toluene-d_8) showed the extracted material to be a 1.78:1 mixture of mono and 1,1'-di-t-butyluranocene contaminated with a small amount of uranocene.

1,1',3,3'-Tetra-t-butylferrocene. -- To a solution of 12.94 g (0.0696 mol) of ferrocene and 25.77 g (0.278 mol) of freshly distilled t-butyl chloride in 200 mL of hexane was added 51 mL (0.418 mol) of 98% $BF_3 \cdot Et_2O$. The resulting red-brown solution was refluxed for 24 h during which time it changed color to a deep red. Upon cooling, the solution was slowly poured onto an ice slush (200 mL) containing potassium carbonate. The phases were separated and the aqueous layer

was washed with 2x100 mL portions of hexane. The combined organic layers were washed with 100 mL of H_2O and dried over $MgSO_4$. Removal of solvent afforded a mixture of alkylated ferrocenes as an orange solid. The tetra-alkylated product was isolated by reduced pressure short path distillation followed by two recrystallizations from CH_2Cl_2; yield 5.101 g, 23.0%, mp 196-197°C (lit.[74] mp 198°C); mass spectrum m/e: 410 (100%). See text for ^1H NMR. ^{13}C NMR ($CDCl_3$): δ 100 (C_1, C_3), 63.9 (doublet of triplets, J_{C-H} = 170.7 Hz and J_{C-H} = 6.2 Hz, C_4, C_5), 63.1 (doublet of triplets, J_{C-H} = 168.7 Hz and J_{C-H} = 6.2 Hz, C_2), 32.2 (quartet of triplets, J_{C-H} = 125 Hz, J_{C-H} = 4.8 Hz, CH_3), 30.5 (C_α).

Anal. Calcd for $C_{26}H_{42}Fe$: C, 76.07; H, 10.31; Fe, 76.26

Found: C, 76.26; H, 10.18

Photodimerization of 4,6-dimethylcoumalin. -- Pyrex test tubes (15 cm x 150 cm) were charged with a concentrated solution of 4,6-dimethylcoumalin in benzene and strapped to the quartz immersion well of a photolysis apparatus. The whole apparatus was immersed in a bucket of water and the solutions were irradiated for several weeks with a 450 watt Harnovia lamp. After ca. 1 week a clear white crystalline precipitate began to form on the bottom of the test tubes. Periodically the crystalline dimers were collected and additional 4,6-dimethylcoumalin was added to the test tubes. ^1H NMR ($CDCl_3$): δ 5.57 (t, 2H), 3.18 (d, 2H), 1.77 (d, 6H), 1.67 (s, 6H). No further characterization was attempted.

1,3,5,7-Tetramethylcyclooctatetraene. -- A 50 mL round bottom flask was charged with 2.713 g (10.9 mmol) of the white crystalline photodimers of 4,6-dimethylcoumalin, fitted with an efficient reflux condenser and thoroughly purged with N_2. The reaction vessel was plunged into a fused salt bath preheated to 280°C. After an induction period of ca. 30 sec voluminous gas evolution occured. Heating was continued for ca. 2 min until no further gas evolved. On cooling the solid residue was rinsed onto a silica gel column and eluted with hexane. Only one band eluted which afforded 0.8828 g (50.4%) of 1,3,5,7-tetramethylcyclooctatetraene: mp 69°C (lit.[109] mp 69-70°C); mass spectrum m/e 160 (100%); ^{1}H NMR ($CDCl_3$): δ 5.40 (s, 4H, ring), 1.73 (s, 12H, CH_3).

1,1',3,3',5,5',7,7'-Octamethyluranocene. -- A 200 mL uranocene reactor was thoroughly flamed-out under a steady Ar purge and charged with 768.2 mg (4.79 mmol) of 1,3,5,7-tetramethylcyclooctatetraene and 100 mL of THF. To this solution was added 375 mg (9.59 mmol) of potassium metal piecewise. The resulting solution was stirred for ca. 5 h during which time virtually all of the potassium disappeared and the solution changed color to a bright orange. In the glove box, this solution was slowly added dropwise to a stirred solution of 909.0 mg (2.39 mmol) of UCl_4 in 50 mL of THF. With the addition of the first few drops, an instantaneous reaction occured as evidenced by a color change from light green to dull red. After stirring for 4 days, the solvent was removed by vacuum transfer affording an olive green solid which was purified

by Soxhlet extraction with hexane. Removal of solvent afforded 371 mg, 27.8% yield of 1,1',3,3',5,5',7,7'-octamethyluranocene. Visible spectrum (THF) λ_{max} 650, 689, 704 and 718 nm; mass spectrum m/e: 558 (39%), 398 (38%), 160 (80%). See text for ^{1}H and ^{13}C NMR data.

Reduction of triphenylmethylcyclooctatetraene with potassium metal. -- Triphenylmethylcyclooctatetraene was prepared from cyclooctatetraene iron tricarbonyl following the procedure of Lewis, et al.[103] Excess potassium metal was added to a solution of 0.457 g (1.32 mmol) of triphenylmethylcyclooctatetraene in 80 mL of THF resulting in a dark red brown solution of the dianion. After stirring for 4 h at room temperature, the excess potassium and the solvent were removed affording 0.55 g of the crude dianion as a pyrophoric tan solid. ^{1}H NMR (THF-d_8): δ 7.70, 6.42, 5.33; ^{13}C NMR (THF-d_8): δ 151.9 (9pso), 131.2 (meta), 126.4 (ortho), 123.0 (para), 92.7 (C_5), 95.2, 91.9, 90.3 (ring).

1,1'-Bis(triphenylmethyl)uranocene. -- A solution of the dipotassium salt of triphenylmethylcyclooctatetraene was prepared by treatment of 0.475 g (1.37 mmol) of triphenylmethylcyclooctatetraene in 80 mL of THF with excess potassium metal. After 4 h the excess potassium was removed and a solution of UCl_4 (0.26 g, 0.685 mmol) in 20 mL of THF was slowly added via syringe. The resulting green solution was stirred for 2 h followed by solvent removal which yielded a green solid, which was purified by Soxhlet extraction with benzene; yield 0.5 g

(78.4). Visible spectrum λ_{max} 627, 652, 674(s) and 755 nm; see text for ^{1}H NMR.

REFERENCES

1) R. von Ammon, B. Kanellakopulos and R. D. Fischer, Chem. Phy. Let., 2, 513 (1968).

2) T. H. Siddall III, W. E. Stewart and D. G. Karraker, Chem. Phy. Let., 3, 498 (1969).

3) R. von Ammon, B. Kanellakopulos, R. D. Fischer and P. Laubereau, Inorg. Nucl. Chem. Let., 5, 219 (1969).

4) R. von Ammon, B. Kanellakopulos and R. D. Fischer, Chem. Phy. Let., 4, 553 (1970).

5) N. Edelstein, G. N. La Mar, F. Mares and A. Streitwieser, Jr., Chem. Phy. Let., 8, 399 (1971).

6) A. Streitwieser, Jr., D. Dempf, G. N. La Mar, D. G. Karraker and N. Edelstein, J. Am. Chem. Soc., 93, 7343 (1971).

7) R. G. Hayes and J. L. Thomas, Organomet. Chem. Rev. A, 7, 1 (1971).

8) N. Paladino, G. Lugli, U. Pedretti, M. Brunelli and G. Giacometti, Chem. Phy. Let., 5, 15 (1970).

9) M. Brunelli, G. Lugli and G. Giacometti, J. Mag. Res., 9, 247 (1973).

10) R. D. Fischer, R. von Ammon and B. Kanellakopolus, J. Organomet. Chem., 25, 123 (1970).

11) R. von Ammon, R. D. Fischer and B. Kanellakopolus, Chem. Ber., 105, 45 (1972).

12) T. J. Marks, A. M. Seyam and J. R. Kolb, J. Am. Chem. Soc., 95, 5529 (1973).

13) H. D. Amberger, J. Organomet. Chem., 116, 219 (1976).

14) S. R. Berryhill, Ph.D. Thesis, UC Berkeley (1978).

15) D. R. Eaton and W. D. Phillips, in "Advances in Magnetic Resonance", J. S. Waugh, Ed., Academic Press, New York, N.Y. (1965), vol. 1, p. 119.

16) "NMR of Paramagnetic Molecules: Principals and Applications", G. N. La Mar, W. DeW. Horrocks, Jr. and R. H. Holm, Eds., Academic Press, New York, N.Y. (1973).

17) G. A. Webb, in "Annual Reports on NMR Spectroscopy", E. F. Mooney, Ed., Academic Press, New York, N.Y. (1970), vol. 3, p. 211.

18) G. A. Webb, in "Annual Reports on NMR Spectroscopy", E. F. Mooney, Ed., Academic Press, New York, N.Y. (1975), vol. 6A, p. 2.

19) R. J. Kurland and R. B. McGarvey, J. Mag. Res., 2, 286 (1970).

20) R. S. Drago, J. I. Zisk, R. M. Richman and W. D. Perry, J. Chem. Ed., 51, 371, 465 (1974).

21) H. M. McConnell and D. B. Chestnut, J. Chem. Phys., 28, 107 (1958).

22) R. M. Golding, Mol. Phys., 8, 561 (1964).

23) B. R. McGarvey, J. Chem. Phys., 53, 86 (1970).

24) J. M. Walker, L. Resenthal and M. S. Quereshi, Inorg. Chem., 10, 2463 (1971).

25) W. B. Lewis, J. A. Jackson, J. F. Lemons and H. Taube, J. Chem. Phys., 36, 694 (1962).

26) N. Bloembergen and W. C. Dickinson, Phys. Rev., 79, 179 (1950).

27) H. M. McConnell and R. E. Robertson, J. Chem. Phys., 29, 1361 (1958).

28) H. M. McConnell and C. H. Holm, J. Chem. Phys., 28, 749 (1958).

29) J. P. Jesson, J. Chem. Phys., 47, 579 (1967).

30) A. J. Vega and D. Fiat, Pure and Applied Chem., 32, 307 (1972).

31) R. W. Kluiber and W. DeW. Horrocks, Jr., Inorg. Chem., 6, 166 (1967).

32) W. DeW. Horrocks, Jr., Inorg. Chem., 9, 690 (1970).

33) W. DeW. Horrocks, Jr. and J. P. Sipe, III, Science, 177 994 (1972).

34) B. Bleaney, J. Mag. Res., 8, 91 (1972).

35) W. DeW. Horrocks, Jr., J. Mag. Res., 26, 333 (1977).

36) E. W. Strout, Jr. and H. S. Gutowsky, J. Mag. Res., 24, 389 (1976).

37) B. R. McGarvey, J. Mag. Res., 33, 445 (1979).

38) A. D. Buckingham and P. J. Stiles, Mol. Phys., 24, 99 (1972).

39) P. J. Stiles, Mol. Phys., 27, 501 (1974).

40) J. M. Briggs, G. P. Moss, E. W. Randall and K. D. Sales, Chem. Comm., 1180 (1972).

41) H. Huber, Tet. Let., 3359 (1972).

42) G. N. La Mar, W. DeW. Horrocks, Jr. and L. C. Allen, J. Chem. Phys., 41, 2126 (1964).

43) W. DeW. Horrocks, Jr. and E. S. Greenberg, Inorg. Chem., 10, 2190 (1971).

44) A. A. Pinkerton and W. L. Earl, J.C.S. Dalton, 267 (1978).

45) C. M. Dobson, R.J.P. Williams and A. V. Xavier, J.C.S. Dalton, 2662 (1973).

46) R. von Ammon, B. Kanellakopulos, R. D. Fischer and P. Laubreau, Inorg. Nucl. Chem. Let., 5, 315 (1969).

47) A. E. Sebala and M. Tsutsu, Chem. Let., 775 (1972).

48) R. von Ammon, B. Kanellakopulos and R. D. Fischer, Radiochim. Acta., 11, 162 (1969).

49) J. H. Burns, J. Am. Chem. Soc., 95, 2815 (1973).

50) J. H. Burns, J. Organomet. Chem., 69, 225 (1974).

51) T. J. Marks and J. R. Kolb, J. Am. Chem. Soc., 97, 27 (1975).

52) D. G. Karraker, Inorg. Chem., 12, 1105 (1973).

53) R. G. Hayes and N. Edelstein, J. Am. Chem. Soc., 94, 8688 (1972).

54) A. Zalkin and K. N. Raymond, J. Am. Chem. Soc., 91, 5667 (1969).

55) A. Avdeef, K. N. Raymond, K. O. Hodgson and A. Zalkin, Inorg. Chem., 11, 1083 (1972).

56) A. Streitwieser, Jr., in "Topics in Nonbenzenoid Aromatic Chemistry", T. Nozoe, R. Breslow, K. Hafner, S. Ito and J. Murata, Eds., Hirokawa Pub. Co., Inc., Tokyo (1973), p. 221.

57) R. von Ammon and R. D. Fischer, Ang. Chem. Int., 11, 675 (1972).

58) R. D. Fischer, in "Organometallics of the f-Elements", T. J. Marks and R. D. Fischer, Eds., D. Reidel Pub. Co., Boston, Mass. (1979), p. 337.

59) M. Miller, Ph.D. Thesis, UC Berkeley (1979).

60) F. H. Kohler, J. Organomet. Chem., 121, C61 (1976).

61) C. G. MacDonald, J. S. Hannon and S. Sternhell, Aust. J. Chem., 17, 38 (1964).

62) H. Batiz-Hernandez and R. A. Bernheim in "Prog. in NMR Spectroscopy", J. W. Emsley, J. Feeney and L. H. Sutcliffe, Eds., Pergamon Press, New York, N.Y. (1967), p. 63.

63) A. Streitwieser, Jr. and C. LeVanda, submitted for publication.

64) A. Streitwieser, Jr., in "Organometallics of the f-Elements", T. J. Marks and R. D. Fischer, Eds., D. Reidel Pub. Co., Boston, Mass. (1979), p. 149.

65) R. F. Dallinger, P. Stein and T. G. Spiro, J. Am. Chem. Soc., 100, 7865 (1978).

66) D. G. Karraker, J. A. Stone, E. R. Jones, Jr. and N. Edelstein, J. Am. Chem. Soc., 92, 4841 (1970).

67) H. D. Amberger, R. D. Fischer and B. Kanellakopolus, Theoret. Chim. Acta., 37, 105 (1975).

68) C. A. Harmon, D. P. Bauer, S. R. Berryhill, K. Hagiwara and A. Streitwieser, Jr., Inorg. Chem., 16, 2143 (1977).

69) R. Bohn and A. Haaland, J. Organomet. Chem., 5, 470 (1966).

70) A. Haaland, Fortshritt der Fosschung, 53, 1 (1975).

71) S. A. Anderson, J. Organomet. Chem., 71, 263 (1974).

72) A. H. Clark in "Internal Rotation in Molecules", W. J. Orville-Thomas, Ed., J. Wiley and Sons, New York, N.Y. (1974), p. 325.

73) L. N. Mulay and A. Attalla, J. Am. Chem. Soc., 85, 702 (1963).

74) T. Leigh, J. Chem. Soc., 3294 (1964).

75) A. N. Nesmeyanov and N. S. Kochetiovia, Dokl. Akad. Nauk. SSSR, 117, 92 (1957).

76) A. N. Nesmeyanov, N. S. Kochetkova, S. V. Vitt, V. B. Bondarev and E. I. Kovshov, Dokl. Akad. Nauk. SSSR, 156, 99 (1964).

77) Z. L. Kaluski, A. I. Guser, A. E. Kalinin and Yu. T. Struchkov, Zh. Strukt. Khim., 950 (1972).

78) A. N. Nesmeyanov, N. S. Kochetkova, E. S. Fedin, E. V. Leonava and P. V. Petrovskii, Dokl. Akad. Nauk. SSSR, 178, 362 (1968).

79) N. Rosch and A. Streitwieser, Jr., J. Organomet. Chem., 145, 195 (1978).

80) B. Schilling, unpublished results.

81) N. Edelstein, A. Streitwieser, Jr., D. G. Morrell and R. Walker, Inorg. Chem., 15, 1397 (1967).

82) H. Burghard, unpublished results.

83) W. Luke, unpublished results.

84) S. E. Anderson and R. S. Drago, Inorg. Chem., 11, 1564 (1972).

85) R. S. Drago and W. D. Perry, J. Am. Chem. Soc., 73, 2183 (1971).

86) A. Zalkin, D. H. Templeton, S. R. Berryhill and W. D. Luke, Inorg. Chem., 18, 2287 (1979).

87) K. O. Hodgson and K. N. Raymond, J. Am. Chem. Soc., 12, 458 (1973).

88) A. Zalkin, D. H. Templeton, W. D. Luke and A. Streitwieser, Jr., submitted for publication.

89) R. Knor, H. Polzner and E. Bischler, J. Am. Chem. Soc., 97, 643 (1975).

90) R. Knor, A. Weiss, H. Polzner and E. Bischer, J. Am. Chem. Soc., 97, 644 (1975).

91) F. Gerson, G. Moshuk and M. Schwyzer, Hel. Chim. Acta., 54, 361 (1971).

92) W. T. Scroggins, M. F. Rettig and R. M. Wing, Inorg. Chem., 15, 1381 (1976).

93) A. W. Spiegl and R. D. Fischer, Chem. Ber., 112, 116 (1979).

94) B. Bak, J. J. Led, L. Nygaard, J. Rastrup-Andersen and G. O. Sorensen, J. Mol. Struct., 3, 369 (1969).

95) G. C. Levy and G. L. Nelson, "Carbon-13 Nuclear Magnetic Resonance for Organic Chemists", Wiley-Interscience, New York, N.Y. (1972).

96) H. Gunther, G. Jikeli, H. Schmicker and J. Prestien, Ang. Chem. Int. Ed., 12, 762 (1973).

97) K. D. Warren, in "Structure and Bonding", Springer-Verlag, New York, N.Y. (1977), vol. 33, p. 97.

98) C. Heller and H. M. McConnell, J. Chem. Phys., 32, 1535 (1960).

99) A. Carrington and P. F. Todd, Mol. Phys., 8, 299 (1964).

100) A. Carrington and P. F. Todd, Mol. Phys., 7, 533 (1963).

101) A. Mannschreck and L. Ernst, Chem. Ber., 104, 228 (1971).

102) D. P. Bauer, unpublished results.

103) B.F.G. Johnson, J. Lewis and J. W. Quail, J.C.S. Dalton, 1252 (1975).

104) E. H. Hillard, unpublished results.

105) D. Doddrell and J. D. Roberts, J. Am. Chem. Soc., 92, 6839 (1970).

106) J. A. Pople, D. L. Beveridge and P. A. Dobosh, J. Am. Chem. Soc., 90, 4201 (1968).

107) R. W. Fessenden and R. H. Schuler, J. Chem. Phys., 43, 2704 (1965).

108) R. W. Fessenden, J. Phys. Chem., 71, 74 (1967).

109) A. Streitwieser, Jr. and C. A. Harmon, Inorg. Chem., 12, 1102 (1973).

CHAPTER 4 DEUTERIUM LABELING OF RING POSITIONS IN 1,1'-DIALKYLURANOCENES

I. INTRODUCTION

In all of the mono- and 1,1'-disubstituted uranocenes prepared to date, the ^1H NMR resonances of the non-equivalent protons in the substituted rings are all well resolved singlets, three of area 2 and one of area 1. From Table 3-7 the total difference between the highest and lowest field resonances at 30°C in such uranocenes varies from 0.9 ppm to 30.66 ppm. In chapter 3 we suggested that the difference in ring proton resonances may arise from differences in the contact shift at each of the non-equivalent positions in the 8-membered ring. In this chapter we will explore this point in some detail.

If the contact shift differs for each of the non-equivalent ring positions, one might expect a correlation between the contact shift and the spin density at the various ring positions. Attempting such correlation requires assigning all of the ring proton resonances in 1,1'-disubstituted uranocenes.

Integration readily differentiates the 5 position, of area 1, from the remaining three positions, of area 2. Inspection of Table 3-7 shows that there is no apparent correlation between the electron-donating or withdrawing character of the substituent and the position of the 5 proton resonance relative to the other proton resonances. In principle, the 2, 3 and 4 positions can be identified by selective deuteration. The requisite deuterated uranocenes require

preparation of selectively deuterated alkylated cycloocta-tetraenes.

II. PREPARATION OF RING DEUTERATED URANOCENES

A) DEUTERATION OF n-BUTYLCYCLOOCTATETRAENE

The simplest and most direct route to a deuterated alkyl cyclooctatetraene is bromination-dehydrobromination of an alkylcyclooctatetraene affording a bromoalkylcyclooctatetraene (Scheme 4-1). Huisgen and co-workers[1] originally brominated-dehydrobrominated bromocyclooctatetraene to give the dibromide 3a. The relative location of the two bromine atoms was established by conversion to the dimethylcyclooctatetraene with lithium dimethyl cuprate, followed by hydrogenation. Comparison with authentic 1,4-dimethylcyclooctane established the 1,4 positions of the bromines in 3a. Paquette and co-workers[2] found that significant amounts of the 1,5 isomer are also produced in the bromination-dehydrobromination of bromocyclooctatetraene. Paquette and co-workers[3] have brominated a wide variety of substituted cyclooctatetraenes and trapped the intermediate 2 with N-phenyltriazolinedione (PTAD) (Scheme 4-1).

Starting with methylcyclooctatetraene and debrominating the adduct 5b with a zinc copper couple afforded 6 as the only product in 30% yield, indicating that the bromine atoms are in the 2 and 3 positions relative to the methyl group in 2b.

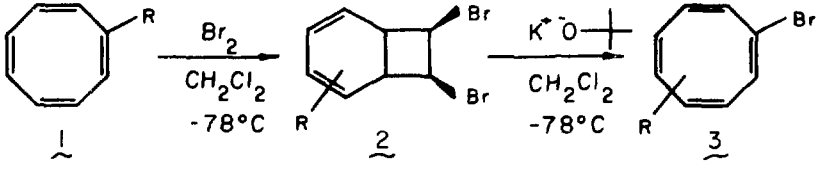

1 ~ 2 ~ 3 ~

R
a) Br
b) CH_3
c) n Butyl

R
a) Br
b) CH_3
c) n Butyl

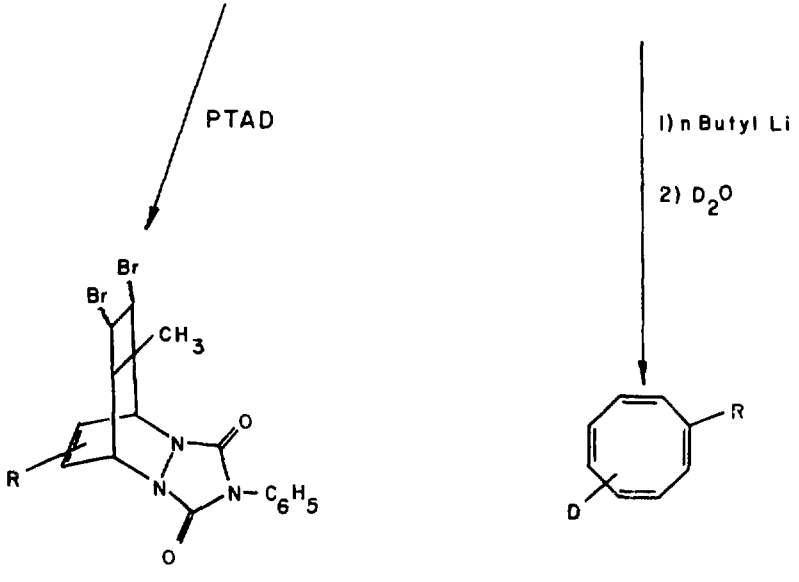

5 ~

R
a) Br
b) CH_3

4 ~

R
a) CH_3
b) n-Butyl

Scheme 4-I

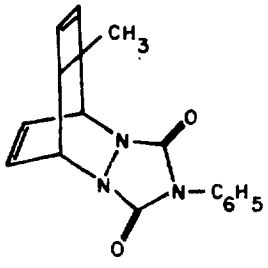

6

Paquette, et al., suggested that the presence of the methyl group might control the initial attack of the bromine, preferentially affording the tertiary carbonium ion 7 which rapidly rearranges to the homotropylium ion 8. Subsequent

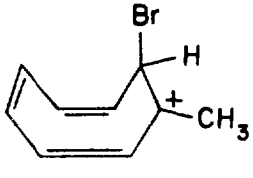

7

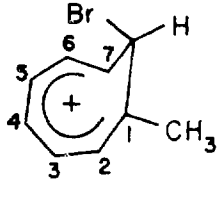

8

bromide ion trapping of 8 at C-7 affords 2b. Precedent for control of the initial electrophilic attack by the methyl group comes from study of the electrophilic attack of chlorosulfonyl isocyanate on methylcyclooctatetraene, which affords 9 in

greater than 97% yield.[4]

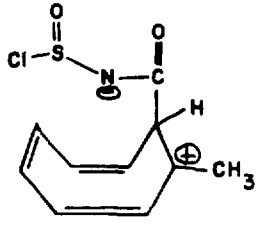

9

Less than a year after their initial report, Paquette and Henzel[5] reported that the bromination-dehydrobromination of methylcyclooctatetraene formed 3b (Scheme 4-1). Treatment of 3b with n-butyllithium and ethylene oxide afforded a 38% yield of 10 as a 3:1 mixture of 2-(4-methylcyclooctatetraenyl)-ethanol and the 5-methyl isomer which could be separated by vapor phase chromatography. The structure of the 4-isomer was established by an unpublished X-ray crystal structure of the $Fe(CO)_3$ adduct 12 (Scheme 4-2).

In both of these reports the bromination of methylcyclooctatetraene was done under identical conditions. Thus, it appears that the bromination of methylcyclooctatetraene leads to a mixture of all the possible isomeric dibromides 2b, and, in principle, then, dehydrobromination can lead to all of the possible isomeric bromides 3b.

As part of a ligand exchange study on uranocenes involving mass spectral analysis, LeVanda[6] prepared a ring deuterated

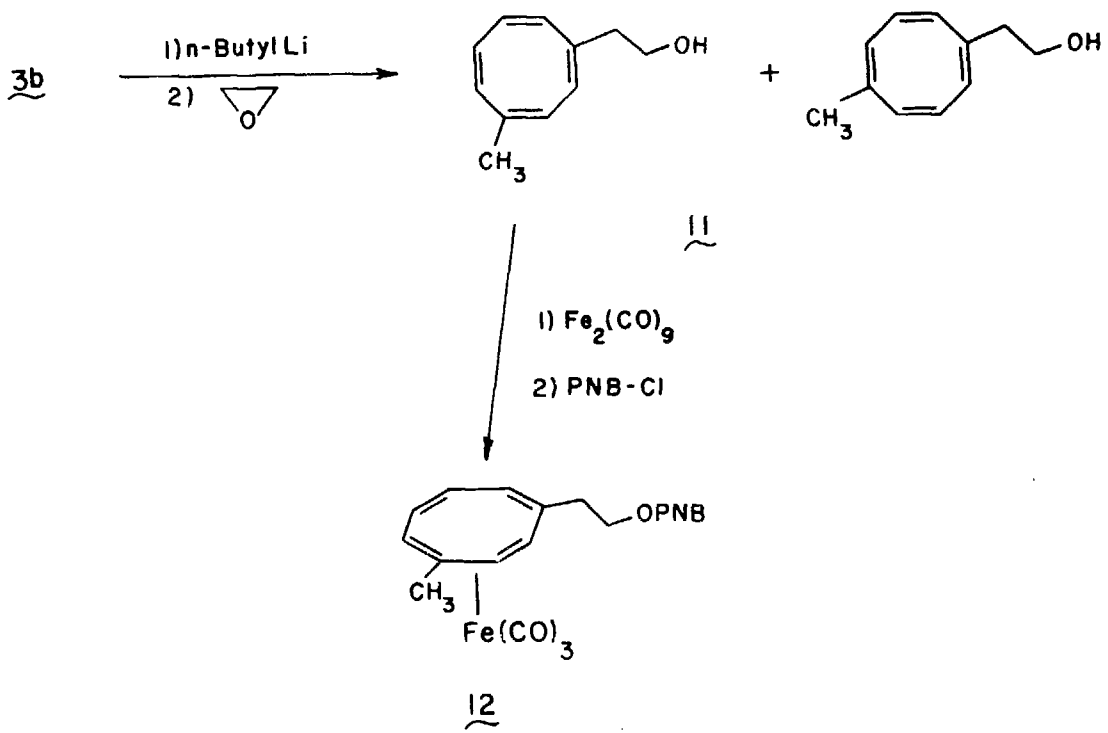
3b
1) n-Butyl Li
2)
OH
CH3
+
OH
CH3
11
1) Fe2(CO)9
2) PNB-Cl
OPNB
CH3
Fe(CO)3
12

Scheme 4-2

1,1'-di-n-butyluranocene from the deuterobutylcyclooctatetraene 4b synthesized according to Scheme 4-1. Prior to the availability of high field FT ^{1}H NMR instruments, integration of uranocene ring proton resonances as a probe for the location of the deuterium label was not possible. Thus, the ^{1}H NMR of this compound was not investigated. The ring proton region of the ^{1}H NMR spectrum of this uranocene is shown in Fig. 4-1. Labeling the ring resonances A-D from low field to high field, comparison with a non-deuterated sample shows the area of the D resonance is unchanged in the deuterated sample. Assuming that 100% deuteration corresponds to complete replacement of one of the hydrogens in the cyclooctatetraene ring, integration relative to the D resonance shows 61% deuterium in the A position, 0% in the B position and 14% in the C position. This implies that only two isomers of 4b were preferentially formed (Scheme 4-1).

In an effort to identify the two isomers we have repeated the preparation of 4b according to Scheme 4-1. Gas chromagraphy of the crude product resulting from the bromination-dehydrobromination of n-butylcyclooctatetraene indicated that it was a mixture of 2 major and 5 minor products. Two different approaches were employed in purifying this crude material.

In run #1 purification was attempted by reduced pressure short path distillation in analogy with the purification of bromocyclooctatetraene.[7] Upon heating above 35°C bromocyclooctatetraene is known to isomerize readily to trans-ß-bromostryene and thus, the distillation is conducted at or below

room temperature at reduced pressure.[1] Under reduced pressure, the bromide 3c distilled at 50-56°C/0.2 Torr accompanied by a large amount of tar formation. Gas chromatographic analysis of the distilled material showed 2 major products with retention times of 7 min and 11.5 min at 145°C (4% SE-30 on carbowax column, 1/4" x 6'). Isolation of these two compounds by preparative gas chromatography and analysis by both ^{1}H and ^{13}C NMR established that the compound with retention time of 7 min was a cyclooctatetraene while the other having retention time of 11.5 min, was a styrene. Further, upon heating or standing for several days at room temperature, the cyclooctatetraene rearranged into a styrene. The NMR analysis was unsuccessful in establishing the isomeric structure of these compounds.

In run #2 the crude bromide 3c was purified by column chromatography on silica gel with hexane elution by analogy with the purification of 3b by Paquette and co-workers.[5] This approach afforded much higher yields of 3c. Gas chromatographic analysis showed that the same 2 major and 5 minor products were present; however, the cyclooctatetraene peak was substantially larger while the styrene peak was substantially smaller.

The bromides 3c from both runs were converted into the deuterated compound 4b by treatment with n-butyllithium at -78°C in THF, followed by immediate quenching with D_2O and purification by column chromatography on silica gel with hexane elution. Comparison of both the proton coupled and decoupled ^{13}C NMR spectra of 4b was unsuccessful in distinguishing whic.

Fig. 4-1 The ring proton region of the ^{1}H NMR of 1,1'-di-n-butyl- and ring deuterated 1,1'-di-n-butyl-uranocenes at 30°C

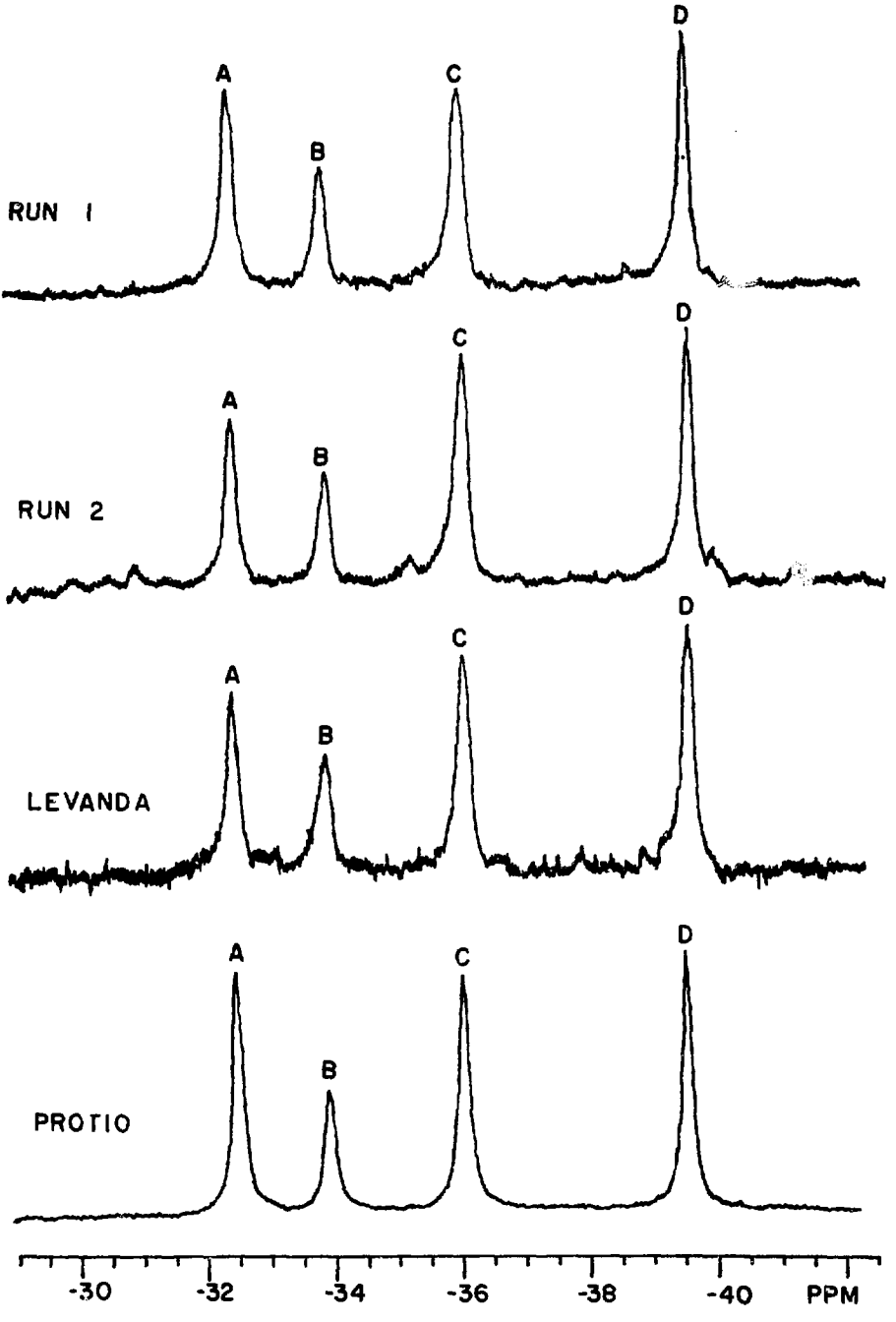
A
B
C
D
RUN 1
RUN 2
LEVANDA
PROTIO
-30
-32
-34
-36
-38
-40
PPM

resonances were associated with carbons bearing deuterium. However, ^{13}C NMR spectra of the dianion suggested that a deuterium was attached to the ring carbon which resonates at 90.7 ppm.

The ring proton region of the ^{1}H NMR spectrum of the uranocenes formed from the deuterated cyclooctatetraenes, 4b, from runs #1 and #2 are shown in Fig. 4-1. Comparison with the unlabeled uranocene shows that there is no apparent deuterium incorporation in the D resonance. Integration relative to this peak gives the deuterium incorporation in the remaining peaks as A 69%, B 20%, C 0% for run #2 and A 28%, B 5%, C 20% for run #1. Again it appears that only three of the four possible isomers of 4b, and, vita infra, 3c are formed in the reaction sequence shown in Scheme 4-1.

Mass spectral data showed that the total deuterium incorporation was 1.59 deuteriums in run #1, 0.93 deuteriums in run #2 and 1.74 deuteriums in the uranocene prepared by LeVanda. Attempted observation of deuterium coupling in the ^{13}C resonances of the uranocene from run #1 was unsuccessful, even at high field (45 MHz), due to the rather large linewidth of the resonances (ca. 100 Hz).

B) 4-DEUTERO-METHYLCYCLOOCTATETRAENE

The ambiguity surrounding the location of deuteration in the alkylcyclooctatetraenes synthesized by Scheme 4-1 requires an unambiguous synthetic route to a labeled alkylcyclooctatetraene. Paquette and co-workers[8] have synthesized the sulfone 16

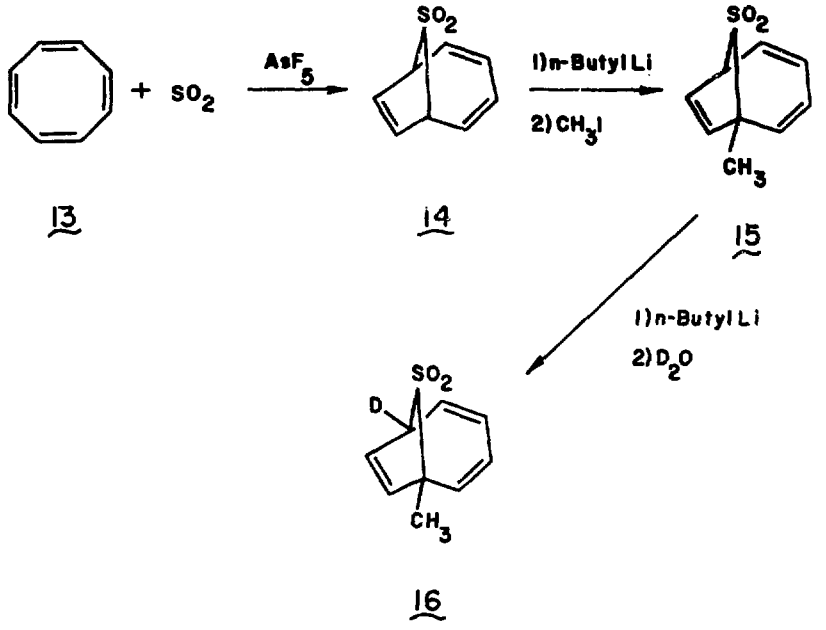

Scheme 4-3

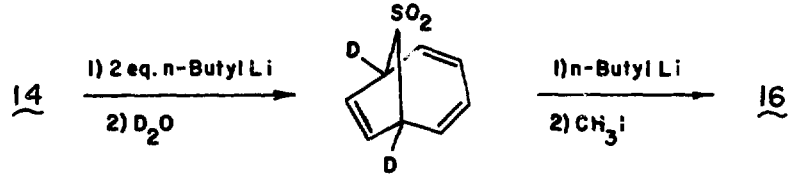

Scheme 4-4

according to Scheme 4-3. Photolysis of sulfones such as 14-16 leads to cyclooctatetraenes in moderate to high yield.[8-13] Ideally, photolysis of 16 would lead to a specifically labeled methylcyclooctatetraene.

Lewis acid catalyzed addition of SO_2 to cyclooctatetraene afforded 14 in 53.5% yield after two recrystallizations from $CHCl_3$/hexane. Treatment of 14 with 1 eq. of n-butyllithium at ca. -78°C in THF afforded a solution of the yellow-brown mono anion, which, when quenched with methyl iodide, yielded a mixture of principally 15 with minor amounts of 14 and 17. Previously, this mixture had been separated by high pressure liquid chromatography.[14] Lacking such facilities we found that

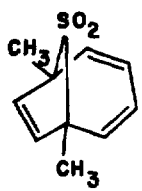

17

the mixtures could be separated by repeated column chromatography on silica gel eluting with diethyl ether. Treatment of 15 with n-butyllithium followed by D_2O at room temperature in THF resulted in a large amount of decomposition and apparent formation of a cyclooctatetraene. To circumvent this we resorted to the

synthesis of 16 shown in Scheme 4-4.

Dideprotonation of 14 afforded a purple dianion which was quenched with D_2O. Subsequent mono-deprotonation and quenching with methyl iodide afforded 16 in 10.3% overall yield from cyclooctatetraene. Purification of these sulfones was greatly simplified by the discovery that they could be readily recrystallized from boiling water. Mass spectral determination of the deuterium content of 16 was impossible since fragmentation involving loss of SO_2 was extremely facile even at low ionizing voltages.

A variety of conditions has been reported for the photoextrusion of SO_2 from 14 and a wide variety of similar systems.[8-13] Ether is generally used as a solvent with varying amounts of acetone as a sensitizer. In some cases Corex or Vicor filters have been employed while in others no filters were used. Using 15 as a model system, several attempts at photolytic extrusion of SO_2 by photolysis of degassed 1:1 or 1:3 acetone/ether solutions of 15, with a Corex filtered 450 watt lamp at room temperature failed to afford methylcyclooctatetraene. Monitoring the photolysis by TLC showed that all of the starting material had disappeared after 20 min, and the reaction mixture possessed a distinct sulfurous odor. However, solvent removal afforded a malodorous oil from which no methylcyclooctatetraene could be isolated by preparative TLC or column chromatography on silica gel with hexane elution. Under similar conditions, photolysis of 17 is reported to afford 1,4-dimethylcyclooctatetraene in 41% yield.[8]

Pyrolytic extrusion of SO_2 from sulfones such as 16 is a

thermally allowed process and does afford the corresponding cyclooctatetraene.[13,15] Slow sublimation of 16 through a pyrex tube packed with glass helices at 400°C afforded the desired methylcyclooctatetraene-4-d in 86.7% yield. Reduction to the dianion with potassium metal followed by reaction with UCl_4 afforded the desired uranocene.

The ring proton region of the ^1H NMR spectrum is shown in Fig. 4-2. Clearly, the A resonance corresponds to the 4-position. Integration shows 1.52 deuteriums incorporated which compares favorably with 1.7 deuteriums incorporated as determined by mass spectral analysis. The absence of deuterium incorporation in any of the other ring positions indicates that the labeled cyclooctatetraene did not undergo degenerative scrambling during pyrolysis. Paquette and co-workers[16] have shown that dimethylcyclooctatetraenes do undergo degenerative rearrangement upon heating above 425°C.

III. ASSIGNMENT OF THE RING PROTON RESONANCES IN 1,1-DIALKYLURANOCENES

From Fig. 4-1 and 4-2, the principal deuterated 1,1'-di-n-butyluranocene is the 4 isomer (vita infra) and thus, the bromination-dehydrobromination sequence in Scheme 4-1 leads principally to the 4-bromoalkylcyclooctatetraene. The ^{13}C NMR spectrum of the deuterated n-butylcyclooctatetraene dianion derived from this bromide indicated that the deuterium was appended to the carbon which resonates at 90.7 ppm, and thus, can be assigned to the 4-position. Peak area and proton

Fig. 4-2 The ring proton region of the ^{1}H NMR of 1,1'-dimethyl- and 1,1'-dimethyluranocene-4d_2 at 30°C

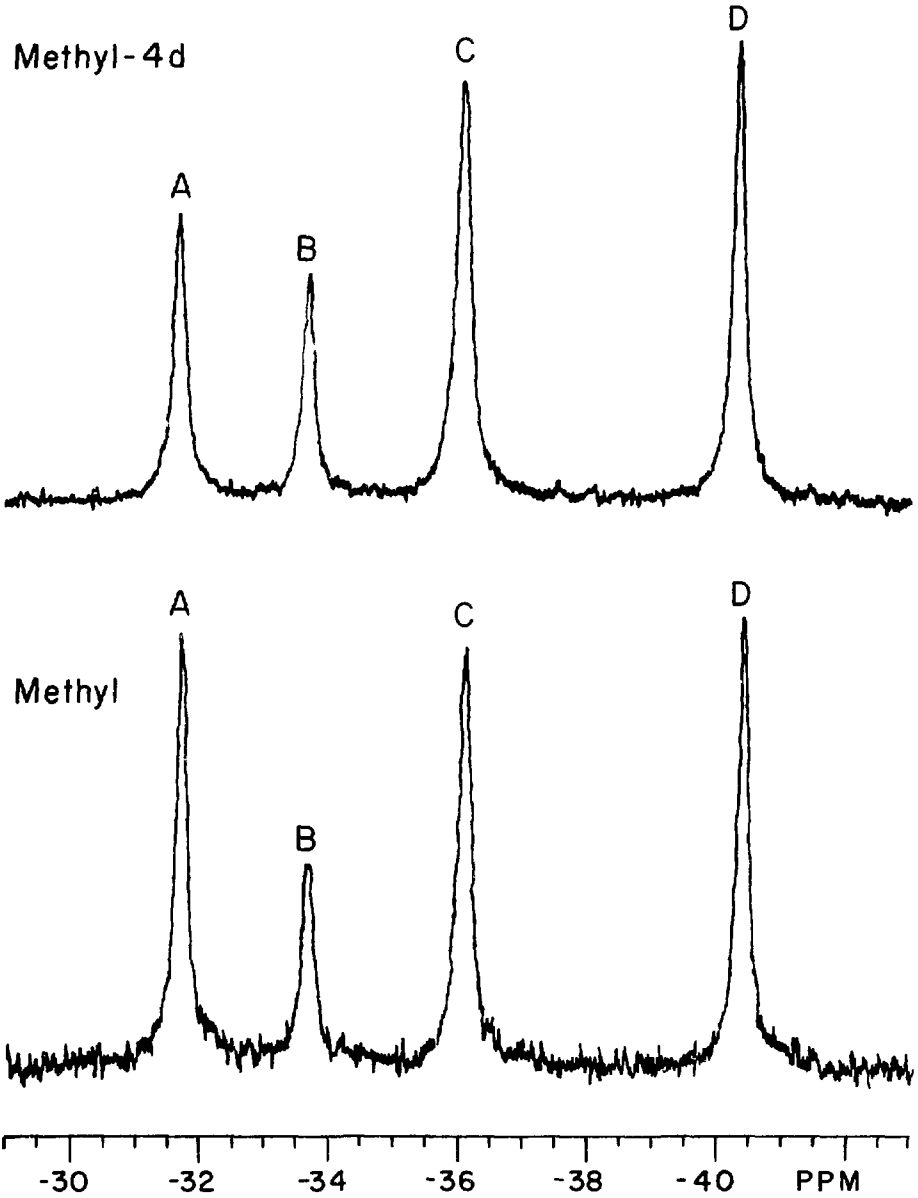
Methyl-4d
A
B
C
D
Methyl
A
B
C
D
-30
-32
-34
-36
-38
-40
PPM

coupled spectra permit assignment of two more of the observed five ^{13}C NMR resonances of the dianion as C1 (101.0 ppm) and C5 (89.3 ppm).

Assignment of the 2 and 3 ring positions in 1,1'-di-n-butyluranocene is less definitive. By analogy with the reported formation of the 2,3-dibromide 2b in Scheme 4-1 by Paquette and co-workers,[3] some of the 2,3-dibromide 2c should also form under identical reaction conditions. Dehydrobromination of 2c could lead to either the 1,2- or the 1,3-bromo-n-butylcyclooctatetraene. If both were formed, the ^1H NMR of the derived uranocene would show deuterium incorporation in both the C and D ring resonances. However, no apparent deuterium is present in position D, within the experimental error of integration which can be safely estimated as ca. 5-10%. Thus, either the 1,2 or the 1,3-bromide 3c is formed preferentially from the 2,3-dibromide 2c. Since bromination of cyclooctatetraene is known to involve primarily cis addition,[17,18] the bromines in the 2,3-isomer 18 will be cis. Assuming that both the monocyclic and the bicyclic tautomers of 18 undergo elimination of HBr, base abstraction of the 2-hydrogen of the bicyclic tautomer will be sterically hindered since the 2-hydrogen is formally bridgehead

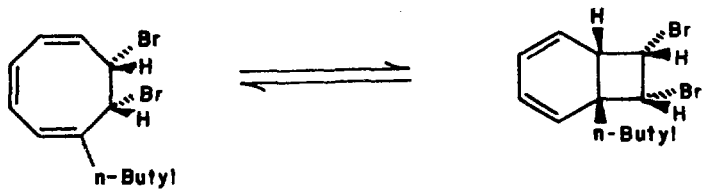

18a 18b

and neopentyl. Similarly, the n-butyl group adjacent to the 2-hydrogen in 18a may also hinder base abstraction of the 2-hydrogen. Thus, base abstraction of the 3-hydrogen in 18 should be preferred leading to preferential formation of the 1,3-isomer of 3c. Thus, the C resonance in Fig. 4-1 can be tentatively assigned to the 3-position. The resulting complete assignment of ring proton resonances from low field to high field in 1,1'-di-n-butyluranocene is 4, 5, 3, 2.

Integration shows that 1,1'-dimethyl-, 1,1'-diethyl- and 1,1'-dineopentyluranocene all have the same ring proton resonance pattern as that of 1,1'-di-n-butyluranocene. Thus, we have also assigned the A, B, C, D resonances in these compounds to the 4, 5, 3, 2 positions, respectively.

In 1,1'-diisopropyluranocene the integrated ring proton pattern is 2, 2, 1, 2. For 1,1'-bis(triphenylmethyl)-, 1,1-bis(trimethylsilyl)-, the substituted rings of mono- and 1,1'-di-t-butyluranocenes, and the high temperature form of di(cyclooctatetraenyl)uranocene the pattern is 2, 2, 2, 1. Although this change in pattern may reflect differences in the electronic effects induced by the substituent, the differences in the inductive effect of an ethyl, isopropyl and t-butyl group are sufficiently small to preclude this approach.

The change in pattern directly parallels the increase in the number, and steric bulk, of the substituents on the α-carbon. Changing the α-carbon from primary, to secondary, to tertiary, changes the pattern from 2, 1, 2, 2 to 2, 2, 1, 2 to 2, 2, 2, 1. A primary substituent can adopt a conformation where the R group is 90° from the ring plane and the ring protons, while

this angle reduces to a maximum of 60° for a secondary substituent and to 30° for a tertiary substituent. Non-bonding interactions between β-protons on the substituent and the 2-position ring protons could force geometry changes at the 2- and possible indirectly at the 3-position of the 8-membered ring.

Alternatively, steric interaction of the substituent with ring protons on the other cyclooctatetraene ligand could affect the conformation of secondary and tertiary substituents which in turn could affect the geometry of ring protons in the ring of attachment. Dreiding models show that the closest approach of a β methyl group and ring protons on the second cyclooctatetraene ligand is less than the sum of the Van der Waals radii for two hydrogens. Thus, it appears that this interaction may force the substituent up out of the plane of the 8-membered ring and away from the uranium atom. Since X-ray crystallographic evidence shows that primary substituents are tipped slightly toward the uranium atom, this difference in geometry of the substituent could account for difference in the relative positions of the 2 and 3 ring protons in primary, secondary and tertiary alkyl-substituted uranocenes. It is important to note that the pattern is controlled solely by the substituent on the ring of attachment and is not affected by a substituent in the second cyclooctatetraene ring. Thus, geometric changes, which will change the pseudo-contact shift rather than substituent induced changes in spin distribution in the 8-membered ring, which would change the contact shift, are probably responsible for the substituent induced changes in the pattern of the

non-equivalent ring proton resonances.

This also accounts for the temperature dependent change in the ring proton resonance pattern of 1,1'-diaryluranocenes. With increasing temperature, on the average the phenyl group will spend more time in conformations where the two carbocyclic rings are coplanar or near coplanarity, and thus, steric interaction between the 2-hydrogens and the ortho hydrogens will increase with increasing temperature. At low temperature, where interaction is minimal, the patterns are 2, 2, 1, 2 for 1,1'-diphenyl- and 2, 1, 2, 2 for 1,1'-bis(p-dimethylaminophenyl)-uranocene, while increasing the temperature results in a change to 2, 2, 2, 1 and 2, 1, 2, 2, respectively. Extrapolation of the variable temperature data for 1,1'-bis(p-dimethylamino-phenyl)uranocene show that above ca. 100°C the ring proton pattern should also be 2, 2, 2, 1. The fact that 1,1'-di-phenyluranocene displays the high temperature pattern at a lower temperature than 1,1'-bis(p-dimethylaminophenyl)uranocene reflects a larger barrier to rotation for the substituted aryl group, consistent with the higher coalescence temperature of the ortho protons in this uranocene.

EXPERIMENTAL

Bromination of n-butylcyclooctatetraene. -- A flamed-out Ar purged 500 mL 4-necked round bottom flask equipped with a dropping funnel, a thermometer, a mechanical stirrer, and a gas inlet tube was charged with 10.34 g (0.0645 mol) of n-butylcyclooctatetraene in 100 mL of CH_2Cl_2. After thoroughly degassing with Ar and cooling to -60°C, a solution of 3.52 mL (0.0645 mol) of bromine in 25 mL of CH_2Cl_2 was added dropwise over a 1 h period. The resulting pale yellow solution was stirred for an additional 1.5 h at -60°C followed by the portion-wise addition of 7.24 g (0.0645 mol) of potassium t-butoxide (Alfa) over a 0.5 h period. The resulting mixture was stirred for 3 h at -70°C followed by overnight warming to room temperature. The mixture was filtered through a course fritt, washed with water and dried over Na_2SO_4. Removal of solvent afforded a yellow-brown oil.

In run #1 this crude material was subjected to short path distillation (65-68°C/10^{-2} Torr). Starting with 9.91 g (0.0619 mol) of n-butylcyclooctatetraene afforded 6.98 g of distilled material.

In run #2 the crude product was column chromatographed on silica gel eluting with hexane. Starting with 10.34 g (0.0645 mol) of n-butylcyclooctatetraene afforded three fractions totalling 7.88 g of chromatographed material.

See text for characterization.

Deuteration of bromo-n-butylcyclooctatetraene. -- An Ar degassed solution of 5.04 g (0.021 mol) of crude bromo-n-butylcyclooctatetraene in 250 mL of THF in a 500 mL round bottom flask was cooled to -70°C and 10.5 mL (0.023 mol) of 2.2 M n-butyllithium was added dropwise over a 5 min period. The resulting solution was stirred for 30 min at -70°C followed by quenching with degassed D_2O in THF. On warming, the reaction mixture was washed with 2 x 100 mL portions of water. The combined aqueous layers were extracted with hexane (2 x 100 mL) and the combined organic layers were dried over Na_2SO_4. Removal of solvent followed by distillation (27-35°/0.2 Torr) afforded n-butylcyclooctatetraene-d, in yields of 20-40%. Mass spectral analysis show deuterium incorporation ranged from 40-70%.

1,1'-Di-n-butyluranocene-2d. -- The labeled n-butylcyclooctatetraenes from runs #1 and #2 were reduced to the corresponding dianion by potassium metal in THF. The dianion from run #2 was isolated as an impure tan solid. Addition of THF solutions of UCl_4 to solutions of the dianions afforded the corresponding uranocene which were purified by Soxhlet extraction with hexane.

9-Thiabicyclo[4.2.1]nona-2,4,7-triene 9.9-dioxide, 14. -- A 1 L 3-necked round bottom flask fitted with a jacketed low temperature addition funnel and a mechanical stirrer was thoroughly flamed out under an Ar purge and charged with 11.5 g (0.11 mol) of cyclooctatetraene (BASF as supplied) and ca. 150 mL of SO_2. The addition funnel was charged with 24 g

(0.11 mol) of antimony pentafluoride dissolved in 100 mL of SO_2. The contents of the addition funnel were added dropwise to the stirred reaction mixture over a 45-65 min period at -70°C. The resulting mixture was stirred for 2.5 hr at -70°C, followed by the addition of cold CH_2Cl_2 (200 mL) and removal of the SO_2 by reduced pressure distillation at 10-20 Torr. The resulting solution was slowly poured onto a vigorously stirred saturated sodium bicarbonate solution (600 mL) cooled in an ice bath. The layers were allowed to separate and the aqueous layer was extracted once with CH_2Cl_2 (200 mL). The combined organic layers were washed with water (2 x 100 mL) and brine (2 x 100 mL) and dried over $MgSO_4$. Solvent removal afforded a tan solid which was recrystallized from boiling water; yield 9.89 g (53.5%); mp 192-193°C. The melting point and spectral properties were identical to those reported in the literature.[14]

Anal. Calcd for $C_8H_8SO_2$: C, 57.12; H, 4.79; S, 19.06; O, 19.02

Found: C, 57.22; H, 4.87; S, 18.86

Inverse addition of a COT-SO_2 solution to the solution of antimony pentafluoride in SO_2 led to significantly lower yields.

1-Methyl-9-thiabicyclo[4.2.1]nona-2,4,7-triene 9,9-dioxide, 15. -- A 250 mL round bottom flask was charged with 1.73 g (102.9 mmol) of 14 and 150 mL of THF. The resulting solution was thoroughly degassed with Ar and cooled to -70°C. Some precipitation occured upon cooling. A 3.95 mL (102.9 mmol) aliquot of 2.6 M n-butyllithium (Alfa) was added dropwise over a 2 min period. The resulting dark purple solution was stirred for 3 min followed by quenching with CH_3I (3 mL) and allowed to

warm to room temperature. Removal of solvent afforded an oil which was taken up in CH_2Cl_2 (100 mL) and washed with 3 x 50 mL portions of water, once with 50 mL of brine and dried over $MgSO_4$. Removal of solvent afforded 1.74 g of a crude mixture of 14, 15 and 18 which was placed on a silica gel chromatography column (4.5 cm x 7.5 cm). Elution with 60:40 hexane/ether resulted in initial elution of 17 followed by 15 and finally 14. Recrystallization of the second fraction from boiling water afforded 0.868 g (46.3%) of 15, mp 114-115°C (lit.[14] 115-116°C); ^1H NMR ($CDCl_3$): δ 5.4-6.2 (m, 6H olefinic), 3.83-4.10 (m, 1H, olefinic), 1.52 (s, 3H, methyl).

Anal. Calcd for $C_9H_{10}SO_2$: C, 59.31; H, 5.53
Found: C, 59.55; H, 5.75

Attempted deuteration of 15. -- A flamed out Ar purged out 200 mL round bottom flask was charged with 0.605 g (3.32 mmol) of 15 in 100 mL of THF. To this solution was added dropwise 1.54 mL (3.9 mmol) of 2.6 M n-butyllithium. After stirring for ca. 2 min the resulting yellow brown solution was quenched with D_2O. Removal of solvent afforded a yellow oil which could not be induced to crystallize. An ^1H NMR of this material indicated that it was principally methylcyclooctatetraene.

1,6-Dimethyl-9-thiabicyclo[4.2.1]nona-2,4,7-triene-9,9-dioxide, 18. -- To an Ar degassed solution of 3.00 g (17.9 mmol) of 14 in 300 mL of THF in a 500 mL round bottom flask at -70°C was added 17.9 mL (39.3 mmol) of 2.2 M n-butyllithium (Alfa).

The resulting deep purple solution of dianion was stirred for 5 min at -70°C followed by quenching with 10 mL of CH_3I. On warming removal of solvent afforded a yellow oil which was taken up in CH_2Cl_2 (200 mL) washed with water (100 mL) and dried over $MgSO_4$. Removal of solvent afforded 3.1 g (88.2%) of a tan solid. The melting point (mp 149°C) and ^1H NMR were identical to those reported in the literature.[8] ^{13}C NMR ($CDCl_3$): δ 134.1, 126.8, 125.1 (olefinic), 65.0 (quaternary), 16.3 (methyl). Recrystallization from boiling water afforded an analytically pure sample.

Anal. Calcd for $C_{10}H_{12}SO_2$: C, 61.19; H, 6.17

Found: C, 61.08; H, 6.42

9-Thiabicyclo[4.2.1]nona-2,4,7-triene-1,6-d_2 9,9-dioxide, 17. -- To an Ar degassed solution of 6.01 g (35.7 mmol) of 14 in 300 mL of THF in a 500 mL round bottom flask at -70°C was added 30.01 mL (75.0 mmol) of 2.5 M n-butyllithium (Alfa). After stirring for 5 min at -70°C the deep purple solution of dianion was quenched with a degassed solution of D_2O in THF. On warming, removal of solvent afforded a tan solid which was recrystallized from boiling water; yield 4.07 g (67.8%), mp 192° (lit.[14] 193-194.5°C); ^1H NMR ($CDCl_3$): δ 6.03 (s, olefinic).

1-Methyl-9-thiabicyclo[4.2.1]nona-2,4,7-triene-6d 9,9-dioxide, 16. Starting with 2.872 g (16.9 mmol) of 15 and following the procedure for preparation of 15, afforded 0.879 g (28.4%) of 16. ^1H NMR ($CDCl_3$): δ 5.4-6.2 (m, 6H olefinic),

1.52 (s, methyl).

Photolysis of 15. -- A 600 mL immersion photolysis apparatus fitted with a quartz well, a Corex filter and a 450 watt Harmonia lamp was charged with 0.201 g (1.1 mmol) of 15 in 500 mL of dry acetone/ether (50:50) and thoroughly degassed with N_2 for 20 min. During irradiation a slow stream of N_2 was passed through the stirred solution. After 15 min of irradiation, TLC showed that none of the starting material remained. Removal of solvent afforded a malodorous yellow oil. Both TLC and ^1H NMR indicated this material was not the starting material or methylcyclooctatetraene. Preparative TLC afforded no identifiable products.

Photolysis for longer periods of time (3 h) or in pure ether afforded similar results, as well as photolysis of both 14 and 17.

Pyrolysis of 16. -- A 0.187 g (1.0 mmol) sample of 16 was slowly sublimed (ca. 60°C/0.2 Torr) through a 1 cm x 17 cm tube packed with 1/4 in glass helices and heated to 400°C over a 5 h period. The pyrolysate was trapped in a U-tube cooled in a dry ice acetone bath. Upon completion of the pyrolysis the contents of the trap were warmed to room temperature affording methylcyclooctatetraene-4d as a yellow oil; yield 0.106 g (86.7%). ^1H NMR ($CDCl_3$): δ 5.4-5.6 (m, olefinic), 1.7 (s, methyl); mass spectrum (12 ev): m/e 119 (100%), 118 (70%), corresponding to 0.83 deuteriums incorporated.

1,1'-Dimethyluranocene-4,4'd_2. -- To an Ar degassed solution of 0.100 g (0.8 mmol) of methylcyclooctatetraene-4d in 50 mL of THF was added excess potassium metal. After stirring for 12 h during which time the solution changed color to yellow brown, the excess potassium was removed and the solution of dianion was slowly added to a solution of 0.152 g (0.4 mmol) of UCl_4 in 15 mL of THF. After stirring the resulting green solution for 3 h, the solvent was removed by vacuum transfer to afford 0.230 g of crude 1,1'-dimethyluranocene-4,4'd_2. See text for spectral analysis.

REFERENCES

1) W. E. Konz, W. Hechtl and R. Huisgen, J. Am. Chem. Soc., 92, 4104 (1970).

2) L. A. Paquette, S. V. Ley, R. H. Meisinger, R. K. Russell and M. Oku, J. Am. Chem. Soc., 96, 5806 (1974).

3) L. A. Paquette, D. R. James and G. Birnberg, J. Am. Chem. Soc., 96, 7454 (1974).

4) L. A. Paquette, J. R. Malpass and F. J. Barton, J. Am. Chem. Soc., 91, 4714 (1969).

5) L. A. Paquette and K. A. Henzel, J. Am. Chem. Soc., 97, 4649 (1975).

6) C. LeVanda, unpublished results.

7) C. B. Grant, Ph.D. Thesis, UC Berkeley (1977).

8) L. A. Paquette, S. V. Ley, R. H. Meisinger, R. K. Russell and M. Oku, J. Am. Chem. Soc., 96, 5806 (1974).

9) L. A. Paquette and R. E. Wingard, Jr., J. Am. Chem. Soc., 94, 4398 (1972).

10) L. A. Paquette, R. E. Wingard, Jr. and R. H. Meisinger, J. Am. Chem. Soc., 93, 1047 (1971).

11) L. A. Paquette, R. E. Wingard, Jr. and J. M. Photis, J. Am. Chem. Soc., 96, 5801 (1974).

12) L. A. Paquette, Tet., 31, 2855 (1975).

13) L. A. Paquette, R. H. Meisinger and R. E. Wingard, Jr., J. Am. Chem. Soc., 95, 2230 (1973).

14) L. A. Paquette, U. Jacabsson and S. V. Ley, J. Am. Chem. Soc., 98, 152 (1976).

15) J. Gasteiger and R. Huisgen, J. Am. Chem. Soc., 94, 6541 (1972).

16) L. A. Paquette and M. Oku, J. Am. Chem. Soc., 96, 1219 (1974).

17) G. Boche, W. Hechtl, H. Huber and R. Huisgen, J. Am. Chem. Soc., 89, 3344 (1967).

18) R. Huisgen, G. Boche and H. Huber, J. Am. Chem. Soc., 89, 3345 (1967).

Chapter 5 ANNULATED URANOCENES PART II
APPROACHES TO DIBENZOURANOCENE

I. INTRODUCTION

The successful synthesis of annulated uranocenes led us to attempt synthesis of a benzannulated uranocene with benzocyclooctatetraene as a ligand. Formally dibenzouranocene, the uranocene complex with benzocyclooctatetraene ligands is the structural homolog of bisindenyliron, the ferrocene complex with indenyl ligands. Such a uranocene is expected to have several interesting properties. In both indenyl anion, and to a greater extent in benzocyclooctatetraene dianion, charge is delocalized into the benzene ring. However, upon complexation in ferrocene-type transition metal complexes, the indenyl anion is always bonded via the 5-membered ring.[1-5] The crystal structure of bisindenyliron has shown that the iron atom is centro-symmetrically located between the 5-membered rings of the two ligands. Effectively, complexation with the metal localizes the charge in the 5-membered ring. Similarly, in dibenzouranocene, would the uranium atom be centro-symmetrically coordinated to the 8-membered ring or would it be displaced toward the 6-membered ring? Further, would conjugation of the fused ring with the 8-membered ring constrain the substituent to coplanarity with the 8-membered ring and thus prevent it from tipping toward the uranium as it does in some alkylsubstituted uranocenes? Also, what effect would such conjugation have on spin delocal-

ization and the NMR of dibenzouranocene?

Mylonakis[6] initially attempted the preparation of dibenzouranocene by the reaction of benzocyclooctatetraene dianion with UCl_4. However, the reaction mixture failed to change color to emerald green, and thus, no complex was assumed to have formed. While most uranocenes, and a large number of other uranium (IV) compounds, are green, both our work and that of Dempf,[7] and Walker, et al.,[8] have shown that not all uranocenes are green in color. Solid 1,1',3,3',5,5',7,7'-octaphenyluranocene is black while solid 1,1',3,3',5,5',7,7'-octamethyluranocene is olive green. However, solutions of the latter material are dull red-brown and look virtually identical to solutions of partially oxidized colloidal uranium metal.

Polarographic studies by Paquette and co-workers[9] have established the second reduction potential of benzocyclooctatetraene as -2.13 volts vs SCE, which is within the range of second reduction potentials of substituted cyclooctatetraenes which form uranocenes. Thus, benzocyclooctatetraene should not reduce UCl_4 to uranium metal.

II. APPROACHES TO DIBENZOURANOCENE

We have pursued two avenues of approach to dibenzouranocene: 1)benzannulation of the uranocene skeleton; 2)preparation of the benzannulated ligand, benzocyclooctatetraene, followed by reduction to the dianion and subsequent reaction with UCl_4.

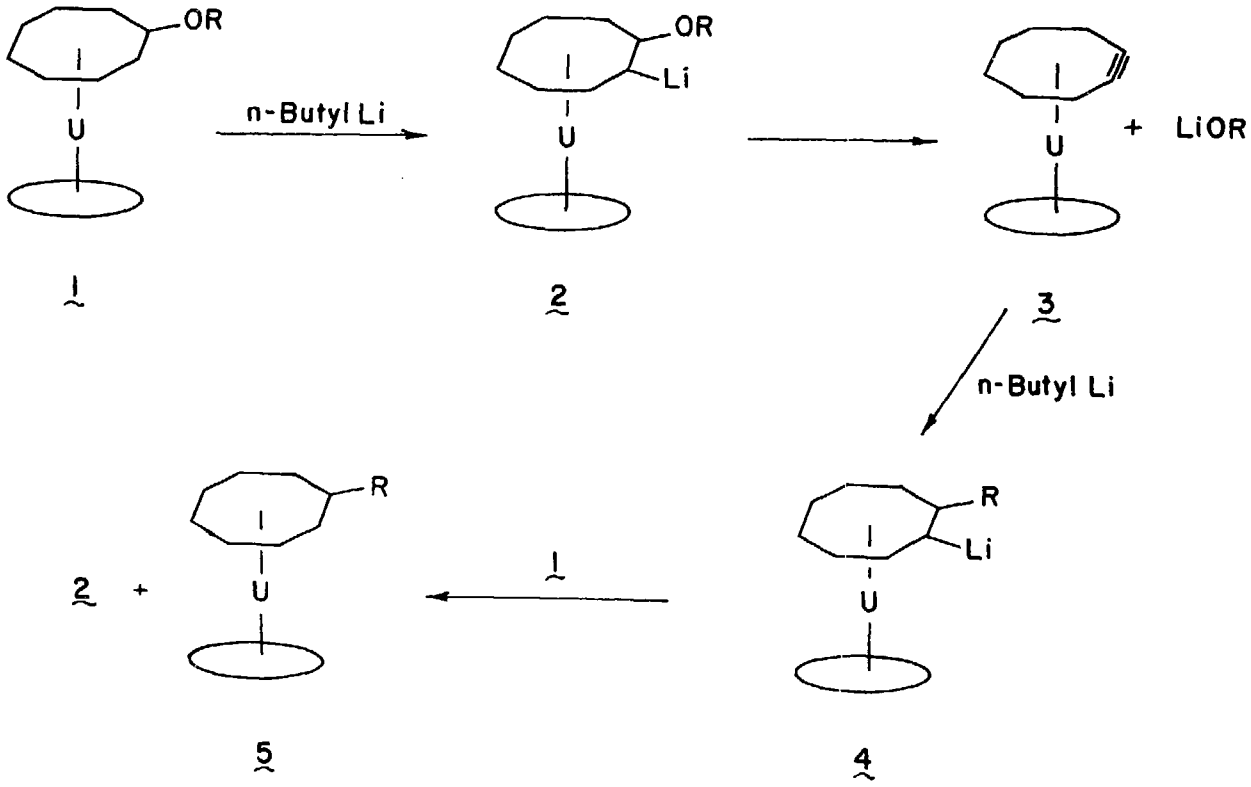

Scheme 5-1

A) ATTEMPTED BENZANNULATION OF URANOCENE

Reaction of 1,1'-dimethoxyuranocene with n-butyllithium is reported to afford 1,1'-di-n-butyluranocene. The proposed mechanism for this reaction involves initial metallation α to the substituent followed by elimination of lithium methoxide, forming a 1,2-dihydro- species, which is trapped by n-butyllithium. The resulting α-litho-alkyl uranocene abstracts an α-proton from an alkoxyuranocene perpetuating the reaction (Scheme 5-1).[10]

Two experimental observations support this mechanism: 1)the reaction does not occur with methyl lithium but treatment of 1,1'-dimethoxyuranocene with n-butyllithium in the presence of a large excess of methyl lithium affords methylated uranocene; 2)only 1.1 eq. of the lithium reagent are required to achieve >95% conversion to 1,1'-di-n-butyluranocene.

In a large number of substitution reactions involving strong base, the presence of eyne intermediates is detected by trapping the eyne with dienes, forming Diels-Alder adducts. Thus, the reaction of bromocyclooctatetraene with alkoxide ions has been shown to proceed via a 1,2-dehydrocyclooctatetraene intermediate which can be trapped by a variety of dienes, Scheme 5-2.[11,12]

If the intermediate in the reaction of 1,1'-dimethoxyuranocene and n-butyllithium is a uranocene species with a planar 1,2-dehydrocyclooctatetraene ligand, then, in principle, it could be trapped by a diene as a Diels-Alder adduct. Such trapping would afford a direct route into annulated uranocenes

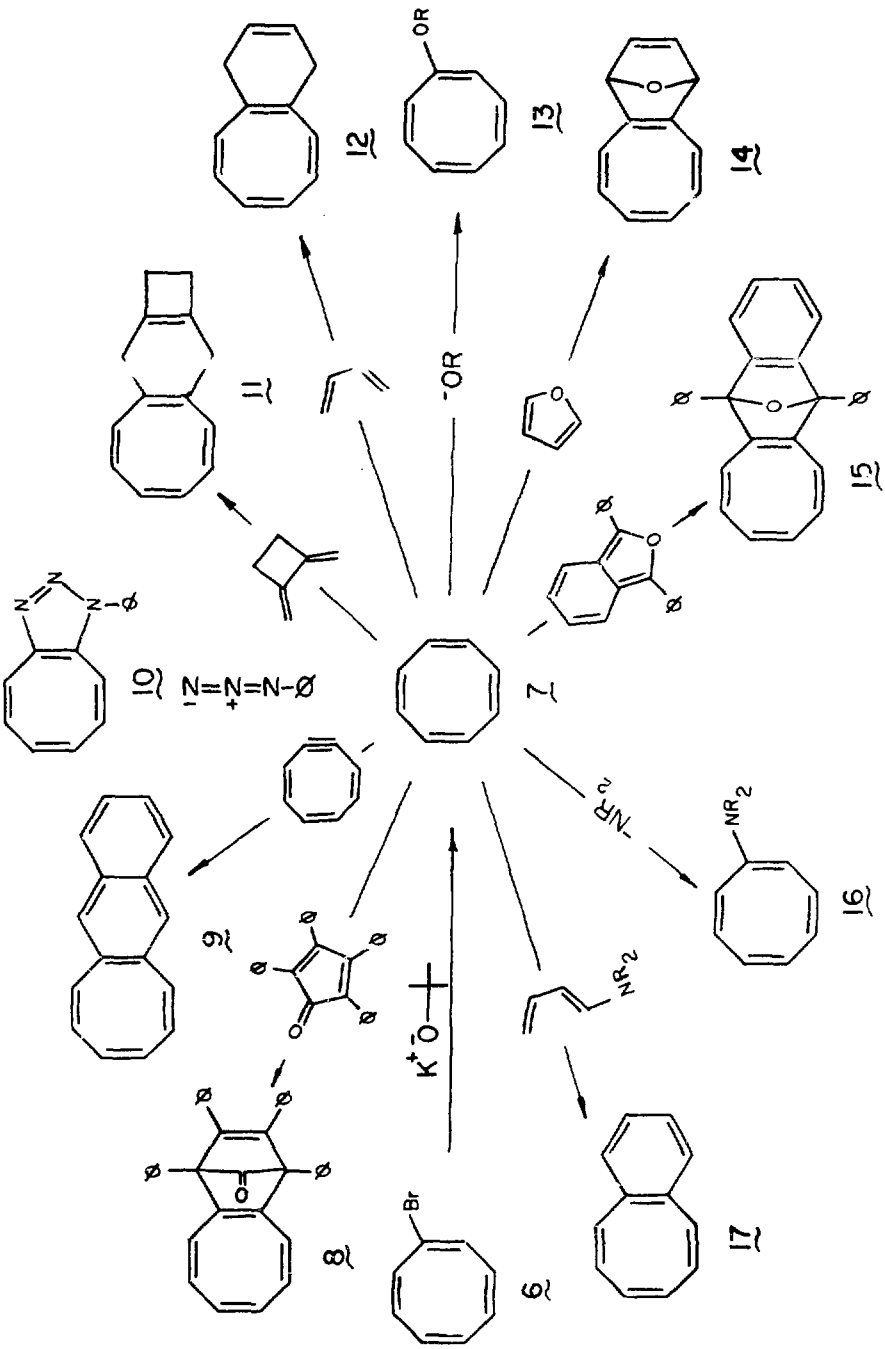

Scheme 5-2

with fused 6-membered rings. Trapping with furan would lead to 18, which upon subsequent deoxygenation would afford a benz-annulated uranocene.

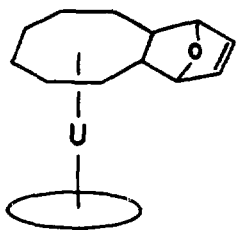

18

Addition of 2 eq. of n-butyllithium to furan solutions of either 1,1'-diallyloxyuranocene or 1,1'-dimethoxyuranocene afforded only replacement of the alkoxy groups by the alkyl group of the lithium reagent and no apparent formation of the desired Diels-Alder adduct as evidenced by a combination of mass and visible spectral analysis. Use of a more reactive trapping agent, 2,5-diphenylisobenzo[c]furan, in THF, afforded only trace amounts of alkyl substitution and a large amount of decomposition. Failure to generate annulated uranocene precursors to benzouranocene via this route led us to pursue a more classical approach to benzouranocene; reaction of benzo-cyclooctatetraene dianion with UCl_4.

B) ATTEMPTED SYNTHESIS OF BENZOCYCLOOCTATETRAENE

1) ATTEMPTED DIELS-ALDER TRAPPING OF 1,2-DEHYDROCYCLO-OCTATETRAENE

Wittig and co-workers[13] originally prepared benzocyclooctatetraene in 0.007% overall yield from o-phthaldehyde according to Scheme 5-3. Since this initial synthesis, five other synthetic schemes with benzocyclooctatetraene as the main product have been reported. They are: 1)cycloaddition of benzocyclobutene and butadiene, (75%)[14]; 2)the silver catalyzed addition of benzyne to benzene, (8.7%)[15]; 3)the protiodebromination of 3,8-dibromobenzocyclooctatetraene resulting from photobromination of biphenylene, (25%)[16]; 4)the dehydrogenation of 12 resulting from 1,3-butadiene trapping of 1,2-dehydrocyclooctatetraene (56%)[17]; 5)the photolysis of sulfone 24, (91%)[18,19] and the pyrolysis of propellane 25, (53%).[20,21] The yields in parenthesis

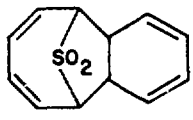

24

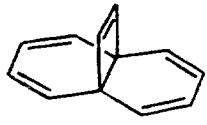

25

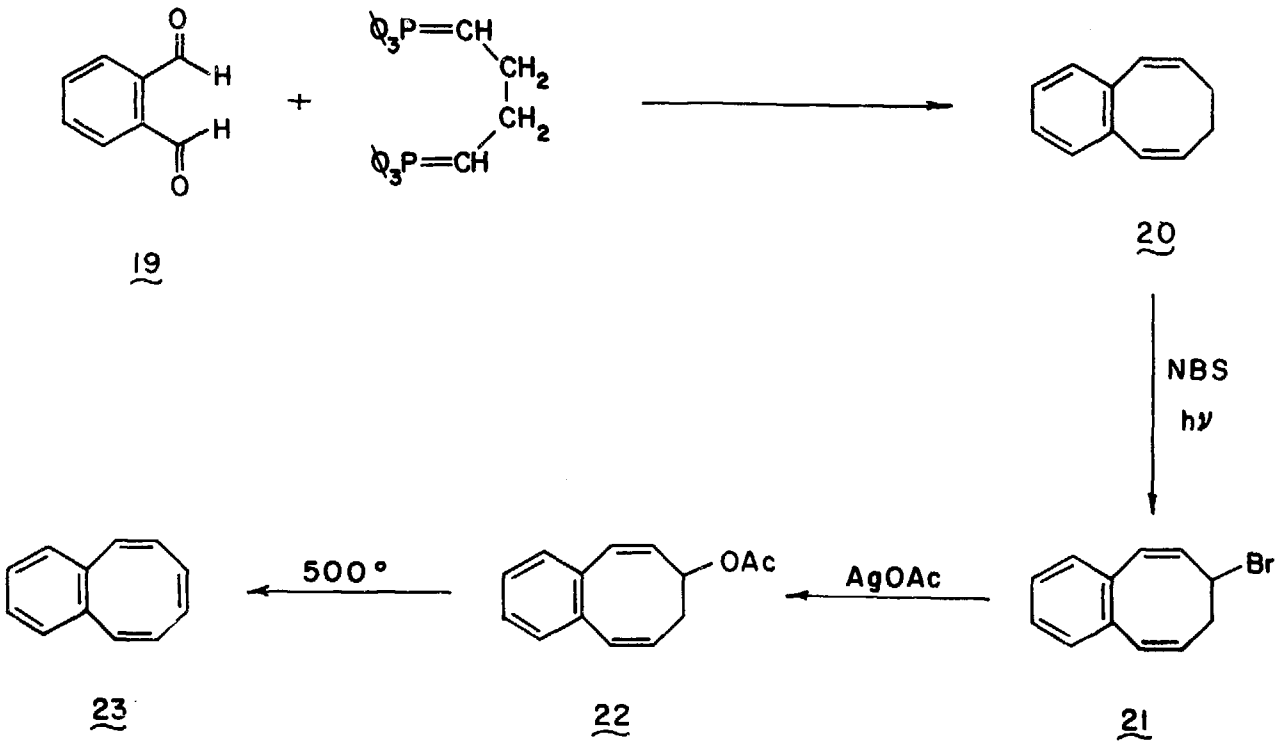

Scheme 5-3

give the yield of benzocyclooctatetraene based on the amount of immediate precursor and are quite misleading since many of the precursors are only available in low yields from multistep syntheses. Of these approaches to benzocyclooctatetraene, the three most commonly employed synthetic schemes are schemes 2, 3 and 4. In light of the explosive hazard associated with isolation of the silver diazonium salt of antranilic acid required in Ag^+ catalyzed addition of benzyne to benzene, and poor availability of biphenylene required in route 3, we elected to synthesize benzocyclooctatetraene according to route 4.

Elix and Sargent[17] have reported that addition of bromocyclooctatetraene and potassium t-butoxide to a 1,3-butadiene saturated solution of ether, followed by 60 hr in the dark affords 9,12-dihydrobenzocyclooctatetraene in 42.6% yield and 51.4% of unreacted bromocyclooctatetraene. We have found that addition of bromocyclooctatetraene to a suspension of potassium t-butoxide in a saturated etherial solution of 1,3-butadiene results in an initial exothermic reaction and formation of a viscous deep purple solution. After stirring for 28 hr a yellow oil was isolated upon workup. Distillation of this material, 42-45°/0.5 mm Hg, afforded a trace amount of bromocyclooctatetraene and t-butoxycyclooctatetraene in 64% yield as the only isolable products.

Reaction under identical conditions followed by isolation and purification of products by column chromatogrpahy on silica gel with hexane elution afforded a small amount of unreacted bromocyclooctatetraene, trace amounts of naphthocyclooctatetraene

and a similar yield of t-butoxycyclooctatetraene. Again, there was no evidence of the desired Diels-Alder adduct. Portionwise inverse addition of potassium t-butoxide to bromocyclooctatetraene in a saturated etherial solution of 1,3-butadiene also afforded a similar yield of t-butoxycyclooctatetraene.

Both 2,3-dimethyl-1,3-butadiene, furan and 2,5-dimethylfuran were investigated as potential trapping reagents. With the former two reagents, only t-butoxycyclooctatetraene in 40-60% yields could be isolated along with trace amounts of naphthocyclooctatetraene. No evidence of the Diels-Alder adducts could be detected. In the latter case, upon addition of potassium t-butoxide to an ethereal solution of 2,5-dimethylfuran, the solution changed color to deep red apparently from α-deprotonation of the furan. Only very low yields of bromocyclooctatetraene, trans-β-bromostyrene and naphthocyclooctatetraene could be recovered from the large amount of tar that formed in this reaction. Treatment of bromocyclooctatetraene with the hindered amide base, lithium 2,2,6,6-tetramethylpiperidide in furan resulted in no apparent reaction after 24 hr of stirring at room temperature.

The exclusive formation of t-butoxycyclooctatetraene as the principal product from these reactions is quite surprising, since Elix and Sargent make no mention of its formation in their original work.[17] Further, neither normal nor inverse addition nor the use of sublimed potassium t-butoxide have any effect on the reaction products. Isolation of small amounts of naphthocyclooctatetraene, which results from rearrangement of the

eyne dimer, indicate that the eyne is formed under the reaction conditions. Thus, the eyne must react faster with the alkoxide than with the diene trapping agents.

Trapping of 1,2-dehydrocyclooctatetraene with alkoxide

trapping of 1,2-dehydrocyclooctatetraene is a well-known reaction. Oth and co-workers[22] have shown that reaction of bromocyclooctatetraene with alkoxides in DMSO leads to high yields of alkoxycyclooctatetraenes. Similarly, Berryhill[23] has found that the replacement of the DMSO with ether affords similar yields of alkoxycyclooctatetraenes.

2) REACTION OF CYCLOOCTATETRAENE DIANION WITH ALKYL HALIDES

Our successful synthesis of cyclooctatetraene dianions by the dideprotonation of cyclooctatrienes suggested that the 9,12-didehydrobenzocyclooctatetraene dianion 27 could be prepared by dideprotonation of the triene 26. Oxidation of 27 followed

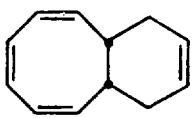

26

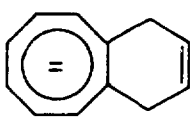

27

by aromatization would afford benzocyclooctatetraene. Alternatively, dehydrogenation of a uranocene derived from 27 would directly lead to benzouranocene.

Formation of 26 was attempted by the addition of an ethereal solution of predominantly trans-1,4-dibromo-2-butene to cyclooctatetraene dianion in liquid ammonia. Upon workup, a yellow oily semi-solid was isolated which rapidly polymerized to a white insoluble solid even with handling under an Ar atmosphere. It is possible that the reaction of the trans-1,4-dibromo-2-butene gives not 26 but polymeric trienes where the two ends of the dibromide have reacted with separate dianions. However, conversion of 98% cis-2-butene-1,4-diol to the dimethanesulfonate followed by reaction with cyclooctatetraene dianion under similar conditions or in THF, afforded similar polymeric material, suggesting that if 26 is formed, it is too unstable to work with.

The reaction of 1,4-dibromo-2,3-dimethyl-2-butene with cyclooctatetraene dianion was also investigated. Presumably, the methyl groups will enhance the solubility of both the benzocyclooctatetraene and the uranocene derived from 29. Sweeting and Johnson[24] have reported that bromination of 2,3-dimethyl-1,3-butadiene affords a mixture of the cis and trans 1,4-dibromo-2-butene, separable by distillation (cis, bp 77.5-79.5°C/5 torr; trans, bp 88-92°C/5 torr, mp 47-47.5°C). Further, the trans isomer could be converted to the cis isomer by photolysis in CH_2Cl_2 or by slow distillation. Without irradiation, the bromination of 2,3-dimethyl-1,3-butadiene affords exclusively

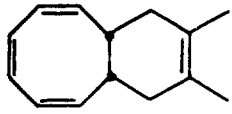

28

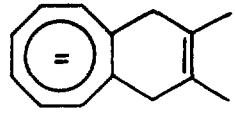

29

the trans isomer in >85% yield.[25] We have found that addition of Br_2 to 2,3-dimethyl-1,3-butadiene in CH_2Cl_2 followed by 12 hr of irradiation with a 400 watt medium pressure Harmonia lamp affords a 63:37 mixture of cis and trans 1,4-dibromo-2,3-dimethyl-2-butene in 43% yield. Attempted separation of the two isomers by fractional crystallization and several fractional distillations resulted in little alteration of this isomer ratio. However, upon storage for several months in the freezer, the trans isomer slowly crystallized as a white solid from a solution of the two isomers.

If, as we proposed in Chapter 2, the initial step in the reaction of cyclooctatetraene dianion with alkyl halides involves electron-transfer radical coupling, then both the cis and the trans isomers could react to form 28. Addition of an ethereal

solution of the isomeric mixture of the dibromides to a suspension of cyclooctatetraene dianion in liquid ammonia afforded a yellow oil upon workup. Reduced pressure distillation (92-94.5°C/3 torr) afforded 28 in 17.8% yield. Attempted classical characterization by treatment with alcoholic $AgNO_3$ did not result in a silver nitrate adduct.

From the yield of 28 it is impossible to tell if any of the trans isomer reacted to form 28. To establish the products resulting from reaction of the trans isomer, the pure trans isomer was subjected to reaction under identical conditions. Upon workup, a yellow tar was isolated which continued to polymerize and harden at room temperature, and none of the triene 28 could be isolated. Thus, only the cis isomer affords 28 upon reaction with cyclooctatetraene dianion. This implies that if the first step in the reaction of cyclooctatetraene dianion with an alkyl halide involves electron-transfer radical coupling, the radical coupling step occurs faster than bond rotation in an allyl radical.

The effect of the fused ring and the two methyl groups in the fused ring in 28 on the stability of the bicyclic and tricyclic tautomers of 28 is interesting. In Chapter 2, we reported that ^{13}C NMR spectra showed that for the two cyclooctatrienes with fused 5-membered rings (n=3) the equilibrium lies totally on the side of 30b. Likewise, when one unit of unsaturation is introduced into the 5-membered ring, the equilibrium still lies on the side of 30b.[26] Cotton and Deganello[27] have shown that a fused six-membered ring is much

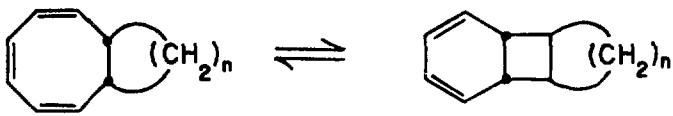

30b 30b

less stabilizing of the b tautomer. At 30°C, the 30a:30b ratio is 7:3 for n=4. The ^{13}C NMR spectrum of 28 shows 6 resonances consistent with tautomer a, and remains unchanged over a period of days. Proton coupled spectra permit assignment of all of the resonances: 140.0 ppm (d, J_{C-H} = 155 Hz) olefinic; 129.3 ppm (d, J_{C-H} = 146 Hz) olefinic; 123.7 ppm (d, J_{C-H} = 142 Hz) olefinic; 121.0 ppm (t, J_{C-H} = 7 Hz) quaternary; 38.1 ppm (d, J_{C-H} = 128 Hz) bridgehead; 36.6 ppm (t, J_{C-H} = 126 Hz) methylene; 20.3 ppm (q, J_{C-H} = 126 Hz) methyl.

Cotton, et al.,[27] have proposed that a cyclohexane ring is less effective in stabilizing the b tautomer because fusion to a planar 4-membered ring forces the cyclohexane ring to adopt a half-chair or tub conformation. Presumably, similar considerations account for the stabilization of tautomer a for 28. However, it is interesting to note that Oth and co-workers[28]

have found that a fused cyclohexadiene ring stabilizes the b tautomer.

III. PREPARATION OF STABLE ANNULATED URANOCENES WITH FUSED 6-MEMBERED RINGS

A) ATTEMPTED PREPARATION OF BIS[10,11-DIMETHYL-9,12-DIHYDROBENZO]URANOCENE

Attempted dideprotonation of 28 with potassium amide in 2% THF/80% NH_3 afforded a red solution and a tan, highly air sensitive, solid upon solvent removal, similar to the dideprotonation of the cyclooctatrienes reported in Chapter 2. Analysis by NMR of the red-brown solutions resulting from redissolution in THF could not unambiguously substantiate the presence of the dianion 29.

Addition of a THF solution of this material to a light green solution of UCl_4 in THF resulted in an immediate color change to brown black. Removal of solvent afforded a silver grey powder which did not give any colored material on washing with hot hexane. Repetition of this reaction with a second preparation of dianion afforded a similar result. Thus, either the dianion 29 is not formed under the deprotonating conditions or, if formed, the dianion 29 does not form a uranocene on reaction with UCl_4.

B) PREPARATION OF DICYCLOHEXENOURANOCENE

To test if any cyclooctatrienes with fused 6-membered rings could be dideprotonated to the corresponding dianion with potassium amide, we attempted dideprotonation of 31. Cotton, et al.,[27] have previously reported preparation of 31

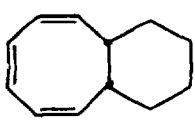

31

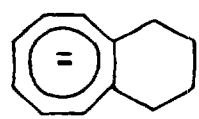

32

by the addition of 1,4-dibromobutane to cyclooctatetraene dianion in liquid ammonia. In our hands, this reaction afforded 31 as a crude yellow oil which could be purified by distillation at 46-47°C/0.65 torr (28.4% yield). Similar to 28, attempted formation of the silver nitrate adduct by treatment with alcoholic $AgNO_3$ failed.

Treatment of 28 with potassium amide in THF/NH_3 afforded a red solution and an extremely air sensitive tan solid upon solvent removal. Analysis by NMR of THF solutions of this

material was unsuccessful in establishing the presence of the dianion 32; however, its formation was confirmed by chemical reaction. Addition of a THF solution of this material to a solution of UCl_4 in THF afforded a green black solution and a greenish-grey solid upon solvent removal. Soxhlet extraction of this material with hexane afforded dicyclohexenouranocene in 17.1% yield. Visible spectra showed the usual uranocene cascade of absorbances with λ_{max} of 628 nm, 655 nm and 672 nm. The mass spectrum showed principal peaks of m/e 554 (98%), 396 (86%), and 158 (75%) corresponding to the parent ion, loss of one ligand and the ligand, respectively. Interestingly, two large peaks of m/e 552 (88%) and 550 (16%), corresponding to loss of two and four protons, respectively, were also present in the mass spectrum, and the relative ratio of these peaks to the parent peak of 554 remain essentially constant regardless of whether the sample had been purified by sublimation or recrystallization or whether the mass spectrum was run at 70 eV or 15 eV. The P-2 and P-4 peaks may reflect the intriguing possibility that the ligand has lost two hydrogens forming 33 which is a direct analog of 34 reported by Sondheimer and co-workers.[29] Possibly, the conformation of the 6-membered ring in dicyclohexenouranocene places the α-hydrogens in a proximity for elimination. In an attempt to induce such elimination in solution, dicyclohexenouranocene, in hexane, was stirred over Pd/C for 1 week, at 30°C. However, monitoring of the visible spectrum showed no change in λ_{max} or the shape of the absorption spectrum.

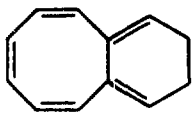

33

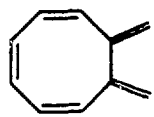

34

The ^{1}H NMR spectrum of dicyclohexenouranocene, at 30°C, shows 7 resonances which could be assigned by a combination of integrated intensities, linewidths, and comparison with the ^{1}H NMR spectra of the annulated uranocenes reported in Chapter 2: -30.64 ppm (ring), -32.53 ppm (ring), -38.70 ppm (ring), -22.35 ppm (β_{endo}, m), -2.94 ppm (β_{exo}, m), -16.42 ppm (α_{endo}, m), 6.56 ppm (α_{exo}, m). In addition to these resonances, the ^{1}H NMR spectrum showed that a paramagnetic impurity was present which could not be removed by either sublimation or recrystallization.

Assuming that the fused ring is in a half-chair conformation, the observation of only 6 substituent resonances requires rapid interconversion of half-chair conformations of the 8-membered ring. Variable temperature ^{1}H NMR spectra of cyclohexenouranocene showed no change in the number of substituent

resonances nor any indication of the onset of coalescence indicating that the energy barrier to interconversion of the half-chair conformations of the 6-membered ring is small.

The bulk magnetic susceptibility of dicyclohexenouranocene was determined by the vibrating magnetometer method from 4.2°K to 97.8°K, with the data plotted in Fig. 5-1. Above 15°K, the magnetic susceptibility shows Curie-Weiss behavior. Using a diamagnetic correction of -187×10^{-6} emu/mole,[30] a least-squares fit of the data from 15°K to 97.8°K gives $\mu_{eff} = 2.65 \pm 0.2$ with $\theta = 23.0$°K and $C = 0.8810$ emu °K/mole, which is comparable to the magnetic properties of other uranocenes listed in Table 3-11.

Fig. 5-1 Plot of 1/X vs T for dicyclohexenouranocene.

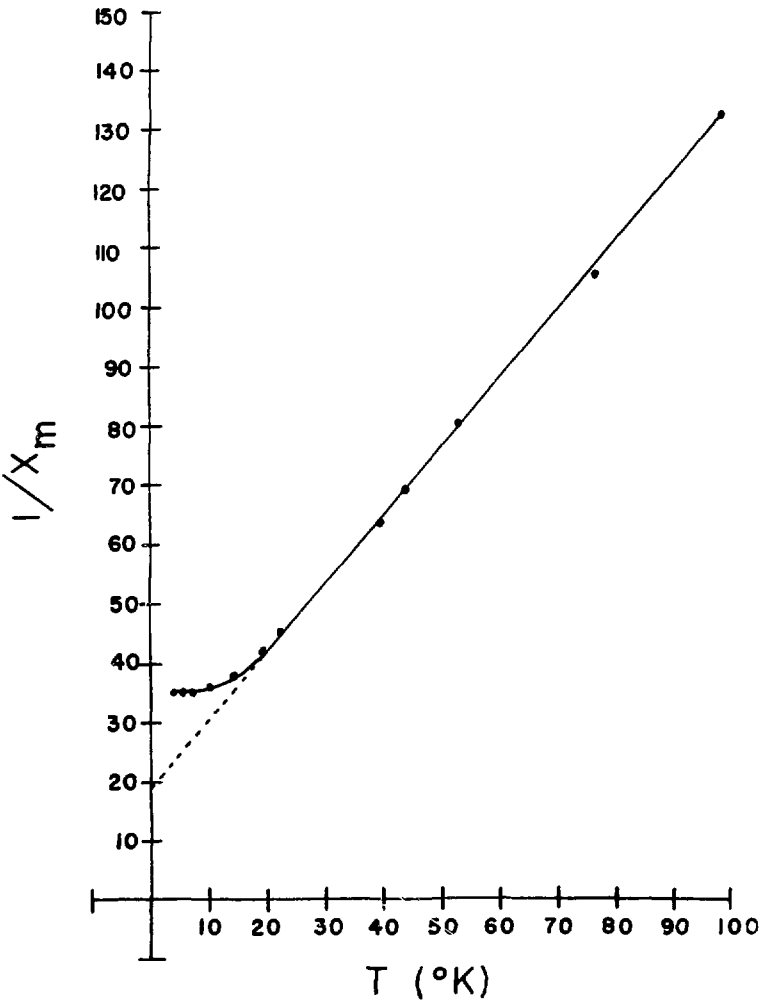
150
140
130
120
110
100
90
80
70
60
50
40
30
20
10
1/χm
10 20 30 40 50 60 70 80 90 100
T (°K)

EXPERIMENTAL

Methoxycyclooctatetraene. -- A 500 mL round bottom flask was flamed out under an Ar purge and charged with 200 mL of DMSO and 21.0 g (0.30 mol) of potassium methoxide. The flask was fitted with a dropping funnel charged with 12.0 g (0.0656 mol) of bromocyclooctatetraene in 100 mL of DMSO, which was added at ca. 1 drop per second to the stirred suspension of base. The flask was wrapped in foil and stirred for 2 days after which time the reaction mixture was deep brown in color. The reaction mixture was transferred to a separatory funnel, 100 mL of water was added and the solution was extracted with 4 x 100 mL of diethyl ether. The organic fraction was dried over $MgSO_4$. Removal of solvent followed by distillation (45°C/1 Torr) afforded 6.12 g (69.5% yield) of methoxycyclooctatetraene. Spectral properties were identical with those reported in the literature.[28]

A 31.6% yield was obtained when sodium methoxide was used instead of potassium methoxide.

1,1'-Dimethoxyuranocene. -- In the glove box, a 250 mL uranocene reactor was charged with 6.0 g (28.3 mmol) of dipotassium methoxycyclooctatetraenyl, prepared by the reduction of methoxycyclooctatetraene with potassium metal in THF, and 100 mL of THF. To this solution was added a solution of 5.42 g (14.1 mmol) of UCl_4 in 75 mL of THF. The resulting deep green solution was stirred overnight followed by removal of solvent by vacuum transfer to yield an olive green solid which was purified by Soxhlet extraction with hexane; yield 5.2 g (72.7%).

The spectral properties of this compound were identical to those reported in the literature.[31]

Addition of n-butyllithium to 1,1'-dimethoxyuranocene in furan. -- To a solution of 0.58 g (1.15 mmol) of 1,1'-dimethoxyuranocene in 150 mL of furan in a 500 mL uranocene reactor was added 0.881 mL (2.29 mmol) of 2.6 M n-butyllithium. The resulting green solution was stirred for 1 day followed by solvent removal. A visible spectrum of the resulting green material showed λ_{max} of 622, 651 and 671 nm indicating formation of 1,1'-di-n-butyluranocene. A mass spectrum showed m/e peaks of 558 (19%; 1,1'-di-n-butyluranocene), 398 (10%; loss of one ligand from 1,1'-di-n-butyluranocene), 532 (15%; 1-methoxy-1'-n-butyluranocene), 372 (3%; loss of one ligand from 1,1'-dimethoxyuranocene). No peak corresponding to the starting material or the Diels-Alder adduct was present.

Treatment of 1,1'-diallyloxyuranocene with n-butyllithium under similar conditions afforded a similar result.

Addition of n-butyllithium to 1,1'-dimethoxyuranocene with added 2,5-diphenylisobenzo[c]furan. -- In the glove box, a 250 mL uranocene reactor was charged with 0.249 g (0.921 mmol) of 2,5-diphenylisobenzo[c]furan (Aldrich), 0.200 g (0.395 mmol) of 1,1'-dimethoxyuranocene and 100 mL of THF. To the resulting blue green solution was added dropwise 0.3 mL (0.78 mmol) of 2.6 M n-butyllithium (Alfa). With the addition of the lithium reagent, the solution changed color to red brown. After stirring for 24 h the solvent was removed affording a greenish brown

solid. A mass spectrum showed no peaks corresponding to 1,1'-dimethoxyuranocene or evidence of the ligand Diels-Alder adduct. A visible spectrum showed no absorptions in the visible region.

Attempted Diels-Alder trapping of 1,2-dehydrocyclooctatetraene. -- A saturated solution of 1,3-butadiene in ether was prepared by bubbling 1,3-butadiene (Matheson) through 500 mL of ether at -20°C in a 3000 mL round bottom flask. To this solution was added 10 g (89.1 mmol) of potassium t-butoxide (Alfa) followed by the dropwise addition of a solution of 10 g (54.6 mmol) of bromocyclooctatetraene in 100 mL of diethyl ether at -18°C. The resulting brown solution was stirred for 4 h at -18°C followed by warming to room temperature and an additional 24 h of stirring. The reaction mixture was washed with brine (150 mL). The aqueous layer was extracted with 2 x 100 ml portions of ether and the combined organic layers were dried over $MgSO_4$. Removal of solvent afforded a golden yellow oil which was placed on a silica gel chromatography column and eluted with hexane. A trace amount of naphthocyclooctatetraene was isolated followed by t-butoxycyclooctatetraene, 5.2 g (52.6%), and trace amounts of trans-β-bromostyrene and unreacted bromocyclooctatetraene. Repetition of the reaction followed by distillation of the crude reaction product (42-45°C/0.5 Torr) afforded t-butoxycyclooctatetraene in 64% yield.

Likewise, inverse addition of sublimed potassium t-butoxide over a 1 h period to bromocyclooctatetraene in a saturated solution of 1,3-butadiene in ether afforded a similar result.

Addition of ethereal solutions of bromocyclooctatetraene to suspensions of potassium t-butoxide in ethereal solutions of 2,3-dimethyl-1,3-butadiene or furan at room temperature afforded only t-butoxycyclooctatetraene in yields of 40-70%.

1,4-Dimethanesulfonyloxy-2-butene. -- To a solution of 26.43 g (0.3 mol) of 2-butene-1,4-diol (91:9, cis:trans, Aldrich), and 70 g (0.7 mol) of triethylamine in 1.5 L of CH_2Cl_2 at 0°C was added 48.76 mL (0.63 mol) of methanesulfonyl chloride (Eastman) dropwise over a 10 min period. After stirring for 45 min, during which time a white precipitate formed, the reaction was quenched by the addition of 250 mL of ice water. The organic layer was sequentially washed with 250 mL portions of cold 10% HCl, saturated sodium bicarbonate, and brine and dried over $MgSO_4$. Removal of solvent followed by recrystallization from hot methanol afforded the dimethanesulfonate as a white crystalline solid; yield, 27.95 g (38.1%). ^1H NMR ($CDCl_3$): δ 6.03 (t, J = 4Hz, 2H, vinyl), 4.97 (d, J = 4Hz, 4H, CH_2), 3.17 (s, 6H, CH_3).

Anal. Calcd for $C_4H_{12}S_2O_6$: C, 29.50; H, 4.95; S, 26.25

Found: C, 29.64; H, 5.04; S, 26.18

cis and trans 1,4-Dibromo-2,3-dimethyl-2-butene. -- Over a 2 h period, 97.32 g (0.61 mol) of bromine in 150 mL of $CHCl_3$ was added to 50 g (0.61 mol) of 2,3-dimethyl-1,3-butadiene in 200 mL of $CHCl_3$ at 0°C. After the addition, the solution was diluted with $CHCl_3$ until the total volume was 600 mL and photolyzed for 12 h with a medium pressure Hg lamp. Removal

of the solvent by reduced pressure afforded a brown oil which was subjected to vacuum distillation through a 1 cm x 25 cm vacuum jacketed column. A forerun, 1.74 g (50-75°C/5 Torr) and a pale yellow lacrimatory liquid, 84.8 g (75°C/5 Torr) were collected. The main fraction appeared to be a 63:37 mixture of cis and trans isomers by NMR. Redistillation of the main fraction through a 1 cm x 40 cm Ta band electrically jacketed column did not alter this isomer ratio. Redistillation through a 2 cm x 38 cm vacuum jacketed column packet with 1/8 in. glass helices afforded one fraction, 75-85°C/5 Torr, 82.0 g (43%) of a pale yellow liquid. NMR ($CDCl_3$) indicated it was a 63:37 mixture of isomers; trans isomer ^1H NMR ($CDCl_3$): δ 3.96 (s, 4H, CH_2), 1.83 (s, 6H, CH_3); ^{13}C NMR ($CDCl_3$): δ 131.9 (quaternary), 34.9 (CH_2), 17.2 (CH_3); cis isomer ^1H NMR ($CDCl_3$)L δ 4.00 (s, 4H, CH_2), 1.80 (s, 6H, CH_3); ^{13}C NMR ($CDCl_3$): δ 132.3 (quaternary), 33.8 (CH_2), 17.6 (CH_3).

Upon prolonged storage of the mixture of the two isomers at -10°C, the trans isomer crystallized as a white solid.

Addition of trans 1,4-dibromo-2-butene to cyclooctatetraene dianion. -- A suspension of cyclooctatetraene dianion in liquid ammonia was prepared by the addition of 10.4 g (0.1 mol) of cyclooctatetraene (BASF as supplied) to a solution of 1.39 g (0.2 mol) of lithium (1% sodium) in liquid ammonia at -40°C. To this solution was added dropwise a solution of trans 1,4-dibromo-2-butene (Aldrich) in 25 mL of ether at -40°C. The resulting solution was stirred for 3 h at -40°C followed by overnight evaporation of the ammonia. The resulting tan semi-

solid was suspended in 200 mL of saturated ammonium chloride and extracted with 3 x 100 mL portions of ether. The combined ether extracts were washed with water (3 x 100 mL) and dried over $MgSO_4$. On standing, a yellow polymeric material began to precipitate from the solution. Removal of solvent left a yellow orange jelly which rapidly solidified to an insoluble polymeric material.

Addition of cis 1,4-dimethanesulfonyloxy-2-butene to cyclooctatetraene dianion under identical conditions afforded a similar insoluble polyermic product.

cis-Bicyclo[6.4.0]doceca-2,4,6-triene, 31. -- Following the reaction procedure for the addition of 1,4-dibromo-2-butene to cyclooctatetraene dianion, addition of 21.6 g (0.1 mol) of 1,4-dibromobutane (Baker) to 0.1 mol of the dianion in liquid ammonia afforded a clear liquid upon workup. Distillation (46-47°C/0.65 Torr) gave 4.55 g (28.4%) of cis-bicyclo[6.4.0]-doceca-2,4,6-triene. Mass spectrum m/e 160; ^1H NMR ($CDCl_3$): δ 5.78, 5.67 (br s, 4.2H, vinyl), 2.65 (br m, 2H, bridgehead), 1.53 (br s, 6H, cyclohexane).

Anal. Calcd for $C_{12}H_{14}$: C, 89.93; H, 10.07

Found: C, 89.85; H, 9.85

Bicyclo[6.4.0]doceca-1,3,5,7-tetraenyl potassium, 32. -- Following the procedure for the dideprotonation of cis-bicyclo-[6.3.0]undeca-1,3,5-triene in Chapter 2, 4.5 g (0.028 mol) of 31 afforded 5.56 g of crude 32.

9,10-Dimethyl-cis-bicyclo[6.4.0]dodeca-1,3,5,9-tetraene, 28. -- Following the procedure for the addition of 1,4-dibromo-2-butene to cyclooctatetraene dianion, addition of 24.2 g (0.1 mol) of a mixture of cis and trans (63:37) 1,4-dibromo-2,3-dimethyl-2-butene was added to cyclooctatetraene dianion in liquid ammonia. Workup and distillation of the crude reaction product (92-94.5°C/3 Torr) gave 4.90 g (26.3%) of the desired triene. ^{1}H NMR ($CDCl_3$): δ 5.8-5.4 (br m, vinyl), 1.8-3.1 (br m, bridgehead and CH_2), 1.92 (s, CH_3). Mass spectrum (70 ev) m/e 186 (5%). See text for ^{13}C NMR.

Similar reaction with the pure trans isomer afforded only polymeric material.

9,10-Dimethyl-bicyclo[6.4.0]doceca-1,3,5,7,9-pentaene potassium, 29. -- Following the procedure for the dide-protonation of cis-bicyclo[6.3.0]undeca-1,3,5-triene in Chapter 2, 4.0 g (21.5 mmol) of 28 was added to 42.9 mmol of potassium amide affording 5.64 g of a highly air sensitive brown solid on solvent removal.

Dicyclohexenouranocene. -- In the glove box a solution of 2.56 g (6.8 mmol) of UCl_4 in 25 mL of THF was added to a solution of 3.0 g (13.5 mmol) of 32 in 100 mL of THF in a 500 mL uranocene reactor. The resulting green solution was stirred for 18 h followed by solvent removal affording a green solid which was purified by Soxhlet extraction with hexane. Yield 0.57 g (15.9%). ^{13}C NMR (dioxane-d_8): δ 308, 297, 270 (ring), 13.4 (C_β), -32.5 (C_α). See text for other physical properties.

Preparation of uranocene in liquid ammonia. -- To 300 mL of ammonia in a 500 mL 3-necked round bottom flask was added 1.65 g (0.04 mol) of potassium metal. The resulting blue solution was stirred at -40°C and 2.19 g (0.02 mol) cyclooctatetraene (BASF as supplied) was added via syringe. The yellow suspension of dianion was stirred for 1 h at -40°C. To this solution was added 4.0 g (0.01 mol) UCl_4 in 35 mL of THF. The emerald green suspension of uranocene was stirred for 1 h at -40°C and allowed to warm overnight while the ammonia was driven off with an N_2 purge. The green solid was pumped to dryness and Soxhlet extracted for 1 week with furan; yield 1.47 g (31.4%).

REFERENCES

1) J. Trotter, Acta. Crystallogr., 11, 355 (1958).

2) J. L. Atwood and K. D. Smith, J. Am. Chem. Soc., 96, 994 (1974).

3) H. P. Fritz and C. G. Kreiter, J. Organomet. Chem., 4, 198 (1965).

4) P. Treichel, J. W. Johnson and J. C. Calabrese, J. Organomet. Chem., 88, 215 (1975).

5) F. H. Kohler, Chem. Ber., 107, 570 (1974).

6) S. Mylonakis, unpublished results.

7) D. Dempf, unpublished results.

8) A. Streitwieser, Jr. and R. Walker, J. Organomet. Chem., 97, C41 (1975).

9) L. B. Anderson and L. A. Paquette, J. Am. Chem. Soc., 94, 4915 (1972).

10) C. A. Harmon and A. Streitwieser, Jr., J. Am. Chem. Soc., 94, 8926 (1972).

11) L. A. Paquette, Tet., 31, 2855 (1975).

12) G. I. Fray and R. G. Saxton, "The Chemistry of Cyclo-octatetraene and its Derivatives", Cambridge Univ. Press, New York, N.Y. (1978).

13) G. Wittig, H. Eggers and P. Duffner, Ann., 619, 11 (1968).

14) W. Merk and R. Pettit, J. Am. Chem. Soc., 89, 4787 (1967).

15) L. Friedman and D. F. Lindow, J. Am. Chem. Soc., 90, 2329 (1968).

16) J. W. Barton and K. E. Whitaker, J. Chem. Soc. C, 28 (1968).

17) J. A. Elix and M. V. Sargent, J. Am. Chem. Soc., 91, 4734 (1969).

18) L. A. Paquette and R. H. Meisinger, J. Am. Chem. Soc., 93, 1047 (1971).

19) L. A. Paquette, R. H. Meisinger and R. E. Wingard, Jr., J. Am. Chem. Soc., 95, 2230 (1973).

20) L. A. Paquette and R. E. Wingard, Jr., J. Am. Chem. Soc., 94, 4398 (1972).

21) L. A. Paquette, R. E. Wingard, Jr. and J. M. Photis, J. Am. Chem. Soc., 96, 5801 (1974).

22) J.F.M. Oth, R. Merenye, Th. Martini and G. Schroder, Tet. Let., 3087 (1966).

23) S. R. Berryhill, Ph.D. Thesis, UC Berkeley (1977).

24) O. J. Sweeting and J. R. Johnson, J. Am. Chem. Soc., 68, 1057 (1946).

25) E Z. Said and A. E. Tipping, J. Chem. Soc. Ferkin I, 11, 1399 (1972).

26) J. F. Monthony and W. H. Okamura, Tet., 28, 4273 (1972).

27) F. A. Cotton and G. Deganello, J. Am. Chem. Soc., 94, 2142 (1972).

28) J.F.M. Oth, H. Rottele and G. Schroder, Tet. Let., 61 (1970).

29) J. A. Elix, M. V. Sargent and F. Sondheimer, J. Am. Chem. Soc., 92, 962 (1970).

30) D G. Karraker, J. A. Stone, E. R. Jones, Jr. and N. Edelstein, J. Am. Chem. Soc., 92, 4841 (1970).

31) C. A. Harmon, D. P. Bauer, S. R. Berryhill, K. Hagiwara and A. Streitwieser, Jr., Inorg. Chem., 16, 2143 (1977).

The Author

The author was born in Pasadena, California in 1953. After completion of grade school and high school in the Los Angeles area he attended the University of Southern California, where, as a chemistry major, he spent 4 semesters and 1 summer in undergraduate research under Professor Thomas C. Flood. Upon graduation with a B.S. in Chemistry in January of 1975 he went to work as a chemist for the Southern California Coastal Water Research Project. In September of 1975 he entered the University of California Graduate School at Berkeley, California, where he spent 4 years of graduate work under Professor Andrew Streitwieser, Jr., receiving both a M.S. and a Ph.D. in organic chemistry.